

McHale

**Proceedings of the
Second Symposium on**

ABNORMAL SUBSURFACE PRESSURE

**January 30, 1970
Louisiana State University
Baton Rouge, Louisiana**

DISCLAIMER

This report was prepared as an account of work sponsored by an agency of the United States Government. Neither the United States Government nor any agency Thereof, nor any of their employees, makes any warranty, express or implied, or assumes any legal liability or responsibility for the accuracy, completeness, or usefulness of any information, apparatus, product, or process disclosed, or represents that its use would not infringe privately owned rights. Reference herein to any specific commercial product, process, or service by trade name, trademark, manufacturer, or otherwise does not necessarily constitute or imply its endorsement, recommendation, or favoring by the United States Government or any agency thereof. The views and opinions of authors expressed herein do not necessarily state or reflect those of the United States Government or any agency thereof.

DISCLAIMER

Portions of this document may be illegible in electronic image products. Images are produced from the best available original document.

Proceedings
of the
Second Symposium on
ABNORMAL SUBSURFACE PRESSURE

January 30, 1970
LOUISIANA STATE UNIVERSITY
Baton Rouge, Louisiana

Sponsored by
The School of Geoscience
and the
Department of Petroleum Engineering

Proceedings Edited by
R. E. Ferrell, Jr. and B. R. Hise

Editor's Introduction

This volume contains the proceedings of the Second Symposium on Abnormal Subsurface Pressure held at Louisiana State University (Baton Rouge Campus). It was co-sponsored by the Department of Petroleum Engineering and School of Geoscience. The conference was attended by some 285 technical people from all disciplines of science and engineering that share a common interest in the characteristics, control and exploitation of the zone of abnormal subsurface pressure.

This volume contains papers of specific interest to drilling, reservoir and research engineers; and to both exploration and production geologists. A feature of the second symposium was a panel discussion on the diagenesis of clay and the relationship these changes have to the characteristics and occurrence of abnormal subsurface pressures.

R.E.F. and B.R.H.
Louisiana State University
Baton Rouge, Louisiana

TABLE OF CONTENTS

TITLE	i
EDITOR'S INTRODUCTION.....	ii
GEOPRESSURES (Abstract)..... Mr. C. A. Stuart	1
THE USE OF SUBSURFACE TEMPERATURE TO DETECT GEOPRESSURE. Mr. E. Rush George	5
PREDICTION OF PORE PRESSURE FROM PENETRATION RATE..... Dr. George D. Combs	35
AN ENGINEERING INTERPRETATION OF SEISMIC DATA..... Mr. E. S. Pennebaker	51
PERFORMANCE OF ABNORMALLY PRESSURED GAS RESERVOIRS IN SOUTH LOUISIANA..... Dr. W. E. Wallace	63
ABNORMAL PRESSURES AND POTENTIAL GEOTHERMAL RESOURCES IN THE RIO GRANDE EMBAYMENT..... Mr. Raymond H. Wallace, Jr.	87
CHANGES IN THE CLAY-WATER SYSTEM WITH DEPTH, TEMPERA- TURE AND TIME. (Abstract)..... Charles E. Weaver and Kevin C. Beck	116
THE DIAGENETIC ISOPLETH..... Mr. J. F. Burst	121
REVIEW OF TECHNIQUES USED IN THE DETECTION AND DRILL- ING OF OVERPRESSURED FORMATIONS..... Walter H. Fertl and Donald J. Timko	131

GEOPRESSURES¹

by

Charles A. Stuart
Shell Oil Company
New Orleans, Louisiana

Abstract

Geopressures play a dominant role in the oil and gas industry. These pore-fluid pressures have been the source of such well problems as blowouts, stuck pipe, no drilling progress, lost circulation, saltwater flows, etc. At one time, offshore drilling did not appear profitable because of high drilling costs. Deep target objectives were rarely attained. The concept of impenetrable rocks was accepted as fact in the Gulf Coast.

Sedimentary rocks have two basic components: the matrix and the contained pore fluids. All present rock classifications are based on some aspect of the matrix. A unique rock classification based on pore-fluid pressures has been introduced here to divide the rock into two broad classes: Hydropressures, in which pore-fluid pressures are generated by the weight of the overlying waters, and Geopressures, generated by a pressuring source greater than waters. A classic example of a hydropressure-geopressure province is the Tertiary Basin which forms a part of the larger Gulf of Mexico Basin.

Clastic sedimentation has been continuous throughout the Cenozoic Era in the Tertiary Basin. All rocks in this system started out as hydropressures. Hydropressures are found today to a certain depth, which ranges from 3,000 to 19,000 feet, below which geopressures are found. A

¹Editors Note: The full text of Mr. Stuart's paper was not available at the time of this printing and only an Abstract is included in these proceedings.

geopressure basin exists at the present coast line, which is approximately at the same position as the Gulf Coast geosynclinal axis. The base of the Tertiary is thought to be as deep as 30,000 to 40,000 feet at this position. In a cross section starting from the Bear field, Louisiana, 50 miles inland and extending to the edge of the continental shelf, geopressures rise and migrate upward through the Eocene, the entire Oligocene, Miocene, Pliocene, and into the Pleistocene-Recent. The ages of these rocks range from 100,000 years through 50,000,000 years. Further inland on the north flank of the Tertiary Basin, geopressures exist in the Lower Cretaceous. Thus, the volume of geopressure rocks probably exceeds the volume of hydropressure rocks in this Basin.

A buried rock is subjected to the temperatures and pressures of the earth's crust. In hydropressures, the geostatic overburden less the water pressure acts grain-to-grain, and compaction (porosity reduction) occurs with burial. Simultaneously, the water is squeezed out. This means that there is a depth limit below which sands will not have sufficient porosity and permeability to yield a productive reservoir. This is a serious limitation to our industry.

Geopressures require both a seal and source of pressures. The seal is shale in this Basin. Shale layers and down-to-basin regional faults seal the geopressure cells in regional fault blocks. The top sealing shale layer, where the pressure gradient abruptly increases, is the mutation zone. When a formation is sealed and buried, the pore fluids assume the geostatic pressure. Thus, geopressures are created. Compaction (porosity reduction) is stopped. A geopressure relationship with porosity is also created. A geopressure cell contains both sands and shales; and a geopressure-porosity relationship exists for either sand or shale taken individually.

The geostatic gradient increases with depth in hydropressures. It is about 0.85 psi/ft. at 2,000 feet and 0.95 psi/ft. at 12,000 feet. The gradient of 1.0 psi/ft. (19.2 ppg), so frequently shown as a theoretical limit, may never occur in many stratigraphic columns. Geopressures approach but have not been observed to exceed the geostatic gradient. The highest geopressure that has been validated is 0.94 psi/ft. (18.1 ppg). All primary geopressuring in the Tertiary Basin can apparently be accounted for by the weight and temperature of the earth's crust.

Often overlooked is the more important fact that porosity preservation applies to geopressure sands as well as shales. Consequently, there should be no depth limit to which geopressure sands can be porous and permeable. This opens new depths for exploration and exploitation drilling.

The hydropressure-geopressure pattern is not only related to the distribution of the pressure component in pore fluids but also to the distribution of another component: oil and gas.

In addition to an increase in porosity, there is a geothermal shift to higher values in geopressures. Drilling rates are inversely proportional to overbalance (hydrostatic head of mud less the pore-fluid pressure) and generally increase as geopressures are entered. Therefore, any log such as electrical, sound velocity, seismic, geophone, density, temperature, rock drillability, penetration rates, etc., in which porosity, overbalance, or temperature is a parameter will provide an empirical or indirect method of geopressure detection. The drilling and completion kick provide the direct method of quantifying pore-fluid pressures.

Drilling problems stem from an adverse relationship between the pore-fluid pressures, formation fracture pressures, and overbalance. Geopressure technology was developed to cope with these problems.

Application of geopressure technology to drilling has shown that the cost of wells could be reduced to 1/6 of the former cost. This success converted the offshore to a profitable venture. The only depth limitation is mechanical. There should be no such thing as an impenetrable formation.

THE USE OF SUBSURFACE TEMPERATURE
TO DETECT GEOPRESSURE

by

E. Rush George
Atlantic Richfield Company
Dallas, Texas

Abstract

Various methods to detect abnormal subsurface pressures have been used at least since 1959. These methods gave reliable answers in some areas, but proved to be less reliable in others.

In this paper, a method is presented that used changes in slope of the vertical temperature profile to indicate changes in subsurface pressure. The change and rate of change appear to be more significant than the specific temperature or gradient.

It is proposed that migrating ground water moved by pressure gradients alters the temperature distribution in the subsurface. It is proposed that a decrease in permeability caused by the high apparent viscosity of the water adsorbed in fine-grained shales or clays traps or seals pressure in low resistivity shales. Cement formed in shales and/or within the sand reduces permeability, thus trapping or sealing pressure in the high resistivity rocks.

Charts, graphs and plots of temperature vs. depth and temperature vs. pressure tend to confirm the above. A plot of temperature vs. pressure for the first well in several reservoirs studied is linear, indicating a reasonable relationship between temperature and pressure.

A chart is presented that may be used to estimate the relative pressure in a zone from the temperature shown on the electric log heading for that zone.

Most of the other methods propose that an increase in apparent porosity indicates possible high pressure; whereas the temperature method suggests that changes in porosity are not important, but that a reduction in permeability may trap pressure.

Introduction

The first known use of log-derived data for the detection of geopressure was by George in 1959 (Fig. 16). By 1964-1965, the technique was in general use. This method uses the electric log response from shales in association with sands to indicate the presence or absence of high pressure. It was observed that shale resistivity, shale conductivity, shale sonic velocity or travel time and/or shale density could be used to indicate zones of abnormal pressure. Refer to the "Discussion" in this paper for the where, when, how, and why pressure is trapped. Gretner (1969) provides a general discussion of the geographic and geologic occurrence of geopressure.

In this report, geopressure, overpressure, abnormal pressure, high pressure, and superpressure means a subsurface formation fluid and/or gas pressure that is greater than the weight of a column of water of average salinity from the subsurface depth in question to the surface. In South Louisiana, this averages approximately 0.465 pounds/square inch/foot of depth, or has a pressure gradient of 0.465.

Temperature measurements in the earth's crust have been made at least since 1664 (Plummer, p. 73). In 1968, the American Association for Petroleum Geologists started a program to systematically measure and record subsurface temperatures for all the North American Continent for the purpose of establishing regional geothermal gradients. In between these dates, many workers have studied the variations in temperature of the earth's crust. In 1931, Plummer and Sargent studied the lateral and vertical temperature distribution in the Woodbine zone in northeast Texas and related their findings to the geology of the area. In 1944-45, Guyod used an electrical model to predict the temperature distribution in and around a salt dome and extended his study to include other geological problems. In these studies, ground water movement was not considered.

In 1964 and 1966, Schneider studied the effect of moving ground water on the subsurface temperature distribution and concluded that it alters the temperature distribution significantly.

Purpose

The purpose of this paper is to (1) help reduce drilling costs and hazards by helping recognize zones of high pressure, (2) stimulate thinking or to arouse curiosity so that others may improve or develop this hypothesis or by further study, reject it.

Limits

This study is limited specifically to South Louisiana onshore and offshore; however, examples from other areas are presented for comparison. This study is limited to the writer's own observations or experience and to published material; therefore, it must be considered as an introduction to the method or as a progress report. It is not intended that this paper is "the" answer. The principles upon which this paper are based are well documented in the literature, but the conclusions drawn from these principles are the writer's and, therefore, may be questioned.

It is not suggested nor implied in this paper that the maximum temperature shown on the electric log heading for each log run is the geostatic temperature for that depth. However, Schoepple (1966) suggests, after examining more than 50,000 well logs, that this temperature is within 5 to 8 per cent of the undisturbed temperature. The change and rate of change in the vertical temperature profile with depth appear to be more meaningful than the specific temperature. The section of the hole near the bottom of the well is exposed to the cooler circulating mud for a minimum of time and all logs are run under this condition; therefore, it is believed that these temperatures are reliable enough for this study.

Methods

Hundreds of well logs from the area of study and from other areas in the Gulf Coast were studied and only those wells with a number of log runs were used in order to obtain a temperature profile as representative of the area as possible.

Temperature at depth as shown on the log heading was plotted on simple graph paper. A horizontal temperature scale of 40°F per inch, starting with a surface temperature of 80°F and a vertical scale of 2000 feet/inch was used. The temperature points were then connected, giving an approximate vertical temperature profile for the well. A diagonal line was also drawn to represent the average rate of temperature increase for a sand and shale sequence with normal pressure in the area of study. This average rate of increase is approximately 1°F per 100 feet of depth. This average line was included so that we may compare the profile with the normal.

For Figures 3, 9, and 10, the minimum shale resistivity for each hundred feet was also included for comparison with the temperature profile in that well. For Figures 3 and 9, the horizontal shale resistivity scale is 0.2 ohms per inch and for Figure 10 is 1.0 ohm per inch.

Where pressure measurements from tests were available, they were shown at the test depths. If pressures were not available, mud weights were shown to imply high pressure.

Examples

Figure 1 is the approximate average vertical temperature profile for the northwest Gulf of Mexico shown with the average rate of temperature increase with depth for normal pressured sand and shale sequences in the same area. This continuous profile is shown so that we may better understand the profiles made from logging depths in wells. It is obvious that the more logging points we have, the better these points represent the real temperature profile.

Figure 2 is a profile from log points in a well offshore South Louisiana which was drilled down the flank of a shallow piercement salt dome. Note that the well penetrated approximately 2200 feet of salt overhang. Temperature is higher than normal above the salt and lower than normal below the salt. This is the response predicted by Guyod (1944-45). Salt is a much better conductor than the sediments next to it so heat is withdrawn from sediments down the flank and is piled up on the less conductive sediments above, a temperature "halo" effect. This effect will be referred to again later.

Figure 3 is from a well that penetrated a high pressure zone from approximately 16,000 feet to total depth. For this example, the minimum shale resistivity is also shown since shale resistivities have been used for a number of years to locate zones of high pressure. Note the shale resistivity decreases below the average trend and the mud weight increases just under the limy high resistivity "cap" at approximately 15,800 feet, both indicating an increase in pressure. The temperature begins to increase above normal at that point and stays above normal to total depth. This also indicates high pressure. Note how suddenly the mud weight had to be increased from 10.5 lbs. to 16 lbs. The sudden increase in pressure below the high resistivity zone suggests that this high resistivity zone is sealing or helping to seal the pressure. This is the zone referred to by Rochon (1967) as "the mineralized zone that traps fossil pressure." This high resistivity zone will be discussed later.

Figure 4 could be called a classic profile because its shape conforms to the hypothesis of this paper. The temperature for the first four log runs plots on the 1°F per 100 foot line on trend with a surface temperature of 80°F. Note also that the mud weight was increased between 12,000

and 13,000 feet. This well was drilled before we were able to recognize high pressure zones from logs. It was a standard practice to raise the mud weight below approximately 10,000 feet in anticipation of high pressure. The large increase in mud weight and the significant increase in temperature above normal between 12,000 and 13,000 feet, both indicate a rather large increase in pressure.

Figure 5 is a profile that suggests two zones of high pressure; a zone of moderate pressure from approximately 11,000 feet to approximately 13,000 feet and a zone of much higher pressure from approximately 13,000 feet to total depth. The writer is familiar with this area and with the drilling foreman responsible for drilling this well. There are two zones of high pressure in the area, but they vary in depth from well to well so the practice is to set protection pipe and raise the mud weight before the zones are drilled. Note also that the temperature is below normal from approximately 5,000 to 13,000 feet. The shape of this profile is quite similar to Figures 1 and 2. This will be discussed in detail later.

Figure 6 depicts a well with pressure data from a test. The pressure estimated from the temperature profile and from tests agrees rather well. Mud weights would indicate that there is a pressure increase in the lower part of this well, but the temperature profile shows the pressure to be near normal. This well was drilled a number of years before logs were used for pressure estimation.

Figure 7 is from an old well as in the previous example. Note that the temperature profile and tests indicate that the well had near normal pressure but the mud weight was raised "just in case."

Figure 8 is from a recent well drilled after the industry had learned how to use logs to locate the top of a high pressure zone. There is very close agreement between the increase in pressure shown by the temperature profile and the increase in mud weight. This, too, could be called a "classic profile."

All the previous examples have been from wells which penetrated sand and shale sequences such as found in South Louisiana. The next two examples are from Hidalgo County near the southern tip of Texas. They are not in the specific area of study, but are included to show that shale data from logs may not be too reliable except in the ideal environment. But even here an increase in temperature above the normal gradient for that area indicates an increase in pressure above normal.

Figure 9 is a profile that penetrated an upper zone (6500 to 9400 feet) of thick, low porosity, limy sands and a thick, low resistivity shale (9400 feet to total depth). High pressure was encountered in both of these intervals, indicated by the mud weight. For this example, the shale resistivity profile is also shown. Note that in the massive "limy" sands, both pressure and shale resistivity increase. In southern Louisiana, the shale resistivity decreases as the pressure increases. But in the lower section from 9400 feet to total depth, the response is the same as in southern Louisiana. Apparently, there are two mechanisms which seal or trap high pressure--low resistivity shale and limy sands. For further details on this, see the discussion section.

Figure 10 is from a well that penetrated a zone of thick, limy, low porosity sands and thin, high resistivity shales. The thick sands contain high pressure. The shale resistivity profile is also included to show that shale resistivity alone in this environment is not useful as a high pressure indicator. The shale resistivity scale had to be changed from 0.2 ohms to 1.0 ohms per inch to keep the profile on the graph. Two zones were tested in this well. One at 9,150 feet had a gradient of 0.71 psi/ft. and the other at 11,400 feet had a gradient of 0.83 psi/ft. The temperature profile indicates high pressure, while the shale resistivity profile does not.

The next three examples are from wells not in our area of study. These wells penetrated zones of limestone, dolomite, and/or anhydrite. These examples are included to show the temperature profile that may be expected in this environment and that care must be used when attempting to predict pressure from the temperature profile without first establishing the rock type.

Figure 11 is a profile from a low pressured well that penetrated massive limestone, dolomite and anhydrite zones. Note the temperature response from the massive anhydrite zone (8,000 to 11,000 feet) and from the highly porous and permeable dolomite zone (11,000 to 12,200 feet). Temperatures are above normal in the anhydrite zone and below normal in the dolomite zone. This will be discussed in more detail later.

Figure 12 is from a well that penetrated a normal sand-shale sequence to approximately 9,000 feet and then a dense limestone section with two porous zones at 12,000 and 14,500 feet that had pressures slightly above normal. The temperature response from the porous zones is not the response for a pressure increase observed in a sand-shale series in South Louisiana. Our previous examples had a temperature increase with an increase in pressure. This

example shows a temperature decrease with an increase in pressure. Why? Refer to the discussion for a possible explanation of this.

Figure 13 is from a well that penetrates very limy tight sands and shales to approximately 10,000 feet and dense limestone from 10,000 to 15,000 feet where a porous limestone with high pressure was drilled. The mud weight increased from 10.5 to 17.5 when the porous zone was penetrated, indicating a sudden increase in pressure. This area has one of the highest temperature gradients for normal pressure (to 15,000 feet) observed in this study. As the pressure increases above normal, there is a corresponding increase in temperature above the normal gradient for that area.

Figure 14 is a plot of pressure from tests (vertical scale, 1" = 2,000 lbs.) and temperature (horizontal scale, 1" = 40°F). In wells not in association with salt domes, the points plot almost exactly on the diagonal; or, for an increase of 50 lbs. in pressure, there is an increase of 1°F in temperature. Wells in association with a salt dome plot too hot on top of the salt and too cool down the flank of the dome just as Guyod (1944-1945) predicted. Wells in an old field plot in the low pressure range, implying that pressure is depleted much faster than the temperature can change. Super-pressured wells that are pressured by leakage up the fault plane from below also imply that the pressure changes in nature are much faster than the temperature changes if the pressure changes are induced by faulting or by production.

Figure 15 is a chart that may be used to approximate formation pressure from its temperature by using the apparent linear relationship of temperature and pressure from Figure 14.

Discussion

High pressure has been found in almost all parts of the world where wells have been drilled in the search for oil and/or gas. It occurs most often in geologically young rocks, in sand-shale sequences such as found in South Louisiana. High pressure is sometimes found in the intermediate age rocks if porous zones are sealed in or between limy sands and/or shales, where the cement forms very fast and early (Newman 1968, Dowlen 1968 and Runnels 1969), such as the massive Frio sands shown in Figures 9 and 10. High pressure is frequently found in association with older rocks such as limestone, anhydrite, marl and/or salt because they are ideally impermeable to begin with (Hubbert and Ruby 1959,

pp. 151-52). Sometimes pressure is trapped in older sands because the weight of the overburden has reduced the original porosity (Atwater 1965 and Thompson 1959) and the silica thus released reforms as cement to trap pressure.

It is proposed that there are two separate and distinct methods of sealing high pressure. Type one is low resistivity shales or clays (Figures 4 and 5). Type two is highly cemented sands, shales, limestones, anhydrites, and/or evaporites (Figures 10 and 13); a combination of the two types (Figures 3 and 9). It is also proposed that type one occurs in the geologically young rocks and that at some point in time it begins to lose its effectiveness and then type two begins to become effective. There are some overlapping of types in the zone of change and in the exceptional case the two types are reversed as shown by the examples in Figures 3 and 9.

A theory of why pressure is sealed by low resistivity type sediments is proposed. Type one is a mixture of clay types along with varying amounts of other fine-grained material (Figures 10 and 13). Therefore, its efficiency as a pressure sealing trap should vary greatly. Some of the reasons for these variations are shown on Table 1 in particular: (1) size range, (2) surface area range, (3) relative resistivity range, (4) layers of bound (adsorbed) water, (5) viscosity of bound water, (6) density of bound water, (7) relative permeability and (8) relative plasticity. It is apparent from the above that "shale" is a complicated mixture that is highly variable, and is not to be overlooked if we wish to understand what is happening in the subsurface. The grain-size of a rock may decrease without appreciably changing the porosity but as the grain size decreases, the pore size between the grains decreases appreciably. When the grain size decreases, there is a drastic increase in surface area. Note in Table 1 the tremendous difference in the surface area of one gram of kaolinite (approximately 50 sq. m.) and montmorillonite (from 700 to 800 sq. m. and more). Also, Hubbert and Rudy (1959, p. 178) quote Archie, "an increase in porosity of about 3% produces a tenfold increase in permeability." The reverse of this is also true--that is, a decrease in porosity produces a drastic decrease in permeability. In discussing the rate of flow of water across shales buried in the depth range of 3,880 to 13,080 feet, Hubbert and Rudy (1959, p. 179) estimate the rate of flow to be about 7.0, 0.8 and 0.2 x 10⁻⁴ cm³/cm²/yr. from the top, middle and bottom of the interval. The above estimates were made using the viscosity of normal water in the calculations.

Water in association with shales, and clays within the shales, may not have the same properties as normal water. Grimm (1962) says that "apparently adsorbed water on clays

is up to several hundred times more viscous than normal water and at times appears ice-like." The presence of this peculiar water has been known for several years. Recently, Derjaguin (1962) and Dresner (1969) have obtained enough of this "thick" water or "polywater" to analyze in the laboratory. This peculiar water, formed in quartz capillaries, has a viscosity approximately fifteen times that of normal water and a density of 1.4 gr/cc. and yet, it was still pure water and nothing else. Dresner (1969, p. 70) says "the existence of polywater in clay might also explain the plastic quality of that material--it's been supposed that polywater may in fact be the more 'natural' form of water, . . ."

Shales contain varying amounts of very fine quartz grains, so we may expect this form of water to be present. This is the water formed or adsorbed on to quartz. Are there other forms of "peculiar" water formed by the other minerals in shales? It is possible.

Now if we recalculate the flow rates through shales as Ruby did, but this time use the viscosity of polywater, we begin to understand why and how these low resistivity, fine-grained, shales or clays seal or trap pressure.

It is suggested that the efficiency of the adsorbed, polywater seal increases with depth of burial and decreases when the temperature increases above a critical value. Powers (1967, p. 1241) cites Burst and others and suggests that as montmorillonite is converted to illite in the subsurface, part of the adsorbed water is desorbed and returns to normal water, and that the conversion is dependent on depth of burial and/or temperature. If this is the case, the desorbed water would revert to its original lower viscosity and again begin to migrate, thus lowering the pressure. Also, when the layers of molecular water decrease to a critical number, the rock is no longer plastic, but becomes a competent rock (Grimm 1962). When this happens, any distortion or movement caused by compaction or by tectonic activity will cause the rock to crack, or break, thus opening "other" flow channels for water to escape, further reducing the trapped pressure.

There is evidence (Grimm 1962, Lang 1967) that the rigidity and therefore the viscosity of the adsorbed water on montmorillonite decreases away from the clay grain. The effect of pressure with depth of burial would be (Lang 1967, p. 468) "to alter the size and strength of hydration envelopes surrounding the clay particles and therefore alter the reservoir permeability."

The start of the water desorption, or as Powers (1967) and Burst (1969) suggest, the start of the conversion of

montmorillonite to illite would be the end of type one seal and the beginning of type two.

If the escaping or migrating water moves out of a sand and through a shale, the shale may become cemented or mineralized as seen in the 15,000 to 16,000 foot zone in Figure 3. If the escaping water moves into or through a sand, the sand may lose porosity and permeability from the formation of cement as shown by the example in Figure 9.

Is this the reason high pressure is seldom found in the intermediate age rocks? Type one seal loses its efficiency because the adsorbed water is being desorbed and type two seal has not yet become effective because cement has not formed in quantities large enough to destroy the permeability of the rock. This would be the reason for an overlapping of the two types. There are exceptions to be sure, but this appears to be the rule.

The highest pressure observed in type one environments has a gradient range of 0.7 to 0.8, whereas pressures trapped by type two seals approach 1.0. Hubbert and Ruby (1959, pp. 155-56) state, "in the Guam Field, Iran, pressure gradients range from 0.9 to 1.0 in 10 of the 15 wells that penetrated the Farris formation sealed by or occurring between marls, limes, anhydrite or salt." This implies that type two seals are more effective and that their effectiveness is not destroyed by high temperature as implied by Powers (1967) and Burst (1969).

A high pressure zone must be sealed in all directions or the pressure would "leak-off" to its normal gradient for that environment. This implies that the sealing rock has very little, if any, permeability. It has been observed in this study that as the permeability decreases to form a seal, the temperature increases or is higher than the 1° per 100 foot gradient for that depth for both type one and type two seals, whereas logs show a decrease in resistivity and a decrease in sonic velocity for type one seals and an increase in resistivity and sonic velocity for type two seals. Logs have not been too useful in locating type two seals because there are many "other" factors that may increase the apparent resistivity and sonic velocity besides the reduction or loss of permeability.

It has been observed that if the shale resistivity decreases significantly below the 0.1 ohm increase per 1000 feet normal gradient for South Louisiana, pressure will be trapped by type one seals. If the shale resistivity increases significantly above the 0.1 ohm per 1000 foot gradient, pressure, if any, will be trapped by type two seals; and for a normal rate of increase, there probably will be no high pressure.

In trying to estimate the pressure sealing capacity of the "cap" in gas storage reservoirs, Thomas et al., 1968, p. 181, says "threshold displacement pressures for low permeability samples of porous media can be predicted if their permeability, porosity and formation resistivity factors are known, . . . threshold pressure is not a function of time . . ." (and p. 177) ". . . the lower the permeability of the core, the larger the pressure increment." This implies that the lower the porosity and/or permeability, the higher the formation resistivity factor and the better the seal becomes. This is the response of type two seals, but as stated before, logs are not too reliable in predicting the occurrence of high pressure in type two environments. In type one environments, logs respond opposite to what the above implies. What then causes the abnormal log response in type one environments? Is it because the shales in a type one environment have higher porosities?

Johnston (1965, p. 719) says "if a given lithology such as a shale is investigated, the acoustic log response will be essentially a response to porosity variations," whereas, Overton (1969, p. 3) in discussing log response from shaly zones says "in shaly sands, the water salinity is lower as seen by the SP curve, since dispersed clay has the ability to bind both water and ions onto its surface. This water is still conductive, however, and causes the solid to conduct."

Table 1 shows that there is a difference in shale resistivities, probably from variations in surface area and/or in variations in the quality of the adsorbed water. Lang (1967, p. 462) found that when pressure up to 7000 lbs. is applied to clay-water mixture, kaolinite shows a very small decrease in resistivity; however, when the same pressure is applied to a bentonitic clay-water mixture, there is a significant decrease in resistivity and the decrease is not linear but is in steps and he says (p. 461) "It therefore seems logical to attribute the abnormally large pressure influence on resistivity in the lower portion of the curve to a pressure-induced breakdown of a viscous and more highly ordered adsorbed water." In discussing the effect that temperature has on this resistivity decrease (p. 463), he says ". . . the structural characteristics of the adsorbed water diminishes with an increase in temperature and, therefore, became less susceptible to pressure breakdown."

It is proposed that the low-resistivity, low sonic-velocity shales in association with high pressured zones is the result of the above and is not because these shales have a higher porosity as assumed by Johnson (1965, p. 719). Let's examine a section of a log from a medium-high pressure zone and notice how the curves respond (Fig. 17). This

example shows a slightly shaly sand zone from 10,930 to 10,985 feet and a shale zone from 10,985 to 11,100 feet. In addition to the induction-electrical log curves, a computer-derived continuous porosity curve made from the sonic log (dotted curve) and the density log (dashed curve) is traced on the example in the conductivity track. All scales are included for reference.

In the sands at 10,930, 10,935, 10,947, and 10,959 feet, note that there is good agreement between the two porosities. The difference of from 2 to 5 porosity per cent is probably due to varying amounts of dispersed shale in the sand. Now refer to the shale from 11,000 to 11,066 feet and note the difference in porosity from the two logs. Porosity from the density log varies from approximately 20 to 22 per cent over the interval. This porosity is approximately what we would expect from this depth. But the sonic log porosity ranges from 40 to 43 per cent in the same zone. The sonic log's "apparent" porosity is approximately 100 per cent higher, but is it measuring porosity or is it measuring or "seeing" the peculiar nature of the adsorbed water in association with the fine-grained, low resistivity shale discussed above?

Compare the changes in resistivity, conductivity and porosity from the sonic log in the interval 10,985 to 11,100 feet and note that they are almost a duplicate of each other. It has been shown above that a decrease in grain size with its greatly increased surface area decreases the resistivity. Also, when pressure is applied, the resistivity decreases further. The log section above shows this to be true. Now if the apparent porosity from the sonic log follows this trend, is it not reasonable to assume that it also is being affected by these changes instead of porosity? The density log indicates that there is little, if any, porosity change in the zone; therefore, it is postulated that the changes observed in the other logs are from a change in grain size, surface area, and to a change in the quality of the adsorbed water and not from porosity changes.

In discussing subsurface pressure and ground-water migration, Hubbert and Ruby (1959, pp. 151-52) say, "the rate of flow of water does not depend upon the magnitude of the anomalous pressure, but upon its gradient or rate of change with distance. . . . Then, unless the rocks are ideally impermeable, it follows that away from any region of greater than normal pressure, the water must be flowing and must continue to do so until the excess pressure is dissipated." In discussing normal pressure (p. 169), they say ". . . the fact that the pressure varies with depth in a manner approximating closely that of hydrostatics implies in this case also the existence, in spite of the very low

permeability of some strata, or an adequate freedom of hydraulic communication in the vertical direction over the long time intervals involved. . . ." We may infer from the above that the rate of pressure change with distance is an indication of the rate of water flow or migration.

It has been shown, by the examples from South Louisiana, that the rate of temperature change with depth may be used to infer the rate of pressure change; therefore, the rate of temperature change may also be used to indicate the relative rate of water flow or migration in the subsurface as stated by Hubbert and Ruby above. This is what we would expect in an environment of type one seals.

There are several factors that may alter the temperature distribution in the subsurface; however, only two will be discussed because of the large effect these two may have upon the temperature distribution. The two variables are (1) the amount of water made available by the conversion of montmorillonite to illite, and (2) the effect that this desorbed water has on temperature when it migrates out of the zone.

Power (1967, p. 1249) says ". . . it was said earlier that interlayer water, especially the last four layers, has a considerably higher density than ordinary water. Therefore, the water must increase in volume as it is desorbed from the montmorillonite." He further states "If 1.4 gm/cc. is used as the average density of the last four layers of water, the volume increase of the water upon transfer is forty per cent. . . ." In discussing the desorption of water from montmorillonite by heat, Burst (1969, p. 80) says "When the heat accumulation is sufficient to mobilize the interlayer of water, one of the two remaining layers is discharged into the bulk system. The amount of water in movement should constitute ten to fifteen per cent of the compacted bulk volume. . . ."

The above would represent a significant volume of water that has reverted to its original viscosity and now is free to move. Also, since its volume increases approximately forty per cent when it is desorbed, it should be cooled by a like amount; therefore, this cooler water would tend to cool the rock it comes out of and the rock it moves through.

In discussing the role of migrating ground water in altering the temperature distribution in the subsurface, Schneider (1964, p. 209) states, "A logical hypothesis is that, owing to the circulation of ground water, the vertical temperature gradient in aquifer systems should be lower than the average regional geothermal gradient, which is generally

determined for some depth in the earth's crust where fluid circulation is negligible. Under certain circumstances, the temperature distribution may be used to interpret some of the essential flow characteristics of the aquifer." On page 210, he quotes Olmsted, "The vertical temperature gradient is steeper in rocks of low permeability than in highly permeable rocks, and the areal pattern of temperature distribution can be explained in part by differences in the rate of ground water flow." Again, Schneider (1966, p. 192) says ". . . 'hot' regions delineate discharge areas where there is a significant upward flow component. . . . 'cold' regions or heat sinks generally coincide with areas of lowest geothermal gradients, and areas where significant recharge occurs. . . ." The flow is from higher (hot) or toward the lower (cold) temperature.

Hot zones or cool zones in the earth's crust, then, would be controlled by circulating ground water just as circulating water in the cooling system controls the temperature in an internal combustion engine. A restriction of flow in any part of the engine causes the temperature to increase in that part, but not necessarily in all parts where adequate circulation still is being maintained. Also, excess circulation in one part will cause that part to be too cool. Uniform circulation would maintain a uniform temperature distribution in all parts of the engine. Differences in the thermal conductivity of the various parts of the engine and in its cooling system would have very little effect on the temperature distribution of the system; however, the rate of flow would be the most important variable.

It is proposed that the temperature distribution in the earth's crust is modified more by ground water movement than by differences in thermal conductivity. The vertical temperature profile, then, is an approximate measure of the permeability distribution or water flow distribution in the earth's crust.

The examples presented show that (1) ideally impermeable rocks, such as limestone, anhydrite and highly cemented sands are the hottest (Figs. 10 and 13); (2) ideally impermeable rocks that contain porous zones (Figs. 10, 11, and 12) show the temperature in the porous zone is dependent upon its pressure; (3) in rocks with good permeability both vertically and laterally (Figs. 4, 5, and 8), the temperature profile is essentially equal to the straight line gradient of 10°F increase per 100 feet of depth and increases at a greater rate as the pressure increases; and (4) the temperature may decrease below the normal gradient as in Figure 5 because of a lateral heat migration as shown by Figure 2 or by lateral water migration, Figure 12, or by cooling from an increase in volume of water as it is desorbed (Powers, 1962, p. 1245) in the change of montmorillonite to illite.

The moderate cooling for the porous zones in Figure 12 implies moderate permeability, and therefore, moderate water movement and moderate pressure. These two cooler zones in a thick, ideally impermeable zone also imply that any water migration must be lateral migration. The degree of cooling in this environment would be controlled by the volume of water moved and time as well as pressure.

The drastic reversal shown in the temperature profile in Figure 11 from 11,000 to 12,200 feet implies that this zone has very good permeability and that much water has moved through this zone and that very little has moved through the hot anhydrite zone from 9,000 to 11,000 feet. The cold zone also implies that cooler waters from above are moving through this zone. For this to happen, the pressure must be below normal and the water moving laterally. Lost circulation is quite a problem when drilling for oil or gas in Florida. The writer has seen wells that had fluid pressure at depths much lower than the 0.433 gradient because the hole could not be filled with fresh water. The fluid level would be several hundred feet below the surface, indicating subnormal pressure just as the temperature profile implies.

In the Gulf Coast study, it was observed that abnormal pressures were accompanied by abnormal temperature. Management decided to find out if circulating (flowing) mud temperature changes would show the top of the temperature-pressure zone. In January 1968, equipment was installed on SO&G Well No. 12 in Eugene Island Black 175 Field, Offshore South Louisiana. At the time the test was started, the well had been drilled to 9844' and protected pipes had been set. The high pressure zone had already been entered since a mud weight of 16.1 lb. was required. The rate of penetration (drilling time) was limited to 10 to 15 feet per hour by alternately drilling and then circulating. The mud weight had to be raised to 17.6 lb. at a total depth of 10,700', indicating a further increase in pressure. One hundred and fifty-six hours were required to drill this 656 foot interval but only 39 hours were drilling and 117 hours were circulating time. The results of this test were not too conclusive and no further tests were made.

The maximum temperature for log runs show an increase from 148° at 9505 feet to 182° at 10,200 feet or a rate of increase of approximately 4.8° per hundred feet which clearly implies a significant pressure increase.

It is suggested that changes observed in the mud flow-line temperature may indicate the top of the temperature-pressure zone if the measurements are started far enough above the pressure zone to establish the normal gradient.

Conclusions

An increase in temperature above normal indicates an increase in pressure above normal in the young, low resistivity sand and shale sequences such as are found in South Louisiana.

The average rate of temperature increase for normal pressured zones in this area is 1°F for each hundred feet of depth. An increase of 1°F above normal indicates a pressure increase of fifty pounds pressure above normal.

In older rocks outside South Louisiana that consist of high resistivity shales and highly cemented sands, the rate of temperature increase is greater than 1° per 100 feet of depth, but the same rule applies. An increase in temperature above the normal gradient for that area is an indication of pressure above normal; however, an estimation of its magnitude is not as accurate as in South Louisiana.

In ideally impermeable rocks such as limestone, anhydrite, marl and evaporites, temperature gradients are the highest and pressure trapped in porous zones within these rocks tend to have higher gradients, often approaching a gradient of 1.0 pound/foot of depth. Here, again, the temperature profile tends to follow the pressure, but with less reliability. It also usually shows a larger rate of change for a pressure change than the other rocks. In normal pressured porous zones in these older rocks, the temperature decreases toward the normal gradient and may decrease below normal if pressures are below normal as has been observed in some of our examples.

REFERENCES

- Atwater, G. I. and Miller, E. E. (1965). The effect of decrease in porosity with depth on future development of oil and gas reserves in South Louisiana: AAPG, V. 49, 1965, p. 334.
- Baillie, A. D. and Vecsey, G. E. (1968). Hydrothermal trends, Harbor BC gas fields: Oil Week, V. 18, No. 52, p. 10.
- Bredhoeft, J. D. and Hanshaw, B. B. (1968). On the maintenance of anomalous fluid pressures: Geol. Soc. Amer. Bull., V. 79, pp. 1097-1122.
- Burst, John F. (1969). Diagenesis of Gulf Coast clayey sediments and its possible relation to petroleum migration: Amer. Assn. Petroleum Geologists Bull., V. 53, No. 1, pp. 73-93.
- Chillingar, George V. and Knight, Larry (1960). Relationship between pressure and moisture content of kaolinite, illite, and montmorillonite clays: Amer. Assn. Petroleum Geologists Bull., V. 44, No. 1, pp. 101-106.
- Derjaguin, Dr. Boris V. (1962). Thick water: Industrial Research, Nov. 1962, p. 29.
- Dowlan, Stuart (1968). The profit takers--scale and corrosion: Baroid News Bull., V. 19, No. 3, pp. 11-14.
- Dresner, Simon (1969). Polywater: Popular Science, V. 195, No. 1, p. 68.
- Drost-Hansen, Walter (1966). The puzzle of water: International Science and Technology, Oct. 1966, pp. 86-96.
- Engelhardt, Wolf V. and Gaida, Karl H. (1963). Concentration changes of pore solutions during the compaction of clay sediments: Jour. Sed. Petrology, V. 33, No. 4, pp. 919-930.
- Fertl, Walter H. and Timko, Donald J. (1970). Occurrence and significance of abnormal pressure formations: Oil and Gas Journal, Jan 5, 1970.

- Frank, Robert C. (1965). Gases-in-solids: Modern Science and Technology, pp. 89-97, D. Van Nostrand Company, Inc., Princeton, N. J., Toronto, New York, and London.
- Gann, Donald P. (1965). Changes in ionic concentrations of effluent from compaction of clays: MS Thesis, University of Houston, August 1965, 96 pp.
- Goldring, L. S. (1964). Selectivity in the electrical transport of ions across ION-exchange membranes: Amer. Chem. Soc. Mtg., Denver, Jan. 19-24, 1964, Abstr., pp. 190-200.
- Graff-Petersen, P. (1967). Interformational deformations and pore-water hydrodynamics: 7th Internat'l. Sedimentological Cong., Reading University, Aug. 10-12, Edinburgh University, Aug. 14-16, 1967.
- Gretener, P. E. (1969). Fluid pressure in porous media--its importance in geology, a review: Canadian Geology Bull., V. 17, No. 3, pp. 255-295.
- Gretener, P. E. and Labute, G. J. (1969). Compaction--a discussion: Canadian Geology Bull., V. 17, No. 3, pp. 296-303.
- Griffin, George M. and Blairs, Parrott (1964). Development of clay mineral zones during deltaic migration: Amer. Assn. Petroleum Geologists Bull., V. 48, No. 1, pp. 57-69.
- Grim, Ralph E. (1962). Applied clay mineralogy: McGraw-Hill, New York, London and Toronto.
- Guyod, Hubert (1944). Temperature well logging (a booklet): Well Log Consultant, Houston, Texas.
- Guyod, Hubert (1945). Caliper well logging (a booklet): Well Log Consultant, Houston, Texas.
- Heald, M. T. and Renton, J. J. (1966). Experimental study of sandstone cementation: Jour. Sedimentary Pet., V. 36, No. 4, pp. 977-991.
- Hecht, A. M. M. Dupont and Ducros, P. (1966). Study of the transport phenomena of adsorbed water in certain clay minerals by nuclear magnetic resonance: SOC Bull., Franc, Mineral Cristallog., V. 89, No. 1, pp. 6-13.
- Holden, W. R. and Caudle, B. H. (1967). Permeability micro-stratification in natural sandstones: 42nd Ann. Fall Mtg., SPE of AIME, Preprint No. Spec. 1819, 12 pp.

- Hottman, C. E. and Johnson, R. K. (1965). Estimation of formation pressure from log derived shale properties: JPT, June 1965, pp. 717-722.
- Hubbert, M. King and Ruby, William W. (1959). Role of fluid pressure in mechanics of overthrust faulting: Geol. Soc. Amer. Bull., V. 70, pp. 115-206.
- Hutt, Jeremy R. and Dekg, Joseph W., Jr. (1968). Thermal and electrical conductivities of sandstone rocks and ocean sediments: Geophysics, V. 38, No. 3, June 1968, pp. 489-500.
- Jones, Paul H. (1969). Hydrodynamics of geopressure in the northern Gulf of Mexico basin: Jour. Petroleum Technology, July 1969, pp. 803-810.
- Kalish, P. J., Stewart, J. A., Rogers, W. F., and Bennett, E. O. (1964). The effect of bacteria on sandstone permeability: Jour. Petroleum Technology, July 1964, pp. 805-814.
- Katchalsky, Aharon (1965). Nonequilibrium thermodynamics: Modern Science and Technology, D. Van Nostrand Company, Inc., Princeton, J. J., Toronto, New York and London, pp. 195-201.
- Kaye, Brian (1965). Sizing solid particles: Modern Science and Technology, D. Van Nostrand Company, Inc., Princeton, N. J., Toronto, New York and London, pp. 341-349.
- Kemper, W. D. and Rollins, J. B. (1966). Osmotic efficiency coefficients across compacted clays: Soil Sci., Soc. Amer. Proc., V. 30, No. 5, pp. 529-534.
- Labute, G. J. and Gretener, P. E. (1969). Differential compaction around a Leduc reef--Wizard Lake area, Alberta: Canadian Geology Bull., V. 17, No. 3, pp. 304-325.
- Land, Carlton S. and Baptist, Oren C., (1965). Effect of hydration of montmorillonite on the permeability to gas of water-sensitive reservoir rocks: Jour. Petroleum Technology, Oct. 1965, pp. 1213-1218.
- Lang, W. J. (1967). The influence of pressure on the electrical resistivity of clay-water systems: Proc. 15th Clay and Clay Minerals Conf., Pittsburg, Pa., Oct. 10-13, 1966.
- Maxwell, John C. (1964). Influence of depth, temperature, and Geologic age on porosity of quartzose sandstone: AAPG, V. 48, No. 5, May 1964, pp. 697-704.

- McCrossan, R. G. (1961). Resistivity mapping and petrophysical study of upper Devonian inter-reef calcareous shales of central Alberta, Canada: Amer. Assn. Petroleum Geologists Bull., V. 45, No. 4, pp. 441-470.
- Meade, Robert H. (1966). Factors influencing the early stages of the compaction of clays and sands-review: Jour. Sedimentary Pet., V. 26, No. 4, pp. 1085-1101.
- Milne, I. H. and Early, J. W. (1958). Effect of source and environment on clay minerals: Amer. Assn. Petroleum Geologists Bull., V. 42, No. 2, pp. 328-338.
- Milne, I. H. et al. (1962). Permeability and salt filtering properties of compacted clay: Proc. 11th Clay Minerals Conf., Ottawa, Canada, Mutual Press Ltd.
- Milne, I. H., McKelvey, J. G., and Trump, R. P. (1964). Semi-permeability of bentonite membranes to brines: Amer. Assn. Petroleum Geologists Bull., V. 48, No. 1, pp. 103-105.
- Morgan, James P. and Anderson, Harold V. (1961). Genesis and paleontology of the Mississippi River mudlumps: Dept. Conservation, Louisiana Geological Survey, Baton Rouge, La., Bull. No. 35.
- Mungan, Necmettin (1965). Permeability reduction through changes in pH and salinity: Jour. Petroleum Technology, Dec. 1965, pp. 1449-1453.
- Myers, Robert L. and VanSiclen, Dewitt C. (1964). Dynamic phenomena of sediment compaction in Matagorda County, Texas: Trans. GCAGS Ann. Conv., Corpus Christi, Texas, Oct. 28-30, 1964, pp. 241-252.
- Newman, Harold (1968). Downhole scale control in South Texas: Baroid News Bull., V. 19, No. 3, pp. 30-34.
- Olodovskii, P. P. (1967). Density distribution of adsorbed water in dispersed media: INZH-FIZ ZH, V. 12, No. 4, pp. 496-501.
- Overton, Harold L. and Gupta, Yugal (1969). Shaly sand logging and ionic absorption: The Log Analyst, March-April 1969, pp. 3-6.
- Plummer, F. B. and Sargent, E. C. (1931). Underground waters and subsurface temperatures of the Woodbine Sand in northeast Texas: Univ. Texas Bull., No. 3138, Bureau of Econ. Geology.

- Runnels, Donald D. (1969). Diagenesis, chemical sediments and the mixing of natural waters: Jour. Sedimentary Petrology, V. 39, No. 3, pp. 1189-1201.
- Powers, Maurice C. (1967). Fluid release mechanism in compacting mudrocks and their importance in oil exploration: Amer. Assn. Petroleum Geologists Bull., V. 51, No. 7, pp. 1240-1254.
- Rickles, Robert N. and Friedlander, Henry Z. (1966). Membrane technology: Internat'l. Science and Technology, May 1966.
- Rochon, R. W. (1967). Relationship of mineral composition of shales to density: Trans. 17th Ann. Mtg. GCAGS, San Antonio, Texas, Oct. 25-27, 1967, pp. 135-142.
- Schneider, Robert (1964). Relation of temperature distribution to ground-water movement in carbonate rocks of central Israel: Geol. Soc. Amer. Bull., V. 75, pp. 209-216.
- Schneider, Robert (1966). Interpretation of the geothermal field associated with the carbonate-rock aquifer system of Florida, GSA Abstracts for 1966, Special Papers No. 101, pp. 191-192.
- Schoepfel, R. J. and Gilarranz, S. (1966). Use of oil well log temperatures to evaluate regional geothermal gradients: Jour. Petroleum Technology, June 1966, pp. 667-673.
- Selig, Franz and Wallick, George C. (1966). Temperature distribution in salt domes and surrounding sediments: Geophysics, V. 31, No. 2, pp. 346-361.
- Serruya, Collette, Picard, Leo, and Chilingarian, George V. (1967). Possible role of electrical currents and potentials during diagenesis (electrodiagenesis): Jour. Sedimentary Petrology, V. 37, No. 2, pp. 695-698.
- Shaw, Daniel B. and Weaver, Charles E. (1965). The mineralogical composition of shales: Jour. Sedimentary Petrology, V. 35, No. 1, pp. 213-222.
- Slaubaugh, W. H. and Stump, A. D. (1964). Surface area and porosity of marine sediments: Jour. Geophys. Res., V. 69, No. 22, pp. 4773-4778.
- Smith, George W. (1967). Liquid-like solids: Internat'l. Science and technology, January 1967, pp. 72-80.

- Thomas, L. K., Katz, D. L., and Tek, M. R. (1968). Threshold pressure phenomena in porous media: Soc. Petroleum Eng. Jour., June 1968, pp. 174-184.
- Thomson, Alan (1959). Pressure solution and porosity: SEPM Spec. Publ. 7, A Symposium, pp. 92-110.
- Tilson, Seymour (1965). Solids under pressure: Modern Science and Technology, pp. 69-80, D. Van Nostrand Company, Inc., Princeton, N. J., Toronto, New York, and London.
- Tragesser, A. F., Crawford, Paul B., and Crawford, Horace R. (1967). A method for calculating circulating temperatures: Jour. Petroleum Technology, Nov. 1967, pp. 1507-1512.
- Warner, Mont M. (1965). Cementation as a clue to structure, drainage patterns, permeability, and other factors: Jour. Sedimentary Petrology, V. 35, No. 4, pp. 797-804.
- Waxman, H. H. and Smiths, L. J. M. (1968). Electrical conductivities in oil bearing shaly sands: SPE Journal, June 1968, pp. 107-122.
- Weiler, R. A. (1967). Surface conductivity and dielectrical properties of montmorillonite gels: 16th Clay Minerals Conf., Denver Univ., August 28-31, 1967, Program, pp. 37-38.
- Winsauer, W. O. and McCardell, W. M. (1953). Ionic double-layer conductivity in reservoir rock: AIME Trans. (SPE), V. 198, pp. 129-134.
- Zierfuss, H. and van der Vliet, G. (1956). Laboratory measurements of heat conductivity of sedimentary rocks: AAPG, V. 40, No. 10, October 1956, pp. 2475-2488.

SOME OF THE VARIABLES IN SHALES
(from Published Material - Several Sources)

	KAOLINITE	ILLITE	MONTMORILLONITE
Relative Density Range	2.6 - 2.68 Avg. 2.63	2.7 - 3.0 Avg. 2.76	2.0 - 2.7 Avg. 2.2
Structure	Balanced 2 Layer Non-Expanding	Balanced 3 layer Non-Expanding	Un-Balanced 3 Layer Expanding
Particle Shape	Flakes	Flakes	Flakes
Particle Size Range	20 to 1 Micron 0.02 - 0.001 MM	20 to 1 Micron 0.02 - 0.001 MM	20 to 1 Millimicron or 1 Angstrom and less 0.02 - 0.000001 MM
Surface Area Range	50 - 58 M approx. per gram	A variable Approx. 50	700 - 800 square M per Gram and more
A sphere 1 MM in diameter filled with equal sized spheric particles 10^{-5} MM in size can contain approximately 10^{15} particles with a total surface area of more than 10^5 square MM.			
Relative Resistivity	1	0.6	0.16
Relative Water Adsorption	Slight	Moderate	Very large
Molecular Layers of Bound Water	1 to 3 (1 Layer = 2.9 Angstroms)	Approx. 3 8.7 Angstrom	From 3 to over 40 8.7 to 116 Angstroms +
Resistivity of Bound Water	Unknown, but should have a wide range.		
Dielectric Constant of Bound Water	Approx. 3	Approx. 3+	From 3 up to 80
Viscosity of Bound Water	Up to several hundred times Normal Water-- at times, appears ice-like.		
Density of Bound Water	Variable--ranging from 0.73 to 1.7 and more		
Acoustical Properties of Bound Water	Unknown, but should have a wide range.		
Swelling in Per Cent	5 - 60%	15 - 120%	Calcium 45 - 145% Sodium 1400 - 1600%
Relative Permeability	Large	Moderate	Very slight
Relative Plasticity	Slight	Moderate	Calcium - Large Sodium - Very large
Base Exchange Capacity Range	3 - 15	5 - 40	60 - 150

TABLE I

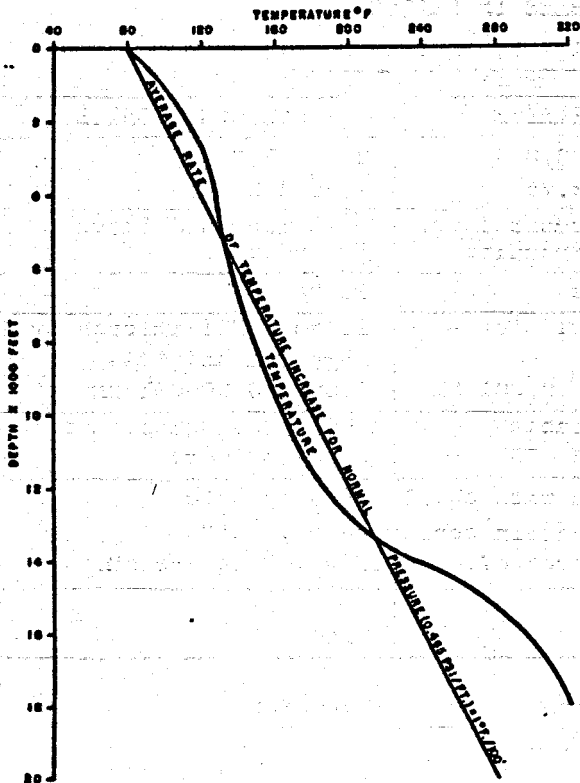


Fig. 1 - Approximate Average Vertical Temperature Profile for the Northwest Gulf of Mexico.

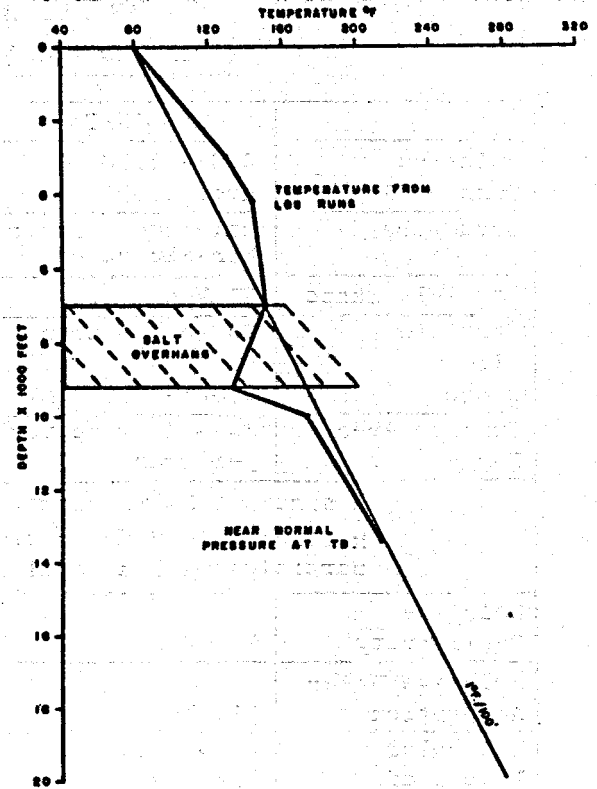


Fig. 2 - Temperature Profile Down-Flank of a Shallow Salt Dome South Timbalier Block SE, South Louisiana, Offshore.

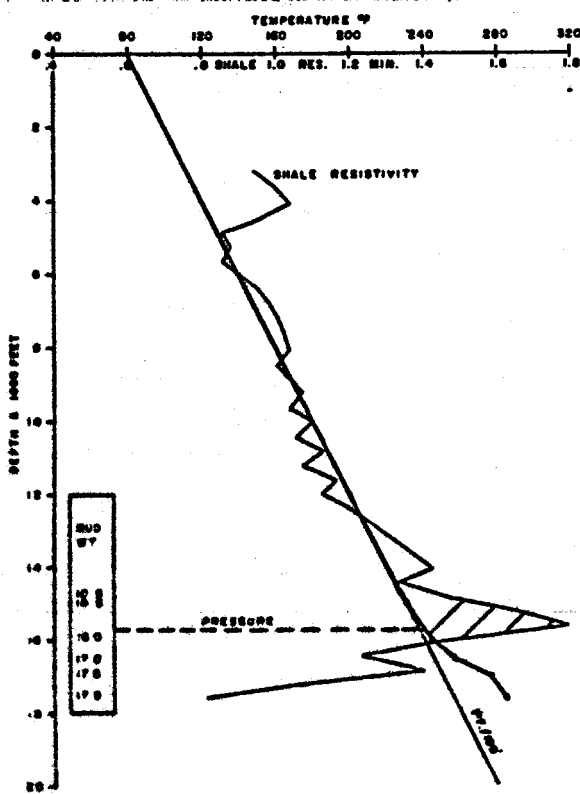


Fig. 3 - Shale Resistivity vs Temperature, Field Well, Vermilion Parish, Louisiana.

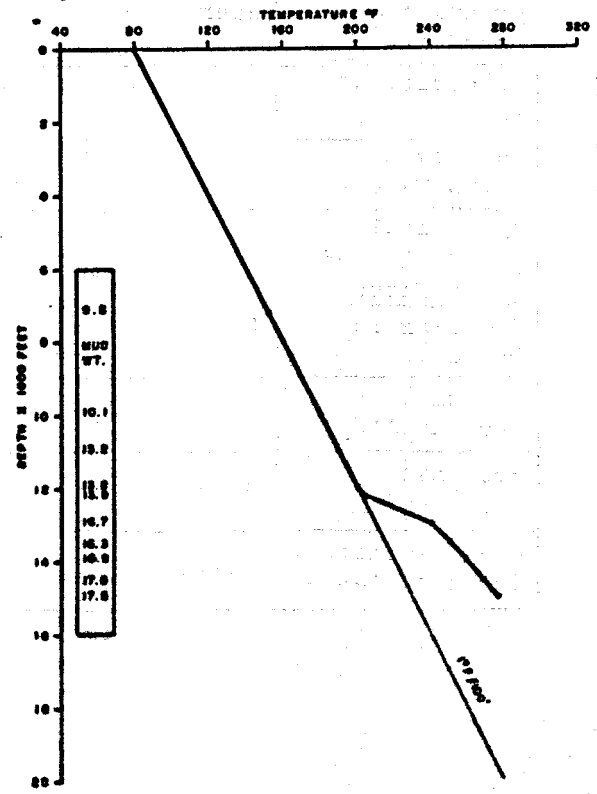


Fig. 4 - Wildcat, Calveston Co., Texas

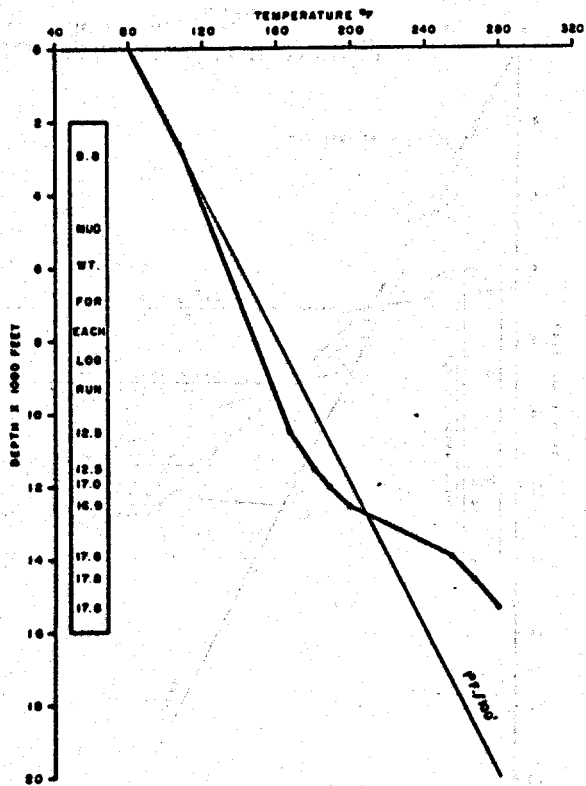


Fig. 5 - Abnormal Pressure, Lafayette Parish, Louisiana.

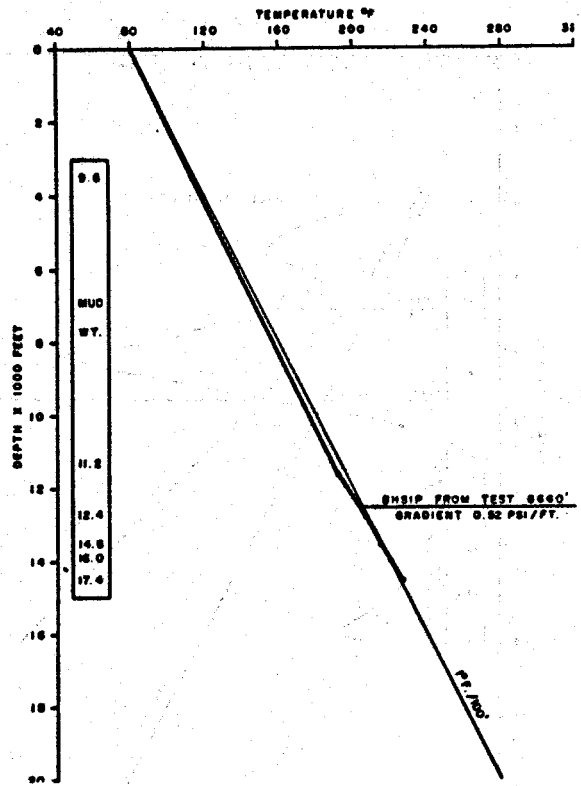


Fig. 6 - Mud Weight Too High, Vermilion Parish, Louisiana.

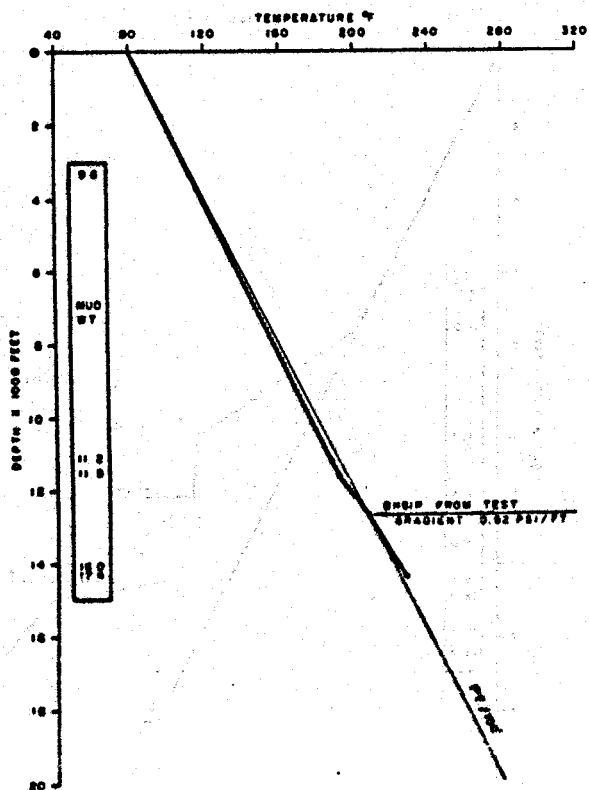


Fig. 7 - Field Well, Vermilion Parish, Louisiana.

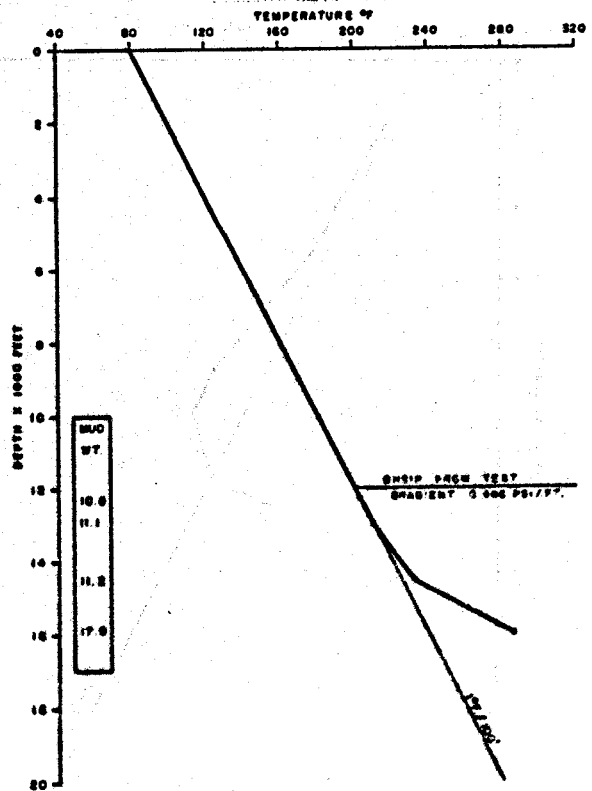
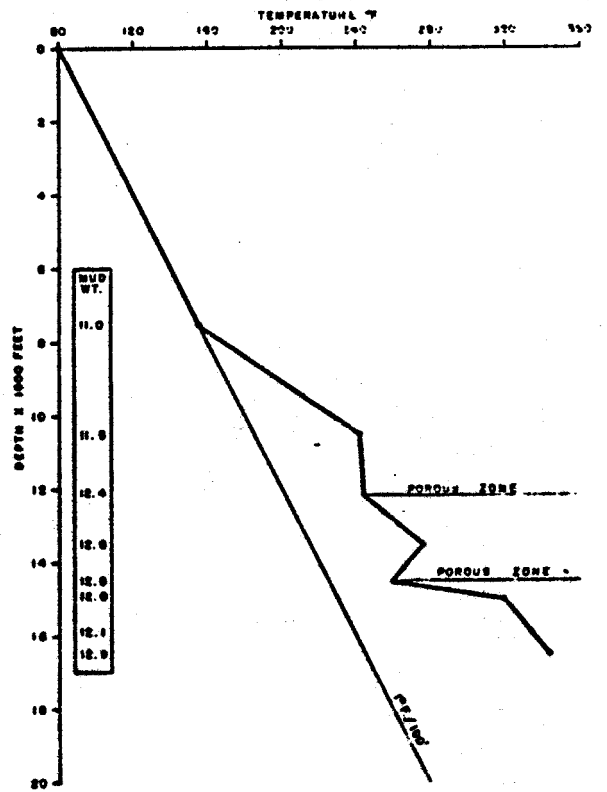
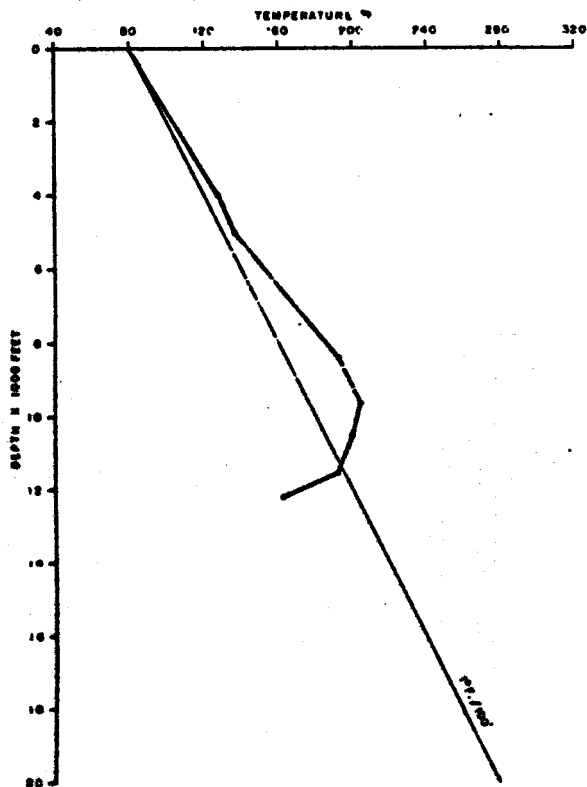
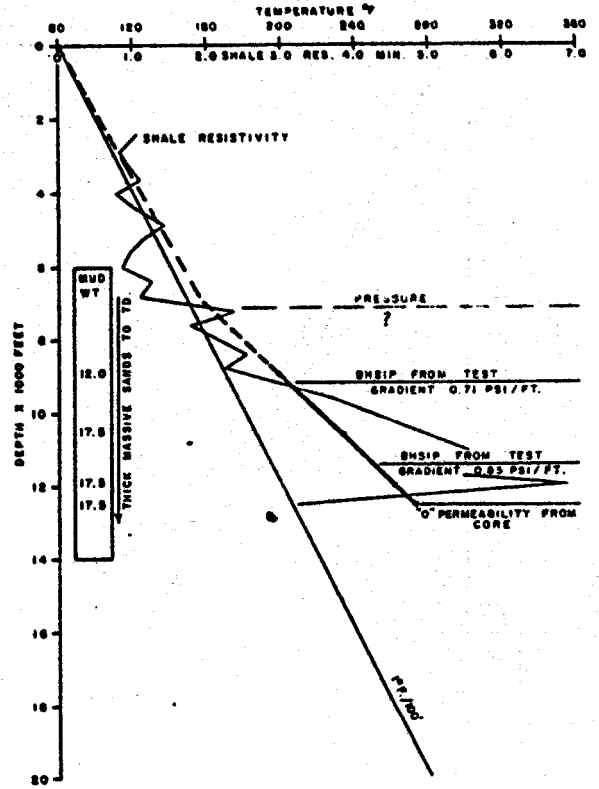
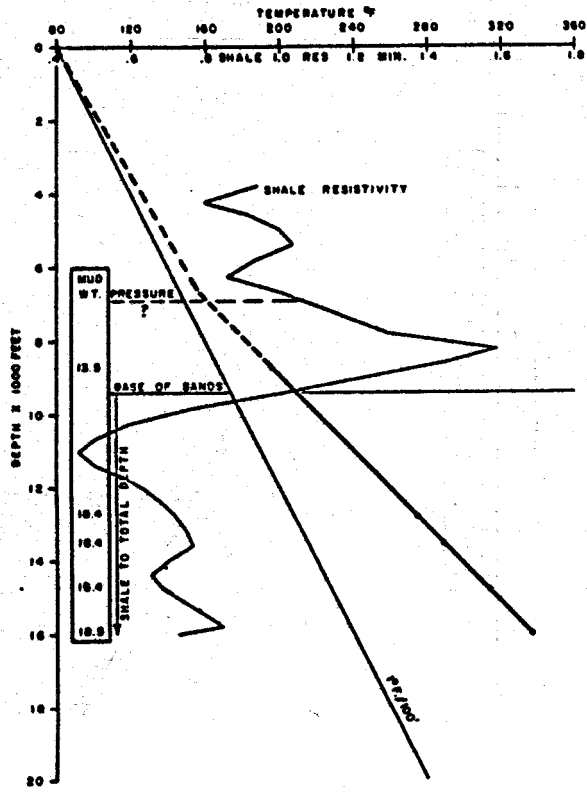


Fig. 8 - Changing Gradient Abnormal Pressure, St. Mary Parish, Louisiana.



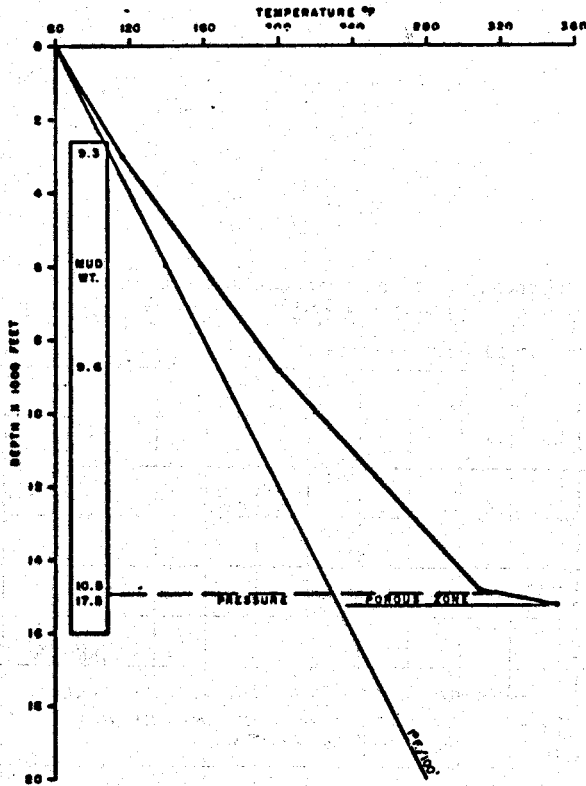


Fig. 13 - Pore Limestone High Pressure, Wildcat, Robertson Co., Texas.

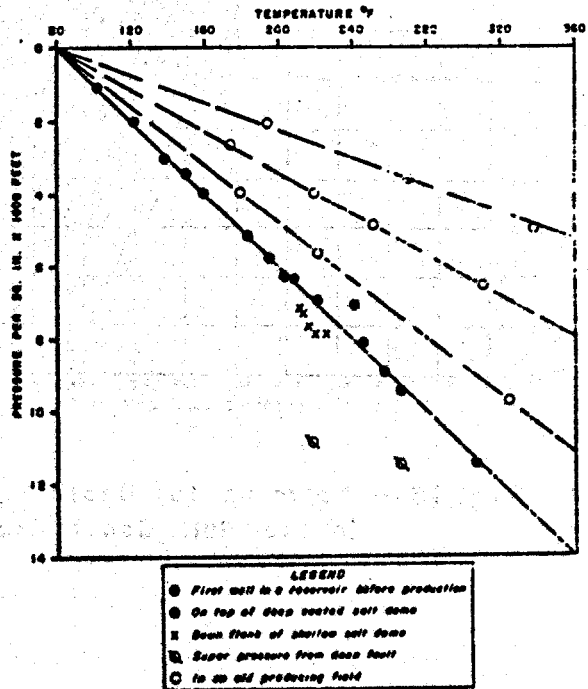


Fig. 14 - Approximate Temperature - Pressure Relationships for South Louisiana.

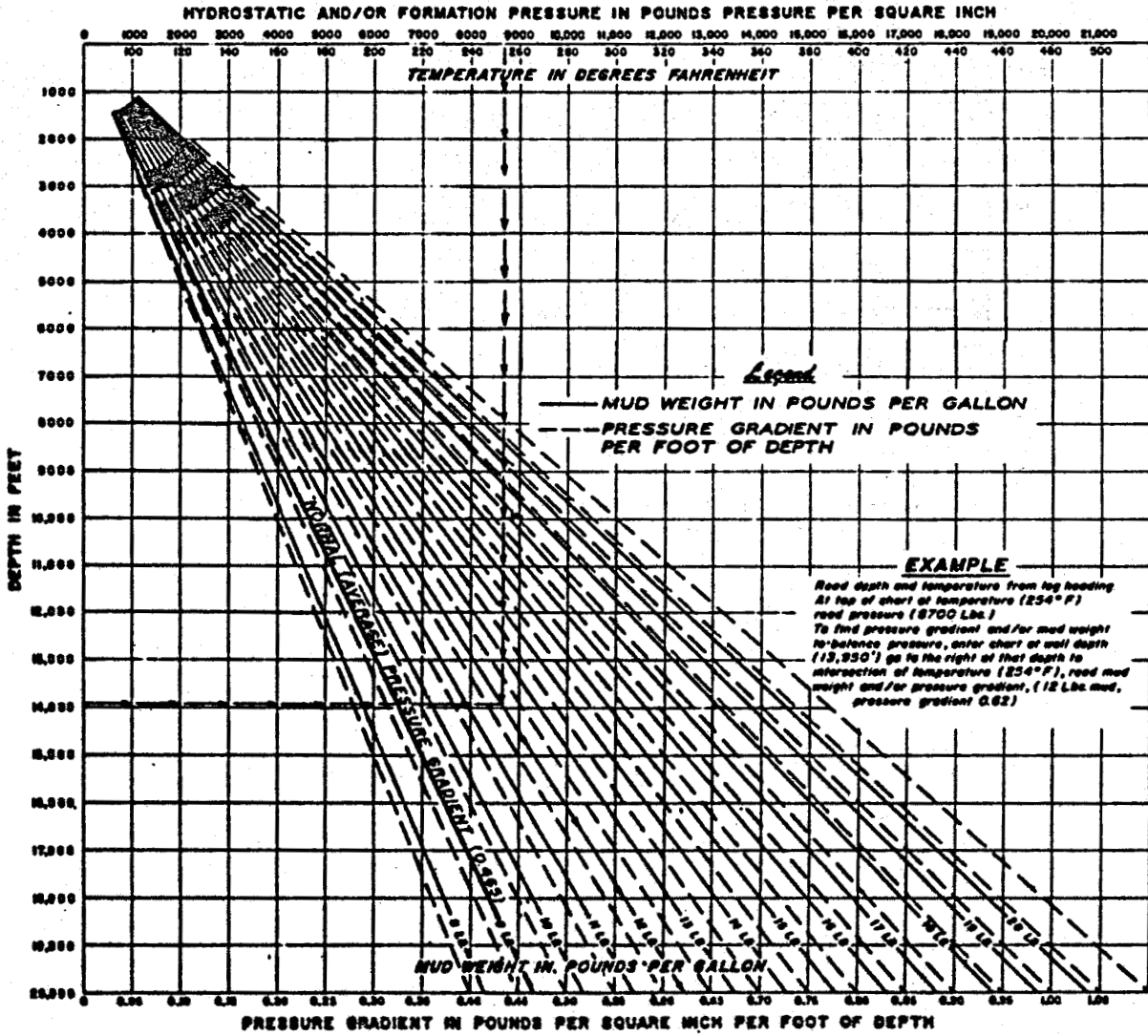


Fig. 15 - Approximate Depth - Pressure - Temperature Relationship in the Gulf Coast Geological Provinces.

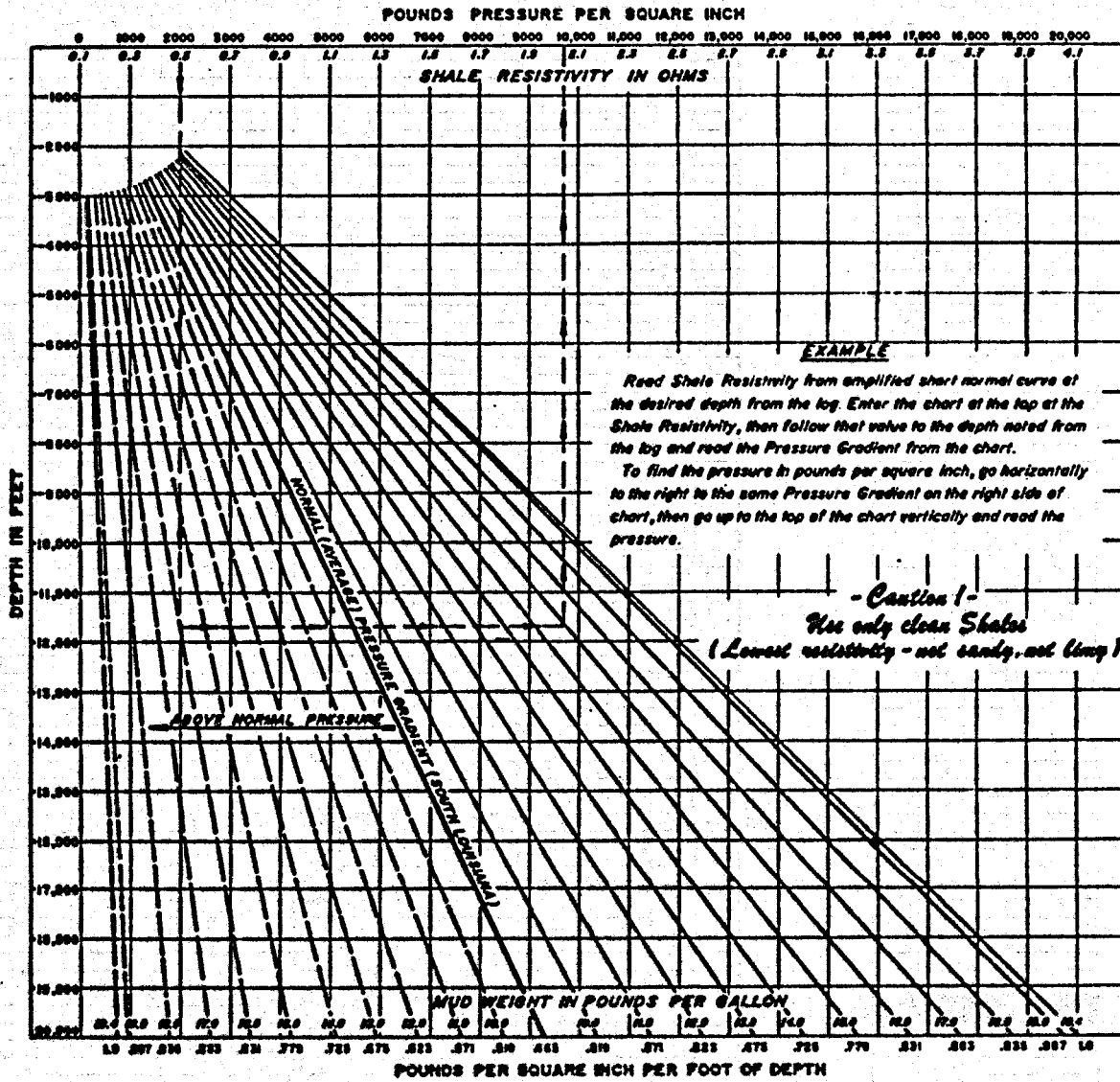


Fig. 16 - Approximate Formation Pressure from Resistivity Logs South Louisiana.

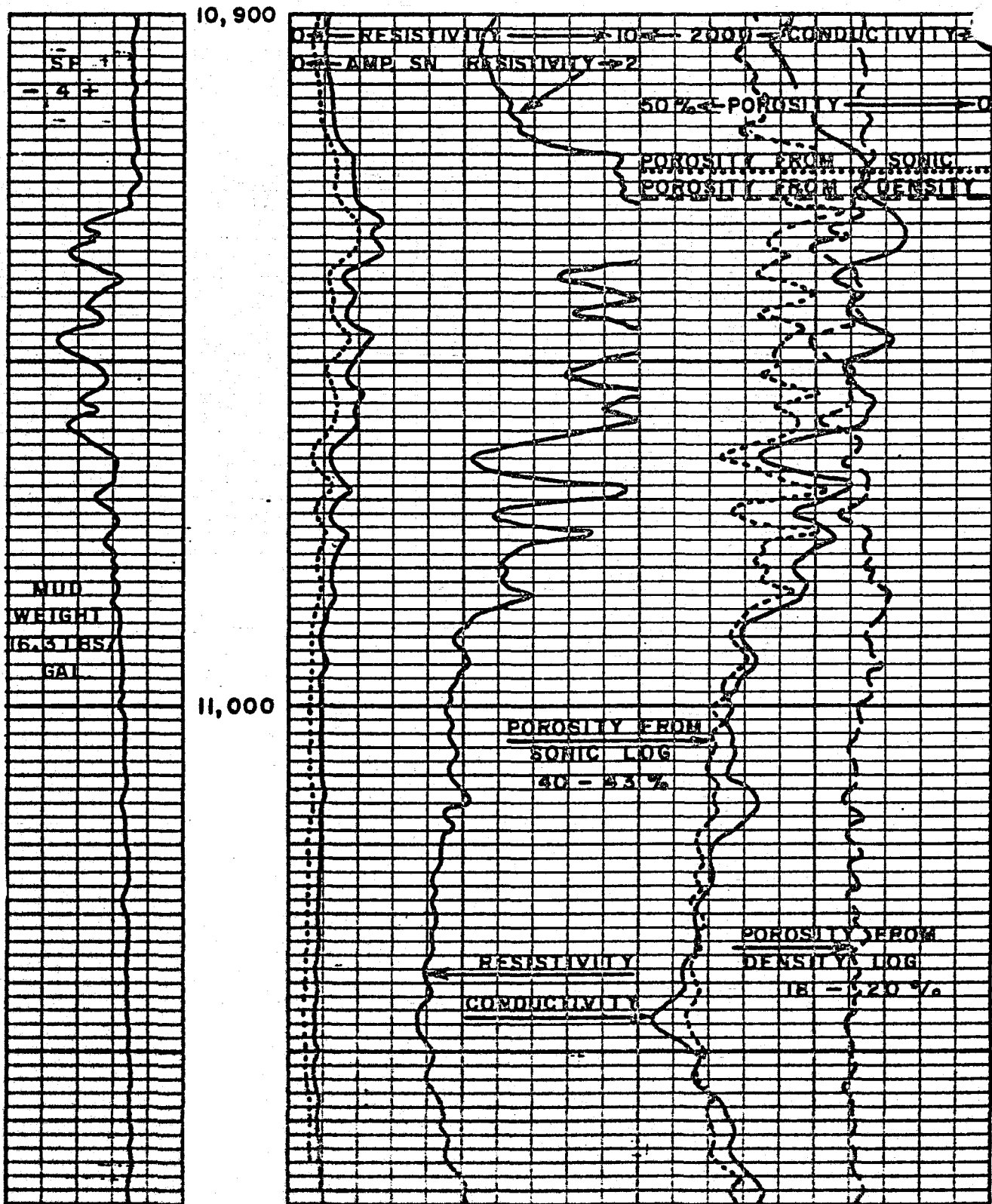


Fig. 17 - Shale in a Geopressure Zone, Aransas County, Texas.

THIS IS A PREPRINT --- SUBJECT TO CORRECTION

PREDICTION OF PORE PRESSURE FROM PENETRATION RATE

By

George D. Combs, Member AIME, Humble Oil & Refining Co., New Orleans, La.

© Copyright 1968

American Institute of Mining, Metallurgical and Petroleum Engineers, Inc.

This paper was prepared for the 43rd Annual Fall Meeting of the Society of Petroleum Engineers of AIME, to be held in Houston, Texas, September 29 - October 2, 1968. Permission to copy is restricted to an abstract of not more than 300 words. Illustrations may not be copied. The abstract should contain conspicuous acknowledgement of where and by whom the paper is presented. Publication elsewhere after publication in the JOURNAL OF PETROLEUM TECHNOLOGY or the SOCIETY OF PETROLEUM ENGINEERS JOURNAL is usually granted upon request of the appropriate journal provided agreement to give proper credit is made.

Discussion of this paper is invited. Three copies of any discussion should be sent to the Society of Petroleum Engineers office. Such discussion may be presented at the above meeting and, with the paper, may be considered for publication in one of the two SPE magazines.

ABSTRACT

A general equation for penetration rate in shales is formulated, and the constants in the equation evaluated by a regression analysis of penetration rate data from six Offshore Louisiana wells. The correlation assumes that penetration rate is proportional to weight on the bit, rotary speed, and a hydraulics term, each raised to a fixed power. A penetration

rate normalized for changes in these variables is found to decrease with increasing differential pressure and with increases in a tooth wear index. The drillability of shales -- defined as the drilling rate at some standard operating condition -- decreases with increasing depth but increases when the pore pressure increases because of the reduced compaction.

References and illustrations at end of paper.

The equation predicts the penetration rate with a standard deviation of 29 per cent. If the other parameters are known, it predicts the pore pressure with a standard deviation of about 1 lb/gal. The penetration rate increases when the pore pressure increases because of the reduced differential pressure and the increased drillability of the shale.

INTRODUCTION

A formal procedure for using penetration rates in shale to detect the beginning of abnormal pressure was presented recently by Jorden and Shirley^{1,2}. They presented field data which demonstrate that penetration rate decreases with increasing depth in normal pressure sections and that a reversal in this trend occurs when abnormally pressured shale is encountered. In order to define this reversal most clearly, they recommend raising the mud density when 1000 to 1500 feet above the expected top of the abnormal pressure and then drilling with constant mud density, rotary speed, weight on bit, hydraulics, etc., until the reversal is detected. Although a correlation between a normalized penetration rate, "d-exponent", and differential pressure is presented, the scatter of the data is so wide that it does not seem suitable for quantitative prediction of the pore pressure in the shale being drilled.

A method of predicted pore pressures from penetration rate would be invaluable because it would allow one to drill ahead without stopping to log until the pore pressure reached the value desired for setting casing. Then the well would be logged to confirm the pore pressure and the casing run. The ideal situation would be to avoid both unnecessary logging runs and kicks.

The work of Vidrine and Benit³ carried the technology another step in this direction. They analyzed data from eight South Louisiana wells and concluded that penetration rate always increases with a decrease in differential pressure in each well, but the percent change in penetration rate for a given change in differential pressure is greatest when a large bit weight is used. At bit weights of 4,000 to 5,000 lb/in their data agree well with

the results of numerous laboratory studies^{4,5,6}. They suggest that the differential pressure can be controlled by adjusting the mud weight so as to maintain a constant penetration rate after correcting for bit wear. This would allow one to predict the pore pressure if the differential pressure which is being maintained is known, e.g., from the differential pressure used to drill the last part of the normal pressure section. This technique assumes that the drillability of the shale does not change significantly with depth or pore pressure. They concluded that this assumption was true for the range of these variables covered in each well. However, they concluded that a general equation for drilling rate could not be developed because of variations in shale drillability between wells and over large intervals in the same well.

It seems likely that the strength of shales and, therefore, their drillability are related to the extent which the shale has compacted. Thus, it should be possible to relate drillability to depth and pore pressure as has been done for resistivity^{7,8}, sonic velocity⁷, and bulk density⁹. This paper proposes an empirical mathematical model for penetration rate in shales in which the penetration rate is a function of depth, pore pressure, differential pressure, weight on bit, rotary speed, hydraulics, and an index of tooth wear. The constants in the equation are evaluated by a regression analysis of data obtained from six wells in the Offshore Louisiana area. The characteristics of the equation and a procedure for using it to predict pore pressures from penetration rate are discussed.

DATA COLLECTION AND REDUCTION

Drilling rate data were obtained from 1000 to 4000 feet above the top of the abnormal pressure section to total depth in six wells in the Offshore Louisiana area. These wells ranged from the South Marsh Island to the South Pass areas. The first five wells are straight, exploratory wells and the sixth is a directionally drilled platform well. Continuous rate of penetration, ROP, charts were available for most of the footage covered, and the operating conditions were recorded

on the ROP charts by the drillers and engineer on the rig. Thus, the data are typical of what is now readily available in the field.

Shale intervals were chosen from the ROP charts since it is assumed that logs will not be available when applying the results of this study to drilling wells. In the few sections where ROP charts were not available, logs were used to pick the shale intervals. The rate of penetration was actually computed in either case from the drilling time charts. The author has observed that both the scale factor and zero setting on the instantaneous ROP charts were often in error. Each data point represents the average drilling rate over a minimum of 10 feet of shale. In long shale sections a maximum of 30 feet was used per data point. On the average, one data point was obtained for each 65 feet of hole that was drilled. The weight on bit, rotary speed, flow rate, bit nozzle sizes, and depths when the bit was run and pulled were taken from the ROP charts and the drillers tour reports. The mud density, plastic viscosity, and yield point were taken from the drillers tour reports and the mud engineers reports. These were plotted versus the depth at the time they were measured and smooth curves drawn through each plot. Values for each data point were read from these curves.

Pore pressures were estimated from a resistivity correlation developed for wells in this particular area but essentially the same as that given by Hottman⁷. Since there was at least one point in each well where the pore pressure was known from kick data and formation tests, the resistivity data were used, in effect, to interpolate between these known pore pressures. The accuracy of the pore pressure estimates should be quite good.

All of the above data were placed on punched cards for processing on a digital computer. The computer program calculated the bit wear index T , Eq. (4), and the equivalent circulating mud density using standard equations for laminar and turbulent flow of Bingham plastic fluids. Henceforth, the mud density will be taken to mean the equivalent circulating density.

The measured depths in the directional well were converted to true vertical depths.

DATA CHARACTERISTICS

Since the correlation to be developed is empirical, it will be most accurate when the various variables are within the range covered by these data. Some of the characteristics of the data are summarized in Tables I and II. Most of these data are at depths from 8,300 to 15,000 feet and about two thirds are in abnormally pressured sections. The weight on bit, rotary speed, and the hydraulics term all decrease as the bit size is reduced. Although some data for diamond bits are shown in some of the figures, these data were not used in the correlation and the data in Table I are only for the part of the hole drilled with conventional bits.

DEVELOPMENT OF A MATHEMATICAL MODEL

The following general form was assumed for the penetration rate equation

$$R = R_0' \left(\frac{W}{D_h \cdot 3500} \right)^{aw} \left(\frac{N}{200} \right)^{an} \left(\frac{Q}{D_h \cdot D_n \cdot 3} \right)^{aq} \cdot f(P_d) \cdot f(T) \quad (1)$$

where R_0' is the drillability of the shale[†]. This is defined as the penetration rate with a sharp bit, zero differential pressure, 3500 lb/in bit weight, 200 rpm rotary speed, and a value of 3 gpm/(in · 1/32 in) for the hydraulics term. The next three terms give the effect of weight, speed, and hydraulics. The terms $f(P_d)$ and $f(T)$ represent functions of differential pressure and a bit wear index T which will be defined later. Equation (1) assumes that the effect of the various variables can be separated, i.e., the exponents on weight, speed, and hydraulics are independent of the value of the other variables and the differential pressure and bit wear functions are the same for all operating conditions. This assumption is necessary if a reasonably simple equation is to be obtained even though it cannot be exactly true.

[†]Nomenclature given at end of paper.

The drillability is assumed to be a function of depth and pore pressure of the form

$$R'_0 = f(H) \cdot f(P_p - 9) \quad (2)$$

because this worked quite well for the resistivity data. In order to handle the regression analysis by standard least-squares techniques, it is convenient to work with the logarithm of Eq. (1).

Furthermore, the author has chosen to define the final drilling rate parameter so that it increases with decreasing drilling rate. Thus,

$$\begin{aligned} K &= \log(1000/R) = 3. - \log(R) \\ &= A - a_w \log(W/D_h \cdot 3500) \\ &\quad - a_n \log(N/200) - a_q \log(Q/D_h \cdot D_n \cdot 3) \\ &\quad + f'(H) + f'(P_p - 9) + f'(P_d) \\ &\quad + f'(T) \end{aligned} \quad (3)$$

where the depth, pore pressure, differential pressure, and bit wear functions are redefined as required, i.e.,

$$f'(H) = -\log \{f(H)\}$$

If each of the unknown functions is assumed to be a polynomial in the given independent variable, this equation can be fitted to the data and all the functions evaluated simultaneously.

Equation (3) was first fitted to only the normal pressure data with the idea that this would best define the base line or trend line to be expected until abnormal pressure is encountered. The leading constant, A, was assumed to be different for each well. In other words, the correlation could be shifted to fit the normal pressure data for each well while retaining the same equation for all of the functions. Equation (3) was then fitted to a set of data made up of all the abnormal pressure data plus the last 1000 to 2000 feet of normal pressure data in each well. This correlation should be the most accurate for actually predicting the pore pressure once the top of the abnormal pressure is located. In this case a single value was used for the leading constant A in all wells.

The details of the reasons for selecting these weight, speed, and hydraulics terms and the specific form of the other functions are given in the following sections. In each case, the result obtained from the two correlations just described is presented.

Effect of Weight, Speed, and Hydraulics

The use of weight per inch of hole and rotary speed raised to a power is common in empirical penetration rate equations^{3,10} and needs no further discussion. The hydraulics term, $Q/D_h \cdot D_n$, was selected because it controls the cross-flow velocity beneath the bit¹¹, and the author feels that this should control the bottom hole cleaning action. The term actually represents the momentum flux or 'hydraulic impact' per unit area of hole.

$$\begin{aligned} \frac{\text{Hydraulic Impact}}{\text{Unit Area}} &\propto \frac{QV}{D_h^2} \propto \frac{Q^2}{D_h^2 \cdot D_n^2} \\ &= \left(\frac{Q}{D_h \cdot D_n} \right)^2 \end{aligned}$$

Three different assumptions were tried for the exponents a_w , a_n , and a_q . First, they were simply left as unknowns and evaluated from the data along with the other functions. Second, values of 1.0, 0.6, and 0.3 were assumed based on the results of previous field and laboratory studies^{3,12,13}. Finally, a simple linear equation was assumed with $a_w = 1$, $a_n = 1$, $a_q = 0$.

The accuracy of Eq. (3) in each case is shown in Table III. The standard deviation of K is given for the individual data points and when the error was averaged over 200 feet intervals. The accuracy of the equation is relatively insensitive to the choice of values for the exponents, but the linear equation seems to be least accurate while the values determined by the least squares fit to the data are most accurate. Because of the small differences in the accuracy of the three choices, the author has chosen to use the values (1, 0.6, and 0.3) suggested by the more carefully controlled studies of Vidrine³ and Eckel¹³. These values also seemed to give more reasonable values for the other functions. The rest of this discussion assumes

that these exponents are used to normalize the data to standard conditions of 3500 lb/in, 200 rpm, and 3 gpm/(in·l/32 in).

Bit Wear Function

In order to account for the effect of bit wear while drilling, i.e., before the bit is pulled and inspected, it is necessary to define a parameter to which the amount of tooth wear or the decrease in drilling rate can be related. This parameter should be defined in terms of the variables which are readily available. The assumption used here is that the tooth wear is related to the number of times that the tooth contacts the bottom of the hole

$$T = \sum_{\text{Bit Run}} \left(\frac{\Delta H_1}{R_1} \right) \left(\frac{N}{200} \right)_i \quad (4)$$

where R_1 is the penetration rate in shale for the interval ΔH_1 . Actually, T has dimensions of hours and may be thought of as an equivalent number of rotating hours at 200 rpm — computed as though the formation were all shale.

Since the equation uses only the penetration rate in shales to calculate the equivalent rotating hours, there is an implied assumption that drilling a given footage of sand will wear the teeth as much as the same footage of shale. This means that wear per tooth contact increases in a sand by the same factor that the penetration rate increases. While this assumption is not precise, it does allow for the increased abrasiveness of the sands in a simple manner.

The bit wear functions obtained from the least squares fits to the data are plotted in Fig. 1. The normalized drilling rate, R' , relative to that with a sharp bit, R'_s , is plotted versus the equivalent rotating hours at 200 rpm. The solid line was obtained from the fit to all the data and the dashed lines for the normal pressure data. The curved dashed line was obtained when a second order polynomial was assumed for the bit wear function. The small difference between this curve and the straight line obtained with a linear fit is not considered

significant; consequently, the straight lines are used to normalize the data for bit wear in the final correlations.

While drilling in normal pressure, the bit wear trends for previous bit runs in the same well can be plotted and these will probably be more accurate than a general curve such as that given here. When drilling in abnormal pressure, however, this is not possible because the pore pressure is also unknown and the effects of bit wear and pore pressure cannot be separated. In this case, one must assume the wear trend that is established in the normal pressure section or from previous wells in the area in which the pore pressure is now known.

Differential Pressure Function

The differential pressure function was approximated by a third order polynomial when fitting Eq. (3) to the data. The results are given by the solid curves in Fig. 2. The penetration rate decreases with increasing differential pressure, but not as much as was found in previous studies^{3,4,5,6}. Vidrine³ concluded that the sensitivity of penetration rate to differential pressure is greatest when large bit weights are used. His results for bit weights of 5300 and 3500-4000 lb/in are also shown in the figure. The curve for 3500-4000 lb/in shows about the same response as this study, but the curve for 5300 lb/in shows a much larger change. In addition, the curve for normal pressure data only shows a greater effect than does the curve obtained from the fit to all of the data, and the average bit weight was larger for the normal pressure data. All of this seems to confirm the effect of bit weight and imply that the differential pressure function presented here should not be used for bit weights significantly different from those used in the subject wells.

Both of the curves obtained from the least squares fit have an increase in slope at differential pressures greater than 2000 psi. This is not considered to be significant in relation to the accuracy of the curve. The dashed lines are used as a more realistic approximation to this part of the curve in the following sections. Also, there were very few data points with negative differential pressures greater than

250 psi, and these data indicated little change in penetration rate compared to that at -250 psi. Therefore, the penetration rate is assumed to remain constant below -250 psi in the final correlation.

Variation of Drillability with Depth and Pore Pressure

Since shale resistivity and drillability should both be related to the compaction of the shale, it was assumed that drillability is best related to depth and pore pressure by the same form of equation that works best for the resistivity in these wells. Pore pressures were known accurately at 12 points in the abnormally pressured sections of these wells. These data were used to test several different methods of relating resistivity to depth and pore pressure, or conversely, to predict pore pressure from the resistivity data. The method of Hottman and Johnson⁷ was the most accurate. In general terms, the form of the equation can be written

$$R_{sh} = R_n \cdot (R_{sh}/R_n)$$

$$\text{or } \log(R_{sh}) = \log(R_n) + \log(R_{sh}/R_n)$$

$$\text{with } \log(R_n) = f(H) \quad (5)$$

$$\log(R_{sh}/R_n) = f(p_p - 9) \quad (6)$$

where R_{sh} is the actual resistivity and R_n is the expected value for normal pressure shale at the same depth. In other words, the resistivity is expressed as the product of a function of depth which describes the normal pressure trend and a function of the pore pressure which describes the deviation from this trend due to abnormal pressure. The same general form was assumed for the drillability as noted earlier in Eq. (2).

The pore pressure function developed by Hottman is shown in Fig. 3. This curve is

nearly linear for pore pressures less than 15 lb/gal. Since most of the drilling rate data were for pore pressures less than this, a linear relationship was assumed for drillability. The dashed line in the figure was obtained from the least squares fit, and this line was used in calculating the standard deviations shown in Table III. Examination of the data for pore pressures greater than 15 lb/gal suggested that the drillability changed more rapidly at higher pore pressures as does the resistivity. Consequently, a second approximation was made in which the ratio between the two curves (0.6) below 15 lb/gal was assumed to continue at higher pore pressures. This gives the other curve for drillability in the figure. This did improve the accuracy of the predicted penetration rates at higher pore pressures although there are insufficient data to test this assumption thoroughly. The curved line is used in the final correlation.

The trend of the logarithm of drillability with depth is essentially linear. When higher order polynomials were assumed, the resulting curve differed little from a straight line and there was little change in the standard deviation of the predicted penetration rates. The normal pressure data gave a slope of $0.104 \Delta \log(R'_0)/1000 \text{ ft}$ and the fit to all the data gave 0.097. The depth and pore pressure functions can be combined to give a general plot of drillability versus depth and pore pressure as shown in Fig. 4. Note that in a transition zone where pore pressure is increasing with depth, the drillability may increase, decrease, or remain essentially constant according to the rate at which the pore pressure increases. This may explain why Vidrine³ did not observe any significant effect of depth and pore pressure in the intervals which he studied.

APPLICATIONS

The various functions which relate penetration rate to depth, differential pressure, etc., can be used to predict the pore pressure if all the other variables are known. In practice, the initial problem is to establish a trend line in the normal pressure section. The trend of drillability with depth and the differential pressure function in Fig. 2 can be combined to give a general plot of

penetration rate versus depth and mud density as shown in Fig. 5. If the mud weight being used at each depth is known, this figure will allow one to easily trace the expected trend of normalized penetration rate with depth in normal pressure shales. If the actual penetration rates are corrected to some standard operating conditions and corrected for bit tooth wear, they should follow a curve which is parallel to this as long as the pore pressure is normal. The absolute value of the penetration rate is not critical since it is assumed that the drillability may be consistently lower or higher in a given well as compared to the average shown here, and that the trend line can be shifted to compensate for this.

An increase in penetration rate relative to the expected trend indicates an increase in pore pressure. This increase occurs because of the decrease in differential pressure and the increased drillability of the shale. These two effects can be combined as shown in Fig. 6 to give the total change in penetration rate due to an increase in pore pressure. The relative drilling rate is plotted versus the overbalance or differential pressure expressed as an equivalent gradient in lb/gal. The curves apply only for pore pressures less than 15 lb/gal where the drillability varies linearly with the pore pressure. For example, consider drilling with 12 lb/gal mud density in normal pressure at 10,000 feet (3 lb/gal overbalance). If the pore pressure increases to 12 lb/gal, the penetration rate will increase by a factor of $1/0.525$ or about 90 per cent relative to the value expected for normal pressure shale. This change is equivalent to 2.5 standard deviations based on the value of 0.11 for the standard deviation of K . Thus, such an increase would be expected in only one case out of 160 due to the scatter of the data, and should be clearly distinguished from the usual variations about the trend line. With this much overbalance it is very unlikely that the pore pressure would increase enough to cause a kick before the increase in pore pressure could be recognized. The smaller the overbalance, the greater the probability of taking a kick.

Figure 6 can also be used to judge the accuracy of the pore pressures predicted

from the penetration rate. Since the sensitivity of penetration rate to pore pressure depends upon the amount of overbalance, the error in predicted pore pressure corresponding to a given error in penetration rate will also change. Based on a standard deviation of 0.11 in K , a depth of 12,500 feet, and a predicted overbalance of 1 lb/gal, for example, one standard deviation about the predicted value would cover the range from 0.2 to 2.3 lb/gal overbalance and two standard deviations would cover the range from -0.3 to 4 lb/gal overbalance. One standard deviation corresponds roughly to 1 lb/gal error in pore pressure. This may be compared to a standard deviation of 0.6 lb/gal which was obtained when using the resistivity data to predict the known pore pressures.

Prediction of Pore Pressure

A trend line can be constructed for any assumed pore pressure once the mud density is known at each depth. The drillability can be traced from Fig. 4 for the assumed pore pressure. Then the effect of differential pressure is read from the curve in Fig. 2 which applies to all the data — normal and abnormal. The effect of drillability and differential pressure are combined to give the predicted penetration rate at each depth for the assumed pore pressures.

The results of such a calculation are shown in Fig. 7 for well number 2. The pore pressure and differential pressure are shown by the curves on the right side of the figure. The expected normalized penetration rates for each pore pressure are shown by the light lines. The observed penetration rates are indicated by the dashed line. This curve is a 'moving, 200-ft average' of the individual data points. The entire set of trend lines has been shifted slightly to give the best agreement with the observed penetration rates over the interval from 7400 to 8600 feet where the penetration rate trend clearly indicates normal pressure. The predicted pore pressure is obtained by interpolation between the given pore pressure trend lines. For example, between 9,000 and 10,300 feet the predicted pore pressure increases from 9 to 13.5 lb/gal. The actual pore pressure

increased from 9 to 13.2 lb/gal over this interval. The expected penetration rate corresponding to the actual pore pressure is indicated by the dark, solid curve.

Figures 8 through 12 show the observed and predicted penetration rates for the other wells. The format of these is the same as for Fig. 7. In each case the predicted curve is shifted to give the best agreement with the observed penetration rates over the last 1000 to 2000 feet of the normal pressure section. The trend line for normal pressure is shown as a dotted line after entering the abnormal pressure section. In general the observed penetration rates do follow the predicted curves but with a fairly large scatter. The standard deviation of the error in K_g^1 is 0.11 for the abnormal section plus the last 1000 to 2000 feet of the normal pressure section. This corresponds to an error of 29 per cent in the penetration rate.

There are several sections where the deviation from the predicted curve is particularly large. In well number 2, Fig. 7, the penetration rate was much larger than predicted below about 15,000 feet. The last sand in this well was at 14,200 feet, and the shale below this depth was apparently deposited in a 'deep marine' environment. Consequently, it is possible that neither the resistivity nor the penetration rate correlations are applicable. The last known pore pressure is at 12,500 feet.

The penetration rate did not indicate the top of the abnormal pressure in well 1, Fig. 8. Although the pore pressure started to increase at 11,800 feet, the penetration rate continued to follow the trend line for normal pressure until about 12,600 feet. The pore pressure had increased to 12 lb/gal at this depth; consequently, if one had drilled into the abnormal pressure with less than 12 lb/gal mud density, the well would probably have kicked.

In well 5, Fig. 11, the penetration rate with the 6-in bit between 14,300 and 14,850 feet was much slower than predicted. This entire interval was drilled under-balanced and a kick occurred at 14,850

feet.

The pore pressure increased very rapidly in the interval from 12,000 to 14,000 feet in well number 6, Fig. 12, and the differential pressure was generally decreasing. The reversal of the normal trend toward lower penetration rates with increased depth is quite dramatic in this interval. The normalized penetration rate increased four-fold whereas it would normally decrease by about a factor of 0.63 if the pore pressure were constant. The hole was sidetracked because of stuck pipe and the interval from 12,000 to 12,800 feet re-drilled with essentially the same differential pressures. The individual data points have been plotted over this interval to demonstrate the repeatability of the observed trend in the penetration rate.

FUTURE WORK

The accuracy with which pore pressure can be predicted from penetration rate can be improved by reducing the scatter of the data and increasing the sensitivity of penetration rate to differential pressure. Vidrine⁵ has suggested that the sensitivity to differential pressure is increased by high bit weights. If this can be confirmed and any other changes in operating conditions made as needed, considerable improvement should result. The most promising technique for reducing the scatter of the data is the use of modern instrumentation to continuously record the rate of penetration, weight on bit, rotary speed, pump rate, mud density, and a normalized penetration rate. Such instrumentation is becoming available and should soon provide more accurate data for correlations such as that proposed herein¹⁴. Finally, improved knowledge of the rotary drilling process plus better field data should lead to the development of more comprehensive penetration rate models.

CONCLUSIONS

Analysis of field data on penetration rate in shales in terms of an empirical model indicates that:

1. The accuracy of the model is not highly sensitive to the choice of

exponents on weight, speed, and hydraulics. The least squares fit gave values of 0.68, 0.39, and 0.39, respectively; however, values of 1.0, 0.6, and 0.3 gave more realistic values for the effect of other parameters.

2. Penetration rate decreases with increases in differential pressure, and is most sensitive to changes in differential pressure when the differential pressure is near zero.
3. Penetration rate decreases as the number of equivalent rotating hours on the bit increases.
4. The drillability of shale, or the penetration rate at some fixed operating conditions, decreases with increasing depth and increases with increased pore pressure. This is consistent with the behavior of other shale properties which indicate a reversal of the normal compaction trend when abnormal pressure is encountered.
5. Although the scatter of the data is large, 29 per cent standard deviation, the effect of each of the parameters agrees qualitatively with the results of laboratory studies or what may be logically predicted. This indicates that the model is realistic and that improved accuracy can be expected as more accurate field data become available.
6. With typical operating conditions, the correlation predicts the pore pressure with a standard deviation of 1 lb/gal.

NOMENCLATURE

A	= Constant
a_w, a_n, a_q	= Weight, speed, and hydraulics exponents
D_h	= Hole diameter, in
D_n	= Bit nozzle diameter, in
H	= Depth, 1000 ft
K	= Log (1000/R)

K'	= Log (1000/R')
K'_s	= Log (1000/R'_s)
K'_o	= Log (1000/R'_o)
N	= Rotary speed, rpm
P_d	= Differential pressure, psi or lb/gal·1000 ft
Q	= Flow rate, gpm
R	= Penetration rate, ft/hr
R'	= Normalized penetration rate, ft/hr
R'_s	= Normalized penetration rate—sharp bit, ft/hr
R'_o	= Drillability or normalized penetration rate—sharp bit, zero differential pressure, ft/hr
R_{sh}	= Observed shale resistivity
R_n	= Shale resistivity in normal pressure
T	= Bit wear index — equivalent rotating hours
V	= Nozzle velocity
W	= Weight on bit, lb
ρ_m	= Equivalent circulating mud density, lb/gal
ρ_p	= Pore pressure gradient, lb/gal
σ	= Standard Deviation

ACKNOWLEDGEMENT

The author would like to thank the management of Humble Oil & Refining Company for permission to publish this paper.

REFERENCES

1. Jorden, J. R. and Shirley, O. J.: "Application of Drilling Performance Data to Overpressure Detection", SPE 1407, Presented at the 41st Annual Fall Meeting, Dallas, Texas (Oct 2-5, 1966).
2. Jorden, J. R. and Shirley, O. J.: "Method for Determining the Top of Abnormal Formation Pressures", U. S. Patent No. 3,368,400 (Feb. 13, 1968).
3. Vidrine, D. J. and Benit, E. J.: "Field Verification of the Effect of Differential Pressure on Drilling Rate", J. Pet. Tech. (July, 1968) 676-682.
4. Cunningham, R. A. and Eenink, J. G.: "Laboratory Study of Effect of Overburden, Formation and Mud Column Pressures on Drilling Rate of Permeable Formations", Trans., AIME (1959) 217 9-17.

5. Garnier, A. J. and van Lingen, N. H.: "Phenomena Affecting Drilling Rates at Depth", Trans., AIME (1959) 216, 232-239.
6. Maurer, W. C.: "Bit-Tooth Penetration Under Simulated Borehole Conditions", J. Pet. Tech. (Dec., 1965) 1433-1442.
7. Hottman, C. E. and Johnson, R. K.: "Estimation of Formation Pressures from Log-Derived Shale Properties", J. Pet. Tech. (June, 1965) 717-722.
8. Foster, J. B., and Whalen, H. E.: "Estimation of Formation Pressures from Electrical Surveys--Offshore Louisiana", J. Pet. Tech. (Feb., 1966) 165-171.
9. Boatman, W. A.: "Measuring and Using Shale Density to Aid in Drilling Wells in High Pressure Areas", J. Pet. Tech. (Nov., 1967) 1423-1429.
10. Bingham, M. G.: "A New Approach to Interpreting Rock Drillability", Oil and Gas Jour. (Nov. 2, 1964 through April 5, 1965).
11. McLean, R. H.: "Velocities, Kinetic Energy, and Shear in Crossflow Under Three-Cone Jet Bits", J. Pet. Tech. (Dec., 1965) 1443-1448.
12. Eckel, J. R.: "Microbit Studies of the Effect of Fluid Properties and Hydraulics on Drilling Rate", J. Pet. Tech. (April, 1967) 541-546.
13. Eckel, J. R.: "How Mud and Hydraulics Affect Drill Rate", Oil and Gas Jour. (June 17, 1968) 69-73.
14. Gill, J. A.: "Applied Drilling Technology", Drilling Contractor (March-April, 1968) 34-50.

TABLE I
SUMMARY OF THE DATA

Well No.	1	2	3	4	5	6	Average
Data Pts. - Normal	38	17	68	30	45	18	216 ⁺
- Abnormal	49	109	60	84	21	67	390 ⁺
Depth Range - From	8,260	7,280	8,240	8,350	9,060	8,540	8,300
- To	15,020	16,230	16,000	15,000	14,730	13,900	15,150
Top of Abnormal Pressure	11,850	8,900	13,800	10,800	13,850	10,100	11,550
Max. Pore Pressure, lb/gal	14.7	16.7	15.5	16.5	14.0	18.1	15.9
Differential Pressure, lb/gal·1000 ft - Max.	47	43	63	40	21	53	44
- Min.	2	-5	5	0	-30	-2	-7
Avg. W/D _h ,* lb/in	3,280	3,390	3,640	3,530	4,760	1,750	3,040
Avg. N,* rpm	162	154	149	139	220	174	155
Avg. $\frac{Q^*}{D_h \cdot D_n}$, $\frac{\text{gpm}}{\text{in} \cdot 1/32 \text{ in}}$	2.7	2.7	2.9	2.9	4.8	2.6	2.9
Bit Sizes - 1	12-1/4	12-1/4	12-1/4	9-7/8	9-7/8	9-7/8	---
- 2	8-1/2	8-1/2	8-1/2	6-5/8	6	8-5/8	---
- 3	---	5-3/4	5-3/4	---	---	5-7/8	---

*For those data points used in the final correlation.
⁺Total.

TABLE II
AVERAGE OPERATING CONDITIONS
VERSUS BIT SIZE

Bit Size	Numbers Data Points	W/D _h lb/in	N rpm	Average Operating Conditions
				$\frac{Q}{D_h \cdot D_n}$ $\frac{\text{gpm}}{\text{in} \cdot 1/32 \text{ in}}$
12-1/4	191	3270	183	3.39
8-1/2 — 9-7/8	278	3170	163	3.17
5-3/4 — 6-5/8	137	2660	110	1.98

TABLE III
EFFECT OF WEIGHT, SPEED, AND
HYDRAULICS EXPONENTS

	Exponents			Standard Deviation of K	
	a_w	a_n	a_q	Individual Data Point	200 ft Average
Normal	1	1	0	0.116	0.103
Pressure	1	0.6	0.3	0.112	0.100
Normal and	1	1	0	0.158	0.134
Abnormal	1	0.6	0.3	0.151	0.128
Pressure	0.681*	0.391*	0.386*	0.140	0.119

* From the least-squares fit.

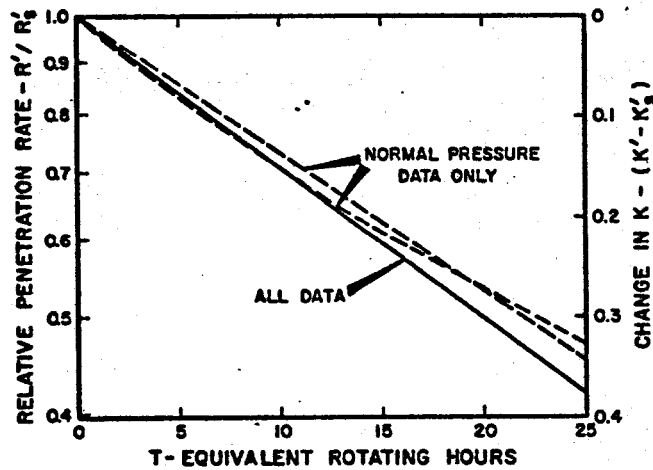


FIG.1 - BIT WEAR FUNCTIONS

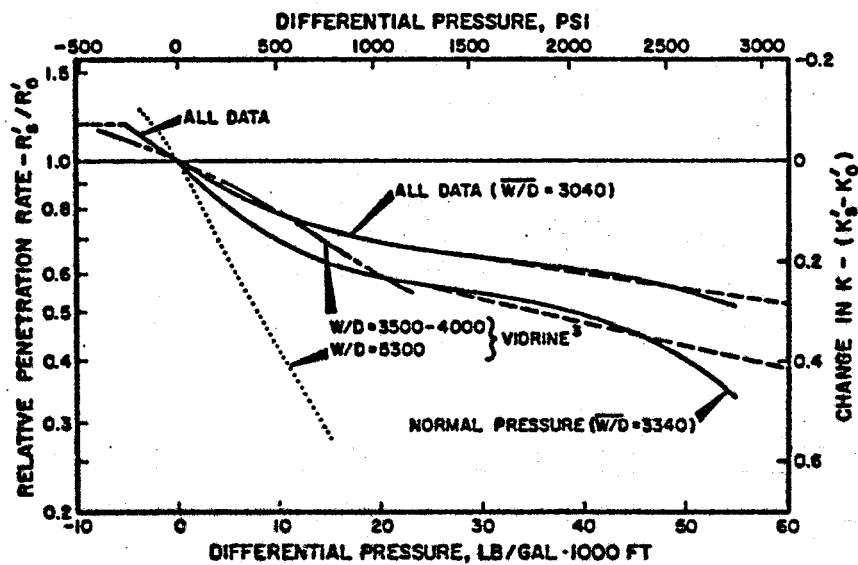


FIG.2 - DIFFERENTIAL PRESSURE FUNCTIONS

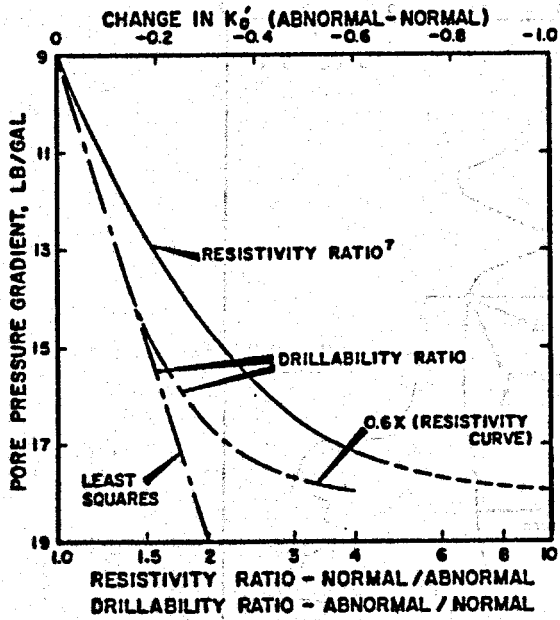


FIG. 3 - VARIATION OF RESISTIVITY AND DRILLABILITY WITH PORE PRESSURE

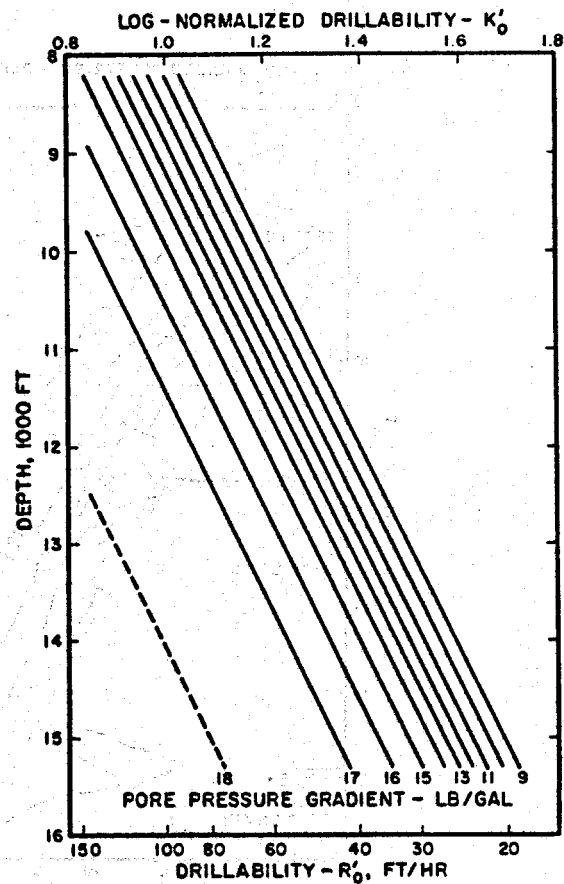


FIG. 4 - VARIATION OF SHALE DRILLABILITY WITH DEPTH AND PORE PRESSURE

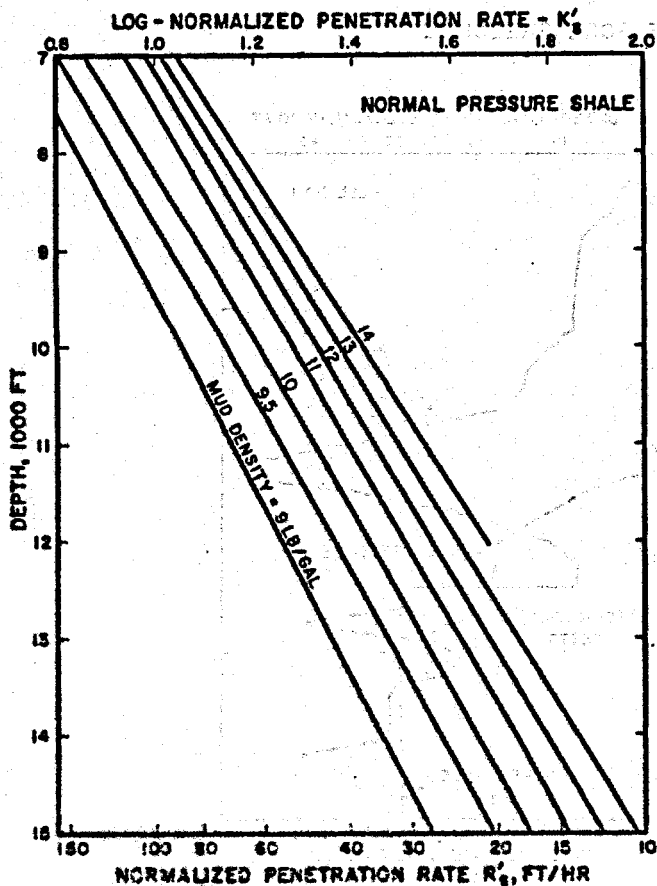


FIG. 5 - PENETRATION RATE IN NORMAL PRESSURE SHALE

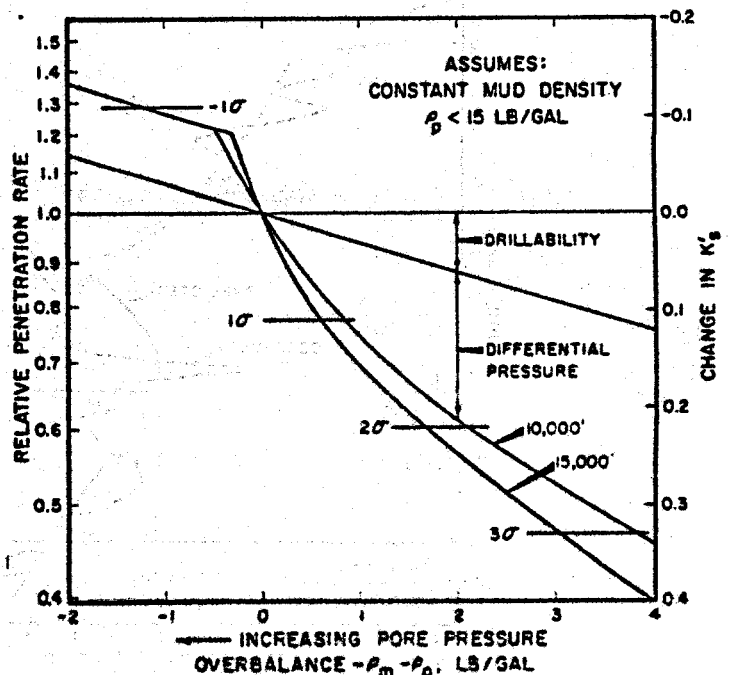


FIG. 6 - SENSITIVITY OF PENETRATION RATE TO PORE PRESSURE CHANGES

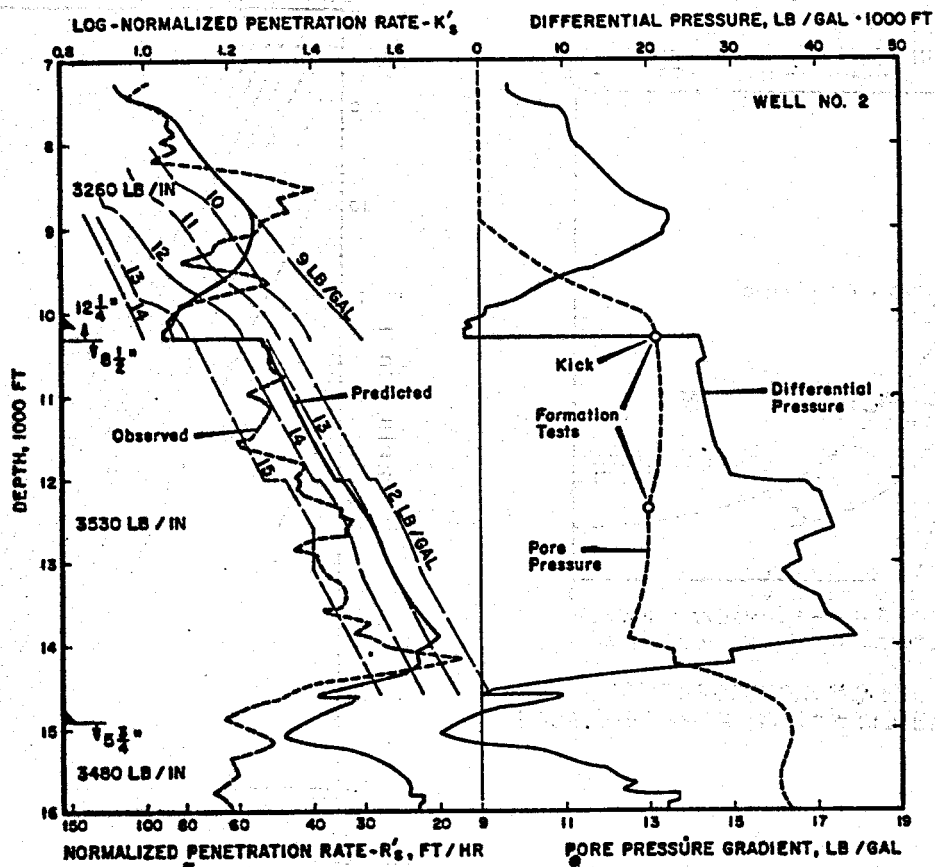


FIG. 7 - PREDICTION OF PORE PRESSURE

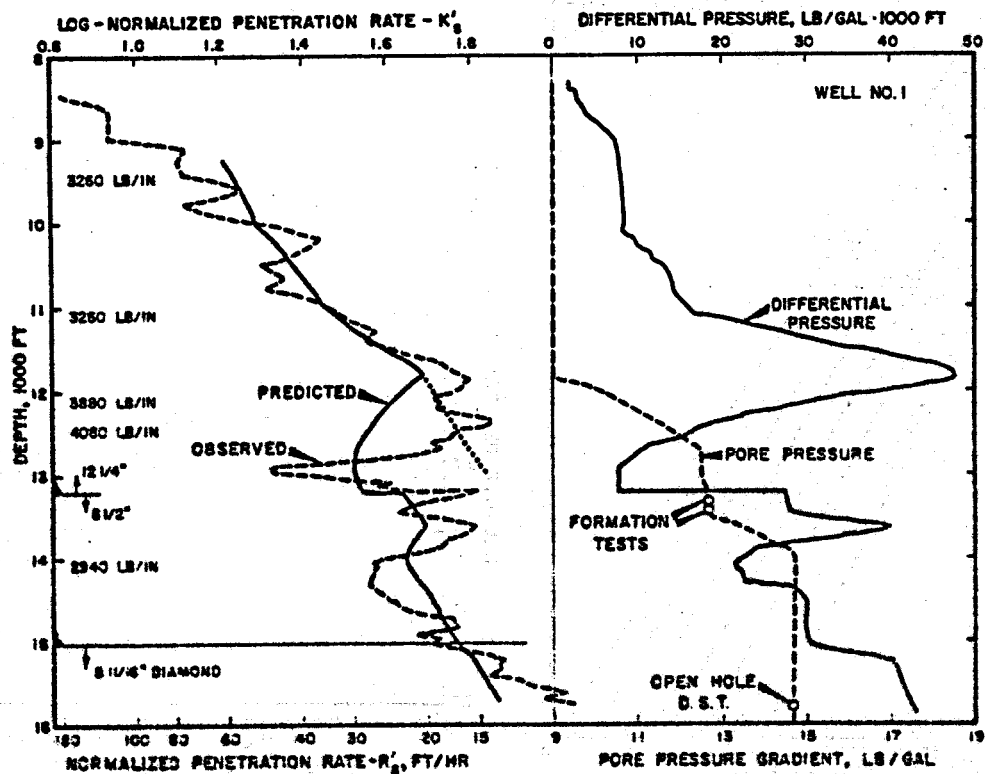


FIG. 8 - COMPARISON OF PREDICTED AND OBSERVED PENETRATION RATES

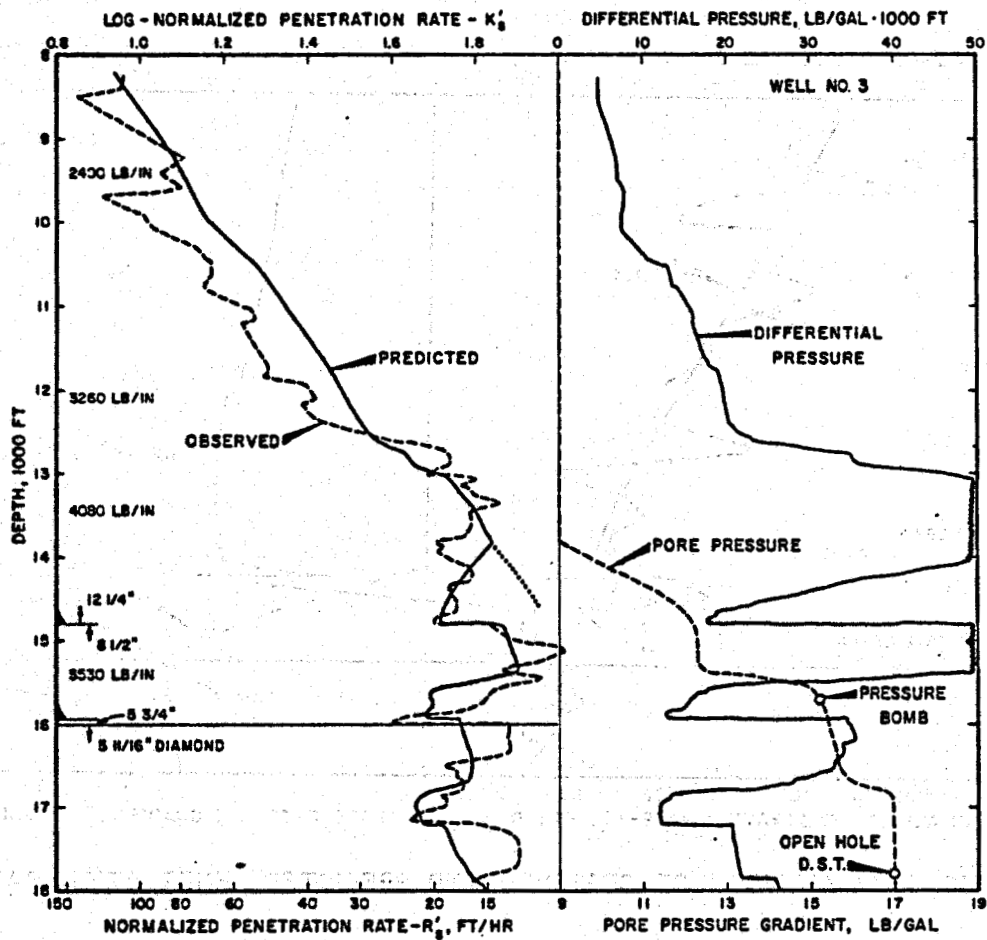


FIG. 9 - COMPARISON OF PREDICTED AND OBSERVED PENETRATION RATES

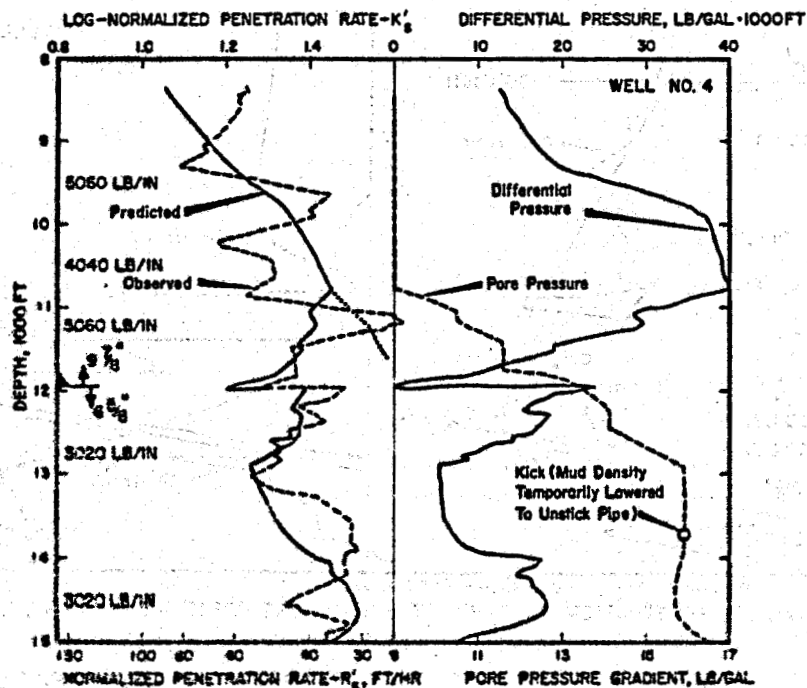


FIG. 10 - COMPARISON OF OBSERVED AND PREDICTED PENETRATION RATES

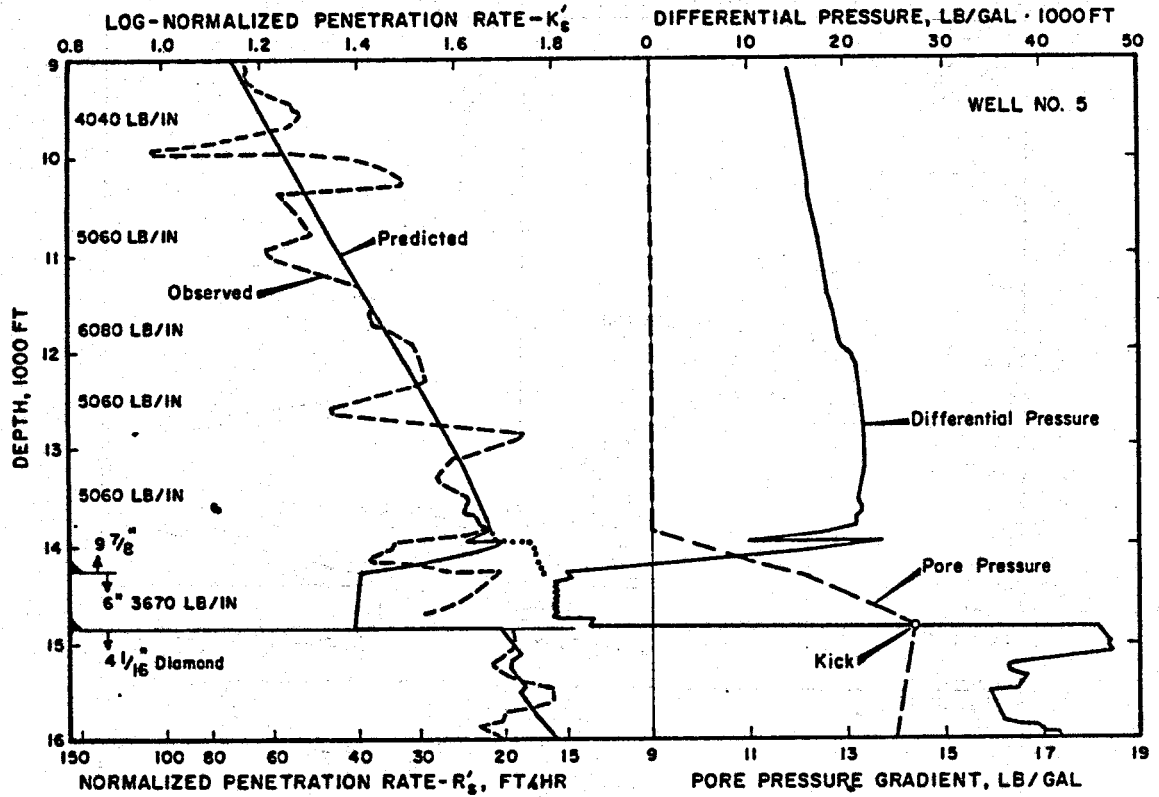


FIG. 11—COMPARISON OF OBSERVED AND PREDICTED PENETRATION RATE

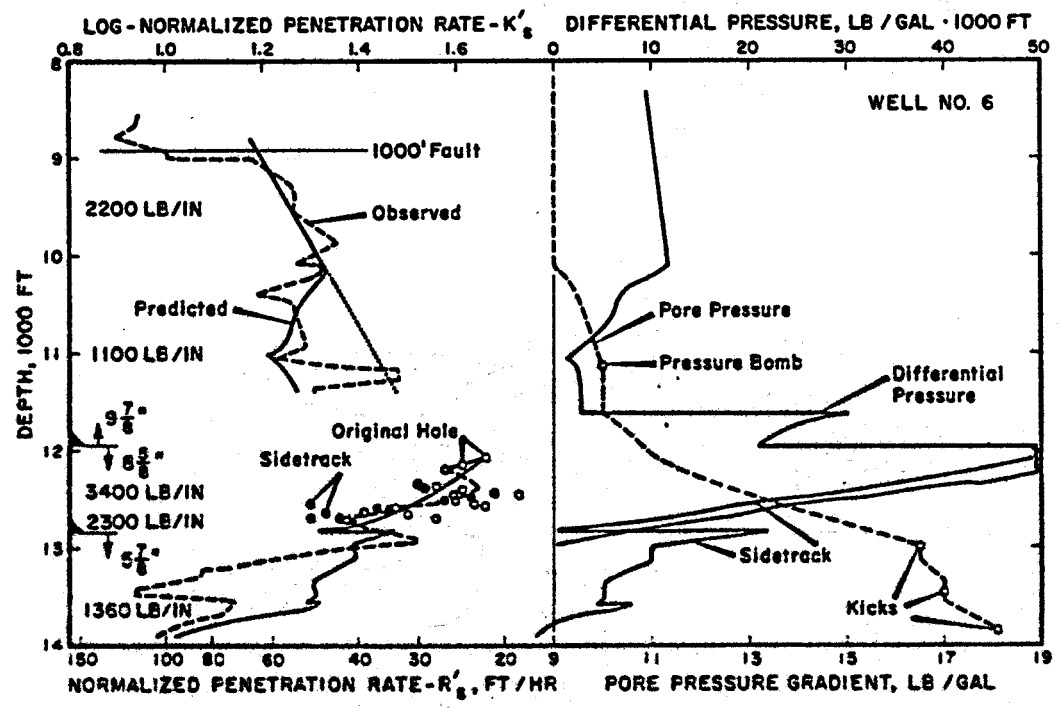


FIG. 12—COMPARISON OF OBSERVED AND PREDICTED PENETRATION RATES

THIS IS A PREPRINT --- SUBJECT TO CORRECTION

An Engineering Interpretation of Seismic Data

By

E. S. Pennebaker, Member AIME, Humble Oil & Refining Co., Houston, Tex.

© Copyright 1968

American Institute of Mining, Metallurgical and Petroleum Engineers, Inc.

This paper was prepared for the 43rd Annual Fall Meeting of the Society of Petroleum Engineers of AIME, to be held in Houston, Tex., Sept. 29-Oct. 2, 1968. Permission to copy is restricted to an abstract of not more than 300 words. Illustrations may not be copied. The abstract should contain conspicuous acknowledgment of where and by whom the paper is presented. Publication elsewhere after publication in the JOURNAL OF PETROLEUM TECHNOLOGY or the SOCIETY OF PETROLEUM ENGINEERS JOURNAL is usually granted upon request to the Editor of the appropriate journal provided agreement to give proper credit is made.

Discussion of this paper is invited. Three copies of any discussion should be sent to the Society of Petroleum Engineers office. Such discussion may be presented at the above meeting and, with the paper, may be considered for publication in one of the two SPE magazines.

ABSTRACT

The reflection seismograph has long been the most important means for obtaining subsurface information prior to drilling. Interpretation of the seismic data is normally made by geophysicists to define subsurface structure. However, considerable information of great value to the drilling engineer is also contained in the seismic information. This paper discusses how the drilling engineer can use these data to estimate depth and magnitude of subsurface formation pressures, predict gross changes in lithology, and warn of possible drilling problems. Techniques are also presented for predicting relative drillability and fracture gradients in rank wildcat areas.

The predictive techniques described have been used with good results over a wide area along the Texas Gulf Coast including Continental Shelf locations and might possibly be applicable to any sedimentary basin.

INTRODUCTION

The only means of obtaining subsurface information other than from drilling is by geophysical prospecting. Although the seismograph has been

used by geophysicists and geologists for many years to help define subsurface structure, it is only recently that engineers have begun to discover useful applications.

One of these applications is the use of routine seismic field data to predict both the depths to abnormal pressure formations and approximate pressure magnitudes.¹ The predictive method results from the fact that velocities between subsurface reflecting layers can be obtained from seismic field data using well known geophysical techniques. Differences in interval velocities between these layers can be used to develop an average interval travel time (reciprocal of interval velocity) profile, which is in effect an acoustic log averaged over fairly long (500' - 1000') vertical intervals.

Analysis of numerous well velocity surveys revealed a close correlation between interval velocity (interval travel time), and factors such as lithology and degree of rock compaction and that interval travel time varies exponentially and predictably with depth. Departure from this normal trend signifies abnormal pressure or gross lithologic changes.

References and illustrations at
end of paper

Additional data such as relative drillability and estimates of fracture gradient complete the information required by the drilling engineer to assure that the proper casing can be available at the drillsite, optimum drilling mud weighting schedule and hole size selection can be made and the proper rig can be chosen.

Drillability information is customarily obtained from bit performance records of nearby wells. Methods of measuring pore pressures from well logs have greatly improved the accuracy of down-hole pressure predictions in areas where there are sufficient wells for adequate control.^{2,3} Empirical fracture gradient correlations for normal pressure formations have been developed from experience in known geological areas.⁴ In areas of poor geological control deep wildcatting can be extremely hazardous and costly for lack of adequate pressure and fracture gradient information.

ROLE OF VELOCITY IN SEISMIC WORK

The reflection seismograph measures time between the earth's surface and various subsurface reflecting horizons. If average velocity of seismic energy through the sedimentary column to a reflecting horizon is known, depth to the reflector can be determined. Thus, if enough reflection information is available, knowledge of subsurface structure can be obtained.

Well Velocity Survey

Techniques for determining velocities are well known in geophysics. The method most commonly used is the well velocity survey. Shots are detonated near the well, and travel times are recorded for energy to travel from the surface to a geophone placed at successive depths (usually 500' - 1000' increments). Difference in arrival times at the various geophone locations can be used to develop an average interval travel time or velocity profile.

Computed Velocities

A second technique is a more indirect method, which uses data from seismic field records to compute interval travel time profiles. In this method every shot in a routine seismograph survey provides data for velocity determination and is the basis for the predictive techniques discussed in this paper. Noteworthy improvements in accuracy of such measurements and resulting calculations have been attained with the advent of new field procedures, digital recording and machine data analysis.

ELEMENTARY REFLECTION PROBLEM

Several methods of computing interval velocities from seismograph data exist.⁵ All are based on

the same elementary reflection problem, as follows:

In Fig. 1, let SS represent the earth's surface. Assume the shotpoint O to be at the surface. When explosives at the shotpoint are detonated, acoustic energy is created in the form of compressional waves. This seismic energy moves equally in all directions. The vertically traveling energy strikes the subsurface plane, RR, and is reflected back to the surface, SS, along vertical path OPO. Energy from the shot also propagates along innumerable diagonal paths to the plane RR in the subsurface, (e.g., path OT) and is reflected back to the surface on path TW. The time required for the energy to travel the two ray paths is recorded by geophones at point O and W, separated horizontally by distance X.

With this information, depth to the reflecting horizon can be calculated and the average velocity in the medium between the surface and the reflecting horizon as follows:

- t_o = travel time along path OPO
- t_x = travel time along path OTW
- \bar{V} = apparent average velocity from surface to reflecting horizon

- From the relation that Distance = Average velocity x Time

$$\begin{aligned} \text{OPO} &= \bar{V} \times t_o \dots\dots\dots (1) \\ \text{OTW} &= \bar{V} \times t_x \dots\dots\dots (2) \end{aligned}$$

After extending the line OP vertically downward to the image point O', from elementary laws of optics:

$$\begin{aligned} \text{OTW} &= \text{O}'\text{W} \\ \text{OPO} &= \text{O}'\text{O} \\ \text{and} \quad \overline{\text{OTW}}^2 &= \text{O}'\text{O}^2 + \text{OW}^2 \dots\dots\dots (3) \end{aligned}$$

Substituting Equation 1 and 2 in Equation 3

$$\begin{aligned} (\bar{V}t_x)^2 &= (\bar{V}t_o)^2 + X^2 \\ \bar{V}^2 (t_x^2 - t_o^2) &= X^2 \\ \bar{V} &= \sqrt{\frac{X^2}{t_x^2 - t_o^2}} \dots\dots\dots (4) \end{aligned}$$

Depth to the reflecting bed may then be found by the relation:

$$Z = \bar{V} \times \frac{t_o}{2} \dots\dots\dots (5)$$

VELOCITY PROFILES FROM SEISMIC FIELD DATA

By making similar time measurements to other reflecting horizons in the subsurface, it is possible to develop a curve of V vs various values of t_0 . The final desired curve, interval travel time vs depth for 1000-foot increments of depth, can then be readily obtained.

In practice a geophone is not usually placed at the shot location, but there are ways to achieve the same result by extrapolating reflection hyperbolae to the zero x distance. Also, to minimize multiple events and enhance accuracy, data from more than one shot are usually combined for each velocity computation. The significant point to be brought out here, however, is the fact that sufficient data are available in records obtained during every routine seismograph survey to compute an interval velocity profile beneath the seismic line.

METHOD OF STUDY

Interval travel time-depth relationships of wells drilled through sand-shale sequences, predominately Tertiary sediments, of the Gulf Coast Basin along the Texas and Louisiana coast were studied. Additional data in limestone and chalk formations of inland Cretaceous zone wells of South Texas were obtained for the study of the effects of lithology on velocity. Confirming data were obtained from wells in California and Louisiana.

Interval travel time vs depth data from well velocity survey logs were plotted on logarithmic paper. Analysis of these curves determined the significance of the variation in interval travel time due to discreet variables such as degree of compaction, lithology, geologic age or geographic location, and abnormal pressure.

Abnormal pressure information was obtained from bottom-hole pressure surveys, wireline formation tests and, in some instances, induction and acoustic well logs. Well velocity surveys from 350 wells in the Gulf Coast Basin were used in this study. Of these wells 148 had encountered abnormal pressure before reaching total depth.

Bit run records were analyzed for a large number of wells in which velocity surveys were conducted to determine correlation between drilling rate and interval travel time. Log-log plots of average drilling rate based on drillers' reported bit runs and interval travel time from the velocity surveys were made for each well as a function of depth.

VARIABLES AFFECTING TRAVEL TIME

The affect of depth on velocity has long been recognized by geophysicists. ^{6,7,8,9} They have

generally agreed that interval velocity varies exponentially with depth according to some power law of the form:

$$V = K_1 Z^n \dots \dots \dots (1)$$

Where: V = Interval Velocity, Feet per Second

- K_1 = Constant
- Z = Depth in Feet

Or in terms of Interval Travel Time, T :

$$T = K_2 Z^{-\frac{1}{n}} \dots \dots \dots (2)$$

Equations 1 and 2 describe a straight line on a logarithmic plot where K_2 is numerically equal to the interval travel time at a depth of one foot, and n is the slope. The power n has been proposed empirically by various investigators between the values 4 and 17. In this study, however, when data from sections containing abnormal pressure, intervals of an unusual amount of shale, or formations other than sand-shale sequences, were carefully excluded, the value n was found to be 4.

The constant K_2 can be further expressed as three independent factors p , l , and a .

Or:

$$T = p l a Z^{-\frac{1}{4}} \dots \dots \dots (3)$$

Where:

- p , l , and a are dependent, respectively, on pore pressure, lithology, and geologic age.

Although Equation 3 was empirically derived from data obtained mostly in one area, there is no reason to believe that the same relation should not hold in other areas.

Equation 3 is significant. It states that at any given location in a sedimentary basin, the interval travel time will normally decrease linearly with depth when plotted on log-log paper; the slope of this line will be $1/4$. A sudden change in any one of the constants will manifest itself as a lateral shift in the line and will appear as an anomaly. Gradual changes such as geologic age (constant a) would not appear as an anomaly, but as a lateral shift in the entire plot.

EFFECT OF ABNORMAL PRESSURE (CONSTANT p)

Geophysicists have long been aware of low-velocity anomalies in the interval velocity-depth trend in certain areas. For instance in the well of Fig. 2, interpreters would have noted that the interval travel times decrease in a normal fashion to about 8500', then begin to increase. The beginning of these "velocity

inversions" were observed to coincide with the tops of certain formations, such as marine Frio, Vicksburg or massive shale sections.

These inversions define zones of abnormal pressure. Velocities are abnormally low because the formations are uncompact.

The degree of departure from a "normal" interval travel time-depth line is directly proportional to the abnormal pressure. Fig. 3 shows this relationship. A transparent overlay of the lines of equal pore pressure gradient (variations in constant p) serves as a convenient means for measuring abnormal pressures from the interval travel time-depth plots. To measure pore pressures the overlay is placed over the plot and is moved laterally until the normal pressure (9 lb/gal equivalent pore pressure) line coincides with the data in the normal pressure formations immediately above the velocity anomaly. Pore pressure gradients are then read from the superimposed lines of equal pore pressure. In Fig. 4 for instance, at 10,000', 18.6 lb/gal equivalent pore pressure is noted.

Pore pressures so determined should be within 1.0 lb/gal of the exact pressure. However, better accuracy can often be achieved.

EFFECT OF LITHOLOGY (CONSTANT 1)

Shale, because of its characteristic low velocity will produce an anomaly similar to a zone of abnormal pressure if it occurs in long intervals (Fig. 5). Undoubtedly the interval from 3000' to 5000' in the Gonzales Co. well was abnormally pressured at one time in its geologic history, but drilling experience indicates that the pressure is no longer present. These zones can usually be identified by their characteristic apparent 14 lb/gal pore pressure reading.

Limestone appears to compact at the same rate as sands and shales, but follows a "limestone compaction line" displaced to the left of and parallel to the "normal" sand-shale compaction line. Dolomite is a harder, more dense rock, and usually transmits energy faster than limestone; therefore it is displaced further to the left, as in the Kendall Co. well, (Fig. 5).

Abnormal amounts of limy or calcareous sands and siliceous shales also decrease interval travel times. In many areas of South Texas and Louisiana a section of calcareous sand and shale overlies deep abnormal pressure zones. This material shows up on the interval travel time-depth profile as an anomaly of lesser interval travel time. Thicknesses have been observed to vary from several hundred to as high as 6000'. Examples are shown in Fig. 6.

In example A such a zone occurs between 8000' and the top of the abnormal pressure zone at 12,500'. To measure pore pressures in such a case the normal pressure base line of the overlay must be shifted to the left to coincide with a new base line established immediately above the abnormal pressure zone.

EFFECT OF GEOLOGIC AGE (CONSTANT a)

It was noted that the wells with generally greater interval travel times were located towards the Gulf. Those with lesser interval travel times were located inland. Intuitively this shift from inland, older sediments, to more recent, less compacted sediments closer to the Gulf is expected. The lateral shift can be observed more readily by noting the depth at which the line crosses a given vertical reference line such as the 100 microsec/foot line. Thus a broad measure of depositional age is the depth at which formations of 10,000 feet/sec velocity are found.

In Fig. 7 Well A, Nueces Co., Texas, penetrated Lower Pliocene and Upper Miocene formations of estimated 8 to 10 million years of age at the same depth in which Well B, offshore Louisiana, found much younger beds. Slopes of the compaction lines for the two wells are the same, but overall interval travel times for the Louisiana well are greater. The sediments have had less time to compact.

Much older formations are present in Fig. 5. The Kendall Co., Texas, well penetrated beds of Cretaceous and Paleozoic age (150 - 250 million years). Note the depth at which we find beds of 100 microsec/foot interval travel time - 1,000 feet, compared to 10,000 feet for the Louisiana well. The formation at 1,000 feet in this well is therefore interpreted to be similarly compacted as the formation at 10,000 feet in Louisiana.

A family of curves showing the relationship of age of burial to the interval - velocity - depth trend in normal - pressure formations of the Gulf Coast area established by this study is shown in Fig. 8.

FRACTURE GRADIENT ESTIMATES FROM SEISMIC DATA

The most critical phase in drilling an abnormal pressure well is setting protective casing in a pore pressure which will permit the use of subsequent higher mud weight without fracturing and losing returns. Fracture gradients have largely been determined empirically. Experience has shown, for instance, that formations break down under substantially lower mud weights, and therefore surface casing must be set deeper in South

Louisiana than in Texas. The lower frac gradient in Louisiana is due largely to the lower overburden weight of the younger beds.

From a knowledge of the overburden gradient and basic rock mechanics^{12,13,14} one can find the frac gradient at a given location using the relation:

$$\text{Frac Gradient} = K (\text{Overburden Gradient} - \text{pore pressure}) + \text{pore pressure} \quad (5)$$

Overburden gradient - Weight of the overburden acting on a formation at a given depth is a function of average bulk density of the rock and the depth. Bulk densities of sedimentary rock are roughly proportional to their degree of compaction.¹¹ Since velocities also depend on rock compaction, a predictable relation between bulk density and velocity can be expected. For instance, in Pliocene - Pleistocene formations of southern Louisiana (100 microsec/ft. interval travel time at 9000' - Fig. 8) overburden gradients would be low compared to those occurring in older formations such as those found in South Texas (100 microsec/ft. at 5000'). Figure 9 shows how this variation with depth changes with geologic age.

Factor K is the effective stress ratio, and can be estimated empirically from hydraulic fracture data. It is the ratio of the effective horizontal stress (computed from the instantaneous shut-in pressure after a frac job) and the vertical stress (computed from the weight of the overburden). Basically it is a function of an elastic constant of the rock (Poisson's Ratio) and long term deformation or creep which tends to equalize stress in all directions. It is quite possible that the latter effect will cause K to vary not only with depth but also with geologic age, or location as reported by Mathews and Kelly.⁴ However, it is believed that overburden gradient, which is in itself influenced by geologic age, is the controlling factor. For the estimating purposes proposed here, the K factor vs depth relation (Fig. 10) is assumed to be the same for all areas.

ESTIMATING FRACTURE GRADIENT FROM SEISMIC DATA

To estimate fracture gradients for a given location first note the depth at which the seismic interval travel time - depth curve crosses the 100 microsec/foot reference line. This will define the proper curve in Fig. 9 for estimating the overburden gradient at that location. Find K from Fig. 10. Compute fracture gradient from Equation 4.

DRILLABILITY ESTIMATES FROM SEISMIC DATA

As a general rule, penetration rate tends to decline with depth. Primarily this decrease is a

result of increased compaction with depth, which increases the mechanical strength properties of the rock. As discussed previously, the compaction force, which is the weight of the overburden, acts on the rock and its contained fluids, or

$$\bar{S}_z = S_z + p_o \dots \dots \dots (5)$$

where

- \bar{S}_z = Total vertical load (gross stress)
- S_z = Rock frame stress
- p_o = Pore pressure

As overburden gradient \bar{S}_z increases with depth and geologic age under constant hydrostatic pore pressure conditions, the rock frame stress, S_z , increases accordingly. Drillability of rocks of a given lithology should therefore vary generally in accordance with variations in S_z . As pore pressure, p_o , increases under abnormal pressure conditions, the rock frame stress, S_z , must decrease, thus an increase in drilling rate results.

Gross changes in lithology can be expected to affect drilling rate because of the basic change in physical strength properties.

Fig. 11 shows that drilling rate decreases exponentially with depth and lithology in a manner similar to interval travel time. The well was drilled with constant bit weight and rotary speed to 8,500 feet in sands and shales. A reduction in drilling rate was noted at the top of the calcareous sand and shale interval, followed by a further reduction at 10,000 feet when rotary speed was reduced from 140 rpm to 70 rpm. At 13,000 feet a sharp increase in drilling rate signals top of abnormal pressure.

A study of similar data from wells drilled in formations of different geologic ages resulted in the series of drilling rate - depth curves of Fig. 12 showing reduction in drilling rate with depth as a function of location as revealed by the interval travel time profile.

To illustrate the use of this chart for predicting potential drilling rate, two seismic interval travel time - depth profiles are shown. The seismic interval travel time profile obtained at Location A intersects the 100 microsec/foot reference line at 2,000 feet. Therefore drilling rate of a well drilled at this location should follow line A-A'. Similarly a well at Location B should follow line B-B'. At 10,000 feet, Well A should drill in a normal sand-shale sequence at the rate of 6 ft/hr and Well B, 70 ft/hr. For other weights and rotary speeds, adjustments are made in the estimates assuming direct dependence of drilling rate on those two parameters.

Estimates thus made are only approximate, but should provide useful data for planning purposes where no other data are available.

FIELD EXAMPLE - WELL B

A routine survey was conducted consisting of a pattern of seismic lines running approximately northwest-southeast and north-south (Fig. 13). Shotpoints for the survey were spaced every 400 feet. For each shot, 24 geophone patterns were located 400 feet apart along the line, starting 400 feet from the shotpoint and extending out to 9,600 feet. Two of these lines, 3-29 and 3-33, helped define a deep-seated structure with its apex directly beneath shotpoint x65-1279 on line 3-29.

The structure was found to dip to the east toward line 3-33, a strike line running north and south along the flank. The contour of the mapped horizon beneath line 3-33 is 400 feet downdip from the high point. Shotpoint x65-1279 on the high point of the structure and on the dip line 3-29 was selected as the location for Well B.

Information on the depth to abnormal pressure and maximum expected mud weight required to drill to 16,000 feet total depth was desired. Also information concerning frac gradients was needed to help plan the casing program.

Unfortunately, field records of the portion of the line directly over the proposed location were missing, so data were selected from seismic records about 3/4 mile down the line as shown. Due to the steep dip along this portion of the line and the presence of diffractions from a nearby fault, good reflections above 11,000 feet at this location were limited. Hence the excellent data from strike line 3-33 are presented here. Conclusions substantiated the first survey but provided more detail.

Fig. 14 presents the results of the computations made from the seismic record representing subsurface coverage from shotpoints x65-3889 through x65-3905 on line 3-33. Each point plotted on the curve is the average velocity for reflection events at various times. The final interval travel time - depth profile obtained from these data is plotted for 1,000-foot vertical increments in Fig. 15.

An engineering interpretation of the seismic data of Fig. 15 was made as follows:

Abnormal Pressure - It was estimated that top of the abnormal pressure zone would be at 10,500 feet. With the calibration overlay shifted to the left to coincide with the normal formations immediately above the abnormal

pressure zone, it was found that formation fluid pressure gradients equivalent to the following would be encountered:

<u>Depth - Ft</u>	<u>Pore Pressure - Lb/Gal</u>
11,000	12.0
13,000	17.0
16,000	18.2

Drillability - The travel time - depth curve crosses the 100 microsec/foot reference line at 4,000 feet. Therefore from Fig. 10 it was estimated that, assuming 4,000 lb/in bit weight and 150 rpm rotary speed, drilling rate would gradually decrease from 70 ft/hr at 4,000 feet to 14 ft/hr at the top of a 2,000 foot calcareous sand-shale interval beginning at 9,000 feet. Average rate through this 2,000 foot interval would slow down to less than 8 ft/hr. At the top of the abnormal pressure zone a marked increase in drilling rate could be expected.

Fracture Gradients - The position of the compaction line with respect to the 100 microsec/ft reference line indicates that the well would be drilled in formations of estimated lower Miocene to upper Eocene age (Fig. 8). Therefore a surface casing setting of 2,500 feet should be adequate.

Calculations (Eq. 4) confirmed that the formations immediately below the surface casing should safely withstand 14 lb/gal mud weight while looking for the 12 lb/gal protective casing seat.

With protective casing set at 11,100 feet in 12 lb/gal pore pressure, the frac gradient immediately below the casing was estimated:

$$\begin{aligned} \text{Frac Gradient} &= .85 (19.9 - 12.0) = 12.0 \\ &= 18.7 \text{ lb/gal} \end{aligned}$$

Therefore unless trouble developed, a liner would not be required to reach 16,000 feet.

COMPARISONS OF PREDICTED AND ACTUAL MUD AND CASING PROGRAMS

Well B was drilled to 16,050 feet. During completion operations accurate subsurface pressure measurements were obtained. Actual drilling rate, mud and casing programs, and formation fluid pressures are compared with the estimates based on seismic data in Table 1.

Fracture gradients measured during hydraulic fracturing operations through perforations at 11,535 feet was 19.2 lb/gal. Measurements obtained during abandonment operations in open hole below the liner seat at 11,640 feet showed

a gradient of 19.7 lb/gal. The calculated fracture gradient based on seismic data was 18.7 lb/gal at 11,100 feet and 19.9 lb/gal at 13,000 feet.

LIMITATIONS

The degree of accuracy demonstrated may not be experienced in all areas. However, less accuracy may be adequate for planning purposes, for which the predictive technique is designed. Accuracy of the velocity computations depend on quality of the original seismic records and on careful data playback and analysis. In general the more recent surveys using long spreads and improved recording techniques are superior, particularly where information at extreme depths is required.

This method has been most successful along the Gulf Coast, where abnormal-pressure zones have been accurately predicted at depths as shallow as 6,500 and as deep as 12,000 feet. The technique is limited to sedimentary basins in which the velocity changes with depth result from compaction phenomena.

Other sources of information, such as paleontological data, log plots of nearby wells, regional geology, and drilling experience in the area should be used for comparison during the planning phase. Density measurements of cuttings, well kicks, penetration rate, temperature measurements, hole instability, and other indications should be watched while approaching the pressure transition zone and used to pick the exact casing depth required for optimum control.

CONCLUSIONS

1. Interval travel time of seismic energy decreases exponentially with depth in normally compacted sediments. Any departure from this normal trend is caused by the presence of abnormal-pressure formations or gross changes in lithology.
2. Methods are available for computing interval travel time profiles from routine seismic data.
3. Engineering interpretations of these seismic profiles have been used extensively and successfully to estimate approximate depth to abnormal-pressure zones and magnitude of the fluid pressures therein, and to obtain estimates of drillability and fracture gradients.
4. The correlations presented in this paper, although developed under Gulf Coast

conditions, should be applicable in any sedimentary basin. Use in offshore areas should be particularly rewarding.

ACKNOWLEDGEMENTS

Appreciation is expressed to Humble Oil and Refining Company for permission to publish this paper. The author is especially indebted to D. C. Meyer, Steve Starr and other Humble Exploration and Esso Production Research Company personnel for their help, encouragement and critical comments in this work.

REFERENCE AND BIBLIOGRAPHY

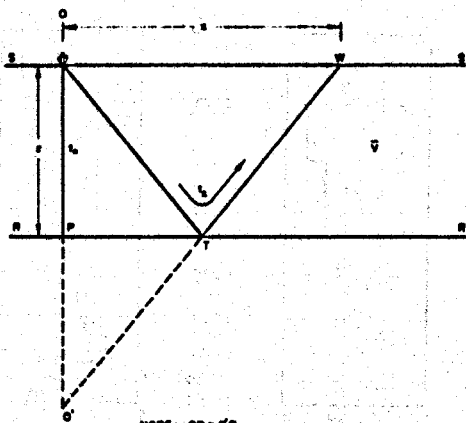
1. Pennebaker, E. S., "Detection of Abnormal Pressure Formations from Seismic Field Records", Paper No. 926-13-C Presented to the Southern District Meeting of API, San Antonio, Texas, March 6-8, 1968
2. Hottmann, C. E. and Johnson, R. K., "Estimation of Formation Pressures From Log-Derived Shale Properties", Jour. Pet. Tech. (June, 1965) pp. 717-722
3. Wallace, W. E., "Abnormal Subsurface Pressures Measured From Conductivity on Resistivity Logs", Oil & Gas Journal (July, 1965) Vol. 63, pp. 102-106
4. Matthews, W. R., and Kelly, John, "How to Predict Formation Pressure and Fracture Gradient", Oil & Gas Journal (February 20, 1967)
5. Dix, C. H., "Seismic Velocities From Surface Measurements", Geophysics (January, 1955) Vol. XX, No. 1, pp. 68-86
6. Faust, L. Y., "Seismic Velocity As A Function of Depth and Geologic Time", Geophysics (April, 1950) Vol. 16, pp. 192-206
7. Kaufman, H., "Velocity Functions in Seismic Prospecting", Geophysics (1953) Vol. 18, pp. 289-297
8. West, S. S., "Dependence of Seismic Wave Velocity Upon Depth and Lithology", Geophysics (1950) Vol. 15, pp. 653-662
9. Sarmiento, R., "Geological Factors Influencing Porosity Estimates From Velocity Logs", Bulletin A.A.P.G. (1960) Vol. 45, No. 5, pp. 633-644
10. Nettleton, L. L., Geophysical Prospecting for Oil, McGraw Hill Book Company, New York, 1940

- | | |
|--|---|
| <p>11. Howell, L. G., Heintz, K. O., and Barry, A. "The Development and Use of a High-Precision Downhole Gravity Meter", <u>Geophysics</u> (August, 1966) Vol. XXXI, No. 4, pp. 764-772</p> <p>12. Hubbert, M. K., and Rubey, W. W., "Role of Fluid Pressure in Mechanics of Overthrust Faulting", <u>Geological Society of America Bulletin</u> (February, 1959) Vol. 70, pp. 115-206</p> | <p>13. Hubbert, M. K., and Willis, D. G., "Mechanics of Hydraulics Fracturing", <u>Transactions, AIME</u>, (1957) Vol. 210, pp. 153-168</p> <p>14. Gretener, P. E., "Can the State of Stress be Determined from Hydraulic Fracturing Data?", <u>Journal of Geophysical Research</u> (December 15, 1965) Vol. 70, No. 24</p> |
|--|---|

Table 1.

COMPARISONS OF PREDICTED AND ACTUAL MUD AND CASING PROGRAMS

	<u>Estimated</u>	<u>Actual</u>
Surface Casing Set at	2,500 ft	2,505 ft
Top of Abnormal Pressure	10,500	10,200
12.0 ppg pore pressure at	11,100	11,000
Protective Casing set at	11,100	10,875
Liner Set at	--	11,640
Fore Pressure Gradients		
10,525 ft	--	10.6 ppg
11,100	12.0 ppg	--
11,306	--	14.8
12,311	--	716.6
13,000	17.0	--
13,965	--	717.3
Maximum Mud Weight	18.1	718.2
Drig. Rate at 4000 ft.	70 ft/hr	76 ft/hr
Drig. Rate at 9000 ft.	14 ft/hr	19.5 ft/hr



NOTE: $OP = O'P$

SS = Horizontal surface of the ground
 RR = Horizontal reflecting surface
 z = Vertical distance to reflection point P
 a = Horizontal distance to geophone W
 v = Average velocity of the medium between the surface and reflecting plane RR
 O = Image of Shotpoint O'
 L = Two way travel time along Path OPO
 t = Travel time along Path OTW

Fig. 1 - Elementary reflection problem

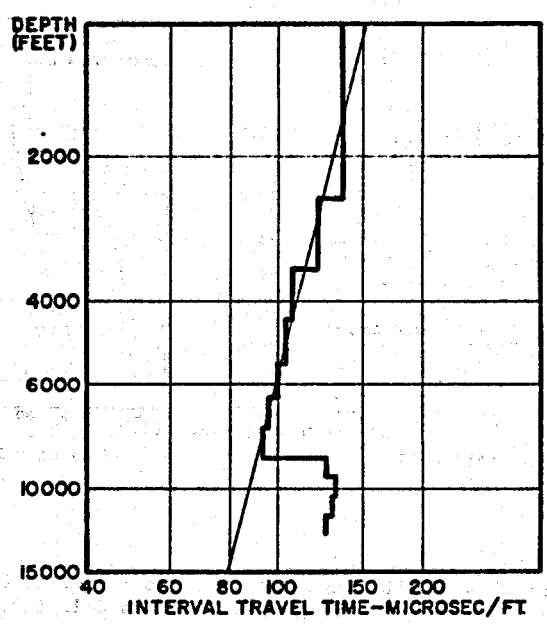


Fig. 2 - Logarithmic plot of interval travel time, Well A, Kleberg County, Texas, showing abnormal pressures below 8500 feet.

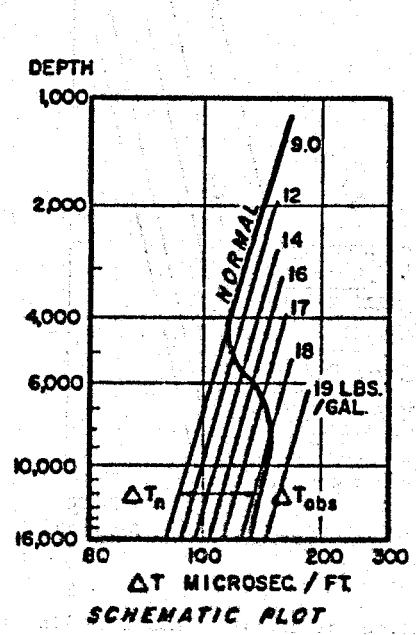


Fig. 3 - Abnormal pressure as related to degree of departure from normal pressure base line.

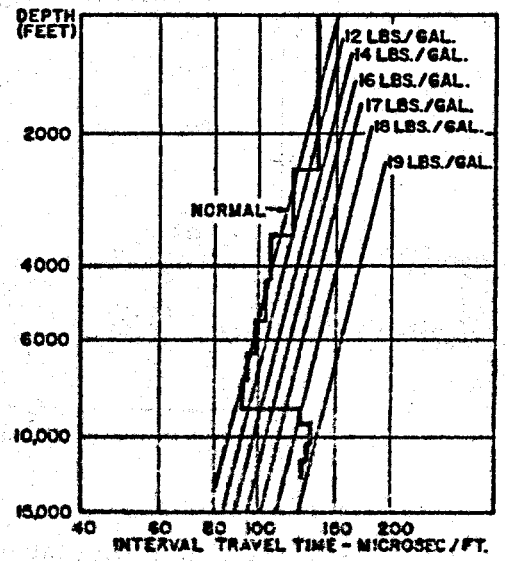
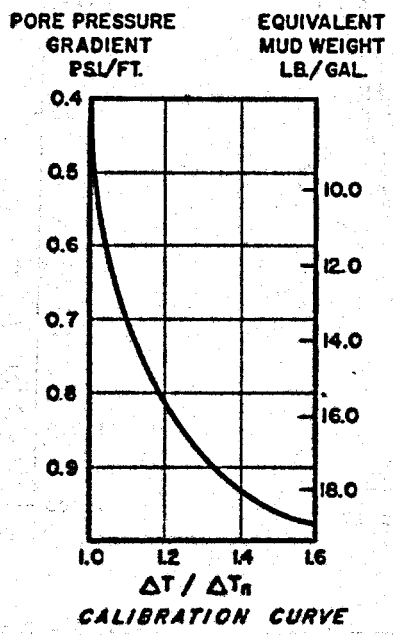


Fig. 4 - Use of calibration overlay to measure abnormal pressure.

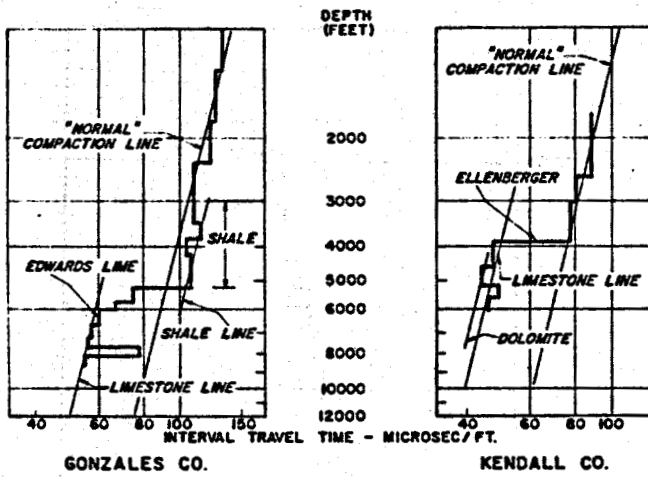


Fig. 5 - Examples showing anomalies in normal base line due to shale, limestone, and dolomite.

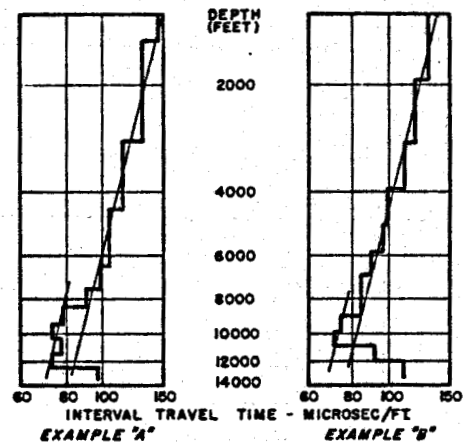


Fig. 6 - Examples showing shifts in the normal base line due to calcareous sands and shales.

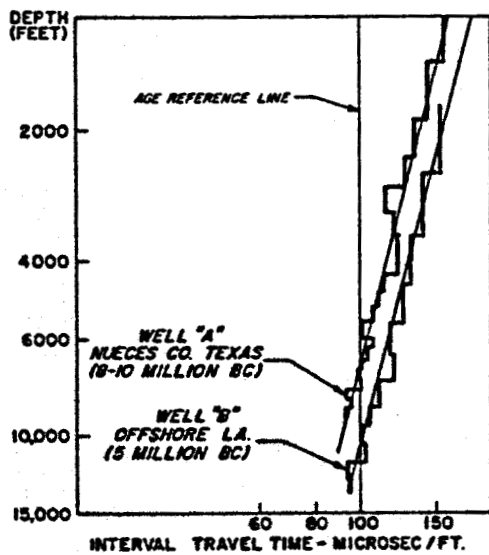


Fig. 7 - Examples showing shifts in normal base line due to Geologic Age of formations drilled.

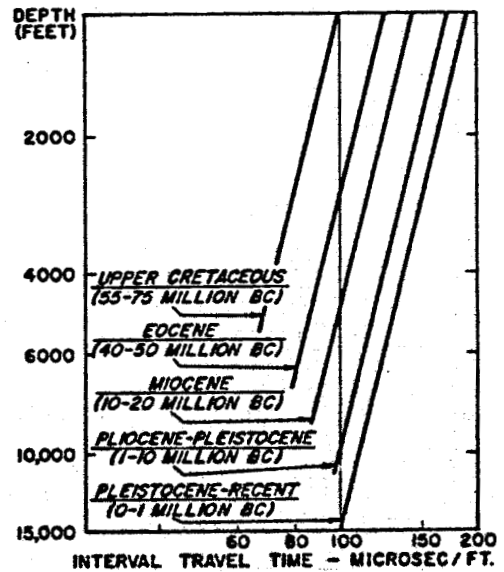


Fig. 8 - Position of normal compaction line as related to Geologic Age of Gulf Coast sediments.

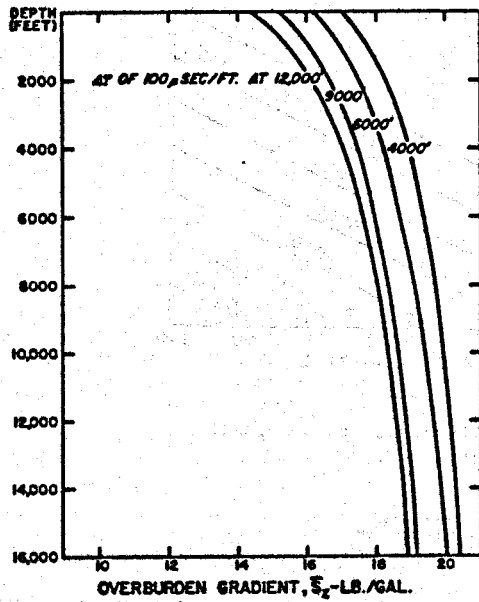


Fig. 9 - Overburden gradient based on average bulk density between depth point and the surface for different Geologic Age base lines. For use in estimating fracture gradients.

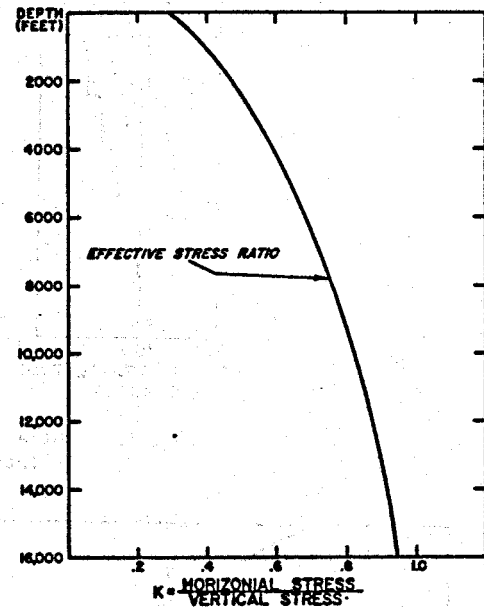


Fig. 10 - Function K vs depth - For use in estimating fracture gradients.

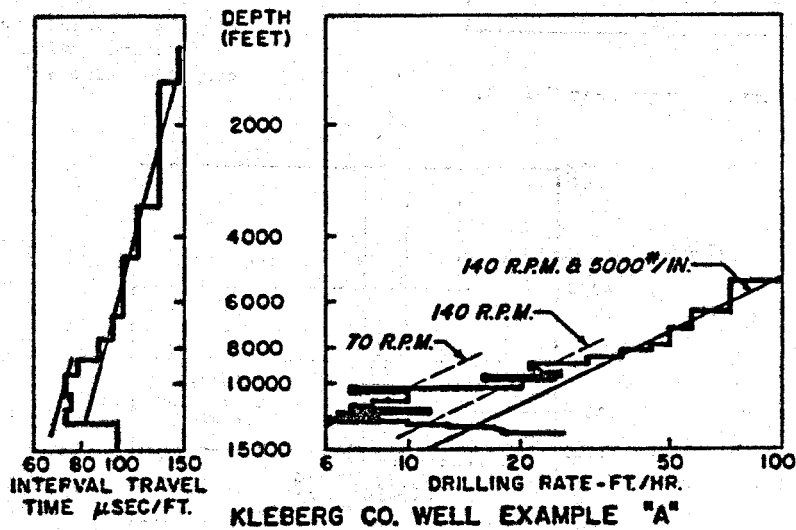


Fig. 11 - Example showing how drilling rate decreases with normal compaction and lithology, and increases due to abnormal pressure.

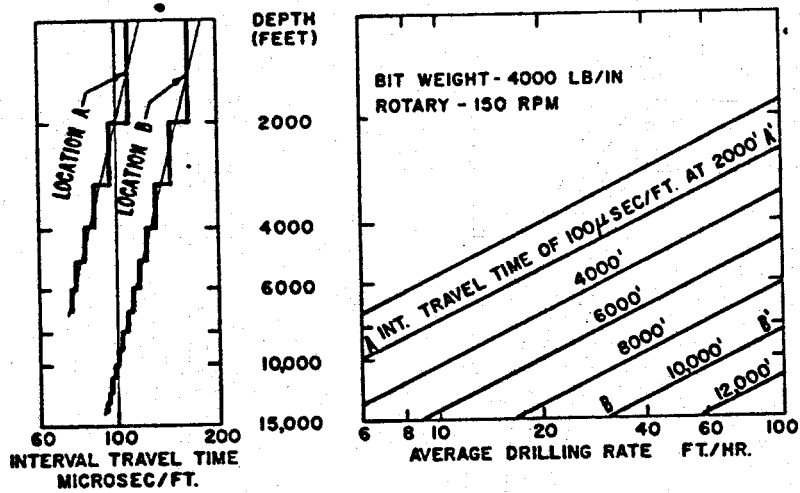


Fig. 12 - Guide for estimating drilling rate from seismic interval travel time profiles.

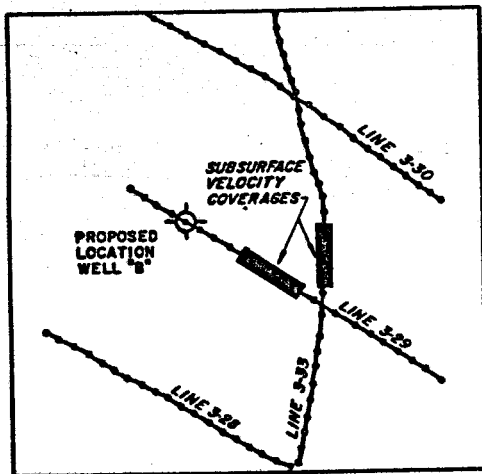


Fig. 13 - Seismic surveys near Well B.

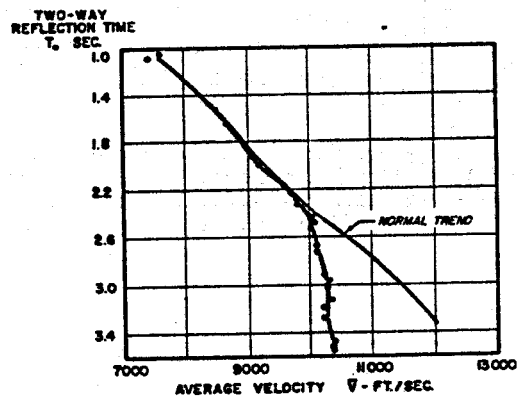


Fig. 14 - Average velocities between the surface and various subsurface reflectors computed from seismic data near Well B.

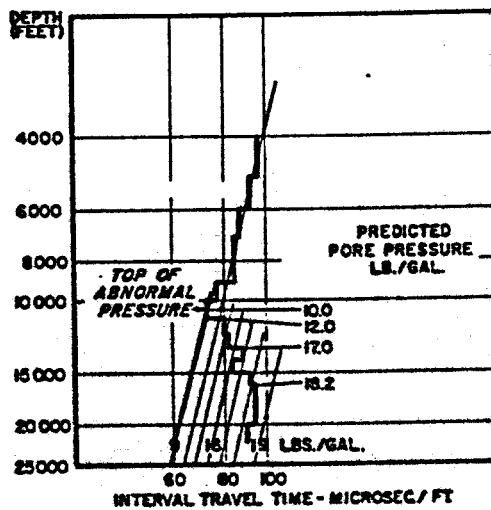


Fig. 15 - Interval travel time profile computed from seismic field data at Well B Location. Abnormal pressure was predicted below 10,000 feet.

THIS IS A PREPRINT --- SUBJECT TO CORRECTION

Water Production from Abnormally Pressured Gas Reservoirs in South Louisiana, Part II

By

W. E. Wallace, Member AIME, Forest Oil Corp., Lafayette, La.

© Copyright 1968

American Institute of Mining, Metallurgical and Petroleum Engineers, Inc.

This paper was prepared for the 43rd Annual Fall Meeting of the Society of Petroleum Engineers of AIME, to be held in Houston, Tex., Sept. 29-Oct. 2, 1968. Permission to copy is restricted to an abstract of not more than 300 words. Illustrations may not be copied. The abstract should contain conspicuous acknowledgment of where and by whom the paper is presented. Publication elsewhere after publication in the JOURNAL OF PETROLEUM TECHNOLOGY or the SOCIETY OF PETROLEUM ENGINEERS JOURNAL is usually granted upon request to the Editor of the appropriate journal provided agreement to give proper credit is made.

Discussion of this paper is invited. Three copies of any discussion should be sent to the Society of Petroleum Engineers office. Such discussion may be presented at the above meeting and, with the paper, may be considered for publication in one of the two SPE magazines.

ABSTRACT

In some cases, when gas is produced from a geopressed reservoir, water will appear in quantity, occasionally to the exclusion of all gas. If a reservoir contained only gas, the P/Z vs. cumulative production plot should be a straight line throughout its producing life. Extrapolation to P/Z = 0 should indicate the original gas in place. In those cases where water appears, this relationship may or may not hold. Often the reservoir fails to produce the calculated recoverable reserve by a substantial margin. This margin may be water which entered the reservoir.

The Gulf Coast area contains many thick sections of undercompacted shales with interspersed geopressed sand lenses. When pressures within these lenses are reduced by gas production, the compaction process, interrupted by a state approaching equilibrium, is permitted to resume. As a result, water is expelled from the shale into the space formerly occupied by the gas and ultimately reaches the well bore.

Uniform shale-water influx may produce a straight line P/Z vs. cumulative plot which represents gas expansion and water influx. This gives an erroneous in-place estimate on the high side. In some cases the shale-water influx varies with the pressure differential causing the P/Z vs. cumulative plot to be curved. Sometimes the drive is sufficient to equal the effect of withdrawal.

Cases with pressure-depth ratios from .5 to .9 are examined.

This condition has been called "retarded water drive", "partial water drive", and the like. The true source of the water is the shale which bounds the reservoir. This activity can be anticipated and calculated if sufficient information about the general conditions are known. If not, the early pressure history should give a strong hint of the ultimate outcome, but in some cases no accurate estimates can be made.

References and illustrations at end of paper.

INTRODUCTION

In this paper we are limiting our investigation to so-called "volumetric" reservoirs; those having sandstone porosity surrounded by shale, containing gas, condensate, and salt water, all under conditions which, at least in the beginning, exceeded a pressure-depth ratio of .465 psi/ft. All examples are taken from fields in South Louisiana and are of ages ranging from Oligocene (Frio) to Miocene. We have included reservoirs which produced gas, condensate, and varying amounts of water. Some produced 100% water, some lesser amounts or no water at all; and the most problematical of all, those in which water influx is only suspected.

A column of sea water has a pressure-depth ratio of .465 psi/ft. This is considered the normal hydrostatic pressure. Larger ratios require special explanations. It has just happened that the majority of our cases have pressure-depth ratios of .8 plus. Only one case of .9 plus was available, although there are others in the area. Examples with much smaller ratios are included to illustrate certain points. We are concerned with the case of the gas well which "watered out" (100% water) but still had a substantial amount of surface pressure. The very low topographic relief in Louisiana precludes any appreciable pressure "head" derived from the elevation of the surface outcrop of a sand. So, greater pressure ratios require special investigation.

In an early phase of this study we noted that several reservoirs went through a more or less definite pressure drop before salt water appeared with the gas. This pressure drop was often in the neighborhood of 1000 psi. There were both variations and exceptions. The expansion of that investigation has become the basis of this report. Our attempt to make a series of simple predictions changed into a list of complicated qualifications. The appearance of water or its failure to appear in wells follows a definite pattern of conditions which we will discuss in the following pages.

In text books the flow of water into reservoirs is termed "water influx" and Craft and Hawkins (1959) in "Applied Petroleum Reservoir Engineering" have a chapter on the subject and numerous references elsewhere. We quote:

"The water which encroaches into a reservoir upon a decline in pressure may be due to one or a combination of the following: (1) artesian flow, where the water-bearing strata outcrops at the surface, (2) expansion of water in the aquifer, (3) expansion of known or unknown accumulations of oil and/or gas in the aquifer, and (4) compaction of the aquifer-rock."

The concept of the water coming from the surrounding shale was apparently not anticipated in item "(4)". We, (Wallace, 1962) presented a paper concerning the water production from abnormally pressured gas reservoirs in which we were primarily concerned with unusual reservoir space arrangements of gas and water, and the expansion of dissolved methane. It is interesting to note that we downgraded the effect of shale compaction as a source of much water. Today we have reversed our stand and feel that shale compaction is a source of the majority of this water with the mysterious origin.

Other references to shale as a source of limited water drive have been rare. Gordon Atwater (1965), in a paper before the American Association of Petroleum Geologists, questioned the possibility of water from shale creating a "partially effective water drive" in a gas field near New Orleans.

The writer has taken the opportunity whenever possible to discuss with experienced engineers the source of water influx into abnormally pressured reservoirs. Frequently the reply has been that the water probably entered as a result of faulty cement jobs, parted or leaky casing, communication with other well streams, breakdown of geological barriers, such as fault seals, and the like. Recently there has been much new literature on shale compaction and water escape as related to drilling and casing problems. Compacted and undercompacted shale have been related to reservoir pressures through conductivity and resistivity logs, density logs, sonic logs, and the rates of bit penetration. There has been very little tendency to relate this and the possible floods of escaping shale water to the "water influx" described in engineering textbooks. Of course, much of this reported water is normally pressured, even so, much of it probably is compressed from shale.

ABNORMAL PRESSURES

Abnormally pressured reservoirs have been found in many of the oil and gas provinces of the world. The list now includes the following states and countries: Louisiana, Texas, Arkansas, California, Oklahoma, Wyoming, Pakistan, Trinidad, north Germany, Burma, Colombia, Argentina, Iran, France, Rumania, Venezuela, Algeria, Netherlands, New Guinea, and Iraq. Two fundamental papers on the subject were by Dickinson (1953) and Thomeer and Bottema (1961). Of outstanding merit are the papers of Hubbert and Rubey (and Rubey and Hubbert, 1959). This joint effort contains a vast amount of observations and deductions on compaction, pressures, and the behavior of fluids in subsurface environment from a mathematical point of view. It is unfortunate that this "gold mine" of material should have appeared under a title including the words "Mechanics of Overthrust Faulting". Most of the basic concepts are introduced or reviewed in these papers. Engineers interested in a broad study of subsurface pressures and their causes should seek out these papers.

The sources of abnormal subsurface pressures are usually attributed to one of the following:

1. The very rapid deposition of large quantities of sands and shales, with shale predominating, may result in sand bodies which are completely surrounded by shale. As the compaction process progresses, water from the shale will be expressed into the available sands. Any water unable to escape, is forced to help support the growing overburden. This increasing overburden is the source of the pressure. The lack of escape routes for the water may be lensing of the sand body, faulting, and impermeability due to mineralization or other causes. The process of deposition is taking place faster than the adjustment of the included fluids.

2. Abnormal pressures are also reported from areas of high topographic relief where the outcrop of the pressured sand is at an elevation sufficient to result in an artesian head. This condition is reported in some of the older fields of Iran, with pressure-depth ratios of .8 and .9+.

3. A third category involves thick gas caps in otherwise normally pressured conditions. It is customary to refer to the pressures at the water/gas interfaces to avoid confusion on this point.

4. There are other miscellaneous causes such as reverse osmosis; (Young and Law 1965) mineral decomposition, release of water of crystallization (Powers 1967) and others which we do not believe have an important bearing on the subject of this paper.

The exact number of abnormally pressured reservoirs in South Louisiana is not known. Accurate data has never been compiled. Gordon Atwater (1965) made a rough compilation for producing reservoirs from DT-1 Reports for December 1962, with the result that 11% were judged to be abnormal out of a total of 2059. The number of abnormally pressured reservoirs to be counted will increase as deeper drilling continues.

SHALE COMPACTION

Shales consist primarily of clay minerals, which have small grains with flat or tabular shapes, with an unusual affinity for water. The initial deposition takes place as soft muds with water contents ranging up to 90%. As these muds are buried by more mud and sand, a gradual compaction takes place. The mineral grains are pressed into more intimate contact with each other and the water in the intervening spaces is expelled. The quantity of water expelled is ultimately larger in volume than the resulting shale. The rock in the final stage has almost 100% mineral solids and 0% water. In the early stages the shale has high values of porosity and relatively high permeability. The escaping water flows to the channel of escape with the least pressure, usually a porous sand layer. Both porosity and permeability decline with increasing depth of burial except when compaction is slowed by limited escape conditions. A firmly compacted shale has usually been reduced by 50% in thickness at about 5000', all due to water loss. Water-wet shales retain their permeability to water long after the surface tension has blocked the further passage of undissolved gas.

Ultimately a state of equilibrium is reached, the pressures being approximately equal in all directions. This state depends on the availability of escape routes, usually the presence or absence of blanket sands, the type of clays present, and other factors.

In the compaction of sand, the grains reach a stage of direct contact with each other almost from the beginning. Compaction of sand at this relatively early stage is essentially complete. Two more types of direct porosity reductions may occur: (1) the forced rearrangement of individual sand grains by extreme pressure, and (2) the solution of the grains at the points of contact. These require high pressures, vast amounts of time, or both.

Shale particles, although flat in general, have relatively "springy" contacts with each other. The compaction process takes place gradually over a great range of pressures and other conditions. In the early stages, the grains touch lightly, if at all. Many of the minerals are in the form of stacks of thin sheets with layers of oriented water molecules attached to each sheet. Each sheet is the crystal surface of a clay mineral. We do not feel that we have space here to enlarge upon the details of clay mineralogy and associated water phenomena.

It is fundamental to our explanation to understand the relation of the different internal pore pressures. A column of sea water will exert an internal supporting pressure of .465 psi per foot of depth. The rock load, including liquids, is approximately 1.0 psi per foot of depth, thus the remainder .535 psi per foot of depth, is supported by the direct contact of the minerals with each other. This concept is explained in detail by Hubbert and Rubey (1959).

If conditions are abnormal, and this can occur in both directions, the internal pore pressure may be either greater or smaller. For example, most of the cases reported in a later part of this report originally had a pressure-depth ratio of .8+ and there are a few known cases of .9+. In the case of the former, the load of 1.0 is supported .8 by pore pressure (fluid or gas) and .2 by the contact of the rock minerals (80% versus 20%). In a depleted reservoir the reduction in pressure may leave a ratio of .3. Thus the support of the pore pressure is .3 and of the minerals .7 (30% versus 70%). The latter case may result in subsidence, which has occurred in many instances.

A recent article by Marsden and Davis (1967) reviewed the case of Goose Creek (Texas), Long Beach (California) and others. In general, the withdrawal does not result in any noticeable surface subsidence although actual subsidence does occasionally occur. In the problem being covered in this paper the subsidence which would be applicable would be due to water squeezed from shale and the loss of thickness of that shale.

Shales surrounding abnormally pressured aquifers and reservoirs contain pore pressures of equal abnormality. In theory, the compaction process has been interrupted or arrested at some time in the past when the depth of burial was less. Meanwhile, added loads of sediment have increased the degree of abnormality. Vast quantities of water would therefore be available if the compaction process should be resumed. This process may be resumed if gas or water are withdrawn from an abnormally pressured "volumetric" reservoir and associated aquifer.

WATER INFLUX AND VOLUMETRIC RESERVOIRS

We are, in this limited case, concerned with the water expelled from shale. We will consider as "volumetric" those closed porous sand lenses which will change little in total volume with internal pressure reductions of several thousand psi. Textbooks contain corrections for the compressibility of water, variations in temperature and solubility of methane in brine. For our purposes we will neglect these and other well known corrections, which serve to improve the reliability of material balance calculations. We are concerned with water which comes in from outside the sand body.

Every square inch of the shale surface surrounding a sand body will give up some water if the pressure differential is large enough (Chilingar and Knight 1960). When there is withdrawal of gas or liquid, the principal pressure drop is at this shale-sand boundary. Any fingers or layers of shale between the sand layers, or within the gross borders of the sand body, will also give up

water, being a part of the shale-sand boundary. Thus the water will come from both the upper and lower surfaces and from above as well as below the gas-water interface. In complex cases, the water may appear in unexpected places and not necessarily as an evenly developed rise of the level of the gas-water interface. The individual complications of interfingering may prevent complete gravity separation of the water. This explains some cases of wells in higher structural positions which watered-out first. In the case of a uniform blanket sand of good permeability, the water may accumulate uniformly and rise steadily as if flowing from beneath the gas cap.

Porosity is the percent of space in a rock. In effect it represents the percent of water filled space or available water. Data on shale porosity are scarce inasmuch as more interest is pointed at the porosity of sands. However, recent interest in logging techniques, as applied to reservoir pressures, has made much information available. It has been found that undercompacted shales, that is, shale with more water than is normal for their depth of occurrence, have the following characteristics or identifying associations:

1. Resistivity logs register low resistivities, frequently .5 ohm/meter or less. Similarly, conductivity values often exceed 2000 millimhos, and on occasion exceed 4000 millimhos.
2. Density logs report shale densities lower than normal for the depth.
3. Sonic or acoustic logs give a velocity inversion. The velocity of sound in shale is less than normal for the depth.
4. The high water content of undercompacted shales permits faster drill bit penetration. These "water-logged" shales are notable for high speed bit penetration, dramatically different from the rates for normally compacted shale.
5. The pressure-depth ratio of a reservoir is often known. This number is directly proportional to the water content of the shale. Underpressured reservoirs are sometimes found, most being the result of hydrocarbon or water withdrawal. Shales adjacent to

zones with lowered pressures are undoubtedly undergoing active adjustment.

The previous five categories indicate five sources of quantitative data on water available to be forced from shale into an aquifer.

The volume of water to be expected is further related directly to the areal extent of the aquifer and reservoir combined, including interbedded shales; more precisely, the area of the shale-sand boundary which we have mentioned earlier. This area is the "cross sectional area of the rock", a part of Darcy's Law (Craft and Hawkins, 1959, p.259). It follows that a quantity of gas contained in a porous sand with the minimum shale boundary area will, when withdrawn, develop only limited water production. A case of this type will be described later. If the gas reservoir is of modest size and the aquifer is extensive as to the shale boundary area, a water influx condition will develop almost immediately. Craft and Hawkins (1959) state that an aquifer 99 times larger than the reservoir will act as if of infinite size. They were referring to water compressibility and other factors. This probably is true whether the aquifer is normally pressured or not. We have examples in the "Cases" section of this paper of several abnormally pressured, productive gas reservoirs in which the reservoir pressure has become stable. One must conclude that the rate of gas withdrawal is precisely equal to the rate of water influx. These special cases are examples under which a quantitative measurement of exact conditions of influx can be made.

There are many instances in which the aquifer limits cannot be determined because of lack of data. We have, in many cases, suspected responsive water influx because of the very low slope of the P/Z vs. cumulative plot, when viewed in relation to geologic limitations of the reservoir. A comparison of the geological dimensions of the reservoir space will make possible a measurement of water influx from the material balance computations by deduction, i.e., the difference. There are cases of reversal of slope and various irregularities. The writer believes that shale-water influx is present in more cases than is usually recognized and most, if not all, of the "Cases" cited. One solution would be to put a precise

pressure recording instrument in the reservoir and leave the wells shut in for an extended period sufficient to measure the pressure increase due to shale-water influx. A device which recorded one static pressure daily would probably serve. Unfortunately, the shutting in of gas wells for an extended period creates many problems, economic and otherwise. This would be analogous to the well "buildup tests" of much shorter duration.

There is a comment, often made, of the production behavior of the abnormally pressured "volumetric" gas reservoir, to the effect that it is only necessary to "get a straw in the barrel" to receive a fair share. It is generally supposed that water encroachment does not actually take place in a "volumetric" reservoir. It cannot by definition. It is the basic theme of this paper that under certain conditions it not only can, but does. We will give cases covering this point later.

An important point is to consider whether a reservoir has or has not been drained completely, when the single well or all wells make 100% water. Several such cases are described later. For example, a well begins to produce gas and condensate from a reservoir of unknown dimensions. The perforations are above any known gas-water interface. Time passes and salt water begins to appear. The quantity gradually increases, to say, 100 barrels per day, while the gas-water ratio gradually changes. Continued flow reaches the point of salt water.

What is the status of gas and fluids in such a reservoir? We interpret the situation as follows: (1) gas has been withdrawn reducing the volume of the gas cap, (2) shale water influx has occurred to the extent that the gas-water interface has risen to, or slightly above, the highest working perforation, (3) a gas cap will be present above this gas-water interface, (4) the gas cap will be reduced in pressure to equalize at the gas-water interface. How much gas remains? The answer is a "gas bubble" of known pressure occupying the reservoir "head room" above the highest working perforation. Part of this "bubble" will have already been produced by gas expansion. If the single well is low in the reservoir, a significant amount of gas may remain, if the single well is high structurally, there may be no gas left. Only geological data or additional wells can get the answer.

MATHEMATICAL MODELS

Bruns, Fetkovich, and Mietzen (1965) have prepared a series of diagrams showing the relation of P/Z to cumulative gas production with varying degrees of water influx. One series was prepared for gas reservoirs with infinite aquifers having varying water encroachment. Another series was prepared for gas reservoirs having finite aquifers with various sizes, permeabilities, and water compressibilities. We have reproduced some of these in our Appendix. Pressures range downward from 5000 psi. The unaffected P/Z plot has a straight slope. Increasing degrees of water influx range upward to complete pressure maintenance. In the case of the infinite aquifer, the intervening plots show various degrees of bending, all concave upward. The resemblance to some of our cases are striking. For the finite aquifer cases, the charts are plotted for two values of water compressibility (3×10^{-6} l/psi and 30×10^{-6} l/psi), a range of three values of Ra/Rr (R=radius, a=aquifer, r=reservoir) of 1.5, 5, and 10, and for aquifer permeabilities ranging from 1 to 10,000 millidarcies. All of these plots exhibit straight lines or some degree of downward, concave curvature. Only one of the cases given in this paper shows such curvature.

It is interesting to speculate on the effect of both of these conditions in which the water compressibility causes a downward concave curvature and water influx alone causes a concave upward curvature. It is likely when both apply equally that a straight line P/Z plot would result, which would give a completely misleading appearance. In our Cases we have ignored water compressibility effect but it is undoubtedly present to an unmeasured degree.

In our Cases with extreme upward concave curvature, the effect of water compressibility has been overshadowed by very active, dominant shale-water drive.

In the mathematical models, the Ra/Rr relationship bears some resemblance to our speculations on the size in area of the sand-shale interface of the combined aquifer and reservoir as a source of water and the gas reservoir in terms of its effect on pressure decline during withdrawal.

IN PLACE ESTIMATES - DISCUSSION

Chierici, Pizzi, and Ciucci (1967) reported on 5 gas fields in the Po River Valley of Italy, which had a combination of "partial water drive" and gas expan-

sion drive. The initial pressures ranged from 1818-2630 psi. We cannot find any depth or indication of abnormality, so we assume that these reservoirs are normal in pressure. The problem is quite clear in this paper, which points out that when an unknown quantity of water is entering a gas reservoir during production, the estimation of gas in place from reservoir behavior is hazardous, to say the least.

In William Hurst's discussion of this paper, the P/Z vs. cumulative plots were prepared in a maneuver similar to the ones which we have used. His plots are straight and give no clues as to water influx. In the field, the story developed differently. A later tally shows twenty-nine wells have been watered out and abandoned with the reservoir 100% flooded with water. Three other fields are reported to have the reservoirs flooded to various amounts, ranging from 35-50%, 65-85%, and 60-80%. Although the plotted data gives a straight line, such a line is no proof that a water drive is absent.

In the cases which we have presented, the straight, or near straight-line plot, is the rule rather than the exception. Although we do not have proof of water influx in many cases, we do in some, and are very suspicious of the rest.

As far as we are concerned, it is impossible to make a reliable estimate of gas in place from the production history alone, inasmuch as a straight line plot does not give a clue to the presence or absence of water influx. In some of our cases the water has not been able to reach any of the wells and arouse our suspicions.

In theory and with good permeability, the material balance should give a straight line P/Z vs. cumulative plot regardless of the withdrawal rates. We have assumed that the reservoir pressure, when measured, had had the opportunity to equalize. In some of our cases the rates of withdrawal have been very uniform, as is customary. In a few cases the rates have varied and so has the plot. It seems evident to us that substantial variations in the rate should confirm the presence or absence of water influx. As we have pointed out elsewhere, a horizontal P/Z plot must indicate a water influx rate equal to the gas withdrawal rate. If the original and current reservoir pressures are known, then the pressure drop required to produce a known water delivery is known. The initial reservoir pressure

represents a no water flow condition, thus two points on the water influx vs. psi curve are known. In the case of the larger aquifers the relation is probably linear.

CHARTS AND CASES - INTRODUCTORY REMARKS

In the section which follows, we have included a number of cases covering the productive history, partial or complete, of reservoirs which have a bearing on our subject. The number of each case is indicative of the pressure-depth ratio of the earliest measurement. For example numbers 8a, 8b, etc. have ratios of .8 plus; 6a, 6b, have ratios of .6 plus. Pressures are given on the left side, cumulative values across the bottom, and years are recorded on the right. A solid line on the right hand side gives the annual production of salt water by calendar years. This is not cumulative. Estimated values are so noted. In some cases water production is given for fractional years.

The cumulative production is in standard cubic feet, plus the barrels of condensate at a fixed ratio of 1 mcf per barrel. We have taken an author's liberty on some matters. Known cases of communication of reservoirs have been adjusted. In the case of numerous pressure points close together, we have plotted them as one. Low readings, suspected of being due to insufficient shut-in-time, have been omitted. We have used surface shut-in pressures, in several cases, to help estimate static bottom hole pressures. We believe this to be reasonable when the wells are gas productive. When water is produced in quantity, the surface pressures are useless. We have used surface shut-in pressures, also, when wells are 100% water productive. Strangely enough, many such pressures go unrecorded.

We distinguish between salt water produced with the gas and fresh water recovered by the low temperature separation equipment. The fresh water we assume to be in a single phase with the gas. The water which we are reporting is the salt or connate water. We are aware that water measurements in the field are indeed crude. Much of the reported water is estimated and may include fresh and salt water. These errors, we believe, are not critical to our conclusions. The "first water" reported is, as well as we are able to judge, the first sizeable quantity of salt water to appear, usually after monthly reports of one to five barrels of fresh water per million cubic feet of gas.

We have chosen to leave the cases unidentified. A number of companies have generously contributed data to this study with the understanding that the locations and field names would not be published. The response to our requests for assistance have been most friendly and cooperative.

Note that the "Cases" are presented according to pressure-depth ratios in ascending order by groups, i.e., .4+, .5+, .6+, .7+, .8+, .9+.

CASE 4a (Fig. 1)

From three wells this reservoir has produced over 20 billion SCF of gas in eleven years. It does not qualify as an abnormally pressured reservoir, inasmuch as the initial pressure has a ratio of .457 psi/ft. of depth. On the other hand, it shows evidence of being "volumetric" but with gas expansion as well as shale-water drive. Two wells are located well up in the 200' gas column and a third has its lowest perforations approximately 12' above the initial gas-water interface. The three wells were salt water free during the production of a cumulative of 17 billion SCF of gas before water appeared in the lowest well. Reservoir pressure decline at that time from initial pressure was 1250 psi.

There is enough subsurface data available to get an idea of the size of the gas reservoir and its configuration. It has been possible to estimate the amount of water required to encroach vertically 12' to the lowest perforation. If we assume 100% replacement of the gas, the volume of influx water would be 1.5 million barrels. This could equal 2.25 billion SCF in reservoir space. These rough figures could change the slope of the P/Z vs. cumulative plot from 52 P/Z per billion to 59 P/Z per billion, a not inconsequential reduction in the estimated recoverable gas. The reservoir area is estimated to be 1300 ac., the aquifer 3000 ac. for a total of 4300 ac.

The water influx has been quite even, as has the rate of withdrawal, and the influx has been unable to equal the withdrawal rate. This is for at least two reasons: (1) the shale is normally compacted for the depth and initial reservoir pressure, and has already given up most of the available water and (2) the actual reservoir pressure drop has only been 1500 psi (bottom hole static) during the production of 20 billion SCF. Water encroachment in this reservoir will not be able to catch up with all of the three wells before reaching the economic limit of

flowing pressure.

CASE 5a (Fig. 2)

This gas-condensate reservoir has produced 6 billion SCF in a period of 6 years from a single well. The reservoir had an original pressure of 6550 psi (.555 pressure-depth ratio). In a very short period the pressure dropped to 5700 psi. All of the subsequent measured reservoir pressures have been either 5700 psi or 5800 psi. In effect, the pressure dropped to a level and has remained the same or has been slightly greater. The first salt water production followed immediately after the 850 psi drop. Water production increased to the year 7-8 and has declined. To some degree this decline may be related to the slight decline in the annual production rate.

The lack of measured reservoir pressures reflects the hesitancy to shut in a well which is producing water. Considering the reservoir pressure relation to hydrostatic water drive gradient this prudence is justified. Presently it is not known whether the pressure-depth ratio is below .465 or not.

The question of interference from leaks or communication with a normally pressured aquifer can be raised. This well is a dual and the other reservoir is presently substantially below normal so communication with it can be ruled out.

We are without complete proof, but in our opinion, this reservoir is limited by faulting. We suspect that it has an aquifer many times larger in area than the gas reservoir which has already produced more than was originally expected. Water drive of some type is undoubtedly present. We estimate a reservoir of 160 ac. and an aquifer of 4100 ac.

CASE 5b (Fig. 3)

This gas-condensate reservoir has produced almost 100 billion SCF of gas and 1 million barrels of water. Only one well is still producing. We have taken some liberties with our chart, in particular, we have eliminated low reservoir pressures, which appeared to be the consequence of low permeabilities and short shut-in times, and several other inconsistencies.

The original pressure-depth ratio of .547 was not far above normal. The present reservoir pressure is below 3000 psi, a drop from an original pressure of 6900 psi. Water appeared at a very early date and increased to the 10th year. The decline after the 11th year is a reflection of sev-

eral wells which watered out.

Well control in this field is adequate to determine a total aquifer plus reservoir of 12000 ac. "boxed in" by faults. The lack of leaks into the 2000 ac. reservoir is proven by the current low reservoir pressure. Any leak into the reservoir would create a pressure increase.

The plot of P/Z appears to be a classic example of gas expansion drive associated with a "volumetric" reservoir. In fact, one million barrels of water have been produced and a material balance calculation using recovered products, pressure decline, and calculated reservoir volume indicates a water influx of 30 billion barrels (including the 1 million which reached the surface). A shale-water drive developed but it was never able to challenge the rate of withdrawal. The low original pressure-depth ratio of .547 indicates an almost normally compacted shale with little water remaining to be squeezed out, despite the very substantial drop in reservoir pressure.

CASE 6a (Fig. 4)

This reservoir produced a total of 5 billion SCF of gas, approximately 4.4 billion before any salt water appeared. At the time of abandonment the well would flow a stream of 100% salt water with 250 psi. The total productive life of the single well was 2½ years. The initial pressure-depth ratio was .637 psi/ft. The P/Z vs. cumulative plot consists of three measured points in a straight line. An estimated point, based on a 100% column of 79,000 ppm chlorides salt water (datum 12110'), gives a value close to, or slightly higher than, that recorded when approximately 3 billion SCF had been produced. This data suggests that the reservoir pressure drop from 7700 psi to 5800 psi was sufficient to develop a shale-water influx equal to the gas withdrawal rate.

The projection of the plot to an economic limit indicates a recoverable total of 15 billion SCF. The role of shale-water here is quite evident. Although the well "watered out" close to a ratio of .465 psi/ft. of depth, it was not "killed" completely but would flow 100% salt water, removing most of the suspicion of communication with a normally pressured aquifer.

The reservoir and associated aquifer are bounded by faults, but the exact dimensions are not known. Nor is it known whether any gas cap remained unrecovered above

the highest perforations. If so, it had been reduced in pressure by gas expansion to a pressure ratio of .468 psi/ft. of depth.

Our guess would be that a 200 ac. gas reservoir was associated with an aquifer 4-6 times larger in area.

CASE 6b (Fig. 5)

This reservoir has produced 32 billion SCF of gas and 1.14 million barrels of water from 4 wells in a period of 8 years. The original pressure-depth ratio was .690, not extremely high. Water production for each year is shown in the lower right part of the graph. The variations in water production represent a series of recompletions intended to shut off the water from several sand stringers. Water reduction has been only temporary. The irregularities in reservoir pressure (and the P/Z) between cumulatives 15-25 billion are related to variations in water production and rate of gas withdrawal.

In this case the influx of abnormally high pressure water is difficult to question. It seems clear that the period of reduced gas withdrawal in year 3-4 resulted in practically an aquilization of water influx and gas withdrawal rates during year 4-5. Resumption of increased water production caused a subsequent decline in reservoir pressure. From this example it may be inferred that controlled variations in withdrawal may make possible better quantitative calculations of ultimate recovery.

Geologic data suggests the following dimensions: sand thickness average net 32±, gas reservoir area 1600 acres, aquifer size not known.

This example gives a suggestion that a time delay is involved in the reaction to change of rate of withdrawal of gas and water.

CASE 7a (Fig. 6)

This reservoir produced approximately 900 million SCF of gas in a period of less than two years without producing any salt water. The initial static bottom hole pressure was 8585 psi, a pressure-depth ratio of .769 psi/ft. The single well was abandoned with a surface pressure of 590 psi after a gas compressor was used to reach pipe line pressure during the final stages.

It is our opinion that this tiny reservoir, in a stray sand, had no aquifer of consequence associated with the gas reservoir. Thus there was little opportunity

for shale-water drive to develop. The overall shale surface of this reservoir was probably small.

It is noteworthy that the P/Z plot does show a slight, but definite, upward swing indicating that the extreme reservoir pressure drop of 6500 psi did start some shale-water influx.

CASE 7b (Fig. 7)

This reservoir has produced almost 8 billion SCF of gas in a period of 2½ years without the appearance of any salt water in the single well. Shut in surface pressures help to supplement the dearth of bottom-hole static pressures.

On the basis of the pressure data and productive history but no geologic data it is impossible to guess the recoverable gas from this reservoir. A reduced withdrawal rate may help determine definitely the rate of shale-water influx. We presume that water influx is giving the P/Z vs. cumulative plot a misleading slope.

From subsurface geology the reservoir has an estimated area of 625 acres with a gas column of 50' and a sand thickness of 85' (gross). As usual, the associated aquifer cannot be accurately defined except to say that it has an area of 1250 acres, minimum. The withdrawal rate of approximately 3 billion SCF per year has been greater than the assumed rate of shale-water influx.

CASE 7c (Fig. 8)

This reservoir has produced 15 billion SCF of gas from two wells in a period of 3½ years. The reservoir pressure has declined from 9600 psi to 8250 psi. An early pressure of 9850 psi was measured but may be inaccurate. Pressures such as this one are often noted and represent either an early decline of several hundred pounds or an error in measurement.

The gas sand is approximately 50' thick (an average of 25' net gas over 600 acres) and covers an area of approximately 600 acres. The associated aquifer is boxed in by faulting and covers an additional 5000 acres, for a total of 5600 acres for aquifer plus reservoir.

If one gives a generous 2.5 million SCF of gas per acre foot, a rough estimate of gas in place would be 25' x 600 acres x 2.5 million SCF = 37.5 billion SCF. During the production of 15 billion SCF the drop has been from 7000 P/Z to 6550 P/Z or 30 P/Z per billion. This would give a pro-

jected estimate of 233 billion SCF of gas in place.

Although no water has appeared in the wells, we feel that an active shale-water influx is cancelling 60% or more of the pressure drop which would be due to gas withdrawal.

Abrupt changes in withdrawal rates should give some measure of the water influx and the time delay in response, if any.

CASE 8a (Fig. 9)

This is one of the larger gas condensate reservoirs, having produced more than 200 billion cubic feet of gas in a period of 11 years. The initial reservoir pressure was estimated to be close to 12,000 psi with a datum of 14,400' or a pressure-depth ratio of .821 psi/ft. The present reservoir pressure is approaching 7000 psi. This is equivalent to the pressure-depth ratio of .465 psi/ft. Approximately 130 billion SCF were produced before any water of consequence was noted and the amount was almost insignificant. Definite quantities of salt water appeared after 190 billion SCF were produced but the amount is not large at present, being 50 barrels of water per million cubic feet from one well and 20 from another.

An unknown quantity of gas was lost in blowouts in the earliest days of discovery and development, all prior to the period of settled production covered by the P/Z vs. cumulative plot. The extension of this plot to zero reservoir pressure indicates a quantity of gas in place far in excess of the geological estimate of reservoir space. For example, the late slope indicates a drop of 62.5 P/Z per billion SCF. At that rate and at a 2000 psi cut off point the reservoir is due to produce a total of 890 billion cubic feet of gas or 222.5 million cubic ft. per acre. Inasmuch as this exceeds the actual space by a large excess, we assume that a large but unknown quantity of water has come from the surrounding shale.

The approximate gas/water ratio of areal extent of aquifer to gas reservoir is believed to be 1:2 (4000 acres of reservoir/8000 acres of aquifer). The water influx is actively cancelling a significant amount of the pressure decline, but is incapable of equalling the withdrawal rate of gas, although the pressure loss is now almost 5000 psi (original reservoir pressure 12,000 psi, now approximately 7000 psi). The large pressure drop is directly across the face of the shale which is surrounding the aquifer and reservoir. The water has only encroached

sufficiently to reach the lowest wells. Water is not being delivered in sufficient quantity to drown the reservoir prior to recovery of most of the gas by expansion drive plus shale-water drive. A high per cent of recovery is predicted. On the other hand, the shale-water influx may cause an error in calculations of ultimate recovery of roughly 1/2 of the amount indicated by the P/Z versus cumulative plot.

CASE 8b (Fig. 10)

This reservoir was abandoned after production of nearly 6 billion SCF by two wells. Both eventually watered out but had substantial surface pressures when 100% water productive. We have been unable to obtain a record of these final pressures. We would guess a residual surface pressure of 1000-3000 psi. The first salt water appeared in one well after a total reservoir production of about 2.5 billion SCF. Water appeared in the second well shortly after. The production versus time plot shows the gradual increase in daily rate until the water appeared and the reduction of rate as the water increased. There were no bottom hole static pressures taken during the period of water production. Lack of information during this period is typical of the concern over "killing" a water producing well.

The high initial pressure-depth ratio of .847 psi would indicate an availability of abundant quantities of shale-water. A limited size to the aquifer is indicated by the rapid reservoir pressure decline. The sand is about 65' thick and the reservoir covers slightly less than 500 acres. The pressure drop of 1350 psi is related to the fact that the gas cap was removed more rapidly than the shale-water could respond. We would guess that the aquifer occupied about 4,000 acres (ratio 1:8). This is analogous to bleeding down a small gas pocket in casing. The gas, if very limited, can be removed much faster than the water influx can replace it and the pressure can be dropped quickly. With a larger gas cap the drop would have been less. There is not sufficient information to determine if at any time the shale-water influx and gas withdrawal rates were equal, but it is very unlikely.

CASE 8c (Fig. 11)

The productive history of this reservoir is not yet complete. In a period of ten years, 21 billion SCF of gas have been produced by 3 wells. The reservoir pressure has been reduced from 10,000 psi to 9650

psi during the production of 11 billion SCF. No bottom hole static pressures have been taken later due to water production. Of the three wells only one makes water. This began after 6.2 billion SCF had been withdrawn.

The P/Z vs. cumulative plot shows remarkably little decline. This is assumed to be due to a readily responsive source of shale-water. Note that the current bottom hole static pressures are 4000 psi greater than normal artesian gradient and a pressure-depth ratio above .8 psi per ft. probably still prevails.

It is impossible to estimate the quantity of recoverable gas without a measure of the rate of shale-water influx. This might be determined by a period of reduced withdrawal to reach experimentally a gas withdrawal rate equal to the rate of water influx.

The reservoir appears to occupy 1000 acres with a gross sand thickness of 100'. Water showed up in the 5-6 year of production and is increasing. But with the current pressure no well has died. The water which has been produced is evidence of shale-water influx. The sustained pressures indicate the influx of a substantial amount of water which remains unmeasured.

CASE 8d (Fig. 12)

Only two bottom hole static pressures are available, giving pressure-depth ratios of .875 (initial) and .868. Seven shut in surface pressures have made possible estimated bottom hole static pressures shown on the chart. Pressure decline in this reservoir has been slight considering the 7.5 billion SCF produced in a period of almost 2½ years. No salt water has appeared and only .9 barrels of fresh water per million SCF of gas has been reported.

The shale-water influx has been very responsive, apparently from the first day of production. A material balance of water influx and gas withdrawal has existed almost from the earliest production. The .875 pressure-depth ratio indicates readily available shale-water subject to sufficient shale area. The geological data indicates a gas reservoir with an area of approximately 380 acres, and aquifer area of approximately 1450 acres or a ratio of 1:4. The reservoir and aquifer are limited in all directions by faulting. The gross sand thickness is 150' and gas column is approximately 200'.

The combination of pressure-depth ratio of .875, aquifer plus gas reservoir of 1830± acres, and reservoir pressure

drop of 100 psi apparently joined to supply water from the shale at almost the exact rate of gas withdrawal.

CASE 8e (Fig. 13)

Two wells have produced 14 billion SCF of gas in a period of 3 years. No salt water has appeared but the history of the reservoir is not complete. Basic pressure data is limited to two bottom hole static pressures. The initial pressure-depth ratio was .881. This is one of the highest of which we have data available for this study.

In addition to the very high pressure-to-depth ratio, the production history indicates a stabilized pressure (surface shut-in) during the withdrawal from a cumulative of 10.2 billion to 13.1 billion SCF. To clarify, the reservoir space being drained of gas was being filled with an equal volume of influx water; thus the reservoir pressure has remained constant.

The P/Z cumulative plot will not truly reflect the quantity of recoverable gas unless the rate of water influx is known. A reservoir pressure decline of 900 psi was required to achieve stable and equal influx and withdrawal conditions. In this case the monthly withdrawal rate has been unusually uniform. We feel that the achievement of stable pressures is proof of active shale-water influx.

From the geological data the gas reservoir is estimated to have an area of 800 acres while the aquifer has an estimated area of 1700 acres. The gas column exceeds 200' in a sand with a gross thickness of 30'. The water free condition, to a degree, is due to the high position of the perforations above the water/gas interface and to the limited size of the aquifer. The total area of 2500 acres is completely "boxed in" by faulting.

CASE 8 f (Fig. 14)

The production from this reservoir has reached 38 billion SCF with the end not quite in sight. Our productive history covers 15 years and 5 wells, not all producing at the same time. The exact time of first salt water production is not known but the earliest well watered out when the reservoir had produced about 19 billion SCF. In plotting the reservoir static pressures we have eliminated low pressures in wells having low permeabilities.

The plot of P/Z vs. cumulative shows no obvious effect of shale-water influx although the produced water indicates that

water is entering the reservoir while the reservoir is 1000 psi or more greater than the pressure/depth ratio of .465.

For a number of years it has been surmised that the geology of the area could not be made to accommodate a gas reservoir of the size indicated by the P/Z cumulative plot. At this stage the remaining wells face a watery grave after a brief period of additional production.

As will be noted, the rate of water influx never approached the gas withdrawal rate although production declined in the late years. The aquifer is believed to be of a size 3 times larger than the gas reservoir (1700 ac. aquifer, 800 ac. gas).

CASE 8g (Fig. 15)

The behavior of this gas reservoir caused the initiation of this project when the well had a residual surface pressure of 3500 psi with 100% salt water production. Because of the mechanical problems no bottom hole static pressures were taken. A number of shut in surface pressures are available and from these bottom hole static pressures and P/Z have been estimated. The original pressure-depth ratio was .847. Salt water appeared after the production of 2.5 billion cubic feet of gas and condensate. We are unable, of course, to use surface pressures during the production of water and gas. Ultimately the well produced 100% salt water and continued to produce 1000 bbls. of salt water per day for a month but no gas appeared.

This reservoir was depleted with a single well. The high sustained pressures suggested a reservoir containing possibly 50 billion SCF. Consequently 3 offset wells were drilled attempting to get into the reservoir. All found the sand filled with water. The gas sand was just above the total depth of the productive well with no water level visible.

At the time of abandonment the well would flow 100% salt water with a shut-in surface pressure of 3500 psi. During abandonment the well got loose and filled the adjacent rice field with hot salt water. At that time the bottom hole static pressure was estimated to be roughly 9000 psi equal to the estimated pressure at the time of first water production 5 years earlier.

After a reservoir pressure drop of 1000 psi the quantity of water coming in matched the quantity of gas being withdrawn. This stable condition of equal volume replacing equal volume is believed to have remained

constant for 5 years.

We make a crude estimate of water influx as follows: (1) 1 million barrels of water was produced during a 5 year period together with 4.1 billion SCF of gas. (2) This represents roughly 3.1 million barrels of reservoir space which emptied. (3) The water influx maintained the same reservoir pressure, so the voided space was filled. (4) The water which entered the reservoir during production, including the 1 million produced barrels, was of the order of 4.2 million barrels. We estimate the reservoir area to be 200 ac. and the aquifer 6000 ac., ratio 1 : 30.

CASE 8h (fig. 16)

This small reservoir has produced 4 billion SCF at the time of writing and water production has occurred only during the past year. Behavior has been typical for the small reservoir of 200 ac. and small aquifer of 700 acres. Both figures, of course, are estimated.

CASE 8i (fig. 17)

This case is definitely one of the most unusual in behavior. The bottom hole static pressures reflect a decline of 12,450 psi to 10,900 psi during the production of about 8 billion SCF of gas. At this point water appeared in one of the two wells. The productivity curve then shows a sharp reduction in daily withdrawal. The pressures responded by increasing slightly but definitely. The producing rate was then increased while the reservoir pressure increased 100 psi. Water production has not really been significant in quantity, but is noticeably increasing.

The P/Z plot is not a straight line. We believe that it reflects the varied flow rates and the very definite shale-water influx. It is clear in this instance that varied flow rates can create a response in the P/Z plot, which may give helpful quantitative information.

We have taken the liberty here of assuming a common reservoir for these two wells because of the identical pressure behavior during the period of production. The geological information suggests two separate reservoirs. The reservoir area is believed to be 1100 ac. The aquifer area is unknown.

CASE 8j (Fig. 18)

This reservoir shows unusual behavior of surface shut-in pressures. An abrupt drop of about 900 psi occurred when production began. Half of this drop was regained during the production of about 3 billion SCF. We do not have detailed reservoir pressures to determine exactly what happened. Apparently a drop in reservoir pressure was followed by a rebounding shale-water drive which appears to be quite effective. The straight line projected between the two P/Z points does not give the details.

Again we see a situation with active, abnormally pressured water drive, the water influx being almost equal to the withdrawal of gas and water. This reservoir will probably end with 100% water production and a high residual pressure.

Reservoir is estimated to have an area of 680 ac. The size of the aquifer is unknown.

CASE 8k (Fig. 19)

This is one of the reservoirs which has had sustained pressures, although water productive, from an early date. Most of the water, some 350,000 barrels, was produced during year 1-2 and the first quarter of year 2-3, at which time the water productive well was shut in. Seven billion SCF have been produced with a reservoir pressure drop of 300 psi. More data would have been very helpful. The surface pressures suggest variations in the reservoir pressure.

We feel that a very responsive shale-water drive is present. The withdrawal of gas and water have been very close to, but slightly greater than, the water influx. Estimation of the gas in place cannot be made from the productive history alone.

The reservoir is estimated to cover 1325 ac. The aquifer size is unknown but is limited by faulting in three directions.

CASE 8l (Fig. 20)

This gas condensate reservoir is in the extremely high range with a pressure-depth ratio of .881. Salt water appeared in year 2-3 but the quantity is small. The water productive well was shut-in in year 3-4. As occurs in several cases, the reservoir pressure has been almost stabilized after water production developed.

The dimensions of the gas reservoir and aquifer are not known. The production

of 33 billion SCF from those wells would lead us to infer the presence of a large aquifer or shale boundary area which developed a strong shale-water drive.

CASE 8m (Fig. 21)

This is our single example of a reservoir with down bending P/S vs. cumulative plot. We estimate a reservoir size of 720 ac. The aquifer appears to have no determinable limitations in size. The resemblance to Bruns, Fetkovich, Meitzen's (1965) curves for water influx with reservoirs and aquifers of finite dimensions and water compressibility effect is striking (their figures 5,6,8,9).

CASE 9a (Fig. 22)

This gas-condensate reservoir is in an area where extreme pressures have already been reported. The pressure-depth ratio of .903 was recorded after a brief period of production. The original reservoir pressure was probably greater. Eighteen billion SCF of gas have been produced in a period of less than five years from a single well. There is no reported water production. The unusual feature here is the decline in reservoir pressure from 12650 psi to 12050 psi and then a subsequent increase to 12275 psi. If we assume that the measurements were correct, it is only reasonable to conclude that shale-water drive or some other type of extremely high pressure drive was developed by a reservoir pressure decline of 600 psi.

The dimensions of this reservoir and aquifer are not known. An examination of the data presented here gives no clue as to the quantity of gas which is in place or which would be recoverable. We guess that the residual pressure will be extremely high when 100% water production ultimately occurs.

CONCLUSIONS

1. Abnormal pressures in South Louisiana have a single cause. The process of deposition of shale and sand is taking place faster than the process of adjustment of the included fluids. The rapidly increasing load must find partial support upon the trapped fluids. This entrapment is due to the decreasing porosity and permeability of the shale during the process of compaction. Older sedimentary basins usually have had time for the pore fluids to arrive at a state of equilibrium, except where the extremely low permeability of evaporite sequences can maintain pressures over long periods of geologic time, i.e., abnormally

pressured zones of Cambrian age are reported by R. Byramjee (1966). The only trapping medium in South Louisiana is shale, evaporites being absent from the Tertiary sediments.

2. The process of shale compaction results in the squeezing out of vast quantities of intergranular water and proportionally lesser amounts of hydrocarbons. Where the loading is more rapid than the escape process, abnormally pressured oil and gas reservoirs and aquifers result. In these cases, the process of compaction may be described as temporarily arrested. The process of shale compaction may be resumed by withdrawal of gas or fluids from the reservoir, thus creating a pressure differential across the shale/sand interface. This initiates a type of abnormally pressured water influx drive which we will call shale-water drive.

3. This shale-water drive is controlled by the factors involved in Darcy's Law. i.e.: (1) the permeability of the shale, (2) the pressure differential across the shale/sand interface, (3) the cross sectional area of the sand interface and (4) the viscosity of the water. The first three are variables over a wide range. The permeability of shale is closely related to the porosity of shale. As porosity declines with compaction so does the permeability decline, and dramatically so (Hubbert and Rubey, 1959). Since the porosity is a direct measure of the fluid content, the higher porosities (and permeabilities) have the most available water. Pressure-depth ratios of .8 and .9 are indicative of the highest water availabilities.

The flow of water is directly proportional to the pressure differential across the shale/sand interface. The higher abnormal pressures make possible extremely high differentials during the productive life of some reservoirs.

The third item, the surface area, may be the one which exerts the most influence on the quantity of water which enters. The flow is directly proportional to the cross sectional area. If we include the upper boundary, the lower boundary, and the surface of interfingering shale layers, the surface area may actually cover many, many square miles. The unit of area used in Darcy's Law, the square centimeter, literally becomes billions in the case of the larger aquifers and associated reservoirs.

4. The shale-water drive is proportional to the area of the shale/sand interface (square miles), the degree of under-compaction (pressure/depth ratio), and the pressure differential (psi) developed by withdrawal during the process of production. Early production

data plus geological data should indicate clearly the behavior of this shale water influx. For some reservoirs, withdrawal rates may need to be manipulated, but ultimately quantitative data should result. The draw-down and build-up procedures described by Matthews and Russell (1967) should, with modification, be applicable with quantitative results.

5. The shale-water drive which we have dwelled upon here in regard to abnormal pressures also is present to a degree in the normal pressure range and to a lesser degree in subnormal pressure conditions. Although the maximum amount of shale-water available is present at pressure-depth ratios in excess of .9, the compaction process will make water available at ratios less than .465 as well. Likewise, the condition is not limited to gas reservoirs alone. In conditions of lesser ratios the water continues to be available but is proportionately less per psi drop.

Case 4a has shown definite evidence of water influx in spite of the fact that all pressures, including the initial pressure were below a ratio of .465.

Case 5b has received an estimated influx of 30 million barrels of water while the ratios declined from .547 to .350.

Textbooks contain many references to water influx in the range of normal and subnormal ranges but few in the higher ranges. Oil reservoirs in any pressure range are also subject to shale-water drive when sufficient pressure differential is present at the shale-sand boundary.

6. The pressures sustained or increased by shale-water influx affect three parts of the complex recovery process. All are favorable:

a. The cancellation partially or wholly of the pressure drop due to gas withdrawal may defer or prevent retrograde condensation in the reservoir and the consequent loss of valuable products.

b. The cancellation of pressure decline will prevent sandstone porosity shrinkage and help prevent reduction in permeability due to such shrinkage. This should improve percentage of gas or oil recovered.

c. The water influx will, as in the case of artesian water drive, sustain the gas pressure to a favorable economic level, if not to the limit, at least for a favorable period of time.

7. An unfavorable consequence of shale-

water influx will be the by-passing of some of the gas. Any gas remaining below the gas-water interface will not be recovered. It is unlikely that the water sweep will be completely effective. Gas in extremely small pockets or "dead end" situations either above or below the gas-water interface, will not be recovered due the high residual pressure remaining when production is terminated.

8. There is a tendency to surmise that a high residual pressure, at the stage of 100% water production from the reservoir, indicates a nearby gas cap supplying such pressure. The presence or absence of such a gas cap cannot be determined from such pressures inasmuch as the gas does not supply the pressure. The residual pressure may not be due to the gas remaining in the reservoir but rather to shale-water drive.

9. The sealing of high pressure reservoirs takes place in two basic stages. These stages may be in reverse order depending upon circumstances. The escape of water takes place along the directions of greatest permeability. In sand beds and along bedding planes the travel will be parallel to the bedding. During this stage the water which has no such opportunity to move parallel to the bedding will travel transversely. If faulting should sever the travel access parallel to the bedding planes, the only escape route remaining will be transverse to the particle arrangement. It is only at this stage that substantial pressure differentials begin to accumulate.

10. A normally compacted shale bed with its extremely low permeability becomes the seal for more permeable but undercompacted shales below. A shale zone 100 feet thick with a ratio of .465 at the top can contain a reservoir with a ratio of .8 at the bottom, the intervening shale being transitional.

ACKNOWLEDGEMENT

The writer is not a reservoir engineer by profession but rather a geologist with a long time interest in the subject. It will be obvious that the author is not a skilled mathematician. It is our hope that the qualitative conclusions given here will lead others to quantitative results. There have been many who have helped in the calculations and in discussions with the author, particularly Ed Villareal. Jack Kleban, Walter Jensen, T. M. Bertch, Marvin Martin, Carlton Sheffield, to mention a few, have given generously of their time and skill.

We are particularly grateful to the

Production Personnel of other companies without whose assistance and generosity this study would have been impossible.

REFERENCES

Byramjee, R., 1966, "Argile non compactees et pressions anormales cas du Nord-Sahara": Rev. Inst. Fran. du Petrole et Ann. des Comb. Liq., v. 21, no. 7-8, p. 1067-1077 (True Nelaton, Paris, 15)

Chierici, G. L., Pizzi, G. and Ciucci, G. M., 1967, "Water drive gas reservoirs: uncertainty in reserves calculation from past history": Jour. Petrol. Tech., Feb., p. 237-244. Discussion and Reply, July, 1967, p. 963-967

Chilingar, G. V., and Knight, L., 1960a, "Relationship between pressure and moisture content of kaolinite, illite, and montmorillonite clays": Am. Assoc. Petroleum Geologists Bull., v. 44, no. 1, p. 101-106

Craft, B. C., and Hawkins, M.F., 1959, "Applied petroleum reservoir engineering": Prentice-Hall p. 437

Dickinson, George, 1953, "Geological aspects of abnormal reservoir pressures in Gulf Coast Louisiana": Am. Assoc. Petroleum Geologists Bull., v. 37, p. 410-432

Dobrynin, Valery M. 1962, "Effect of overburden pressure on some properties of sandstones": Soc. Petrol. Eng. Jour., Lec. p. 360-366

Hubbert, M. K., and Rubey, W. W., 1959, "Role of fluid pressure in mechanics of overthrust faulting. I. Mechanics of fluid-filled porous solids and its application to overthrust faulting": Geol. Soc. America Bull., v. 70, p. 115-166

Marsden, S. S. Jr., and Davis, S. N., 1967, "Geological Subsidence": Scientific American, v. 216, no. 6, p. 93-100 and 155-156

Rubey, W. W., and Hubbert, M. K., 1959, "Role of fluid pressure in mechanics of overthrust faulting. II. Overthrust belt in geosynclinal area of Western Wyoming in light of fluid-pressure hypothesis": Geol. Soc. America Bull., v. 70, p. 157-205

Thomeer, J. H. M. A., and Bottema, J. A., 1961, "Increasing occurrence of abnormally high reservoir pressures in boreholes, and drilling problems resulting therefrom": Amer. Assoc. Petrol. Geol. Bull., v. 45, no. 10, p. 1721-1730

Wallace, W. E., 1962, "Water production from abnormally pressured gas reservoirs in South Louisiana": Trans. Gulf Coast Assoc. Geol. Soc., v. 12, p. 187-193

Weller, J. M., 1959, "Compaction of sediments": Am. Assoc. Petroleum Geologists Bull., v. 43, no. 2, p. 273-310

Powers, Maurice C., 1967, "Fluid - release mechanisms in compacting marine mudrocks and their importance in oil exploration": Amer. Assoc. Petroleum Geologists Bull., v. 51, no. 7, p. 1240

Matthews, C. S. and Russel, D.G., 1967, "Pressure buildup and flowtests in wells": Soc. Pet. Eng. of A.I.M.E. Mono. v. 1

Young, Allen and Low, Philip F., 1965, "Osmosis in argillaceous rocks": Amer. Assoc. Petrol. Geol. Bull., v. 49, no. 7, p. 1004-1008

APPENDIX

The following figures are from the JOURNAL OF PETROLEUM TECHNOLOGY (March, 1965, p. 289) article entitled, "The Effect of Water Influx on p/z Cumulative Gas Production Curves", by J. R. Bruns, M. J. Fetovich and V. C. Meitzen:

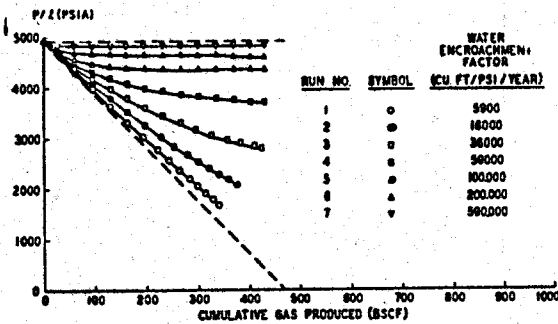


Fig. 2—Curves of p/z for gas reservoirs with water influx, Schilthuis method.

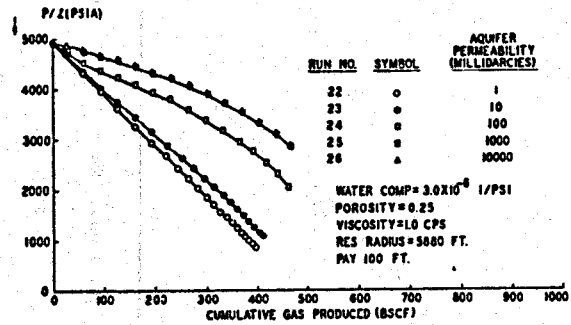


Fig. 6—Curves of p/z for gas reservoirs with water influx, van Everdingen-Hurst method, finite, $R_e/R_o = 10$.

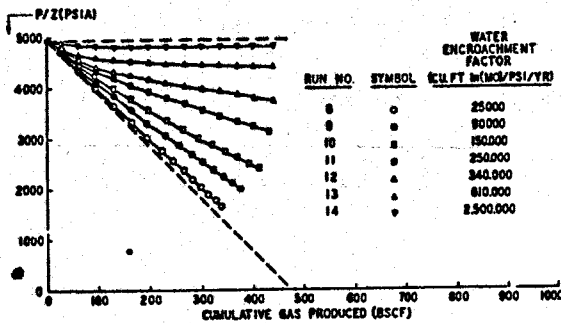


Fig. 3—Curves of p/z for gas reservoirs with water influx, Hurst simplified method.

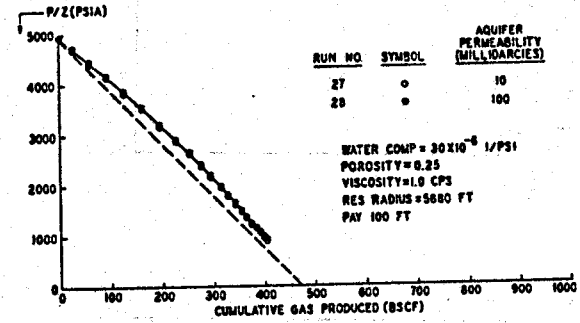


Fig. 7—Curves of p/z for gas reservoirs with water influx, van Everdingen-Hurst method, finite, $R_e/R_o = 1.5$.

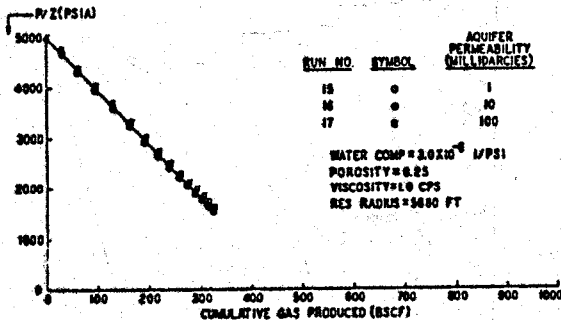


Fig. 4—Curves of p/z for gas reservoirs with water influx, van Everdingen-Hurst, finite, $R_e/R_o = 1.5$.

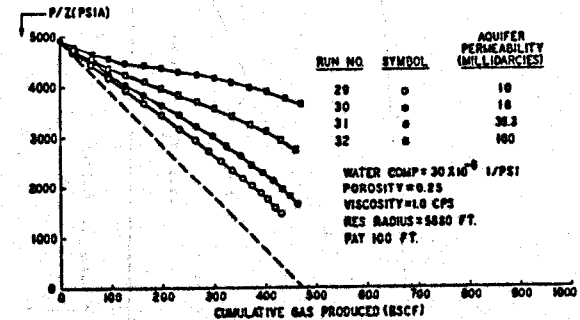


Fig. 8—Curves of p/z for gas reservoirs with water influx, van Everdingen-Hurst method, finite, $R_e/R_o = 5$.

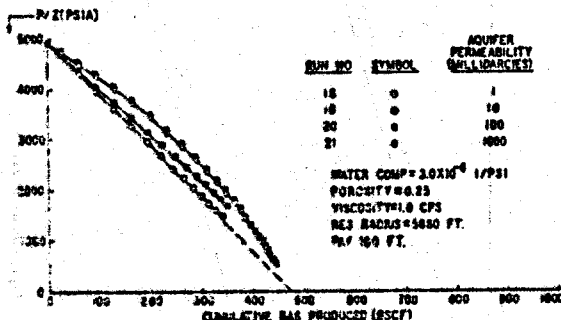


Fig. 5—Curves of p/z for gas reservoirs with water influx, van Everdingen-Hurst method, finite, $R_e/R_o = 3$.

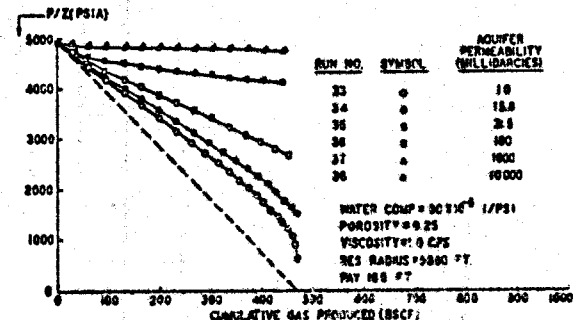


Fig. 9—Curves of p/z for gas reservoirs with water influx, van Everdingen-Hurst method, finite, $R_e/R_o = 10$.

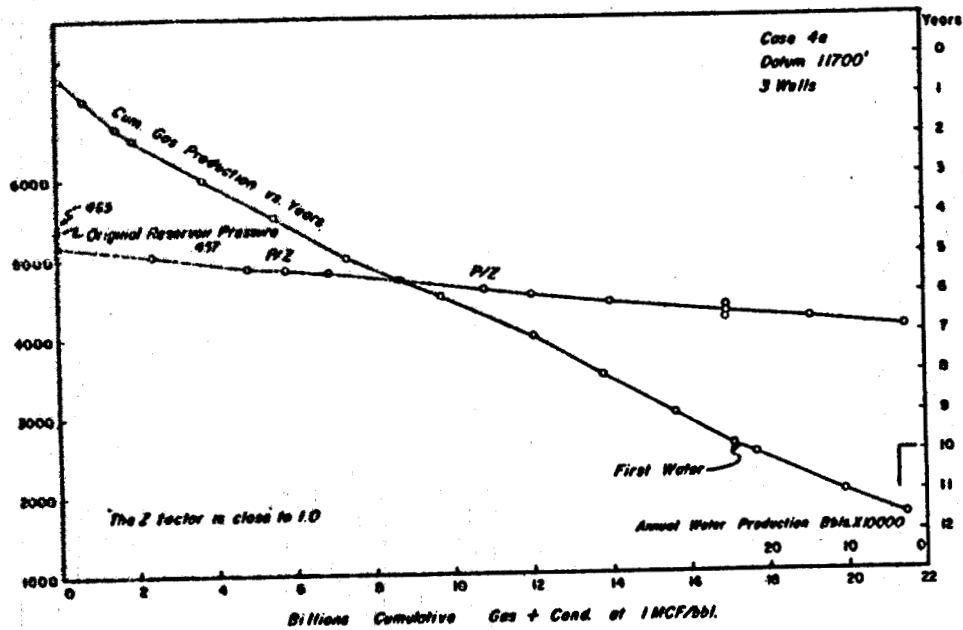


Fig. 1.

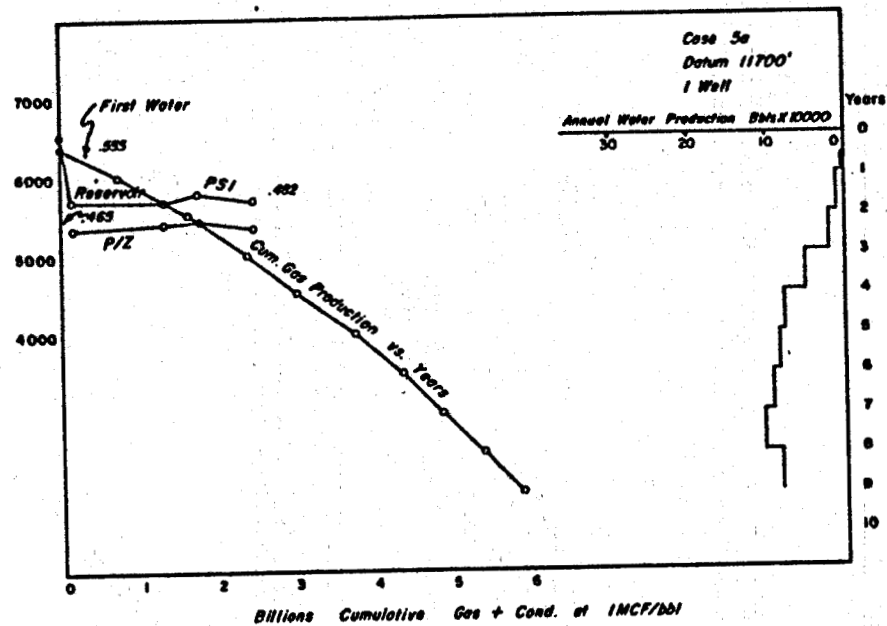


Fig. 2.

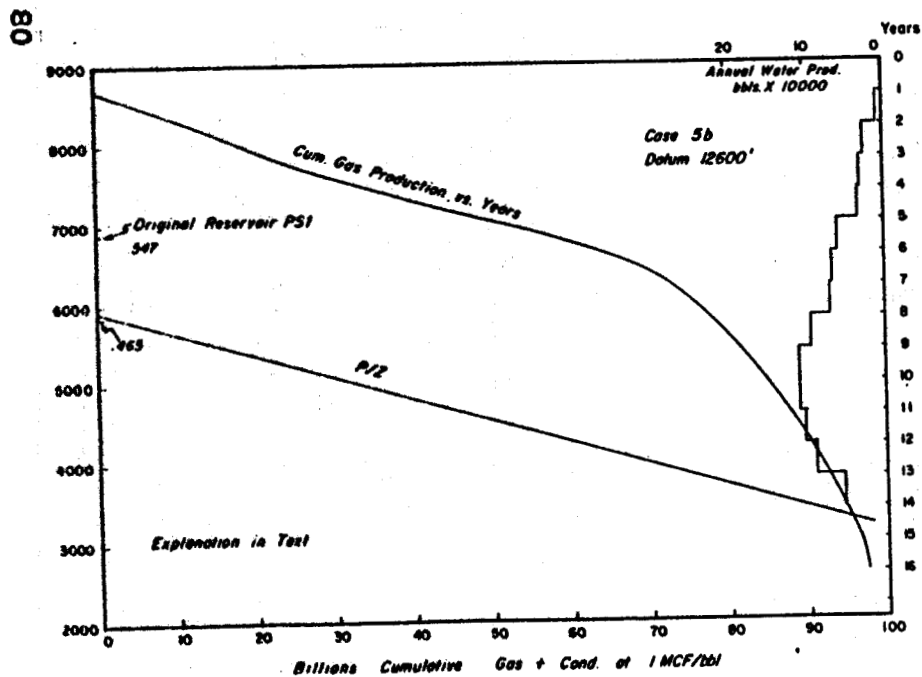


Fig. 3.

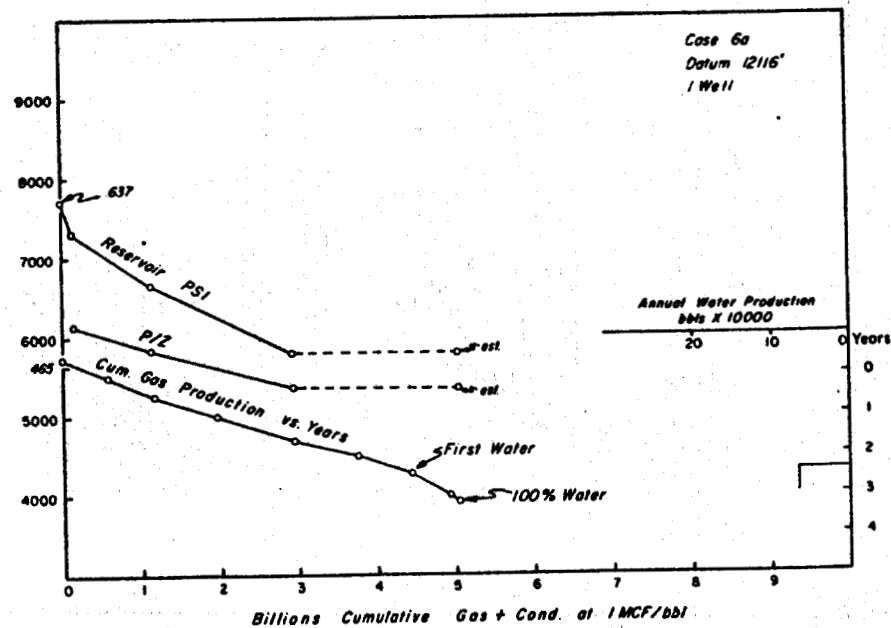


Fig. 4.

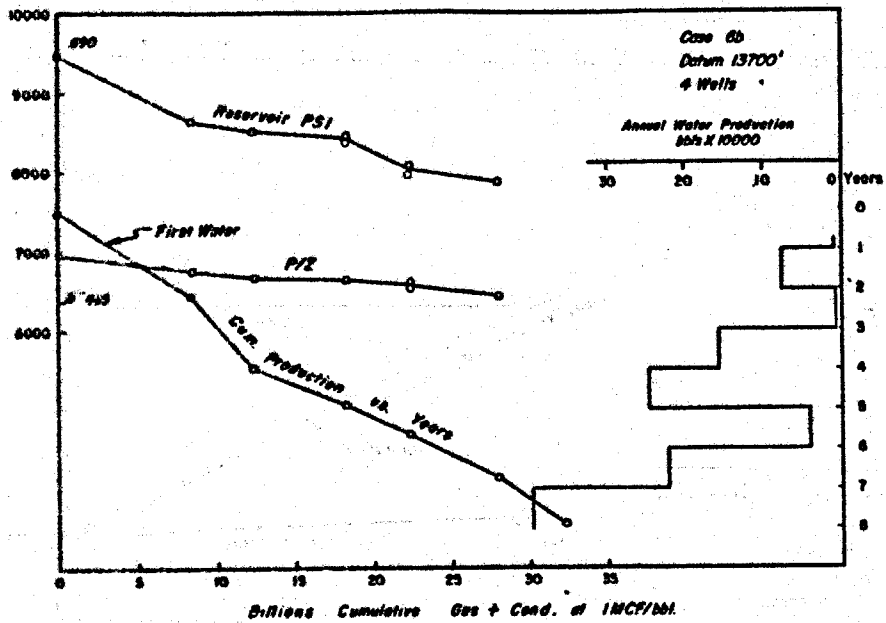


Fig. 5.

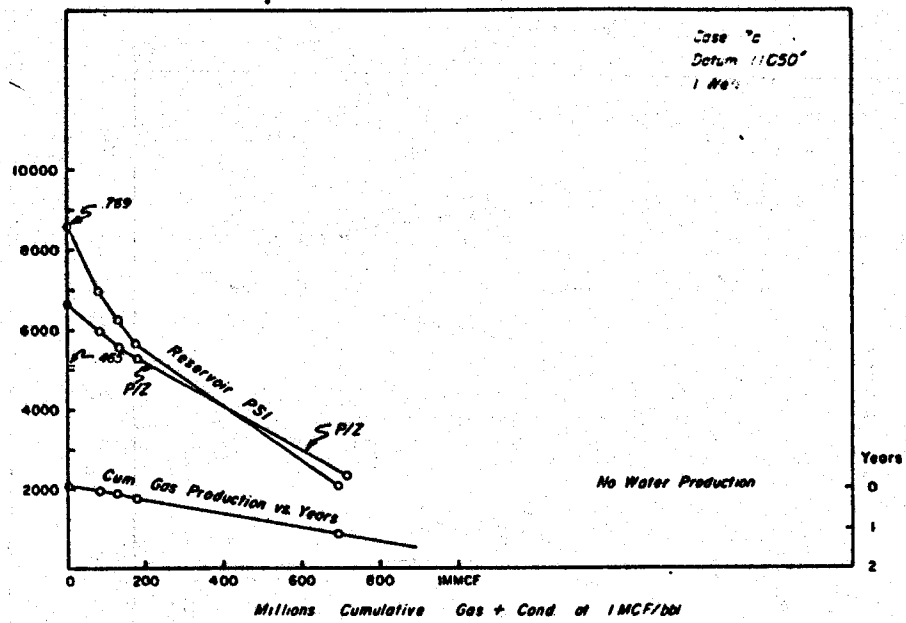


Fig. 6.

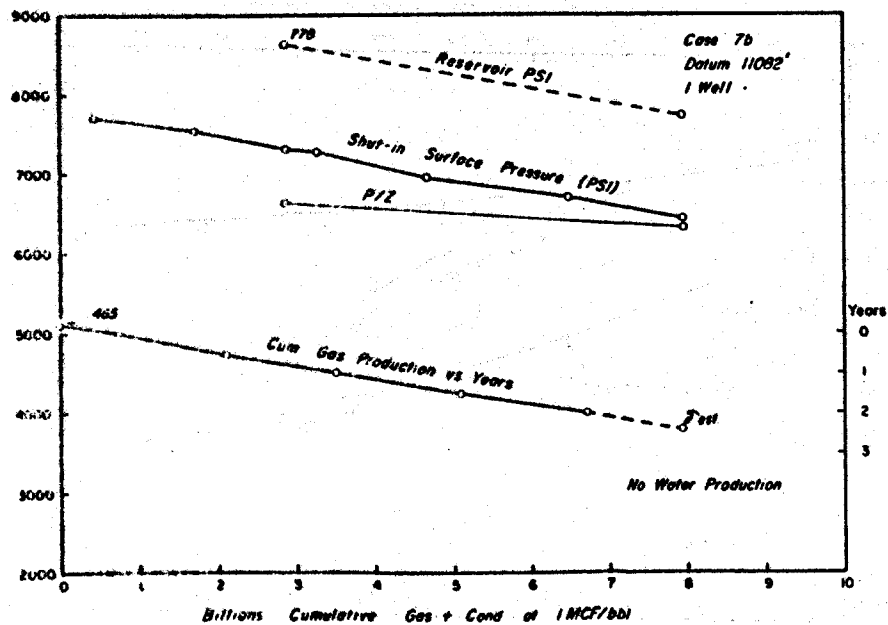


Fig. 7.

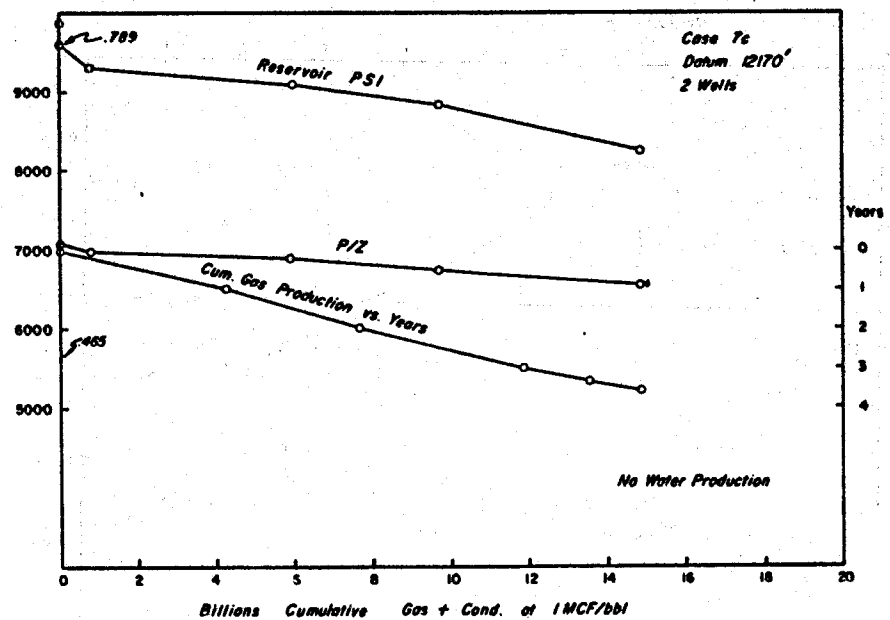


Fig. 8.

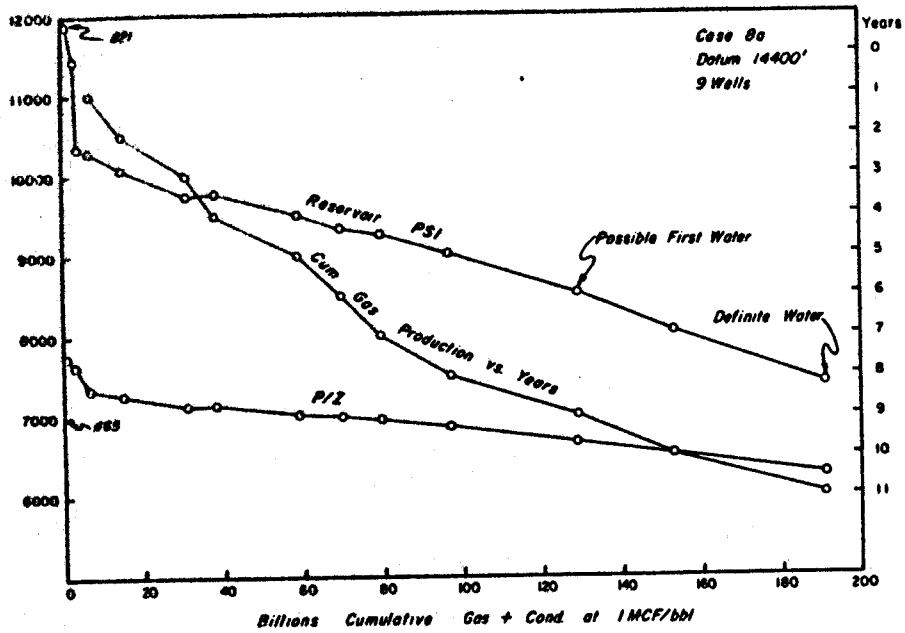


Fig. 9.

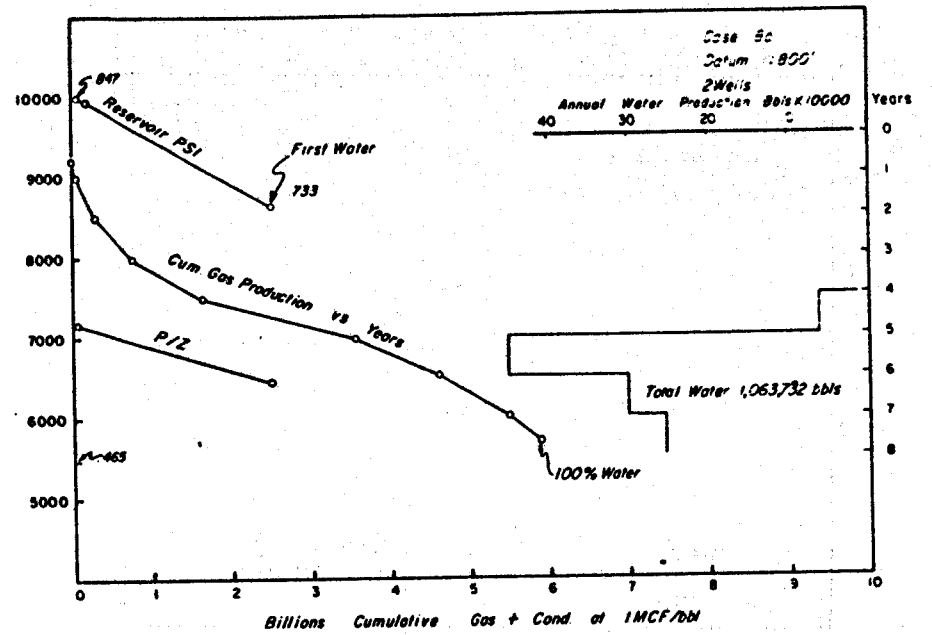


Fig. 10.

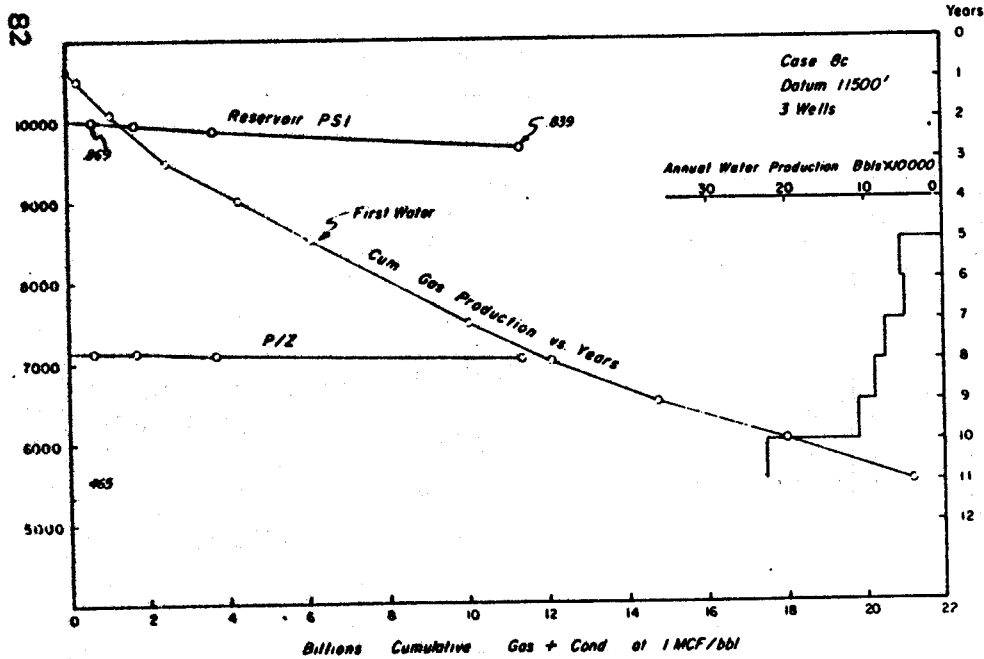


Fig. 11.

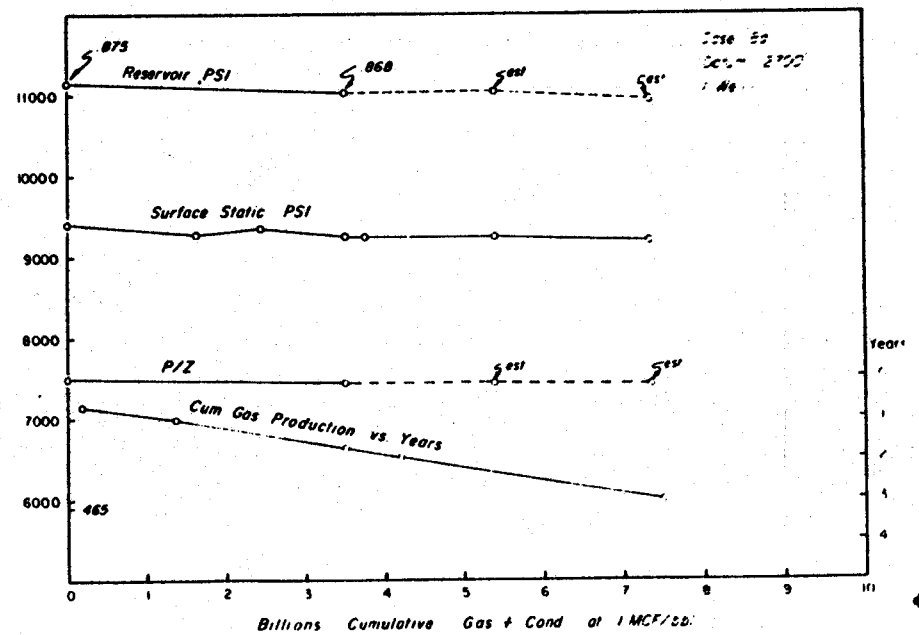


Fig. 12.

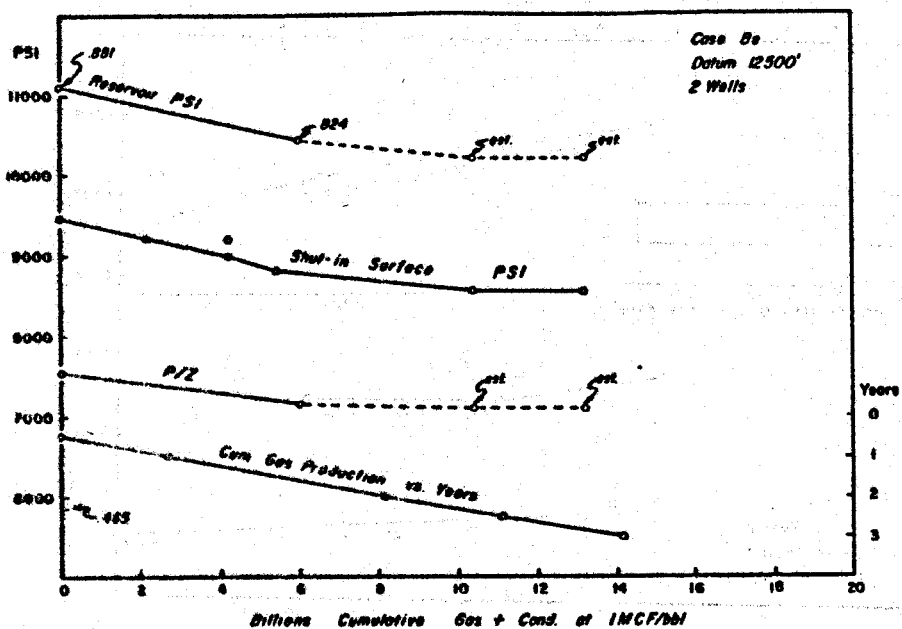


Fig. 13.

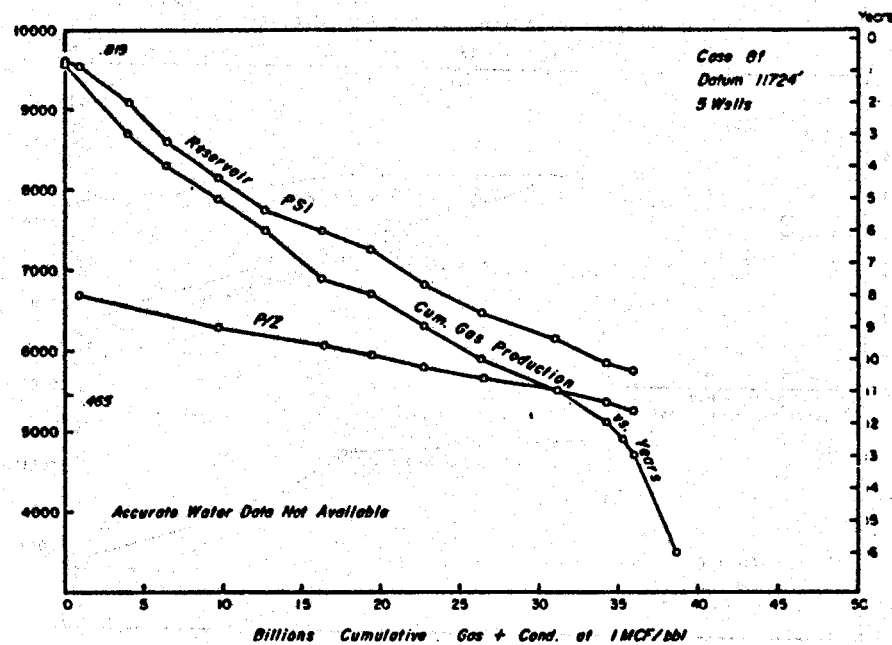


Fig. 14.

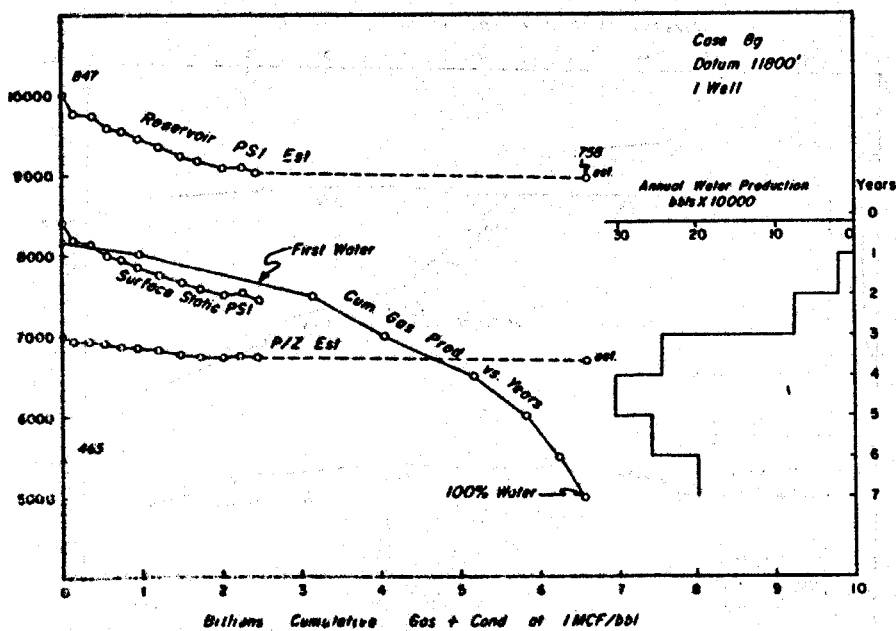


Fig. 15.

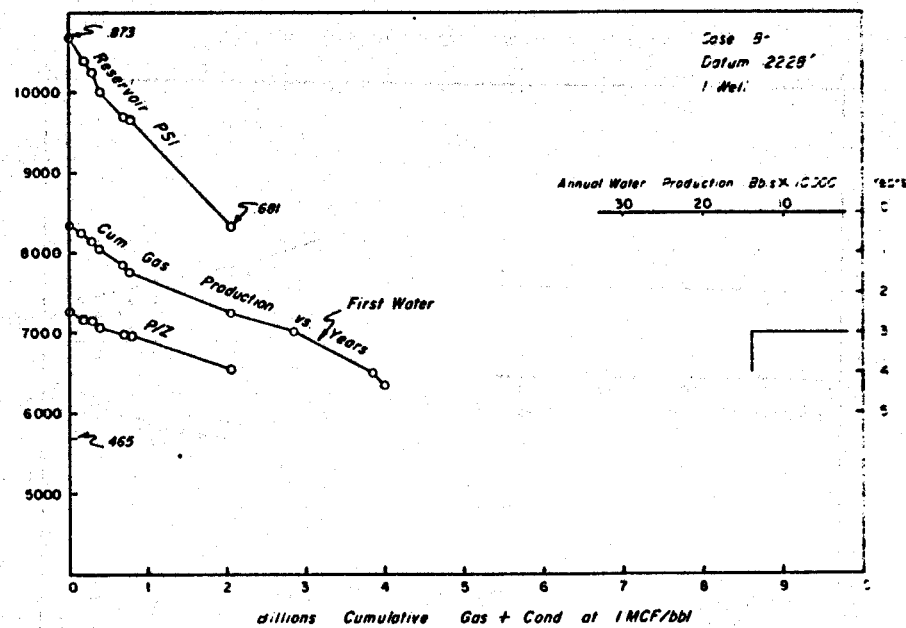


Fig. 16.

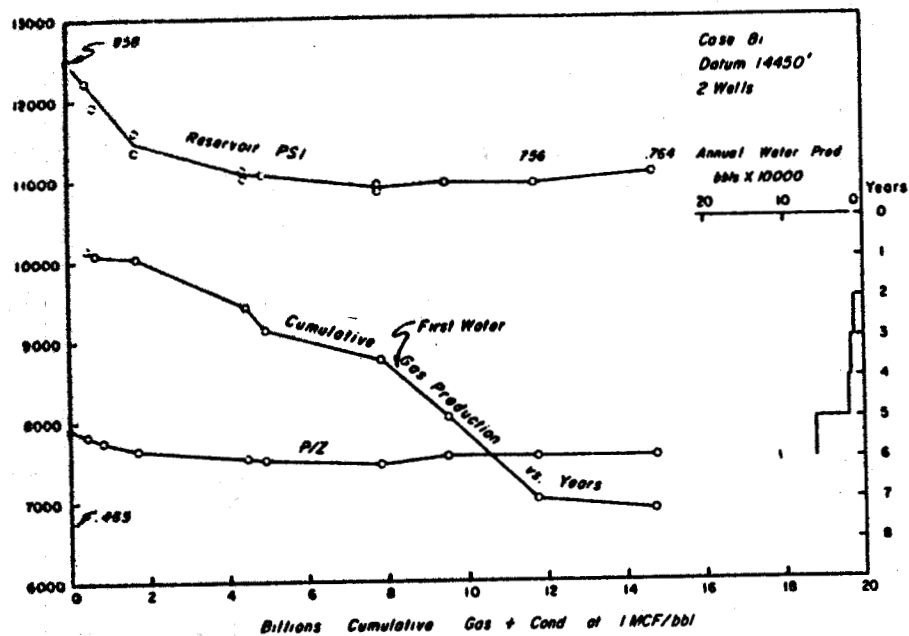


Fig. 17.

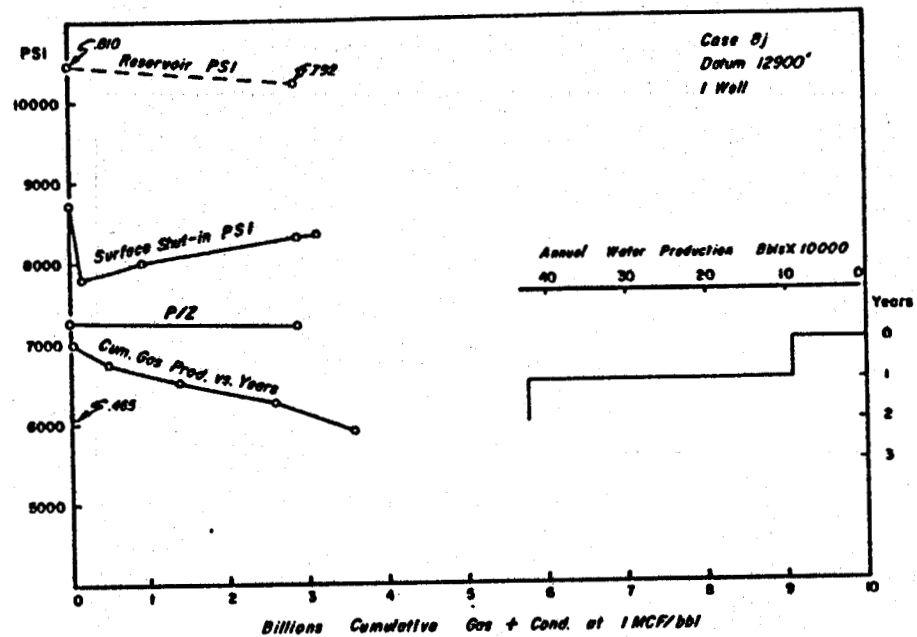


Fig. 18.

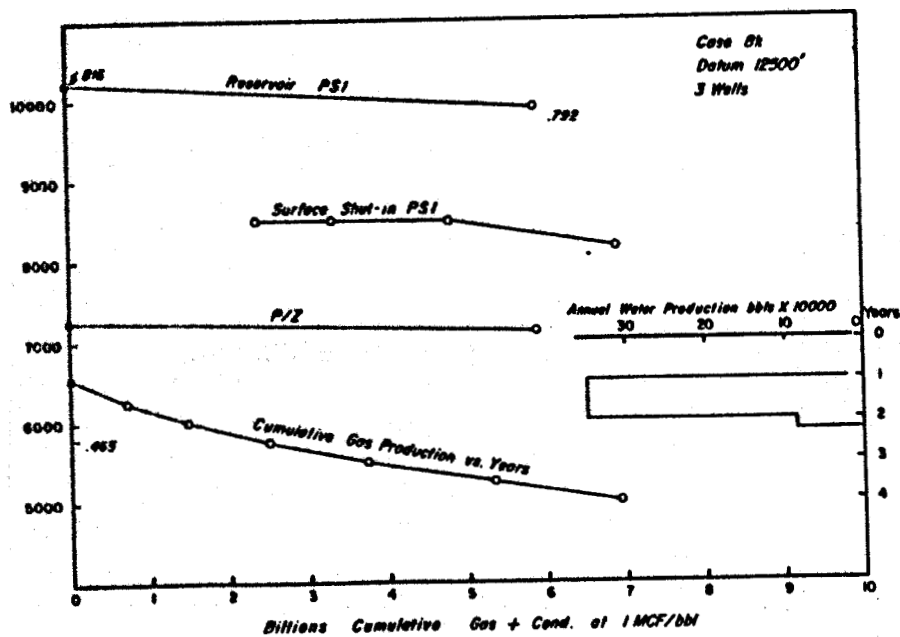


Fig. 19.

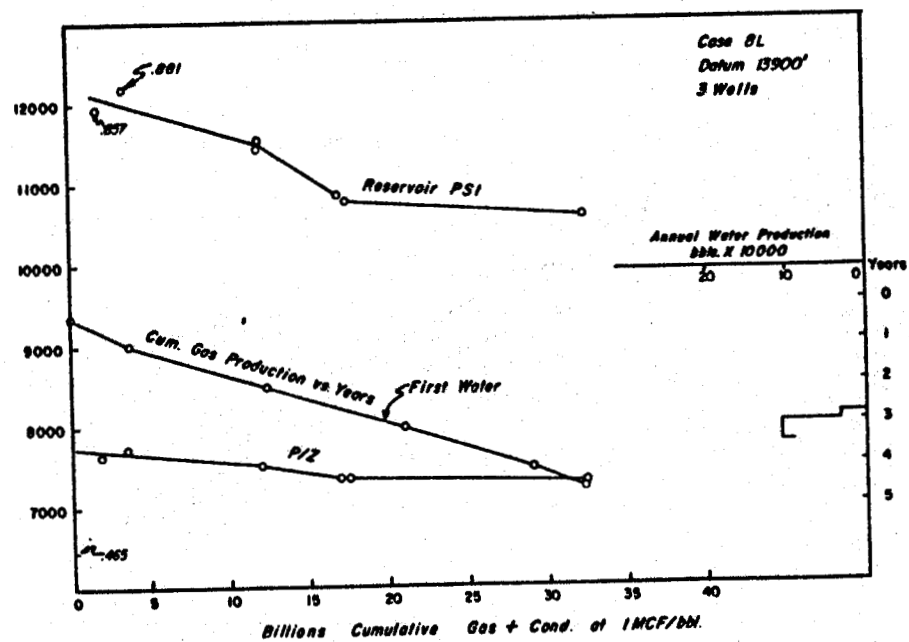


Fig. 20.

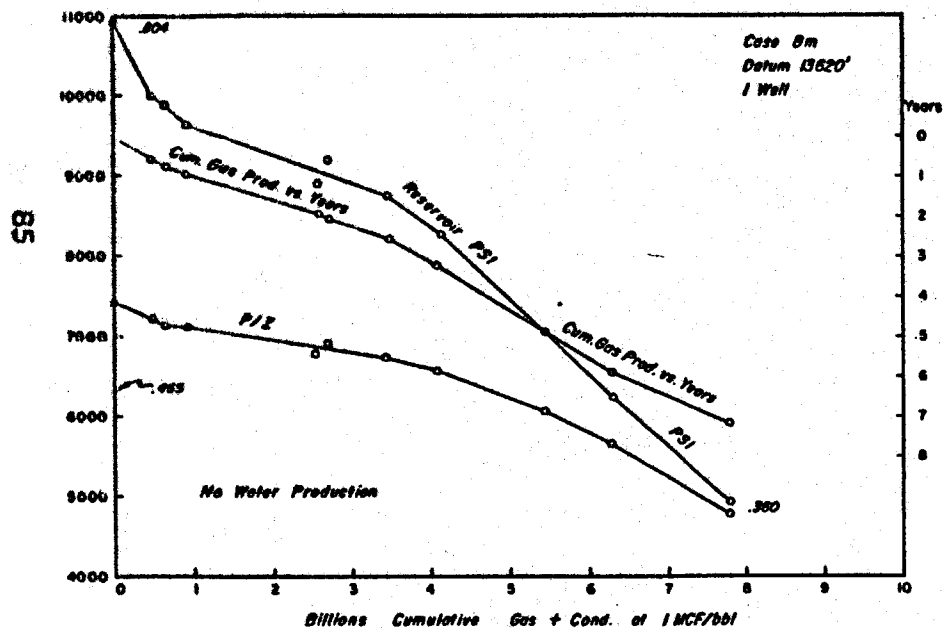


Fig. 21.

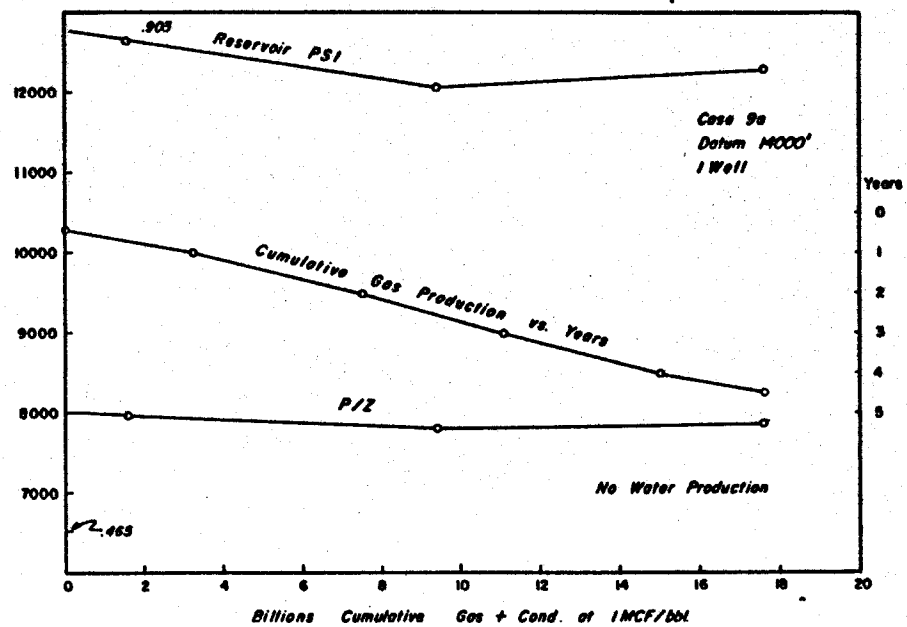


Fig. 22.

ABNORMAL PRESSURES AND POTENTIAL GEOTHERMAL
RESOURCES IN THE RIO GRANDE EMBAYMENT
OF TEXAS¹

by

Raymond H. Wallace, Jr.²

Abstract

Abnormally pressured deltaic and near-shore marine deposits of Cenozoic age in the Rio Grande Embayment of Texas contain large quantities of fresh to moderately saline ground water in which dissolved solids are commonly less than 10,000 milligrams per liter.

Vertical variations in geothermal gradients in zones of geopressure range upward to 16°F. per 100 feet, and gradients in excess of 2.5°F. per 100 feet are common. Isogeothermal surfaces at relatively shallow depths in the Rio Grande Embayment probably reflect the shift of the depocenter from south Texas to the Mississippi Embayment during Neogene time. Igneous and metamorphic activity along the margins and within the Rio Grande Embayment is also believed to have been a factor in the upward displacement of isogeothermal surfaces.

A preliminary investigation of the Tabasco-Weslaco area in Hidalgo County, Texas reveals that geothermal gradients and isogeothermal surfaces are strongly affected by growth faulting and diapirism; and that "deep basin" hydrodynamic processes--thermal diagenesis of clay minerals, chemical and thermal osmosis, and redistribution of salinity --appear responsible for the hydrologic conditions.

¹Publication authorized by the Director, U. S. Geological Survey.

²Geologist, U. S. Geological Survey, Gulf Coast Hydroscience Center, MTF-NASA, Bay St. Louis, Mississippi 39520.

Geologic and hydrologic conditions in the Rio Grande Embayment appear favorable for development of geothermal resources; however, further detailed investigations are needed, and engineering and legal problems must be solved before the resource potential can be exploited.

Introduction

The First Abnormal Subsurface Pressure Symposium (April, 1967) included discussions concerning the relations of geologic structure, abnormally high temperature and pressure, and clay-bed phenomena responsible for observed hydrologic conditions in buried deltaic and near-shore marine deposits of the northern Gulf of Mexico basin. A sizable water-resource and thermal-energy potential is evident, apparently the result of dynamic evolutionary processes unique to young sedimentary basins. To identify and evaluate the principal factors in this hydrogeologic process, the Rio Grande Embayment area was selected for detailed investigation, and research leading to this report was conducted by the U. S. Geological Survey. Later, studies will be extended into parts of the basin that are characterized by less advanced stages of hydrologic evolution, as well as those more advanced. The Rio Grande Embayment was selected because the results of geologic reconnaissance, correlated with regional data collected, reveal well-defined conditions of structure, temperature, pressure and water quality.

The most prominent structural feature in the western Gulf of Mexico basin is the Rio Grande Embayment (Fig. 1) which plunges southeastward from the Del Rio Ridge of Texas toward the Gulf of Mexico. It includes within its flanks a large part of southeastern Texas and parts of the Mexican States of Coahuila, Nuevo León, and Tamaulipas (Murray, 1961, p. 128).

The Sierra Madre Oriental which forms the southwestern boundary of the Rio Grande Embayment (Murray, 1961, p. 128), arose from the narrow Mexican geosyncline during the Late Cretaceous Laramide orogeny. Following this event, violent diastrophism in early and middle Eocene time resulted in numerous southeastward-plunging folds, the Coahuila Marginal Folded Belt (Fig. 1), which trends parallel to the axis of and lies within the Rio Grande Embayment northeast of the Sierra Madre Oriental front (Alvarez, 1949, p. 1330; Humphrey, 1956, p. 28; Fowler, 1956, p. 41). Volcanic activity also occurred at this time along the southwestern and upper northeastern margins of the Rio Grande Embayment (Lyons, 1957, pp. 8-9), and continued into Miocene time. Ash beds and volcanic detritus in Tertiary deposits of the Gulf basin provide evidence of the extent of this activity.

During periods of basinal subsidence, very thick and extensive deposits of deltaic and delta-associated sands and clays accumulated in the Embayment. These deposits were contemporaneously deformed by regional down-to-the Gulf faulting (Figs. 1 and 2). Some faults have displacements exceeding 1 mile and can be traced for over 50 miles. These

growth-faulted deposits (Ocamb, 1961, p. 139) characterize the Gulf Coast side of the Rio Grande Embayment. Growth-fault systems such as the Mirando-Provident City, Sam Fordyce-Vanderbilt, McAllen and Willamar (Fig. 1), formed where succeeding younger deltaic sand masses overrode massive prodelta and near-shore marine clays deposited during the preceding deltaic cycle. Growth faults mark sediment facies boundaries.

Compartmentalization of sand-bed aquifers by faulting contemporaneous with continued sedimentary loading restricts the normal up-dip release of fluids (Fig. 3) from the compacting, rapidly-buried sequences of sand and clay in the Rio Grande Embayment (Jones, 1967, pp. 126-127). These water-logged sands and clays form an abnormally-pressured belt approximately 100 miles wide (Fig. 4) in the southeastern Rio Grande Embayment; the top of the geopressed zone (Jones, 1969a, p. 803) occurs at depths generally in excess of 5,000 feet.* Geostatic ratios reflecting fluid pressure exceeding 0.9 times the weight of the overlying deposits have been observed in this zone.

Comparison of published and unpublished geothermal gradient maps (Figs. 5 and 6) for the Rio Grande and Mississippi Embayments reveals an apparent upward displacement of isogeothermal surfaces in the Rio Grande Embayment. These geothermal conditions may reflect the shift of the Gulf Basin depocenter to the Mississippi Embayment area of the Gulf Coast geosyncline during Neogene time (Williamson, 1959, p. 25); or they may be the result of tectonic activity in the Rio Grande Embayment. Perhaps both factors are important. Tectonic activity capable of providing the thermal energy required is evident within and adjacent to the northern margin of the Embayment, and along the steep southwestern flank of this triangular slightly asymmetrical basin. Uplift of the Sierra Madre Oriental, for example, could have been accompanied by isostatic upwarp of the upper mantle to the northeast. This upwarp would bring the upper mantle closer to the basal sediments in the Rio Grande Embayment, initiating metamorphism and driving superheated water upward. Another possibility is that dynamic and thermal metamorphism associated with pre-upper Eocene folding, aided by aqueous emanations, has caused a rise of isogeothermal surfaces.

Rising temperature within great thicknesses of deeply-buried water-filled deltaic and near-shore marine sediments in the Rio Grande Embayment should (1) accelerate diagenesis

*All depths cited in this report are in feet below mean sea level unless otherwise indicated.

and dehydration (Burst, 1969, p. 90) of montmorillonite clays, releasing large volumes of "fresh" pore water to dilute formation waters in adjacent sands; (2) increase thermal conductivity while reducing porosity and permeability as aqueous emanations move upward in the system; (3) decrease viscosities of interstitial fluids; (4) produce high geothermal gradients and pressures immediately beneath beds which are most effective in retarding the upward discharge of superheated water (Jones, 1969, pp. 71-72).

Deltaic and near-shore marine deposits in the Rio Grande Embayment including (1) extensive thick aquifer systems which commonly contain water one-third as salty as normal sea water [35,000 mg/l (milligrams per liter) dissolved solids] at depths in excess of 6,000 feet, and in which formation waters freshen toward their down-dip pinch-out (Fig. 7); (2) a general decrease in the porosity and permeability of sand-bed aquifers toward the southwestern flank, at comparable depths (Johnson and Mathy, 1957, p. 212); and (3) increased geothermal gradients in the upper part of zones of abnormal pressures.

Salient features of a relatively small area within the Rio Grande Embayment are described and explained in this paper, which is based upon preliminary findings of a detailed investigation of the hydrogeology of the Rio Grande Embayment, and some preliminary observations are made as to the geothermal potential. The area of investigation covers about 425 square miles and is located north of the Rio Grande in southern Hidalgo County, Texas (Figs. 1 and 8). The eastern and western margins are defined by the 98°00' and 98°30' meridians (W Longitude), respectively.

Geologic Setting

Growth faulting associated with the build-out of Frio "sands" over Vicksburg "clays" dominates the structural scene in the Gulfward part of the Rio Grande syncline. Four major northeast-southwest trending, down-to-the-Gulf faults cut across the study area. (See Fig. 8.) From west to east, these are the Tabasco-Monte Christo, Mission, McAllen, and Donna faults. The Mission fault merges with the Tabasco-Monte Christo fault northeastward, and the Donna fault joins the McAllen fault system. The Tabasco-Monte Christo and McAllen fault systems, are traceable for many miles north-eastward generally paralleling the Gulf coastline. Southwestward into Mexico these fault systems adopt a more southeasterly course (Yzaguirre, 1957, p. 195), possibly reflecting the influence of Sierra Madre Oriental structures.

The McAllen fault and its splinter faults control the

geologic setting in the study area. This is a classic growth fault exhibiting all the significant characteristics. Miocene beds of the Lower and Middle Frio formation* were deposited contemporaneously with maximum fault movement and thicken tremendously across the fault. Collins (1968, p. 82) states that maximum throw is immeasurable, but estimates 5,000-7,000 feet of displacement in Lower Frio beds as opposed to 1,000 feet in Upper Frio beds. The dip of the fault plane decreases from 55° SE in shallow beds to 45° SE at about 11,000 feet. Frio sands and clays show a marked northwestward reversal of stratigraphic dip that increases with depth along the downthrown side of the fault plane.

The Shepherd fault, downthrown approximately 2,500 feet to the northeast, trends northwest-southeast between the McAllen and Donna faults. Thickening of beds across the fault is greatest along the fault plane from east to west, reflecting the structural dominance of the McAllen fault. A myriad of smaller down-to-the northeast faults are into the Pharr-McAllen field from the downthrown block of the Shepherd fault, but these die out upward beneath a shale bed at a depth of about 8,500 feet. According to Collins (1968, p. 82), the top of this shale bed represents a hiatus or unconformity in the Frio; below it, the pressure gradient increases abruptly.

The oldest beds penetrated by the drill on the upthrown side of the McAllen fault are in the Vicksburg formation of Oligocene age. They are predominately shales that were deposited gulfward from the very sandy shallow marine facies of the formation (Holcomb, 1964, p. 24). Shales of the Lower Frio deep-water marine facies are the oldest beds penetrated on the downthrown side of the fault, with one exception. A well in the Donna field logged the top of the Vicksburg formation at a depth of 10,530 feet which is stratigraphically 4,000 feet shallower than in surrounding areas (Collins, 1968, p. 81). A piercement-type shale diapir is responsible for this anomaly.

Continental and marine sands and shales of the Miocene Frio formation with cumulative thicknesses greater than 10,000 feet have been penetrated in the study area in the search for oil and gas. The top of the formation lies approximately 4,000 feet below the land surface in the Pharr-McAllen field, and the formation dips generally south-eastward. The sediments of the Frio formation are mainly medium- to very fine-grained quartzose sand and montmorillonite-illite clay. Immediately downdip from the major

*The nomenclature used in this report is not necessarily that of the USGS.

faults the degree of sorting is generally poor, reflecting an extremely high rate of deposition contemporaneous with fault movement. With increasing distance from the faults, however, the degree of sorting increases significantly, presumably as a result of winnowing by longshore currents. The areal continuity of individual beds is poor; it generally is somewhat better in the direction of strike than in other directions. Individual sand and clay beds range in thickness from less than 1 foot to about 1,000 feet. According to Fisher (1969, p. 250), Frio sediments were deposited by a "wave-dominated high-destructive delta system," they formed in distributary channels, in extensive shallow embayments subject to marine transgressions, and in strand-plain and coastal-barrier systems similar to those of the modern Rhone delta.

Delta-lobe deposition occurs in high-destructive delta systems as in high-constructive systems, but the lobes are less numerous (that is, the modern Mississippi delta versus the Rhone delta) (Fisher, 1969, p. 260).

The Anahuac formation of Miocene age overlies the Frio formation in the eastern part of the study area. Westward, the Anahuac wedges out in the vicinity of the McAllen fault. A maximum thickness of about 600 feet was penetrated in a well in the South Weslaco field. The remainder of the stratigraphic section overlying the Frio and Anahuac beds is represented by sandy deposits of the Catahoula, Oakville and Lagarto-Goliad formations (Corpus Christi Geological Society, 1954).

Hydrology of Deposits

Chemical analyses of more than 100 formation waters from oil-test and production wells in the Tabasco-Weslaco area (Fig. 8) show dissolved solids (salinity) ranging from about 2,000 to about 150,000 mg/l at depths between 5,353 and 11,836 feet. The samples analyzed were collected during drill-stem and wire-line testing of potential gas or oil reservoirs. Reported results of many drill-stem tests where produced water was analyzed, and a number of reports involving salinity estimation by taste indicated relatively high flow rates of brackish and fresh water at the well-head. According to Collins (1968, p. 84), hydrocarbons are presently produced from several "water-drive" reservoirs within the abnormally pressured zone in the Pharr-McAllen field.

With few exceptions, electrical and induction-electrical logs of wells in the study area show subdued negative or small positive deflections of the spontaneous potential curve

opposite massive sand beds below a depth of about 10,000 feet. Calculations of interstitial water salinities show that they are commonly less than 10,000 mg/l (dissolved solids as NaCl).

Salinity-distribution maps have not been completed for the Tabasco-Weslaco area, but preliminary investigation suggests that there is a general decrease in formation-water salinity with depth and down-dip--highly complicated by faulting; also, that extensive "fresh" to brackish-water aquifer systems occur at depths greater than 6,000 feet and extending below 14,000 feet.

Low salinity waters in aquifers within the abnormally-pressured zone are believed to be derived from bound and intracrystalline water in the adjacent clay beds, as a result of thermally controlled diagenesis of montmorillonite (Fig. 9). This produces free pore water, as described by Burst (1969, pp. 80-87). Some of the free pore water appears to have escaped into adjacent sand beds. Jones (1967, p. 164) states, "water released by clay dehydration is fresh water and its volume may be equal to 10-15 per cent of the bulk volume of the clayey sediments." Movement of this "fresh" water into adjacent aquifers would tend to flush out and dilute the original waters of deposition. Production of fluids from these aquifers would lower the head in them and cause release of additional free pore water from adjacent clay beds. Continued freshening of aquifer waters could thus occur.

Formation waters of the so-called Frio brackish-water sediment facies in this area (Corpus Christi Geological Society, 1954; Johnson and Mathy, 1957, p. 207; Holcomb, 1964, p. 29; and Collins, 1968, p. 86) are commonly 25 times more saline than waters from sediments deposited in "inner-middle neritic" and "open-to-the-sea" marine environments. Redistribution of dissolved solids has taken place in these sediments since deposition (Fig. 9).

The brackish-water sediment facies in the Pharr-McAllen field occurs just above a 100-foot-thick shale bed at a depth of about 8,500 feet, beneath which abnormally high fluid pressures exist (Collins, 1967, p. 10). Available water analyses indicate that salinities decrease upward across this confining shale layer, which is immediately underlain by massive sands. Upward freshening of waters by hyperfiltration has probably occurred (hyperfiltration is a process whereby selected ionic species are allowed to pass through clay-shale membranes while others are retained and concentrated). Jones (1967, pp. 170, 172-173) considered this process an important mechanism in salinity redistribution in Neogene deposits of the northern Gulf of Mexico basin.

Porosity and permeability data presently available are insufficient to permit reliable conclusions regarding their relation to the hydrologic setting. General indications are that in the abnormally pressured sand beds, porosity is about 20 per cent at depths of about 11,500 feet; and that permeability is highly variable, but generally lower than in the overlying normally-pressured deposits. Low permeability is, however, offset somewhat by low fluid viscosity of relatively fresh water in the geopressured zone. As shown in Figure 10, fresh water at 250°F. is about 40 per cent less viscous than a brine containing 240,000 mg/l dissolved solids. Effective permeability and the specific yield of wells would be increased by the relatively high temperatures of the geopressured zone.

Geothermal Regime

Bottom-hole temperature measurements recorded on electrical log headings for approximately 150 deep oil and gas test wells were used in preparation of isogeothermal and geothermal gradient maps of the Tabasco-Weslaco area. Extrapolated data were used only where the observed temperature was within 10°F. of the isogeotherm mapped. No correction factors were applied to the log-heading temperature data.

Considerable skepticism has been expressed concerning the accuracy of nonequilibrium bottom-hole temperature readings made during drilling operations, and there is a general reluctance to use these data. Recent research by Ramey (1962, p. 427 to 433) and Schoepel and Gilarranz (1966, p. 672) indicates that without correction log-heading temperatures provide valuable information for regional temperature studies. The merit of bottom-hole temperature information is further attested by a decision of the Research Committee of the American Association of Petroleum Geologists, in April, 1968, to use this data source in its Geothermal Survey of North America. The use of log-heading temperatures is attacked mainly on the grounds that the measurements are made before the bore-holes have reached thermal equilibrium and, therefore, do not represent true geothermal conditions. There is general agreement that bottom-hole temperatures measured during drilling operations will be lower than actual temperatures at bottom-hole depths. However, Schoepel and Gilarranz (1966, p. 672) state that "observed temperatures are likely to be within 5 percent of the formation temperature."

Temperature Distribution

The depth of occurrence of the 200°F. isogeothermal surface (Fig. 11) in the Tabasco-Weslaco area, with reference to mean sea level, ranges from about 6,000 feet, immediately downdip from the Tabasco-Monte Cristo fault, to about 10,760 feet at the eastern margin of the area. Maximum relief on the 200°F. isogeothermal surface thus exceeds 4,100 feet. The surface usually occurs between depths of 8,000 and 10,000 feet, and slopes generally southeastward.

The McAllen, Shepherd, and Tabasco-Monte Cristo faults appear to control subsurface temperature distribution. The northeast-southwest alignment of isogeotherms between the McAllen and Donna faults reflects the myriad of smaller faults extending northward from the downthrown block of the Shepherd fault. The effect of these structures on subsurface temperature distribution is best illustrated by a northwest-southeast cross-section (Fig. 12). Continuing movement along the McAllen fault with time has resulted in a westward migration of structural apexes (Collins, 1968, p. 83). In most instances it is evident that structural highs and thermal highs are coincident (for example, between wells 2-3, 6-7, 10-11, 11-12, 12-13). The geopressuring or capping shale bed (see Fig. 12) appears to be a relatively effective thermal barrier in the vicinity of the line of section. There are two areas, one between the McAllen fault and well 3, and another beneath well 7, where the 200°F. isogeotherm is above the capping shale. Lewis and Rose (1969, p. 1) state "wherever flowing heat meets an obstacle (an insulator) there is a build-up of heat against its face. The temperature rises on this face until a higher temperature gradient exists across the obstacle. Enough heat will then flow through the insulator to balance the flow of incoming heat." It appears that heat transmission is achieved most efficiently by temperature buildup beneath the highest point on a structure. Upward continuity of bedding type and the geometry of fault planes are also factors that combine to determine geothermal gradients and isogeothermal surfaces.

The depth of the 250°F. isogeothermal surface (Fig. 13) ranges from about 8,160 to 11,900 feet below sea level and its average depth of occurrence is about 11,000 feet. Regionally the surface dips southeastward and maximum relief is greater than 3,700 feet. The pattern of the 250°F. isogeotherm reflects the same general structural controls indicated for the 200°F. isogeotherm--but regional anomalies are more apparent.

The elongate northwest-southeast-trending high at the Shepherd-Donna fault juncture is the isogeothermal expression of a piercement-type shale diapir. The 250°F. isogeotherm

occurs at its shallowest depth in this area--within 8,150 feet of the land surface. One well in this vicinity has a recorded temperature of 340°F. at a depth of about 10,000 feet.

Geothermal highs on the map of the 200°F. isogeotherm are also geothermal highs on the 250°F. isogeotherm with few exceptions. However, the 250°F. isogeotherm has about 400 feet less relief than the 200°F. isogeotherm and appears to be less irregular, probably because the latter is nearer the top of the abnormal pressure zone. This relief difference is caused principally by the shale diapir anomaly mentioned above, and it is reasonable to expect that, at progressively greater depths below the confining layer, temperature distribution should become more uniform.

Geothermal Gradients

Geothermal gradient maps published by Nichols (1947, p. 44) and Moses (Fig. 6) show isogradient lines in the Tabasco-Weslaco area; the gradients increase inland from 1.9°F. per 100 feet to 2.1°F. per 100 feet. This is a reasonably accurate representation of conditions above the zone of abnormal pressures -- above a depth of about 8,000 feet in the study area. A geothermal gradient map of the depth interval between the 200° and 250°F. isogeotherms (Fig. 14) indicates a geothermal gradient generally higher than 2.5°F. per 100 feet for the interval. This thermal interval occurs mainly in the upper part of the abnormal pressure zone, where maximum geothermal gradients would be expected. Nichols' and Moses' maps are probably adequate to describe subsurface temperatures under normally pressured conditions, but the gradients they show should not be extrapolated into the abnormally pressured zone.

Geothermal gradient patterns in the Tabasco-Weslaco area appear to reflect two alignments; one northeast-southwest attributed to the effect of growth faulting; and the other, a series of northwest-southeast trending "high" with intervening "lows" interrupted by faulting. The northwest-southeast orientation conforms with the general alignment of the folded province northeast of the Sierra Madre Oriental front (Fig. 1) and with the general axis of deposition in the area.

Effects of Lithology on Geothermal Gradients

Studies were made to determine the effect of lithology on the geothermal gradient in the depth interval between the 200° and 250°F. isogeotherms.

The maximum geothermal gradient in the area (see Fig. 14) ranges upward of 10°F. per 100 feet; the maximum recorded gradient, 16.7°F. per 100 feet, occurs above the shale diapir in the vicinity of the Donna field. It can be seen (Fig. 15) that the percentage of sand in the depth interval between the 200° and 250°F. isotherms is greatest in the areas of maximum geothermal gradient. In the Donna area, the sands are very fine grained and have good porosity but very low permeabilities. This loss of permeability appears to be caused by precipitation of calcium carbonate in the sands. Adjacent shale beds have also become indurated by precipitation of calcium carbonate. Water, or possibly gas --which has 25 times the insulating effect of water--appears to be locked within the interstices between the sand grains, reducing or eliminating convective heat flow and restricting thermal conductivity to that of the mineral grains and trapped water. Since structural highs are the most favorable areas for heat and fluid release, it is suspected that waters of different chemical species, channeled by faults and driven by diapiric movements, have mixed in the sands above the diapir, the reactions and changes in the physical conditions (temperature and pressure) resulting in cementation (Runnels, 1969, pp. 1188-1201). If the observed geothermal gradients continue downward, sericitization of clays, which occurs at temperatures on the order of 570°F., could be in progress at depths as 11,000 feet in this area. Unfortunately, no information on conditions at depth below these zones of maximum gradients is available.

An isopach map of the depth interval between the 200° and 250°F. isotherms (Fig. 16) shows the distribution of thickness reflecting differences in the thermal conductivity of the deposits. These differences identify areas with high insulating values. Areas with lower geothermal gradients have lower insulating values. The data generally conform to heat flow theory as presented by Guyod (1946, pp. 5-39) and by Lewis and Rose (1969, pp. 1-8). Areas of maximum geothermal gradient are also areas of abnormal pressures.

Geothermal Resources Development

Thermal resources of deep geosynclinal basins are not dependent upon recharge and deep circulation of meteoric water; their thermal waters are derived from the sediments themselves, and fluid depletion occurs with energy release. However, the very large amount of water in storage makes possible a continuing large-scale rate of energy production. Development of the resource must result in dynamic compaction of the sediments of the geothermal reservoir and subsidence must occur with pressure depletion--the rate and extent of

the subsidence depending upon the physical dimensions and drainage function of the reservoir.

Potential uses of this resource have been discussed by Jones (1967, p. 173; 1968, p. 124; 1969, p. 88); they include production of electrical energy by flashing superheated water to steam to drive generators; self-distillation of low-salinity waters to produce fresh water; extraction of industrial chemicals precipitated as a result of distillation; and injection of superheated water or steam from geopressured zones into pressure-depleted reservoirs at shallower depths, for secondary recovery of oil or gas. Two of these processes are patented.

Geothermal energy production does not result in air pollution, and concentrated brines can be pumped back into saline aquifers in the hydrostatic zone. There are, however, many engineering and legal problems which must be solved before this resource can be developed.

Summary and Conclusions

The Rio Grande Embayment is an area of increased geothermal flux. Rapid sedimentation across regional growth-fault systems in a subsiding basin produced large-scale stratigraphic separations of deltaic and near-shore marine sand-shale sequences. Upward drainage of these deposits has been restricted; as a consequence of this restriction, coupled with rapid sedimentation, broad areas are underlain by deeply buried, undercompacted sediments with high interstitial fluid pressures. Restriction of drainage from water-filled sediments in an area of high geothermal flux has, because of the insulating effect of the water, resulted in subsurface temperatures which are higher than those in nearby better-drained areas.

High geothermal gradients within geopressured zones have apparently hastened thermal diagenesis of swelling clays, creating large reservoirs of low-salinity water. High temperatures also decrease viscosities of interstitial fluids, but associated geochemical effects reduce porosity and permeability as formation water moves upward in the system.

The geothermal regime within the upper part of the geopressured zone in the Tabasco-Weslaco area appears to be dominated by the structural controls. Faulting and diapirism, by altering spatial relations and physical characteristics of confining clay layers as well as the aquifer systems, have greatly affected the hydrology of the system. Therefore, structure directly or indirectly influences fluid migration

(and hence salinity distribution); it defines areas of thermal and fluid release; it facilitates mixing of chemically different waters with positive or negative effects on the permeability of reservoirs; and it brings superheated aquifers closer to the surface, where they can be more economically exploited.

An accurate appraisal of geothermal resources in the Tabasco-Weslaco area and in the Rio Grande Embayment is not possible at the present time. Preliminary studies indicate, however, that geological, thermal, hydrological, and hydrodynamic conditions in the study area favor geothermal development. Future detailed research efforts will define more fully the geothermal resource potential of the Rio Grande Embayment.

REFERENCES

- Alvarez, Manuel, Jr. (1949). Tectonics of Mexico: Am. Assoc. Petroleum Geologists Bull., V. 33, No. 8, pp. 1319-1335.
- Baker, R. C. and Dale, O. C. (1961). Ground-water resources of the lower Rio Grande Valley area, Texas: Texas Board Water Engineers, Bull. 6014, 81 pp.
- Burst, J. F. (1969). Diagenesis of Gulf Coast clayey sediments and its possible relation to petroleum migration: Am. Assoc. Petroleum Geol. Bull., V. 53, No. 1, pp. 73-93.
- Charygin, M. M. and Bogomolov, Y. G. (1969). On geothermal regime of certain tectonic structures: Internat. Assoc. Sci. Hydrol. Bull. 14, No. 4, pp. 127-130.
- Collins, J. W. (1967). The geology of the McAllen-Pharr field area: Corpus Christi Geol. Soc. Bull., V. VIII, No. 4, pp. 7-32, Dec.
- Collins, J. W. (1968). The geology of the McAllen-Pharr field area, Hidalgo County, Texas: Gulf Coast Assoc. Geol. Soc. Trans., V. k8, pp. 81-97.
- Dale, O. C. (1952). Ground-water resources of Starr County, Texas: Texas Board Water Engineers, Bull. 5209, 47 pp.
- Fisher, W. L. (1969). Facies characterization of Gulf Coast basin delta systems with some Holocene analogues: Gulf Coast Assoc. Geol. Trans., V. 19, pp. 239-261.
- Fowler, Phillip (1956). Faults and folds of South-Central Texas: Gulf Coast Assoc. Geol. Soc. Trans., V. 6, pp. 37-42.
- Guyod, Hubert (1946). Temperature well logging: Well Instrument Developing Co., Houston, Texas, 47 pp.
- Hedberg, W.H. (1967). Pore-water chlorinites of subsurface shales: Univ. Wis., Ph.D. dissertation, Dept. Geol. 121 pp.

- Holcomb, C. W. (1964). Frio Formation of southern Texas: Gulf Coast Assoc. Geol. Soc. Trans., V. 14, pp. 23-33.
- Holmes, G. T. (1967). West Edinburg field, Hidalgo County, Texas: Typical oil and gas fields of south Texas, Corpus Christi Geol. Soc., pp. 198-206.
- Humphrey, W. E. (1956). Tectonic framework of northeast Mexico: Gulf Coast Assoc. Geol. Soc. Trans., V. 6, pp. 25-35.
- Jaeger, J. C. (1965). Application of the theory of heat conduction to geothermal measurements: Geophys. Mon. 8, Am. Geophys. Union, pp. 7-23.
- Jam, P. L., Dickey, P. A., and Tryggvason, Eysteinn (1969). Subsurface temperature in south Louisiana: Am. Assoc. Petroleum Geol. Bull., V. 53, No. 10, pp. 2141-2149.
- Johnson, R. B. and Mathy, H. E. (1957). The south Texas Frio trend: Gulf Coast Assoc. Geol. Soc. Trans., V. 7, pp. 207-218.
- Jones, P. H. (1967). Hydrology of Neogene deposits in the northern gulf of Mexico basin: Proceedings of the First Symposium on Abnormal Subsurface Pressure: Baton Rouge, La. State Univ., April 28, pp. 91-207.
- Jones, P. H. (1968). Geochemical Hydrodynamics--a possible key to the hydrology of certain aquifer systems in the northern part of the Gulf of Mexico basin: XXIII Internat. Geol. Cong., V. 17, pp. 113-125.
- Jones, P. H. (1969a). Hydrology of Neogene deposits in the northern Gulf of Mexico basin: La. Water Resources Research Inst. Bull. GT-2, 105 pp.
- Jones, P. H. (1969b). Hydrodynamics of geopressure in the northern Gulf of Mexico basin: Jour. Petroleum Tech., V. 21, No. 7, pp. 803-810.
- Jones, P. H. (1970). Geothermal resources of the northern Gulf of Mexico basin: paper prepared for presentation at the International Symposium on the Development and Utilization of Geothermal Resources, Pisa, Italy, Sept. 22-Oct. 1 (in press).
- Landes, K. K. (1967). Eometamorphism, and oil and gas in time and space: Am. Assoc. Petroleum Geol. Bull., V. 51, No. 6, pp. 828-841.

- Lee, W. H. K. and Uyeda, Seiya (1965). Review of heat flow data: *Terrestrial Heat Flow*, *Geophys. Mon. 8*, Am. Geophys. Union, pp. 87-190.
- Levorsen, A. I. (1967). *Geology of Petroleum*: San Francisco, W. H. Freeman and Co., 724 pages.
- Lewis, C. R. and Rose, S. C. (1969). A theory relating high temperatures and overpressures: *Soc. Petroleum Engrs., AIME, S.P.E. 2564*, Preprint, 8 pp.
- Lohse, E. A., Middour, E. S., Fipps, E. L., Barfield, W. G., Clarkson, L. B., Goodson, W. P., Hoover, L. E., Minton, J. W., Moyer, G. L. (1954). *Rio Grande cross-section--Zapata to Cameron Counties, Texas*: *Corpus Christi Geol. Soc.*
- Lyons, P. L. (1957). *Geology and geophysics of the Gulf of Mexico*: *Gulf Coast Assoc. Geol. Soc. Trans., V. 7*, pp. 1-10.
- Maxwell, J. C. (1964). Influence of depth, temperature, and geologic age on porosity of quartzose sandstone: *Am. Assoc. Petroleum Geol. Bull., V. 48, No. 5*, pp. 697-709.
- McNitt, J. R. (1965). Review of geothermal resources: *Geophys. Mon. 8*, Am. Geophys. Union, pp. 240-266.
- Moses, P. L. (1961). Geothermal gradients now known in greater detail: *World Oil*, V. 152, No. 6, pp. 79-82, May.
- Murray, G. E. (1961). *Geology of Atlantic and Gulf Coastal province of North America*: New York, Harper and Bros., 692 pp.
- Nichols, E. A. (1947). Geothermal gradients in Mid-Continent and Gulf Coast Oil Fields: *Trans., Am. Inst. Min. Met. Engrs., V. 170*, p. 44.
- Ocamb, R. D. (1961). Growth faults of South Louisiana: *Trans. Gulf Coast Assoc. Geol. Soc., V. 11*, pp. 139-175.
- Powers, M. C. (1967). Fluid-release mechanisms in compacting marine mudrocks and their importance in oil exploration: *Am. Assoc. Petroleum Geol. Bull., V. 51, No. 7*, pp. 1240-1254.
- Ramey, H. J. (1962). Wellbore heat transmission: *Jour. Petroleum Tech., V. 225*, pp. 427-433, Apr.

- Runnels, D. D. (1969). Diagenesis, chemical sediments, and the mixing of natural waters: Jour. Sedimentary Petrology, V. 39, No. 3, pp. 1188-1201, Sept.
- Schoepfel, R. J. and Gilarranz, Santos (1966). Use of well log temperatures to evaluate regional geothermal gradients: Jour. Petroleum Tech., V. 237, pp. 667-673, June.
- Timm, B. C. and Maricelli, J. J. (1953). Formation waters in southwest Louisiana: Am. Assoc. Petroleum Geol. Bull., V. 37, pp. 394-409.
- Walker, K. R. (1964). Influence of depth, temperature, and geologic age on porosity of quartzose sandstone--discussion: Am. Assoc. Petroleum Geol. Bull., V. 48, No. 12, pp. 1945-1946.
- Walker, Terry (1959). Log interpretation in the brackish water - Frio Trend: Gulf Coast Assoc. Geol. Soc. Trans., V. 9, pp. 171-178.
- White, D. E. (1965). Saline waters of sedimentary rocks: in Fluids in Subsurface Environments: Am. Assoc. Petroleum Geol. Mem. 4, pp. 342-366.
- Williamson, J. D. M. (1959). Gulf Coast Cenozoic history: Gulf Coast Assoc. Geol. Soc. Trans., V. 9, pp. 15-29.
- Yzaguirre, L. A. (1957). Petroleum geology of the Anahuac and Frio formations of northeastern Mexico: Gulf Coast Assoc. Geol. Soc. Trans., V. 7, pp. 191-206.

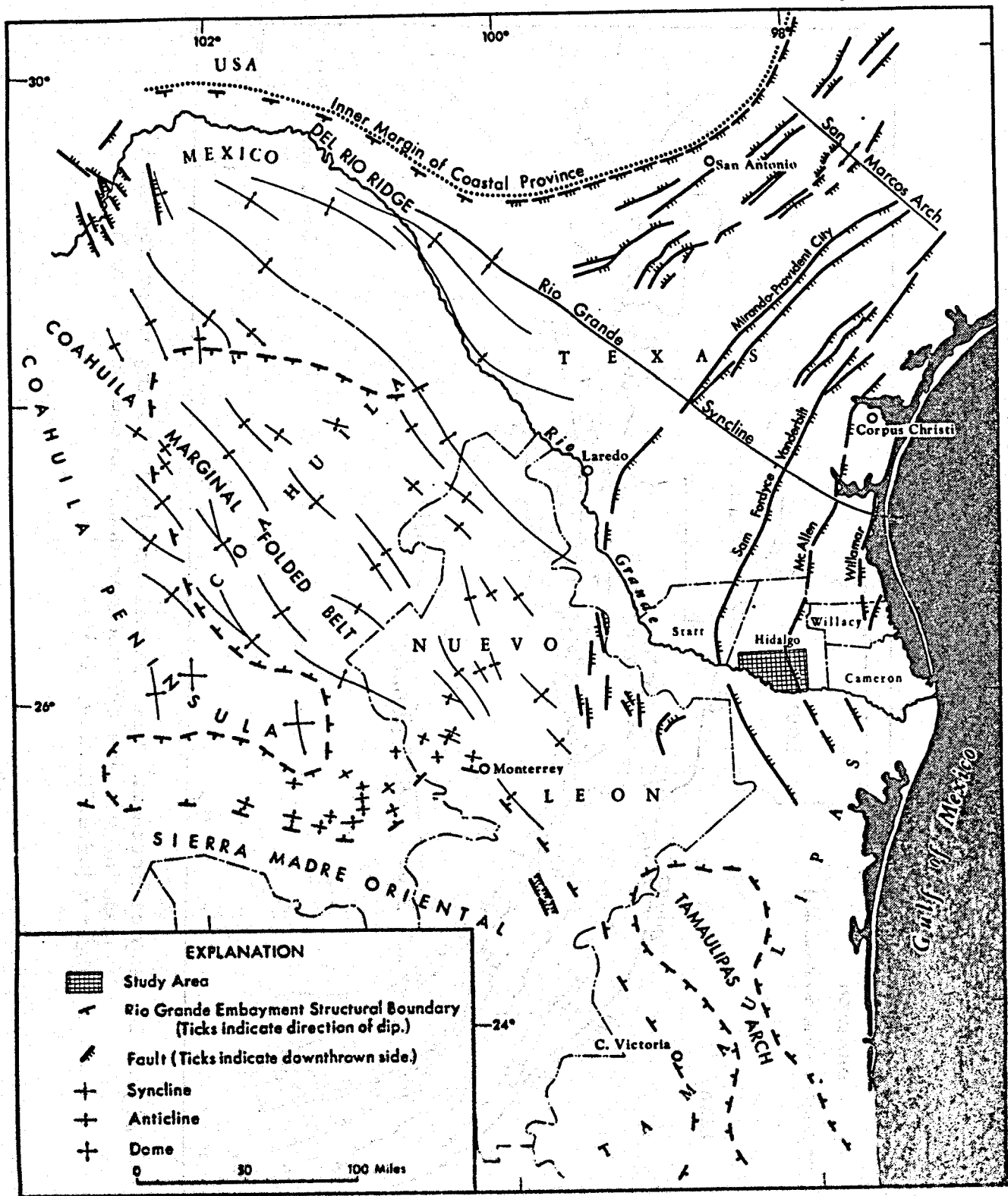


Figure 1. Tectonic map of the Rio Grande Embayment in relation to study area for this report (modified from Barton, 1936 and Murray, 1961).

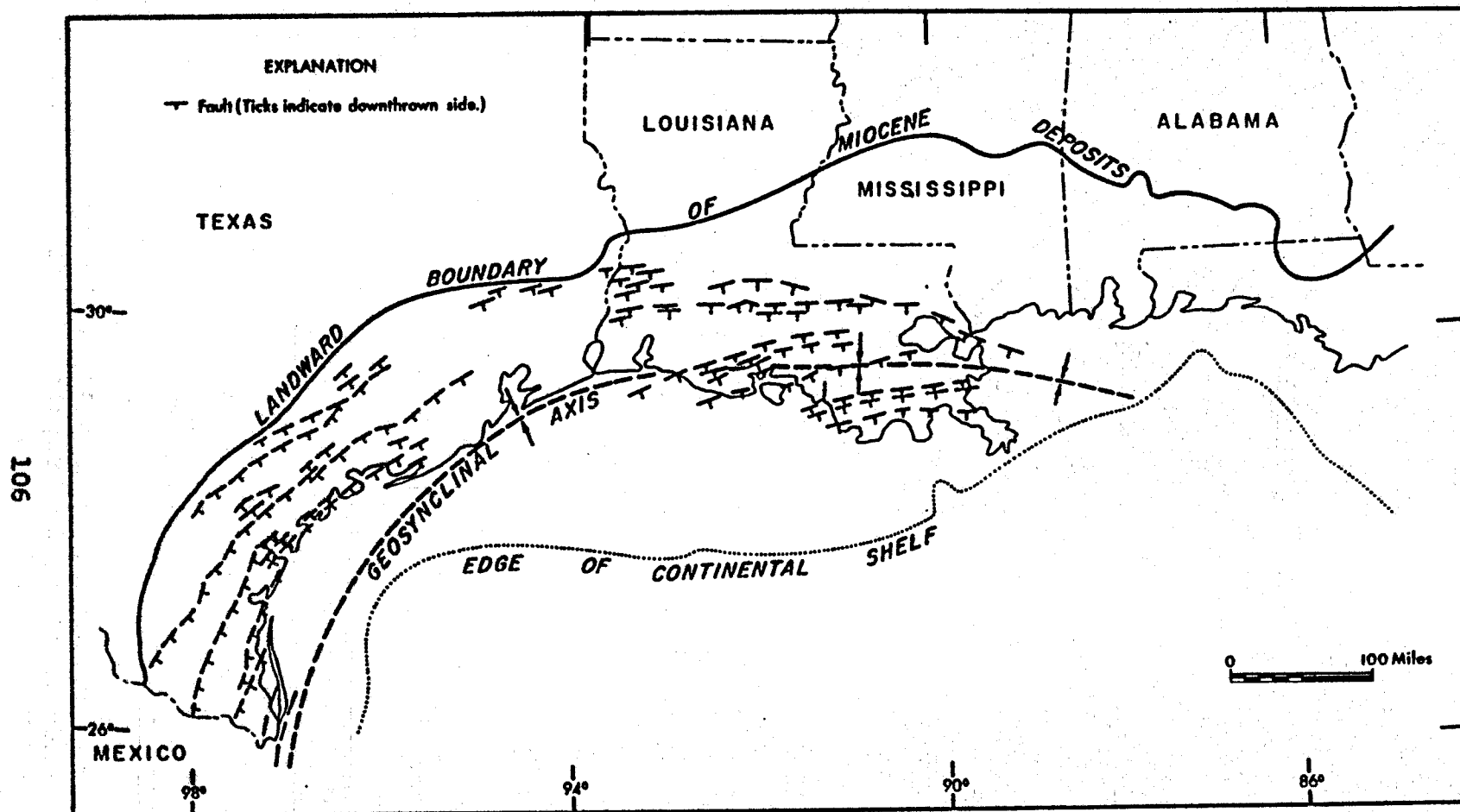


Figure 2. Map of Northern Gulf Coastal Province showing major regional systems of Miocene and younger down-to-the-Gulf growth faults (after Murray, 1961).

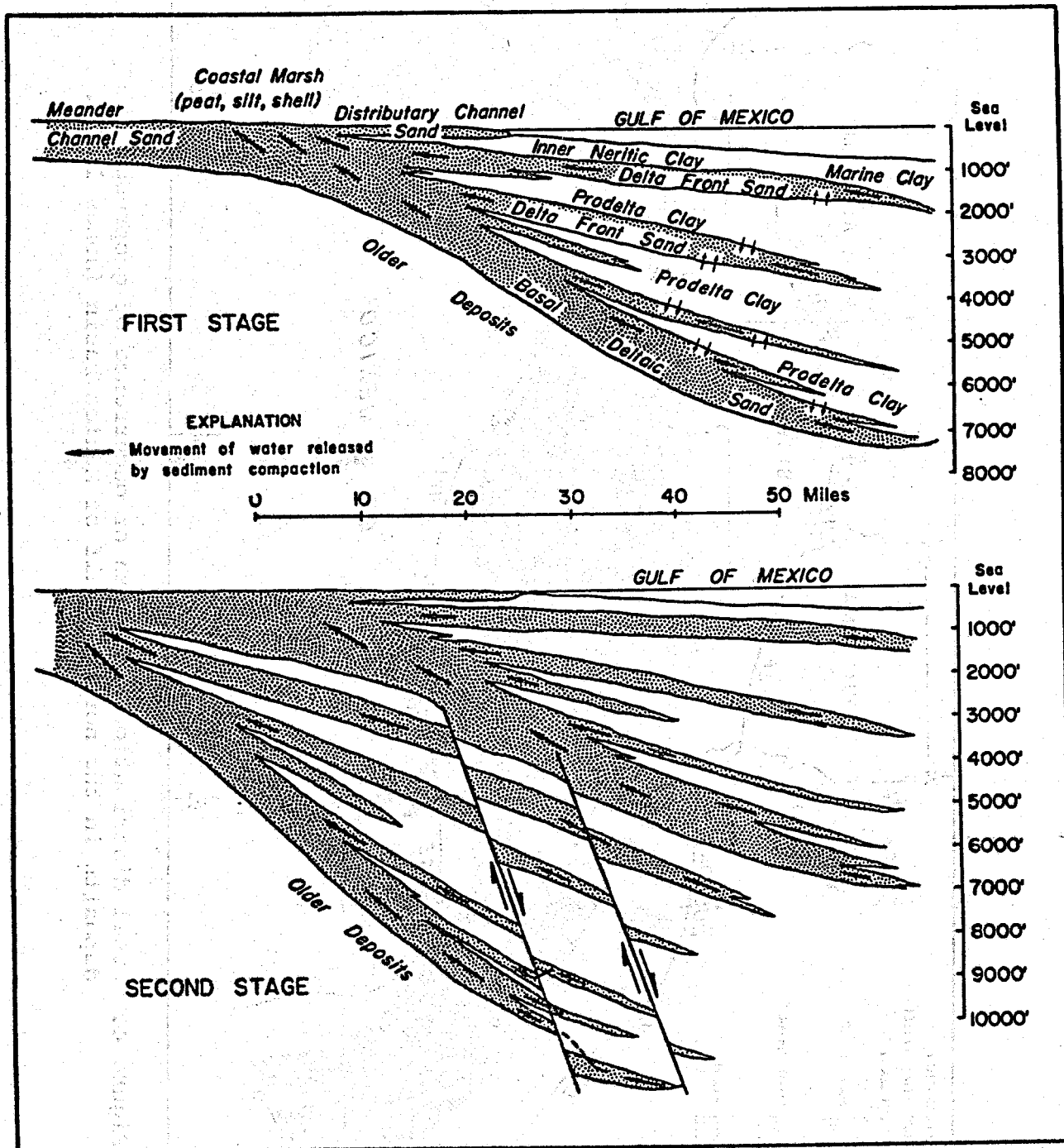


Figure 3. Schematic cross-section through deltaic and near shore marine deposits showing the effect of faulting on normal up-dip release of fluids (Jones, 1967).

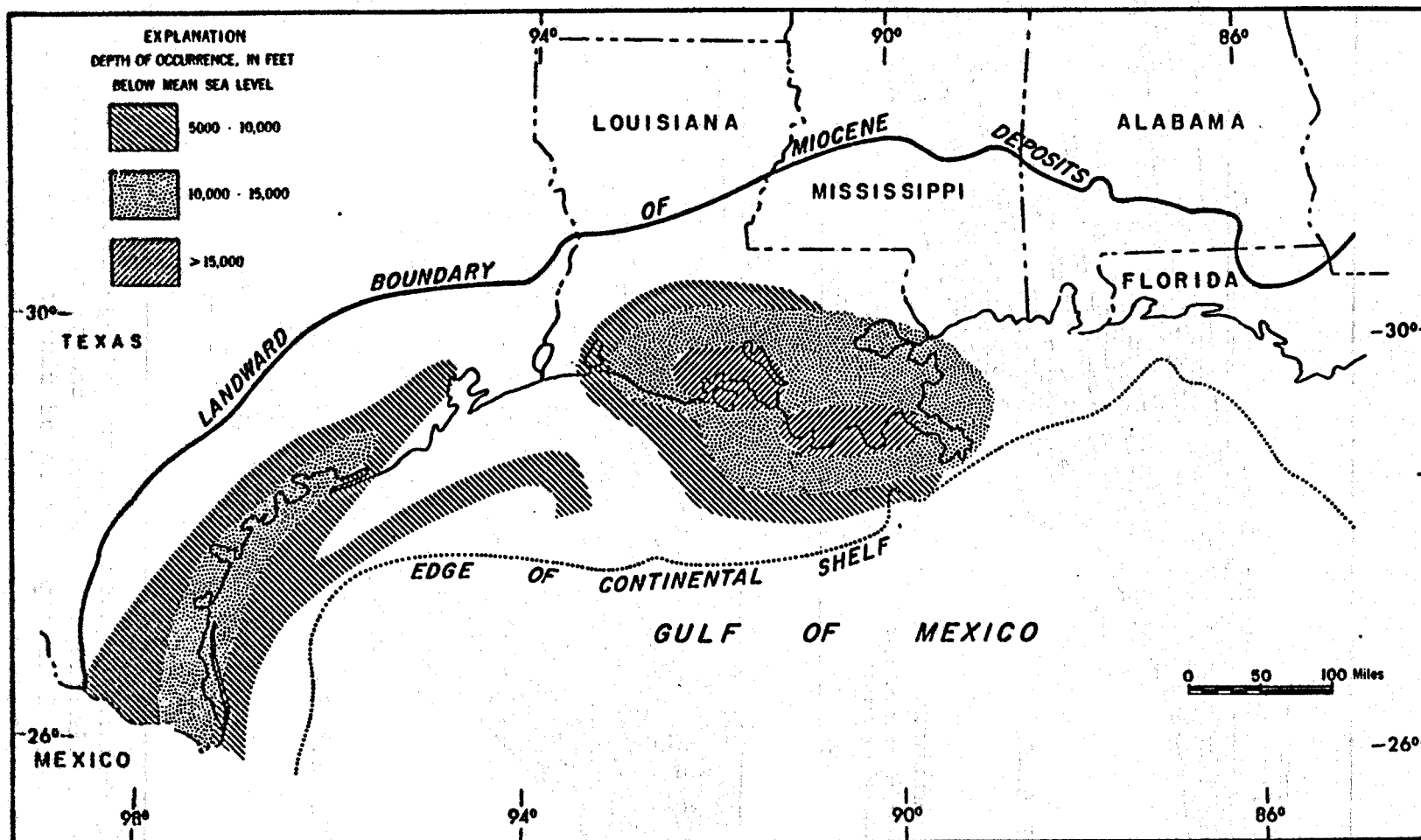


Figure 4. Areal distribution and depth of occurrence of geopressed deposits in the northern Gulf of Mexico basin (Jones 1967).

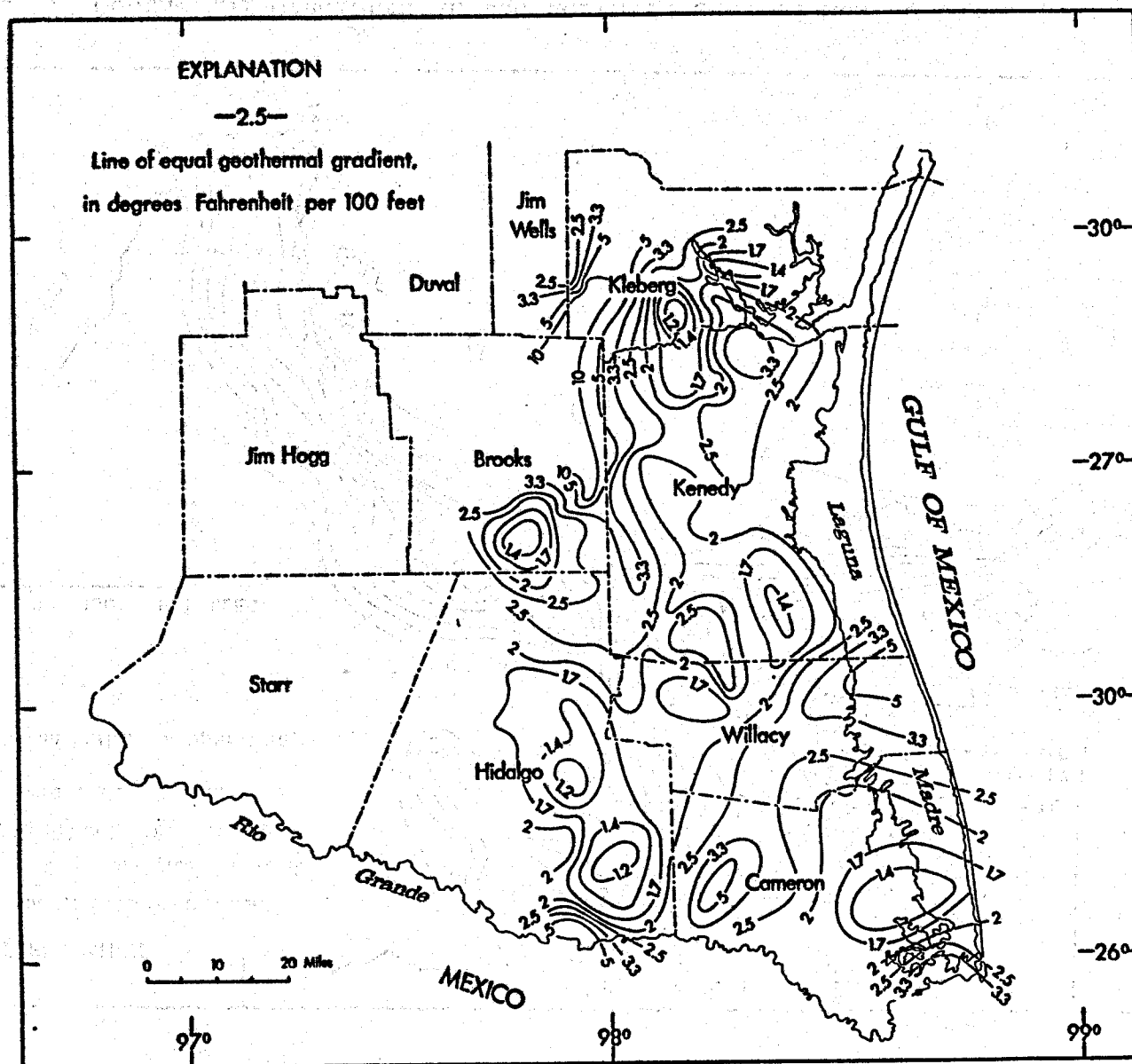


Figure 5. Map of geothermal gradient between 250°F. and 300°F. isotherms in Southeast Texas.

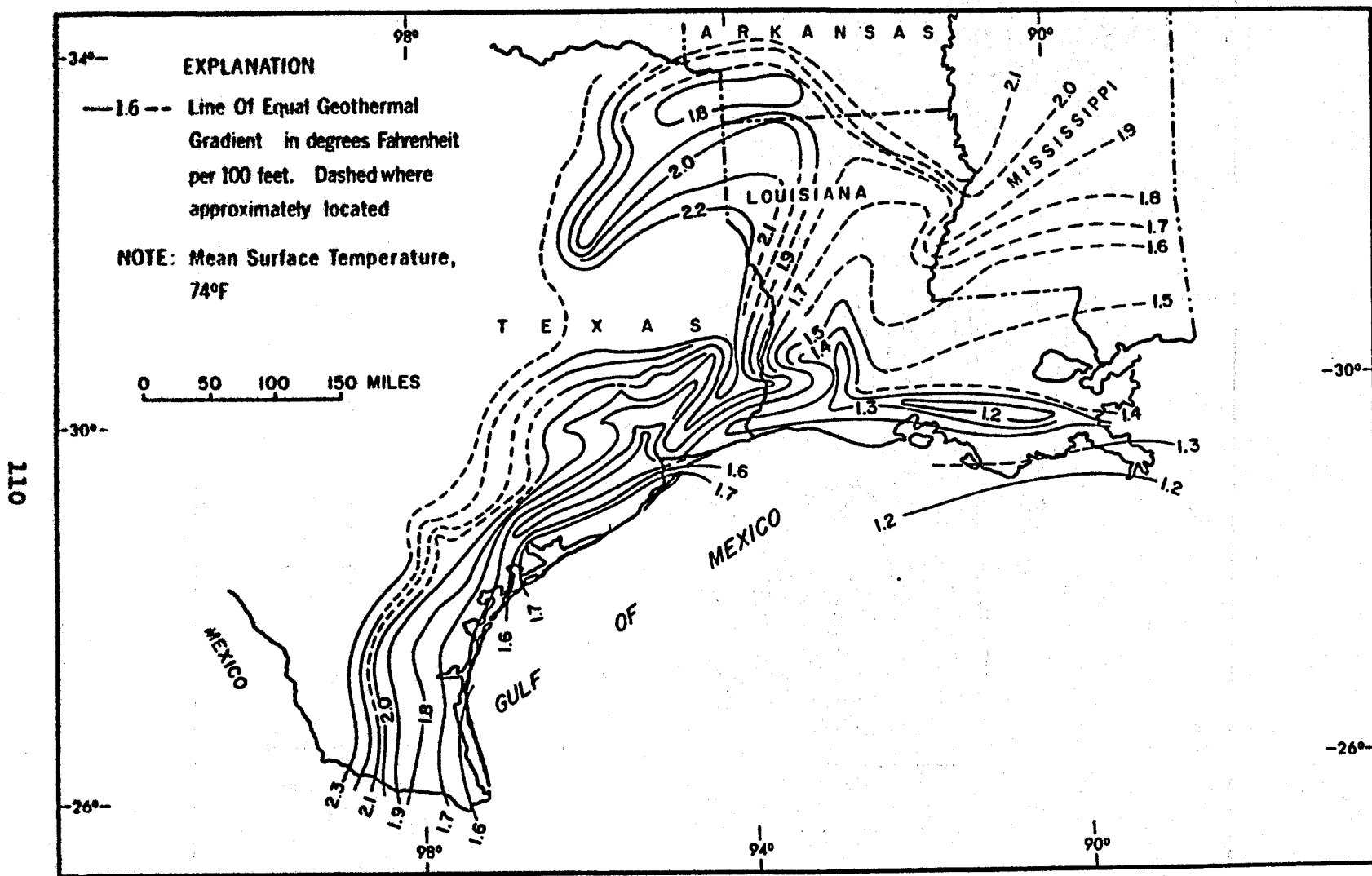


Figure 6. Geothermal gradients in the northern Gulf of Mexico basin (Moses, 1961)

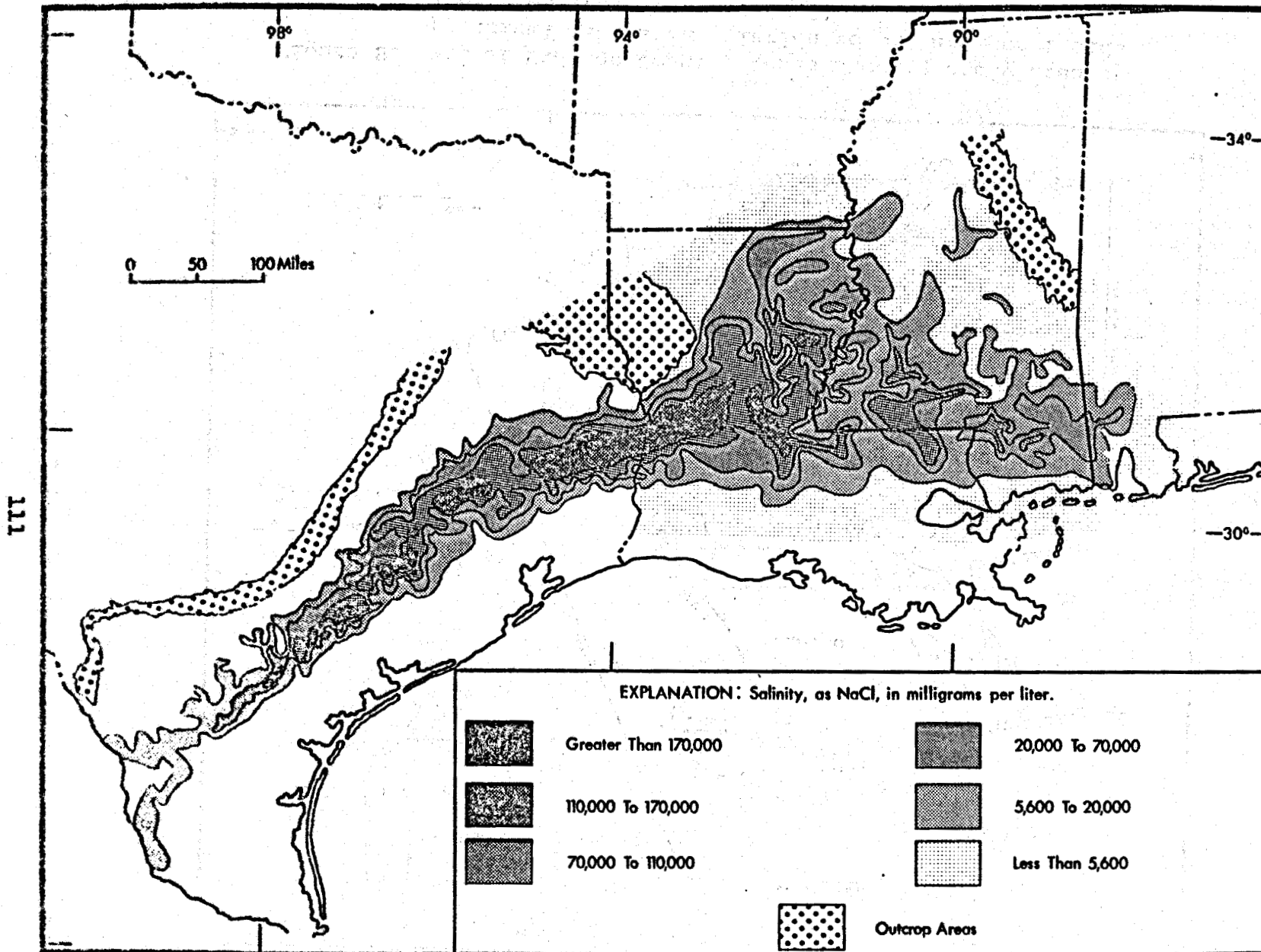


Figure 7. Distribution of formation water salinity within 100 feet of the top of the Wilcox Formation in the northern Gulf of Mexico basin (Courtesy of Tom Hingle, Mobil Oil Corporation).

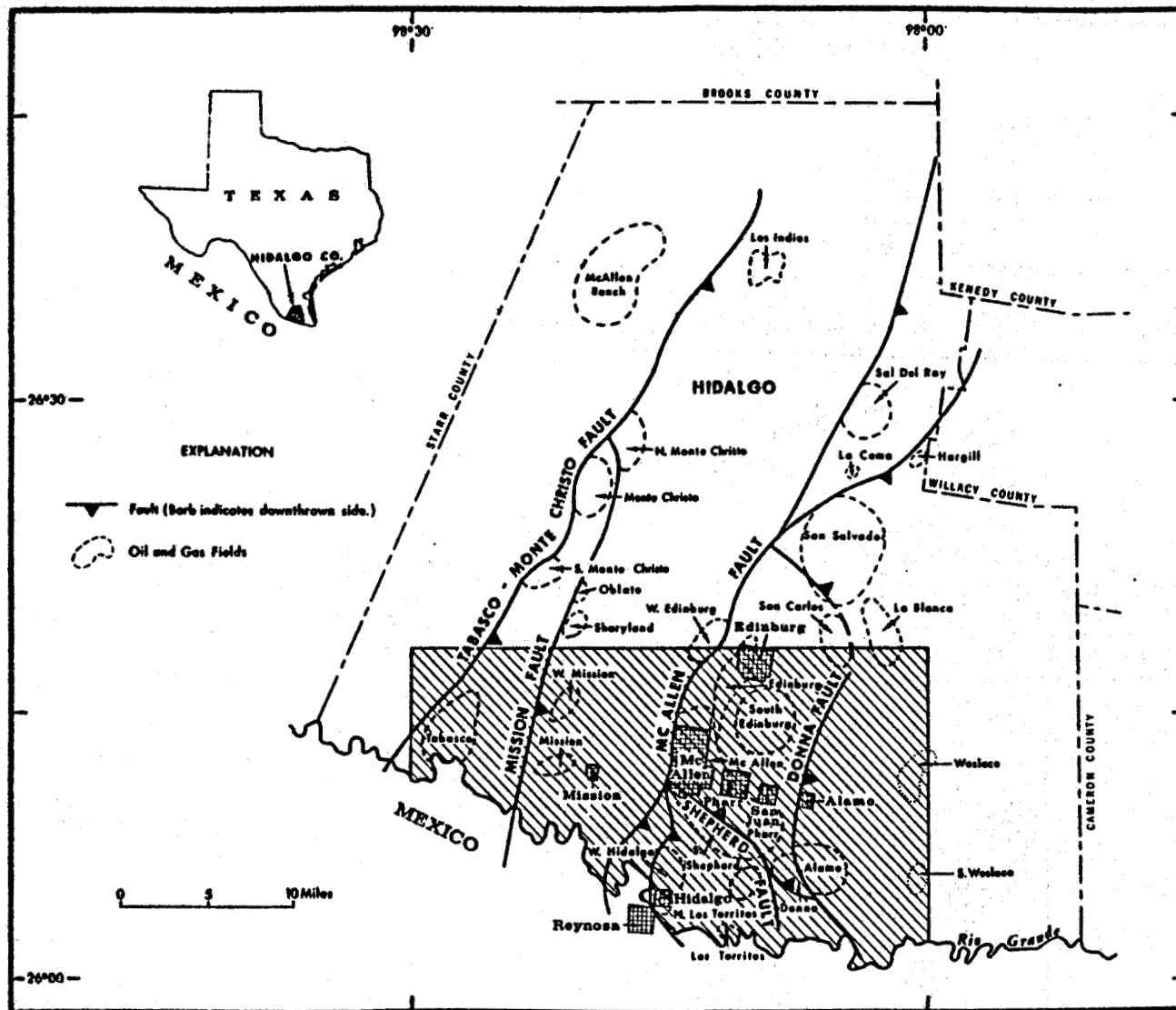


Figure 8. Map of Hidalgo County, Texas showing study area and principal faults in relation to oil and gas fields (modified from Collins, 1968).

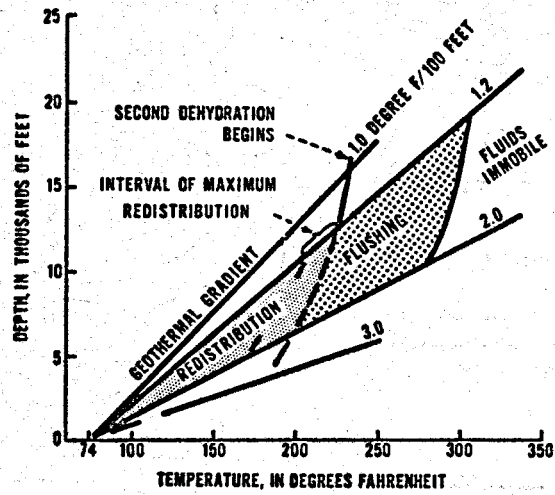


Figure 9. Fluid redistribution model for the northern Gulf of Mexico basin (from Burst, 1969).

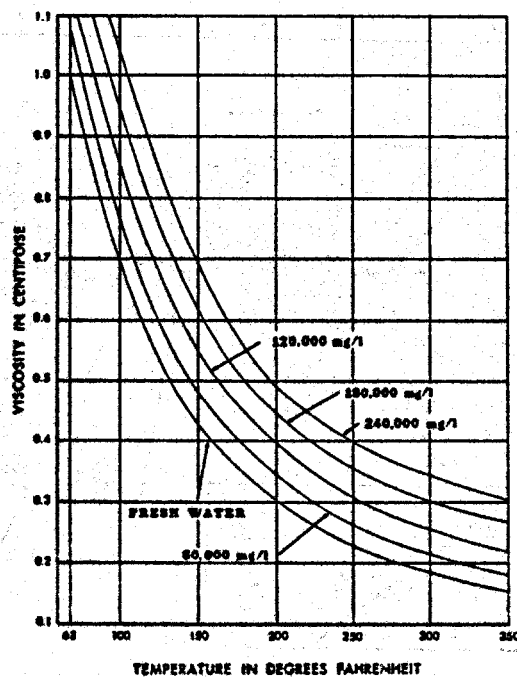


Figure 10. Relation between the viscosity, temperature, and dissolved solids content of water. (Pirson, 1963, figures 4 - 6.)

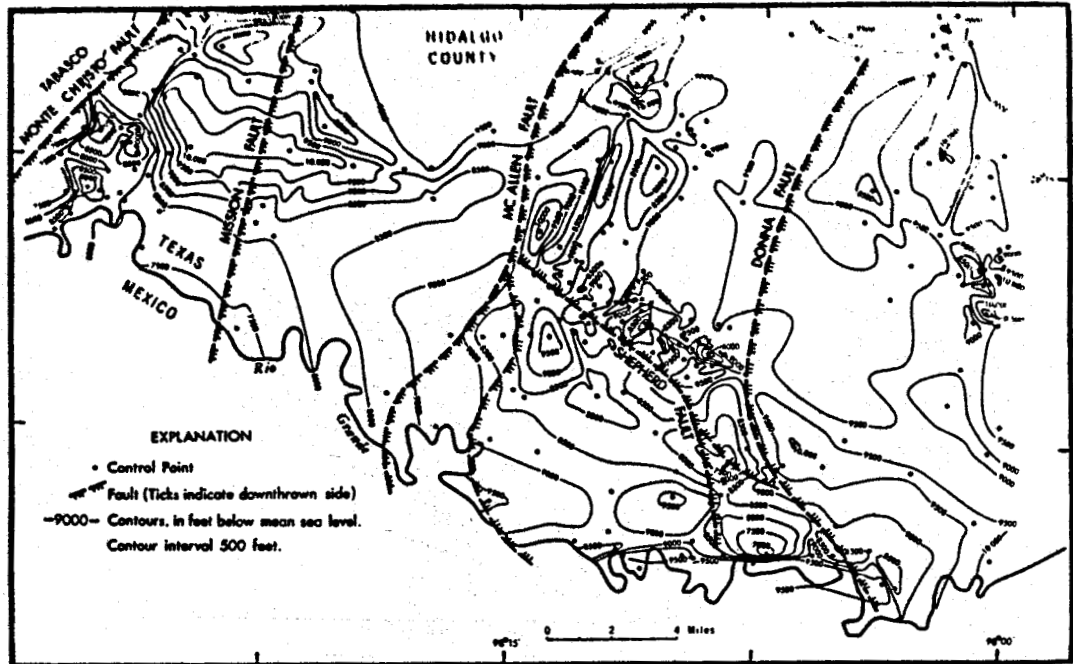


Figure 11. Depth of occurrence of the 200°F. isogeotherm within the study area outlined in Figure 8.

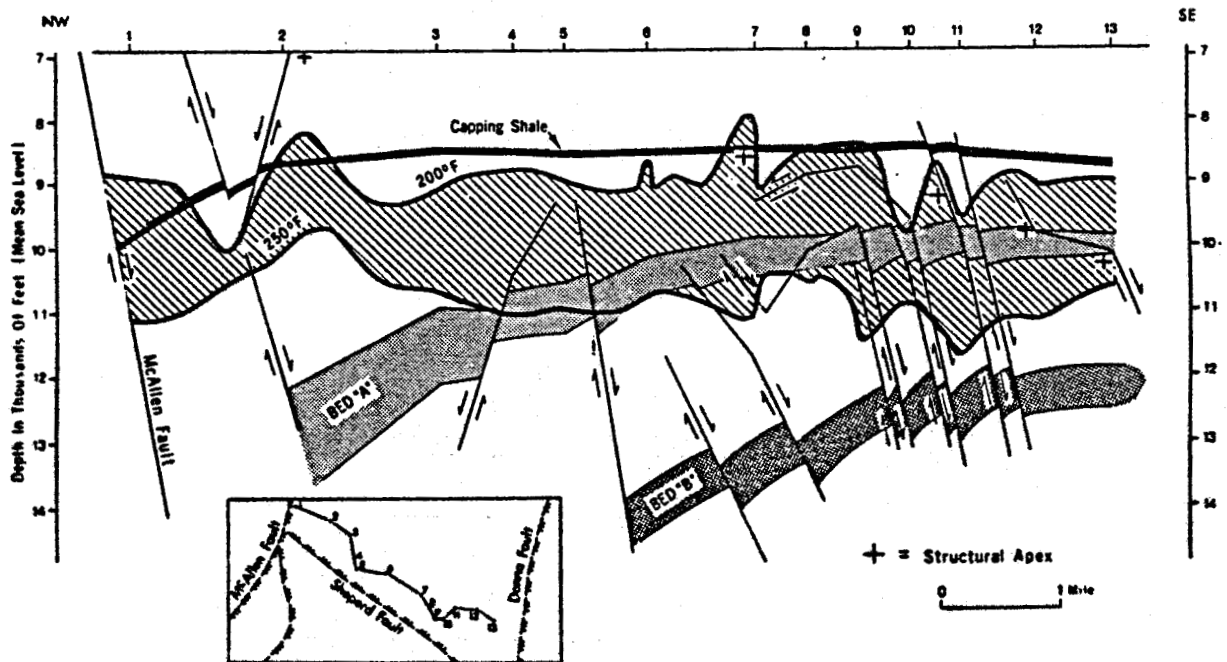


Figure 12. The 200°F. and 250°F. isogeotherms related to structure in the Pharr-McAllen Field area of Hidalgo County, Texas. (Modified from Collins, 1968).

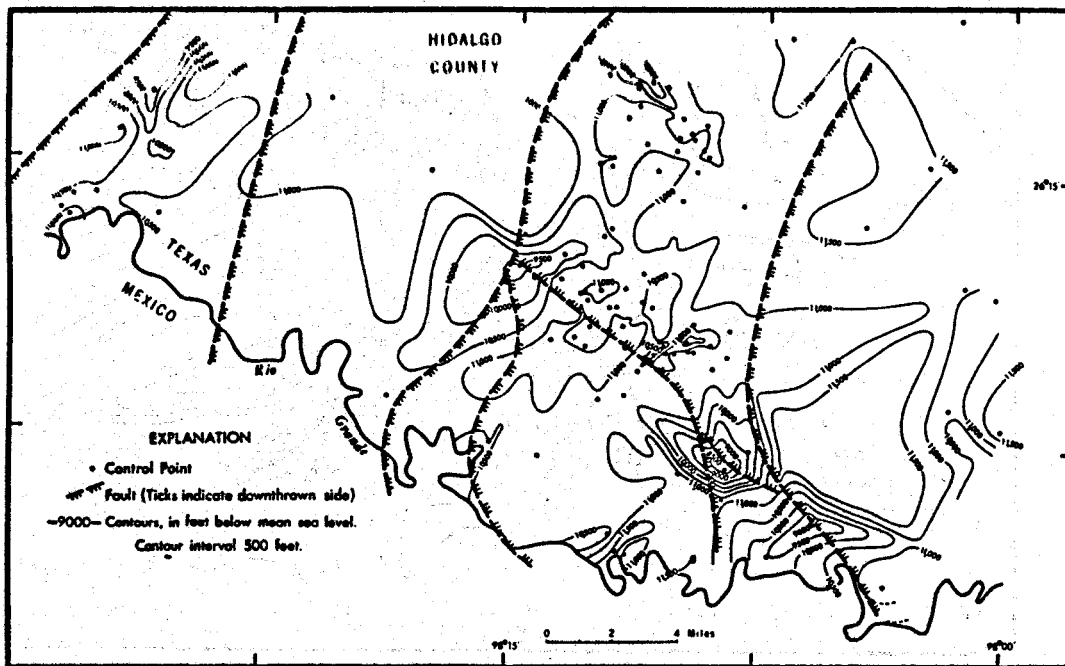


Figure 13. Depth of occurrence of the 250°F. isotherm within the study area outlined in Figure 8.

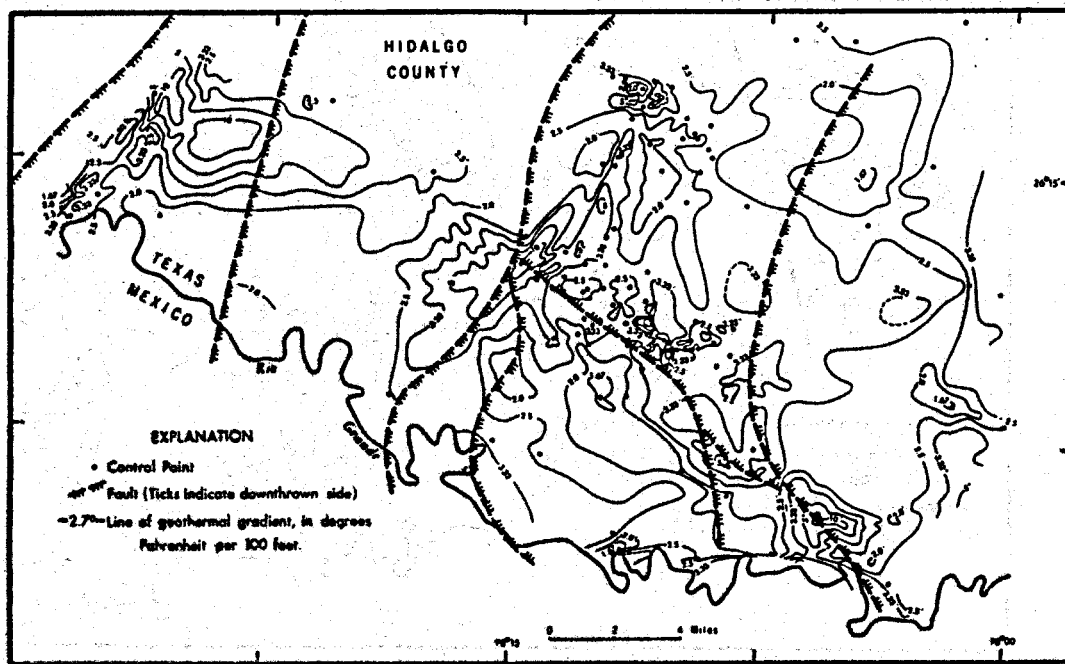


Figure 14. Map of geothermal gradient in the interval between the 200°F. and 250°F. isotherms within the study area outlined in Figure 8.

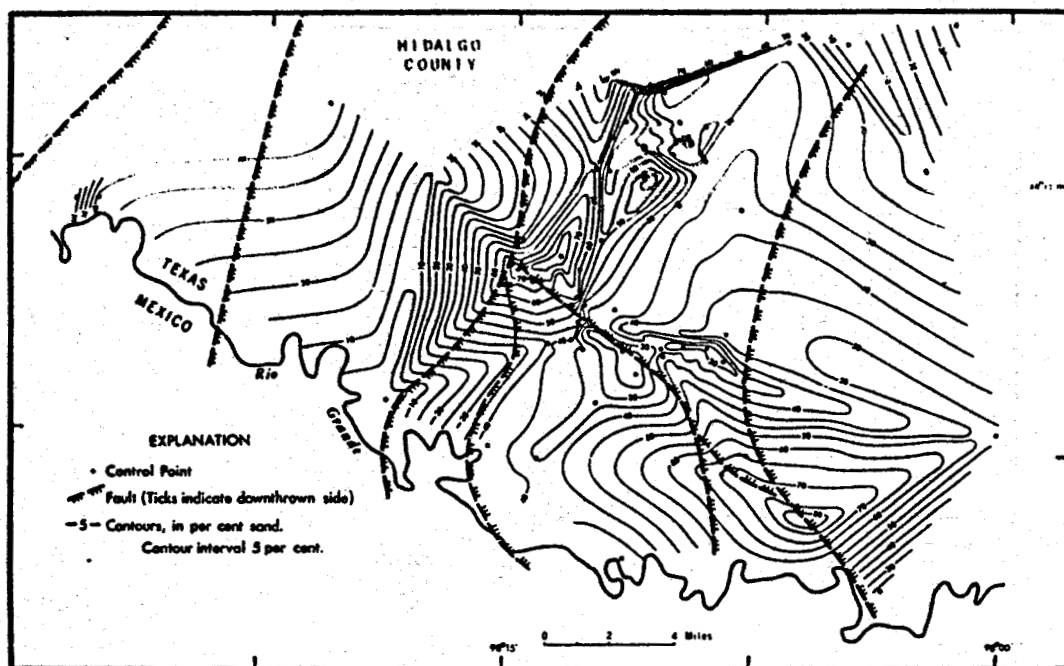


Figure 15. Per cent sand in the interval between the 200°F. and the 250°F. isogeotherms within the study area outlined in Figure 8.

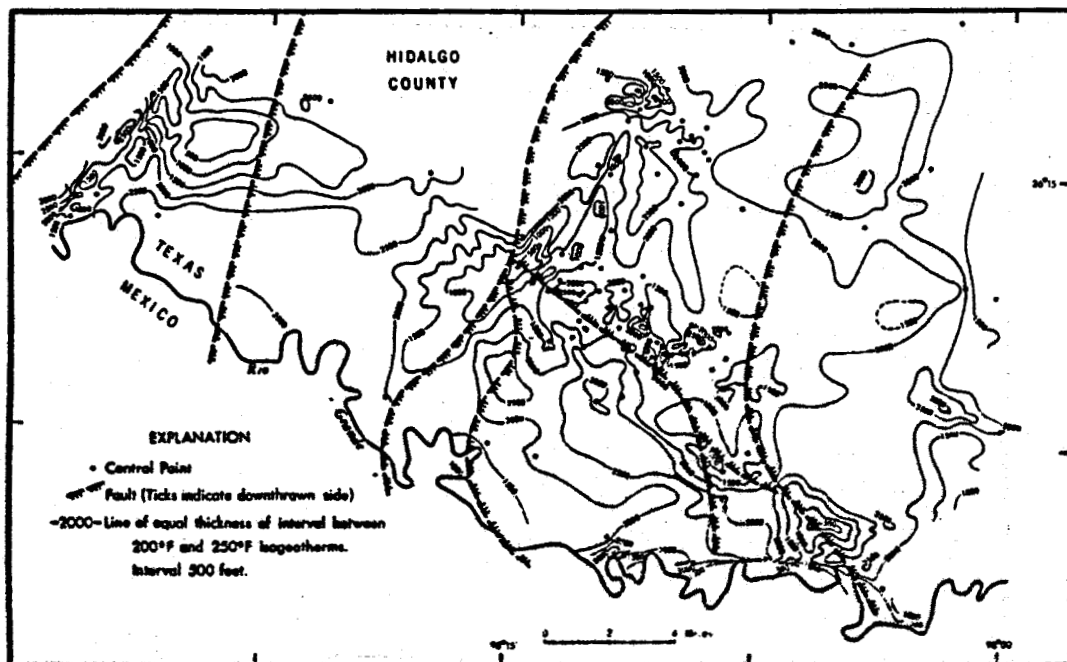


Figure 16. Isopach map of the interval between the 200°F. and 250°F. isogeotherms within the study area outlined in Figure 8.

CHANGES IN THE CLAY-WATER SYSTEM WITH
DEPTH, TEMPERATURE, AND TIME

by

Charles E. Weaver and Kevin C. Beck

School of Ceramic Engineering
in cooperation with
Water Resources Center
Georgia Institute of Technology
Atlanta, Georgia 30332

Abstract

Mineralogic studies of muds and shales have shown that the clay minerals are modified by deep burial. Side wall core samples from 4,223 to 16,450 feet in the Gulf of Mexico (courtesy Chevron Oil Co.) and from the surface to 24,003 feet in the Anadarko Basin, Oklahoma (courtesy Shell Oil Co.) were studied in order to obtain additional information to the processes involved.

With depth the montmorillonite in these montmorillonite-rich shales is altered to mixed-layer illite-chlorite-montmorillonite; the regularity of the mixed-layer phase tends to increase with depth. Much of the interlayer hydroxy material is Al and Fe, acquired before deposition. K is acquired from the river and sea water, and after deposition, from K-feldspar. Increase lattice charge in the montmorillonitic layers (largely beidellite) is due to the reduction of iron in the octahedral layer and the incorporation of additional Al in the tetrahedral layer. It is suggested that the latter phenomenon is caused by the migration of interlayer Al into the hexagonal holes in the oxygen sheet. The oxygen tetrahedra rotate sufficiently to incorporate the Al into the Si-rich tetrahedral layer. Most of the loss of expandable layers occurs by 12,000 feet.

With increasing depth and temperature kaolinite is destroyed and the Al is deposited between the expanded layers as hydroxyl-Al to produce layers of dioctahedral chlorite. Both discrete dioctahedral chlorite and mixed-layer illite-

dioctahedral chlorite-montmorillonite (ultimately mixed-layer illite-chlorite) is formed. During regional metamorphism the sequence is kaolinite and mixed-layer illite-montmorillonite \longrightarrow mixed-layer illite-dioctahedral chlorite $\xrightarrow{K, Mg, Fe}$ muscovite + chlorite.

The cation population of the interstitial waters of the Pliocene-Miocene muds of the Gulf Coast is approximately twice that of sea water. The cation concentration increases to 10,000 feet, abruptly decreases by 20 percent, then remains relatively constant. Na and K are more concentrated than sea water; Ca and Mg less. K and Mg increase with depth; this is presumably a function of the increase in temperature. In the shallow samples the Na concentration increases as the pore water decreases. In deeper samples the ratio remains relatively constant. The pore water systematically decreases to 10,300 feet; abruptly increases by 10,530 feet and then systematically decreases. The abrupt change in pore water content coincides with the top of a high pressure interval.

The anion concentration is $HCO_3 > SO_4 > Cl$. Cl systematically decreases with depth and is one-fourth the concentration of sea water by 10,000 feet. This is presumably due to selective flushing. Over the same depth interval SO_4 increases by a factor of 6-7, comparable to the decrease in pore water, suggesting concentration by selective filtering. HCO_3 increases in concentration to 10,000 feet and then remains constant. The high HCO_3 values are due to the decomposition of organic matter and calcite.

The total exchange cations (Na+K+Mg+Ca) averages 30 meq/100 gms down to approximately 8,000 feet; deeper samples average 20 meq/100 gm. The C.E.C./ Al_2O_3 values decrease to 10,000 then remain constant, confirming the X-ray interpretation. Na is the dominant exchange cation in the shallow samples and Ca in the deeper samples. Most of the exchangeable Mg is used to form dolomite or is flushed into the sands where it combines with montmorillonite to make chlorite.

The Al_2O_3 content of the bulk samples ranges from 9.94 to 17.47 percent. This is equivalent to approximately 55 to 75 percent clay minerals. The Al_2O_3/K_2O , Al_2O_3/MgO , and Al_2O_3/Fe_2O_3 values of the Chevron and Mississippian (except for Al_2O_3/MgO) samples indicate a deficiency of K, Mg, and Fe with respect to the Paleozoic and Precambrian shales. There is no increase in these cations with depth. These montmorillonite-rich clays cannot be converted to the typical illite-chlorite clay suite of the older shales without the addition of these ions from external sources. Dioctahedral chlorite, both as discrete chlorite and as mixed-layer illite-chlorite, is present in most Paleozoic and Precambrian shales and will be even more abundant in deeply buried

Tertiary shales unless cations are added from outside the system. The data indicate that in areas where the conversion of montmorillonite-rich clays to illite-chlorite clays occurs the geothermal gradient is relatively high and K, Mg and Fe are added from below. The possibility exists that geothermal gradients were higher in the Paleozoic and Precambrian, particularly preceding the middle Carboniferous break-up of the continents.

The release of interlayer water may be necessary but not the controlling factor in the development of high pressures in the Gulf of Mexico. Loss of permeability appears to be more critical. In the Chevron well the top of the high pressure interval occurs at the top of a thick mud section, underlying a mixed sand and mud section.

Expandable layers exist to temperatures of at least 200°C. On the basis of certain assumptions it appears that through the top of the high pressure zone interlayer water decreases to 0.8 percent and pore water increases by 5 percent; there is no abrupt mineralogic change through this interval. The increase in pore water correlates with an increase in Al_2O_3 or clay content. It is suggested that ions migrate through the permeability barrier even though water does not.

THE DIAGENETIC ISOPLETH¹

by

J. F. Burst

Technical Director
General Refractories Company
Philadelphia, Pennsylvania

Diagenesis is alive and well--it lives, among other places, in the Gulf Coast of the United States and apparently contributes effectively to the economic importance of the area by providing a medium for the accumulation of petroleum hydrocarbons. This, in itself, should be sufficient basis for our interest. Diagenesis, as a precursor to metamorphism has been recognized in geologic history for many decades. Its use, however, as a tool in petroleum geology has been limited to the past two decades when techniques and instrumentation for measuring low-level energy responses in sediments were developed. Although Winkler has established the upper limit of diagenetic reordering as 300°C, its usefulness in petroleum exploration appears to be limited to the lower half of that temperature range. Evaluating rock changes which have occurred below 150°C (302°F) limits investigation essentially to liquid, gaseous, and semi-solid phases. Interesting contributions regarding low temperature thermal history are also possible from measuring the opacification of pollen exines by progressive carbonization.

Running quickly through the alternatives, it doesn't take long to figure that the three-layer clay minerals, with their capacity for absorbing and desorbing water in response to their environment, offer an opportunity to evaluate diagenetic impact. All things considered, the clay minerals must rank as the diageneticists principal working tool.

¹This is the text of Dr. Burst's oral presentation, for references cited see J. F. Burst (1969) "Diagenesis of Gulf Coast Clayey Sediments and its Possible Relation to Petroleum Migration," AAPG, Bull., V. 53, 73-93.

Clay mineral changes aren't limited to water content readjustments, of course, they run the gamut from slurry to slate, tripping over the diagenesis--metamorphosis boundary somewhere in between. The changes are environmental reactions which develop a characteristic mineral population. The natural population of organics and inorganics with which we are familiar at the earth's outer surface is stable to an elevation of about 10,000 ft. above sea level. Finding limitation not in elevation per se but in environment, principally temperature and atmospheric content. By coincidence, perhaps, the same population is stable to burial depths of about 10,000 ft. (perhaps a bit less). Dependent once again, not on burial depth, but principally on conditions of temperature and atmospheric content. Research work in the relatively shallow subsurface indicates a general population alteration wherein clays densify principally through the loss of water, solid organic material adjusts its carbon-hydrogen ratio in a coalification process and simple liquid and gaseous hydrocarbons mature to characteristics which resemble petroleum. Other secondary effects, such as unusual adjustments in formation water salinity and thermal gradient fluctuations have also been observed. An interesting aspect of these various chemical, structural, and volumetric changes is that they occur in close relationship with one another within rather narrow and well defined burial limits related to energy input. A plateau seems to exist in the subsurface wherein the balance of many surficial chemical and physical systems is broken and these systems begin a re-equilibration to their new energetic environment. The plateau lends itself to subsurface contouring. The re-equilibration zone can be isopached and within it the second stage of clay dehydration can be selected as a level of equivalent energy input which I refer to as the diagenetic isopleth. I have found it useful as a subsurface marker.

Geopressures, which occur within this zone, represent a portion of the subsystem which is unable to re-equilibrate and exists therefore as a disequilibrated anomaly. Characteristics of the diagenetic isopleth are much less obvious than the more familiar indicators of metamorphism and they require more sophisticated tools for recognition. The geologic importance of the diagenetic isopleth may be equally as great as the common metamorphic markers however, and its significance with respect to petroleum geology may be considerably greater.

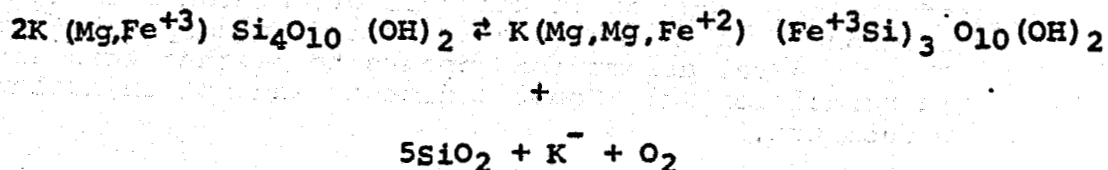
Pressure, time, and temperature are the three agencies responsible for diagenesis--as well as, I presume, most every geologic alteration. Unfortunately, somewhere along the way, popular dimensioning of the effects of pressure and temperature led to the erroneous conclusion that overburden pressure produced diagenetic changes.

More recent work argues that temperature is the principal agency with pressure and time minor contributors. Examination of the kinetic formulae for reaction rates clearly demonstrate the exponential effect of temperature and the fractional exponential of time which relegates it to a relatively ineffective role in diagenetic processes. Equally clear is the greater effectiveness of temperature vs. pressure. A 10% rise in temperature is equal to an increase of overburden pressure equal to several thousand atmospheres. Even using the classic rule of thumb that a 10°C rise in temperature doubles reaction rate gives us some idea of its relative effectiveness over pressure and time as we can equate such a temperature rise to an appropriate overburden pressure increase on the basis of geothermal gradient (10° rise = 18°F rise = 1000 ft. of sediment in Houston area) and to time on the basis of sedimentation rate.

The relative effects of these various parameters may also be judged from direct observation. Figure 1a shows the effects of squeezing hydrated Wyoming bentonite at 40,000 psi and room temperature. Alterations are confined to infilling of air space. In Figure 1b, a similar cylinder of semihydrated montmorillonite clay squeezed at the same pressure but, at a temperature of 50°C shows lineation and micaceous flakes forming. Further heating showed more pronounced flake development (Fig. 1c). X-ray investigation showed that the swelling capacity of the flake material was reduced about 25% indicating a permanent loss of interlayer water.

In the subsurface, where countless nucleation centers occur in the form of clay platelets, diagenetic growth generates crystal building such as the delicate lath development in Figure 2 shows and it encourages the extension of crystal faces such as indicated by the transparent border on the biotite flake shown in Figure 3.

This type of reaction is generated by the partial reduction of the ferric iron components of mica lattices in a muscovite to biotite type transition:



(Dioctrahedral Celadonite plus Heat and Pressure = Trioctahedral Lepidomelane + Quartz)

The reaction, which has been confirmed in the laboratory, accounts for deep burial biotite formation, the development of siliceous binding agents in shale members and a source of potassium for the illitization process.

Actually, this process begins toward the end of the diagenetic sequence and continues through the metamorphic stage. More pertinent to our considerations are the pre-recrystallization changes effected principally by mineral lattice water loss. This subsurface reaction expresses itself in a variety of measurable dimensions. Interlayer water is non-saline, probably as a result of an anion repulsion in which the net negative charge of the clay lattice prevents the Cl^- ion from entering the particle. A simple demonstration of this phenomenon can be observed if a quantity of dehydrated, but still active, montmorillonite is mixed with saline water. As the montmorillonite absorbs its normal complement of water, the salinity of the remaining liquid phase will rise in linear proportion.

Considering what must obviously happen in reverse as waterloaded montmorillonite dehydrates during early diagenesis, a freshening of subsurface waters in the diagenetic isopleth should be apparent.

Subsurface salinity measurements usually reflect the character of sandstone pore brines. This limits confidence in any measurement taken in strata under hydraulic gradient, because they may be transporting water unrelated to the immediately adjacent dehydrating shales. It also makes salinity measurements near evaporites or salt plugs of questionable value.

In spite of these difficulties, anomalies resulting from shale dehydration have been reported. According to Timm and Maricelli (1953) salinity values are an inverse function of shale volume and degree of compaction. The authors note that connate waters in younger sediments (Miocene-Pliocene) in the Gulf Coast were generally more saline than those in older (Eocene and Oligocene) sediments and that in sediments of the same age, salinities are often higher in the updip sections than in more deeply buried downdip extremities. Their general assumption appears to be that this situation is normal for Gulf Coast sediments and not an isolated phenomenon.

On the basis of more recent interpretations of the water escape properties of shales, the higher salinity measurements in younger sediments can now be expressed as an inverse relation between connate brine salinity and the volume of interlayer water expelled from an adjacent shale. Similarly, Timm and Maricelli's second conclusion now can be

thought to suggest that the dehydration point at which inter-layer water is released presently occurs above Eocene sediment burial depth and often traverses dipping strata of the same age.

As plotted in their report, the Timm and Maricelli data appear to be subdivided into several unrelated groups, each containing a few data points. A replot of their data, referenced to the calculated level of clay dewatering in the area under study, shows that the salinity anomaly may be more specifically associated with shale dewatering than the casual salinity-shale volume relationship reveals.

Figure 4a shows that the Timm and Maricelli points are not necessarily divided into isolated groups but may all be related as a function of their distance from the calculated clay dehydration point. The relationship between salinity and clay dehydration appears to be independent of the stratigraphic position or relative age of the samples. Salinities measured near or below the dehydration level are significantly lower than those above. The average salinity in samples below clay dehydration and up to 300 feet above it is 20.6×1000 ppm. Samples from 300 to 4955 feet (the most distant) above clay hydration point average 70.4×1000 ppm. This may be explained as a dilution of pore water salinity by fresh water from adjacent shales during clay dewatering. Above this point, a gradual increase in salinity values reflects the gradually decreasing effect of clay dewatering as its effluent is mixed with the higher salinity pore waters above.

A three-point moving average of the data (Figure 4b) graphically illustrates the salinity variation as an orderly zone of adjustment between two consistent bases. This is regarded as evidence that the interval at, and just above, the clay dehydration point is most favorable for subsurface fluid redistribution.

In comparison to the three-point moving average referenced to the diagenetic isopleth, a three-point moving average of the Timm and Maricelli data, plotted solely as a function of burial depth is shown as Figure 4c. Its irregular configuration demonstrates that a purely depth reference would not reveal the nature of salinity reduction to be a dilution process between two rather consistent salinity bases.

The double base line--intermediate transition zone presentation of the diagenetic isopleth is a convenient and instructive format. Figure 4b for instance, can be compared favorably with Figure 5 wherein the actual measurement of lattice dehydration is plotted versus sample recovery depth. This is the parameter to which other diagenetic indicators

such as salinity reversals, BHT anomalies and geopressuring are apparently related and from which they may be derived. Plotted here is a lattice dehydration log which also shows an adjustment to new subsurface conditions through a transition zone. In this case however, the adjustment is assumed to represent a direct measurement of water loss rather than the secondary salinity effect. Still another similar curve was presented by Fertl and Timko earlier this month in the Oil and Gas Journal although their data did not quite get down to the second base line.

We have talked sufficiently about clay dehydration thus far and its relationship to a specific zone in the subsurface that I feel we should spend a few minutes in an explanation of its possible uniqueness. The continuous diagenetic effects of time, temperature, and pressure experience a discontinuity with respect to sediment dewatering at the stage where the clay lattices in shale sections contain only two water interlayers. At this stage, the attractive forces generated by exchange sites within clay lattices cause the last two water layers to be

1. Spread slightly to accommodate the charge distribution;
2. Infilled with extra water molecules at the rate of one additional water for each eight molecules normally present; and
3. Compacted in an overlapped geometry due to the hexagonal close-pack rule.

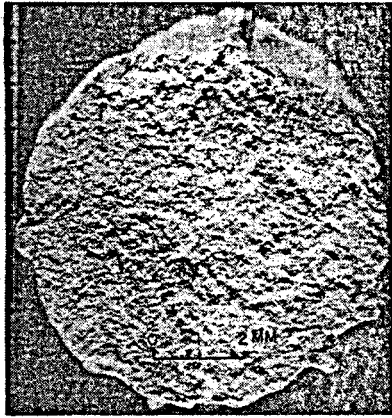
This results in a configuration in which the water trapped within the clay mineral lattice occupies less space inside the clay lattice than it would in the pore space. Pressure therefore is no longer an effective dewatering agent and the shaley interval resists the normal diagenetic progression as it waits for formational temperatures to increase sufficiently to force the stabilized interlayer water into the pores. The vertical extent of this stabilized zone depends essentially upon the rates of sedimentation and pore water expulsion. In rapidly depositing sections, heat accumulation is slow due to excessive entrapped water. This results in a lowering of the geothermal gradient and a deepening of the interlayer dewatering level. Under normal circumstances the sediment temperature eventually rises sufficiently to mobilize the interlayer water and it drains out through the pore system. If the system is closed, however, perhaps by the self-sealing action of monolayer immobility in thick shale sections, the pore space cannot accommodate the mobilized water which is attempting to increase its volume by 10 or 15% upon liquefaction and the condition of overpressuring develops.

This can perhaps be illustrated by Figure 6 where the density of interlayer water is plotted against the number of water interlayers in swelling clay lattices. The upper curve shows suggested density variations when the lattice is overpacked due to the in-filling of voids in those water layers immediately adjacent to the lattices. These water layers, as I mentioned previously, have been restructured in accordance with the lattice charge distribution. When only two water layers are present, dewatering cannot take place without thermal assistance even against pore water densities of three times sea water salinity. Without the overpacking, dewatering is viewed as considerably less difficult although even in this instance the normal close packing tendencies of the lattices densifies interlayer water to the point that dehydration is inhibited.

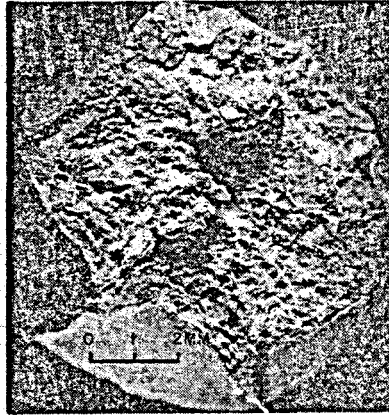
The density reversal at the two interlayer water level must have some effect on subsurface pressure relationships. It represents a fluid flow stability interval between the point at which the free flow of pore water to the surface diminishes and the point at which thermally activated interlayer water flow begins. The stability zone is the optimum interval for shale over-pressuring as neither of the two major dewatering processes operates effectively and overburden pressure can increase without engendering appropriate volume adjustment in the sedimentary section.

The system is essentially "closed" and overpressuring develops as the thermally excited water molecules press against the confining pore water. Even though sufficient water molecules are present to form a continuous phase, the water is not in liquid form and refuses to respond to the pressure gradient.

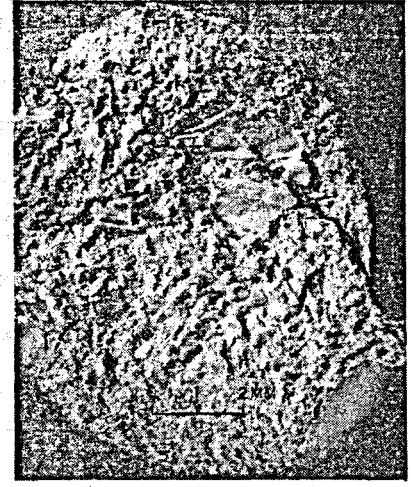
The effect of this condition is observed in bulk density, conductivity, resistivity, and sonic measurements by inversions or reversals which are certainly reflecting a change in sediment water characteristics. There is little likelihood that these can be attributed to a rewatering phenomenon. The diagenetic process appears to be unidirectional. They must represent various stages of dewatering and inasmuch as the clay minerals control in large measure, the dewatering of sediments, it can only be construed as prudent to carefully examine the characteristics of the clay mineral suite in sedimentary sections. Clay mineral dewatering is the key to sedimentary diagenesis, the basis for many measurable secondary effects, and the principal transport control for petroleum hydrocarbons. Each stage of geologic development is best studied by some particular research technique and insofar as I am able to perceive, diagenesis belongs to the clay mineralogist.



WYOMING BENTONITE
40,000 psi
50% RH
ROOM TEMP.
(a)



WYOMING BENTONITE
40,000 psi
0% RH
150° C
(b)



WYOMING BENTONITE
40,000 psi
0% RH
250° C
(c)

EFFECT OF TEMPERATURE AND LOW HUMIDITY DRYING
ON HIGH PRESSURE COMPACTION TESTS

Figure 1

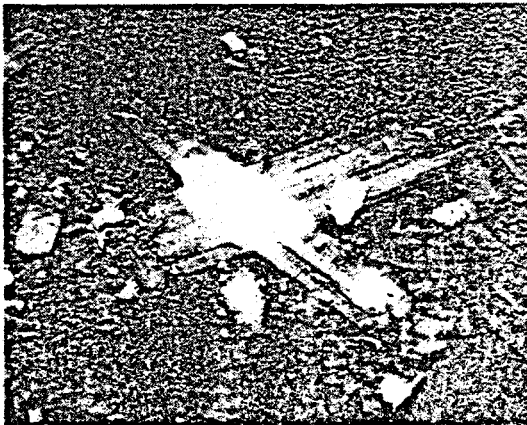


Figure 2

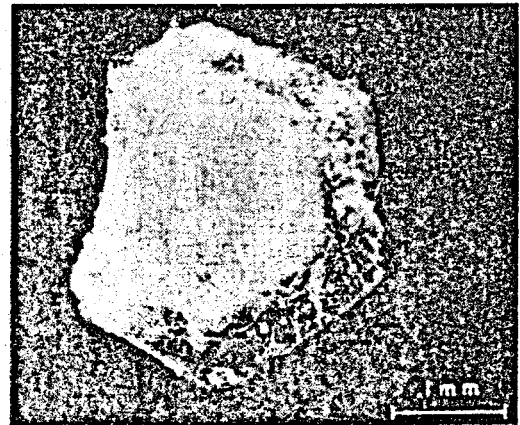


Figure 3

**SALINITY ADJUSTMENTS
at the
INTERLAYER WATER ISOPLETH**

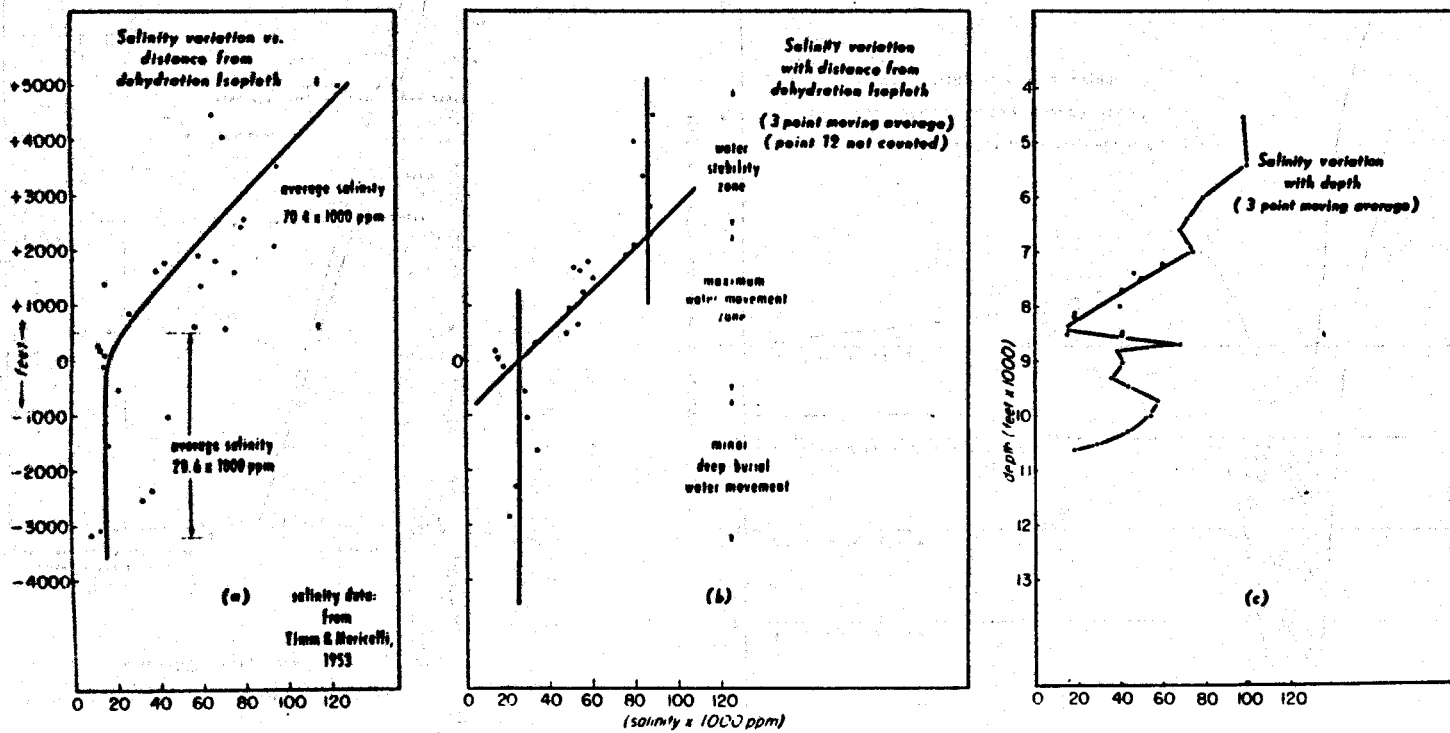


Figure 4.

STEP-WISE DENYDRATION OF CLAY IN GULF COAST WELL,
CHAMBERS CO., TEXAS

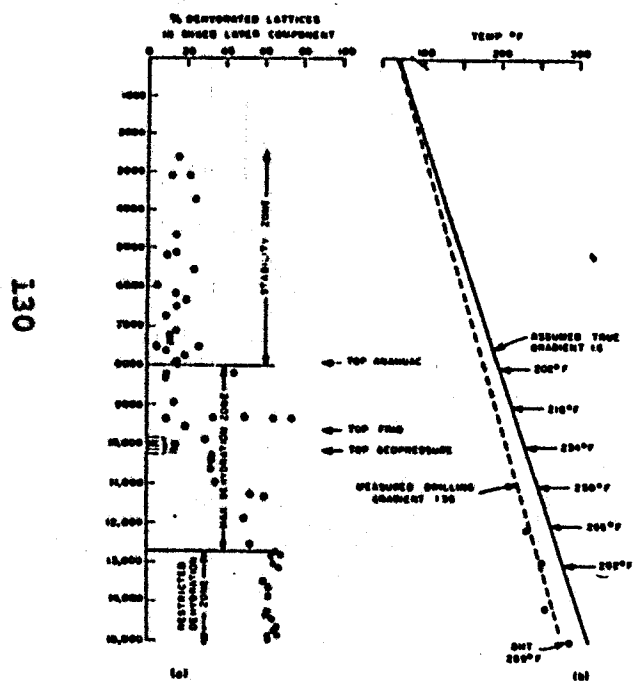


Figure 5.

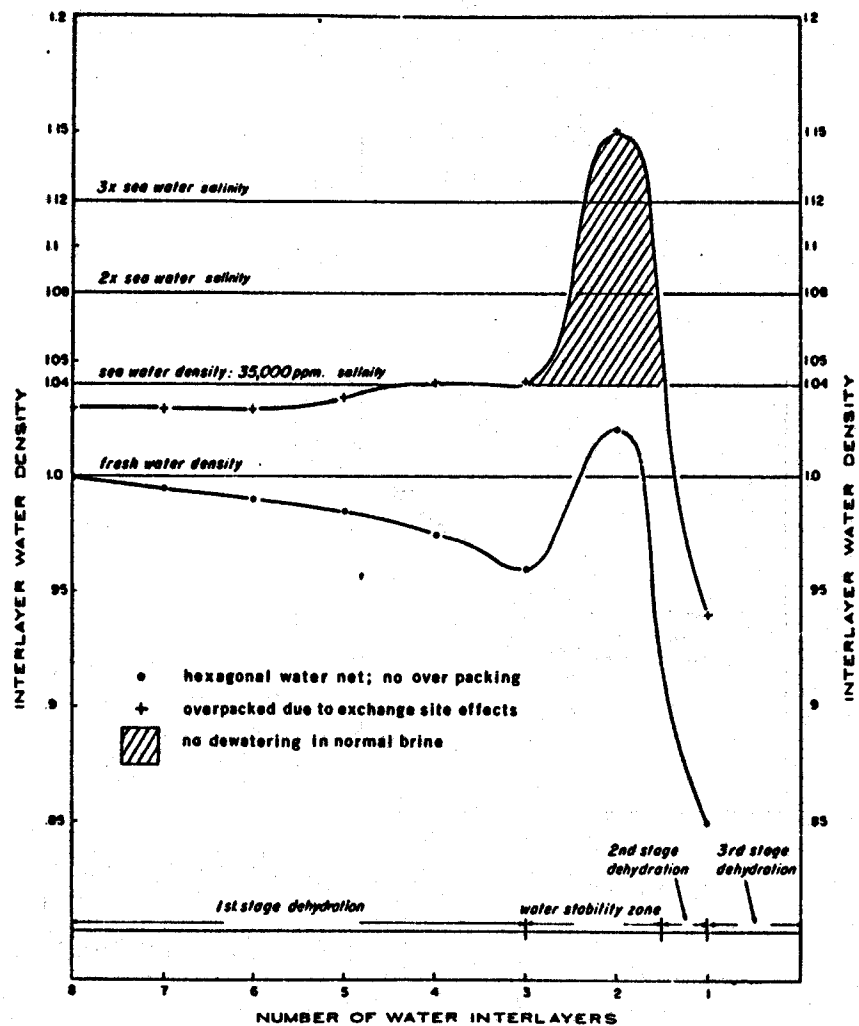


Figure 6.

REVIEW OF TECHNIQUES USED IN THE DETECTION
AND DRILLING OF OVERPRESSURED
FORMATIONS

Walter H. Fertl, Continental Oil Co., Ponca City, Oklahoma
Donald J. Timko, Continental Oil Co., Houston, Texas

Presented by

Aldo M. Zanier
Continental Oil Company
to the

2nd Symposium on Abnormal Subsurface Pressures
L.S.U. - January, 1970

Abstract

Formation pressures higher than hydrostatic occur worldwide and are important factors in the successful planning and drilling programs in the search for oil and gas. It has been noticed in several areas that the distribution of hydrocarbons appears to be related to the pressure environments in the area. Observed changes in the properties of shales can be used to detect overpressured formations. These parameters include in situ and/or surface measurements of shale resistivity, sonic travel time, bulk density, clay mineral abundance ratio, and salinity changes. Also, bore hole temperature and rate of penetration by the drill bit are used to detect overpressures. Knowledge of the expected pore pressure and fracture gradient is the basis for efficiently drilling wells with correct mud weights and casing programs. This prevents a breakdown of exposed formations and contains the high pressure fluids in deeper formations, thus enhancing the chances of successfully drilling these zones. Examples from the Gulf Coast illustrate the various techniques of detecting and drilling of overpressured formations.

Worldwide Occurrence of Geopressures

In the worldwide search for oil and gas, geopressures have been encountered in many countries (Figure 1). Geopressures or abnormally high subsurface pressures are defined as any pressure which exceeds the hydrostatic pressure of a column of water containing 80,000 parts per million total solids. We have compiled a list of areas where geopressures have been reported in the literature (no claim, however, of a complete listing is being made). These areas include the USA (Arkansas, California, Louisiana, Oklahoma, Texas, Wyoming), Europe (Austria, France, Germany, and the Carpathian and Caucasian Regions of eastern Europe), Africa (Algeria), Middle East (Iran, Iraq, Pakistan), Far East (India, Burma, Indonesia, New Guinea, Japan), and South America (Argentina, Colombia, Trinidad, Venezuela). It is believed that increasing exploratory efforts in new areas, on- and off-shore, and the general trend to deeper drilling will further broaden the areas of overpressures which are accompanied by associated drilling and production problems.

Geological Significance of Geopressures

One of the first and certainly most extensive studies of geological aspects related to geopressures has been carried out by Dickinson (1953), who summarized some of his observations as follows "High pressure zones commonly make drilling of wells most difficult in a belt about 50 miles wide along the coastal plain northwest of the Gulf of Mexico from the Rio Grande to the Mississippi Delta. Dangerous abnormal pressures occur commonly in isolated porous reservoir beds in thick shale sections developed below the main sand series. Their locations are controlled by the regional facies change in the Gulf Coast Tertiary province, and they appear to be independent of depth and geological age of the formation.

The high pressures are caused by compaction of the shales under the weight of overburden which is equivalent to approximately one pound per square inch per foot depth. Difference in density between gas and water causes abnormal pressure where hydrocarbon accumulations occur above water, irrespective of whether the water is at normal or abnormal pressure. The magnitude of this pressure depends on the structural elevation above the source of pressure in the water and may cause very high pressure gradients in isolated sand bodies. However, the trend of pressures in the Gulf Coast region indicates that maximum pressures probably do not exceed 90 percent of the overburden pressure." In a more recent work, Dickey et al. (1968) observed that "the pattern of the high pressure zones is not obvious but

appears to be related to the peculiar patterns of faulting contemporaneous with sedimentation which are characteristic of the Gulf Coast." Harkins and Baugher (1969) discuss some pressure anomalies being associated with salt domes. In addition, they stress the relationship between geopressure and stratigraphy. They also suggest that "to develop abnormal pressures the shales usually must be over 200 feet thick." It is normally accepted that thick clay masses have to be deposited rapidly over considerable areas, to prevent any hydrostatic reservoir equilibrium.

Vast field evidence shows that transition zones between normal and overpressured zones may be abrupt or may extend over more than 1000 feet. Our experience also indicates that the presence of fault planes may or may not mark pressure discontinuities, which become an important factor in planning offset wells. The nature of a permeability barrier, the so-called caprock, normally encountered at the top of geopressures, will be discussed in more detail.

Movement of water through a shale section overlying geopressured reservoir rock takes place mainly along the directions of greatest permeability and may cause slow lithological changes in the character of the shale section. Escaping water carries dissolved solids such as carbonates and silica, and gases. Pressure and temperature drop across the transition interval and cause precipitation and mineralization in this zone. Fine grained sediments, such as clays, act as semipermeable membranes permitting dissolved solids in the remaining pore space to react chemically with the clay. The filling of the pore space causes a decrease in the formation porosity. Presence of such an indurated limey shale barrier, which acts as a sealing cap, normally is found in the shale overlying geopressured zones. Evidence is observed on well logs as a relatively high bulk density, an increase in electric resistivity (or decrease in conductivity), and a decrease in measured sonic travel times. Sidewall samples which have been taken in the caprock confirm such observations.

Thickness of the caprock seems to vary greatly. We have observed thicknesses as low as a few feet to as much as several hundred feet. Occasionally a sequence of several sealing barriers may be encountered. Such conditions are thought to have originated by imperfect sealing and/or disturbances caused by tectonic movements over geologic times. In any event, very low shale permeabilities (in the order of 10^{-5} to 10^{-6} millidarcies) in connection with non-Newtonian behavior of the water in the finer interstices of sediments require consideration of the time factor in forming such a sealing barrier. The rate of solid precipitation responds to changes in physical and chemical environments which are

dependent on the composition of brines and clay minerals, pressure, temperature, and the path taken by escaping water, all of which are largely speculative.

Composition and Abundance of Clay Minerals and Their Effect in Drilling

Not much data has been published in the clay abundance ratio in wells penetrating geopressured zones. Kerr and Barrington (1961) in such a study of four wells in the Caillou Island Field, Louisiana, noted major changes in the relative amounts of montmorillonite, illite, and kaolinite comparing geopressured and normal pressured formations. Their study showed compaction reversal. The decrease in montmorillonite seems to represent a sharp change in contrast to the increase in illite. However, one well showed a decrease in the amount of illite associated with an increase in kaolinite. This was interpreted as a change in mineral composition coinciding with the geopressured zone.

Also, some recent work of commercial mud logging companies using methylene blue tests on shale cuttings have shown increasing percentages of high cation exchange capacity clays as high formation pore pressures and high temperatures are encountered in deep wells.

The results of a field case study carried out on sidewall cores in a well in Cameron Parish, Louisiana, are given in Table I. Note that the two cores taken in the highest pressure and temperature at 10,393 feet and 10,415 feet show increasing percentages of montmorillonite.

Another factor in the drilling of long shale sections is the danger of bore hole instability caused by any disturbance of the physical and/or chemical equilibrium conditions due to penetration by the drilling bit (stress relief) or reaction with the drilling fluid (van Olphen, 1963; Browning and Perricone, 1963; Kelly, 1968; Darley, 1969; Chenevert, 1969).

Chenevert (1969) stresses the major role of the hydration effect over erosion and mechanical actions. Darley (1969) distinguishes two modes of shale hydration, the surface hydration ("crystalline swelling") and osmotic swelling. These reactions cause softening and large volume increases which lead to unstable bore hole conditions. Mondshine (1969) extends the osmotic concept to the determination of oil-mud salinity needs in shale drilling. Such oil base muds should be considered as special purpose drilling fluids, which are being used in the Gulf Coast area particularly in deep, high temperature wells. However, these muds are

expensive, may result in reduced penetration rates, and drilling crews do not particularly like to work with them.

Figure 2, plots of depth versus shale resistivity and sand salinity, strikingly shows the fluid sensitive shales. Drilling operators, to avoid hole problems in this area often use air or gas as the drilling medium.

Osmosis and Semipermeable Flow Conditions Through Shale Zones

An osmotic pressure can arise when two solutions of different concentrations (or a pure solvent and a solution) are separated by a semipermeable membrane. Irrespective of the mechanism by which the semipermeable membrane operates, the final result is the same. Osmotic flow continues until the chemical potential of the diffusing component is the same on both sides of the barrier. Of utmost importance to geopressured formations is the fact that if the flow takes place into a closed volume, the pressure inside necessarily increases until equilibrium conditions are obtained. Any disturbance, physical or chemical, would cause a resumption of flow until equilibrium conditions are reestablished.

The behavior of the fine grained sediments, such as shales, siltstones, and shaly sands, as semipermeable membranes ("salt sieves") that allow water to pass out of the formation while retaining and concentrating dissolved salts has been recognized for years by many investigators alike (DeSitter, 1947, etc.).

McKelvey and Milne (1962) gave experimental evidence of the salt filtering ability of compacted bentonite and clay, whereas Young and Low (1965) measured osmotic flow of water and pressures in shales and siltstone. Shales, and especially shaly sands, obviously may not be considered as perfect membranes. However, their efficiency should increase with higher compaction.

In the Gulf Coast, waters fresher than sea water are encountered down to approximately 3000 feet. This appears to be the critical compaction depth where shales begin to act as semipermeable membranes. Figure 3, plots of shale resistivity versus depth, readily shows fresh waters in these shallow intervals.

Practical application of some of these concepts has been proposed by Firson (1967) in the application of well logs to seek "osmotic" entrapment of hydrocarbons.

Jones (1968) states that "the pressure difference across a simple clay bed could, under natural conditions, exceed 3500 psi. In known geopressured reservoirs, stepwise increments of osmotic pressure with depth through a series of bedded sands and clays could, as by a multistage pump, produce any of the reservoir pressures observed to date in the northern Gulf of Mexico basin. Conceivably, osmotic derived fluid pressure could equal or exceed that due to the weight of the overburden causing reservoir rupture and diapirism, especially where heating had reduced the load-bearing strength of clay beds."

In a study of the pressure-hydrocarbon-salinity relationship in the Gulf Coast area, Fowler (1968) suggests the salinity variations in the Frio section to be results of selective ion concentration by the shale membrane effect. It is interesting to note that the "freshest formation waters are found at the base of the normally pressured section in the Lower Houston Farms Sand." Overton and Timko (1969) have shown similar examples of freshening of waters above overpressures.

Figure 4, a plot of salinity versus depth made from log data and sidewall core data, shows this freshening at 6000 feet which is above the pressure transition zone starting at 8000 feet.

These concepts may explain also the long known evidence why downdip freshening of aquifer waters has been widely observed in the Gulf Coast. A field case from South Louisiana (Timm and Marcelli, 1953) indicates in the updip direction a marked salinity increase from 12,500 ppm to 72,500 ppm. In addition, saline waters at the top of a sand sequence and relatively fresher waters at the bottom have been observed in the recent field study by Fowler (1968). Similar results for Southwest Louisiana were published earlier by Timm and Marcelli (1953), who found that "a relative decrease in saline concentrations of connate waters becomes apparent in: (a) massive continental sands above and below intertonguing marine shales, (b) marine sands which are grading downdip into solid marine shales, (c) older more marine parts of a regressive phase as compared with its younger (except very top) non-marine part. . . ."

Geopressure Detection Techniques

The technique of "balanced pressure drilling" is now used effectively in the oil industry. The balanced pressure technique applies hydrostatic pressure equal to the maximum pressure of the uncased formations, adding only a few hundred psi to contain the formation while tripping the drill pipe

to change drill bits. The method offers several advantages. These include faster penetration rates, minimized lost circulation, and differential sticking, less hole instability, and decreased formation damage. However, proper pressure balance is a precise operation with only little difference between effective control and threatened blowouts (O'Brien and Goins, 1960; Goins, 1968). Therefore, experienced drilling personnel and pressure control equipment are needed. Drilling in this manner does provide a direct indication of formation pore pressures.

Detection and evaluation of downhole geopressures may be inferred from a number of different sources, one of the best being well logs. "Well logging" denotes any operation, wherein some characteristic data of the formations penetrated by a bore hole are recorded in terms of depth. Unfortunately, wire-line logging methods and their evaluation are "after the fact" techniques, i.e., after penetration of the drill bit. Nevertheless, it is a significant advancement in well planning, even though sometimes very short zones have to be logged to continually monitor pore pressure variations. These measurements in the shales include:

Bulk density measurements.--Such measurements can be carried out in situ by means of the Density log (Ham, 1966) or on shale cuttings (Boatman, 1967).

Basically, the Density log consists of a gamma ray source irradiating the formation with gamma rays which react with electrons surrounding the bore hole and are back scattered. A detector records the intensity of the back scattered rays which varies with the bulk density of rocks surrounding the bore hole. Bulk density measurements on shale cuttings are commercially carried out by several service companies.

Figure 5, plots of bulk density of shales versus depth by the two methods are shown. Note that the bulk density from the cuttings is less than in the situ log measurements. An exception is apparent in the caprock at 10,500-11,000 feet, where flushing of the cuttings has not been severe because of the caps lower permeability and mineralization. The magnitude of the bulk density data here are similar.

Conductivity measurements.--With the Induction log, formations are energized by electromagnetic induction. Resulting electromotive forces (eddy currents) are detected by receiver coil and transmitted to the surface where both conductivity and its reciprocal, resistivity, are recorded.

Transition to overpressured shale zones is indicated

situation as gas can evolve from formation cuttings as they come to the surface. Generally, it is a good policy to circulate out gas before drilling and weighting up the mud system to be positive that the gas cutting is actually due to geopressures.

Refinements in Geopressure Determination

It has been shown (Timko, 1968) that refinements in the conventional techniques of determining pore pressures from well logs are often necessary. For example, for the well in Figure 11, shale resistivity and shale travel time are plotted in the conventional manner on a depth scale of a half inch to 1000 feet. Two gas zones are present at 7820-90 and 10,160-210 feet. Both plots confirm that the upper zone has normal hydrostatic pressures while the lower zone has a gradient in the vicinity of 0.75 psi/ft.

In drilling the interval from 9600-10,500 feet, the well required mud weights exceeding 15.0#/gal. This on-site data further confirmed the log calculated high pressures. Because of the expected high pressure in the lower zone, it was decided not to dually complete in the two gas zones but to complete only in the lower zone through a tieback string all the way to the surface. When the lower zone was completed and tested, the expected high pressure did not exist. The actual pressure was 0.55 psi/ft instead of 0.75 psi/ft.

Figure 12 is an expanded scale plot of a half inch to 100 feet for the interval 9600-10,500 feet. The pressure variations are seen in more detail.

Note that the shales exhibit a decreasing pressure gradient from 9925 feet to the sand and an increasing gradient below the sand. The sand, therefore, is not at the same high pressure as the shales 100 to 150 feet above and below. To determine true pore pressures in sands, it is a necessity to use the shales immediately adjacent to the zones of interest which can readily be seen on an expanded depth scale.

Engineered Approach

The best engineering approach for the detection and evaluation of geopressures is the study of a combination of several measured parameters as discussed in this paper. This statement is based on our experience, and that misinterpretations may be made when relying on one type of measurement or technique only.

Such conditions, as changes in lithology, can affect in some manner all the detection techniques. An example of this lithology change is shown in Figure 13 where at 16,300 feet, the shales become limey and more resistive, but the pressure gradient remains the same. Drilling rate and bulk densities would also change. We must undertake to develop new techniques to compensate for such pitfalls.

Conclusions

Concepts and methods as outlined in this paper are used in the petroleum industry to detect and evaluate geopressured zones.

Such geopressures are related to the geology of an area and need to be understood for efficient operations. They affect modern drilling techniques, are blowout hazards, influence completion methods and are a factor in producing characteristics of a reservoir. Since most of the pressure data is derived from shales, additional clay research will be necessary to fully understand and cope with these problems.

Acknowledgments

The authors wish to thank the Management of Continental Oil Company for permission to publish this paper and Mr. R. J. Cavanaugh for his assistance in providing laboratory data.

by greater than normal conductivity due to higher than normal water content (Wallace, 1965; McGregor, 1965) and porosity. These measurements are affected by the salinity and temperature of the formation water and tool instrumentation problems in very high conductivities.

Figure 6 is an example from a well located in offshore Louisiana.

Resistivity measurements.--The Electrical log measures the resistivity of the media surrounding the tool. Commonly several different electrode configurations are used in combination to estimate resistivity parameters in formations penetrated by the drilling bit.

In overpressured shales the so-called Short Normal curve shows a departure from the "normal" trend, indicating the high water content and increasing porosity in these shales (Hottman and Johnson, 1965; Ham, 1966). As in the case of conductivity measurements, this log is affected by the salinity and temperature of the formation water.

Figures 2, 3, 7, and 11 are plots of this technique.

Neutron measurements.--The Neutron log measures the hydrogen density of the formations. The increase of porosity and corresponding water allows application of this tool for overpressure detection. However, experience has shown this device is not as accurate for quantitative pressure data as other logging tools.

Pulsed neutron measurements.--A downhole accelerator or neutron generator bombards the rocks with 14 Mev neutrons in a time sequence pattern. During the time the accelerator is off, a gamma ray detector records two readings spaced a few microseconds apart, thus determining how long the neutron exists, or how fast they are captured. This measures the so-called thermal neutron capture cross-section of the formation and its contained fluids. The advantage of this device over the conventional neutron described above is that casing and cement have small effects on the overall response. Figures 7 through 9 exhibit a particularly useful application of the pulsed neutron. In Figure 7, we have plotted shale resistivity versus depth for a well drilled in 1946. All the sand zones listed in the figure below 8200 feet have been productive in this field for at least 25 years. This particular well was producing from the Klump series, but production was lost because of casing problems below 8100 feet. It was planned to get the well back on production by recompleting in the Homeseekers "A" sand at 9060 feet by sidetracking above the fish and redrilling to the Homeseekers "A" zone. The mud weight requirements needed to drill this

well initially in 1946 to the Homeseekers "A" was approximately 14.0#/gal, since the sands and shales contained geopressures of this magnitude.

However, because of production and pressure depletion over the years, most of the sands presently have producing pressure gradients throughout the field considerably less than hydrostatic. Therefore, it is known that the formations would not sustain the high mud weights used originally. The pulsed neutron was run in the old cased hole to evaluate present pressure conditions. Figure 8 is the plot of the response of the device versus depth to 9110 feet. As shown in the figure, the maximum mud weight requirements as determined from the pulsed neutron to reach the Homeseekers "A" sands were 10.2#/gal.

Figure 9, a plot of depth versus formation pore pressure of the shales, shows the change in shale pressure due to pressure depletion of the sands.

The well was sidetracked at 8120 feet in 1968 and drilled to 9215 feet without difficulty with a mud weight of 10.4#/gal, where originally 14.3#/gal was required. Figure 10 shows how the salinity of the formation water has increased with pressure depletion.

Transit travel time (sonic) measurements.--The Sonic log records the transit time of elastic waves through the rocks for use in estimating porosity. A transducer creates elastic wave pulses which travel through the formation and are picked up by receivers on the logging tool. The time required for the signal to travel a predetermined distance in the formation is recorded as travel time. For practical purposes, this log is unaffected by temperature and salinity.

A normal trend of transit time in shales is plotted versus depth. Pressure anomalies will be indicated by an increase of transit time because of the increase in porosity in overpressured shales (Hottman and Johnson, 1965).

Figure 11 shows an example of this technique.

Shale formation factor measurements.--This method, proposed by Foster and Whalen (1965), assumes the shale water to have the same salinity as water in adjacent sands. The shale formation factor is derived from this data and plotted versus depth. The major criticism of this technique is the assumption that sands and adjacent shales have exact salinities, which is open to question.

Salinity variations measurements.--Salinity measurements, related to the detection of geopressures, can be

carried out in situ with proper logging tools or at the surface on shale cuttings (Overton and Timko, 1969). As discussed previously, salinities decrease with increasing pore pressures.

The limitation of this technique is that formation salinities can vary quite markedly with rock stresses due to tectonics such as faulting, unconformities, salt dome uplift and other local or regional geology.

Figure 2 shows a salinity plot, previously discussed.

Geophysical measurements.--The seismograph has been used over the years primarily as a tool to determine subsurface structure. Recently, techniques (Pennebaker, 1968) have been developed using seismic data to predict the depth at which abnormal pressures occur and the magnitude of such pressures. This information is particularly valuable in drilling operations where little is known of geopressures as in a rank wildcat area.

The technique is to determine the changes of interval velocity energy with depth. Undercompacted and overpressured shales existing at depths exhibit a decrease in the interval velocity trend as calculated in the compacted formations above.

Penetration rate of drilling bit measurements.--Drilling rate has been recorded for many years, its relation to overpressured zones being recognized in the last decade only. Jordan and Shirley, in 1966, developed a technique for identifying the first occurrence of overpressured formations from interpretation of drilling performance data. A general equation for penetration rate in shales has been given by Combs (1968), wherein the constants have been evaluated by a regression type analysis of penetration rate data from several wells. Forgotson (1969) suggests that "an increase in the rate of penetration of shales, in which the increase is a minimum of 200 percent of normal, is an indication of the proximity, either vertically or horizontally, of a high-pressure fluid reservoir."

Bore hole temperature measurements.--It has been reported that as geopressures are encountered, formation temperatures increase (Jones, 1968). There are numerous logging devices to make such measurements. Continental Oil Company routinely measures mud flow line temperatures for such pressure detection.

Presence of gas in mud system measurements.--The presence of gas in the mud system is often interpreted as an underbalanced condition. However, this is not always the

REFERENCES

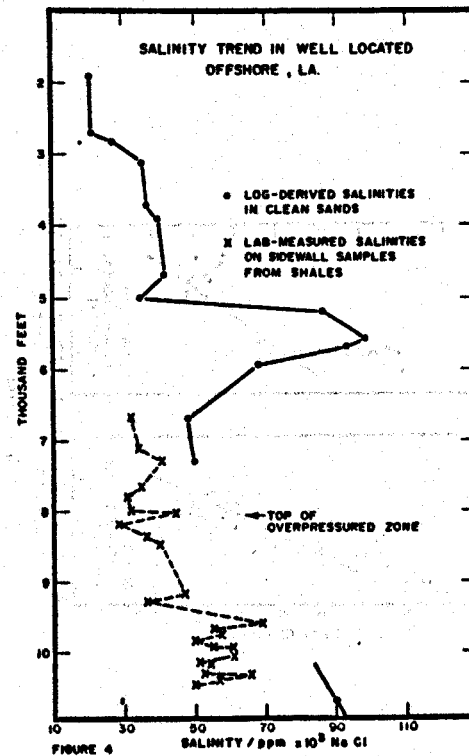
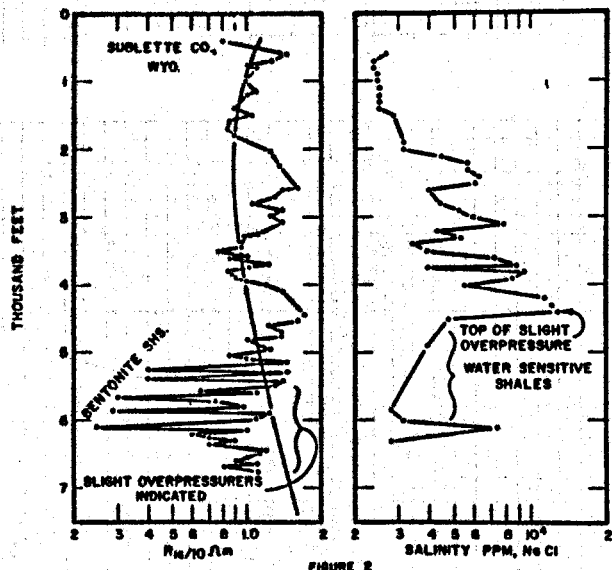
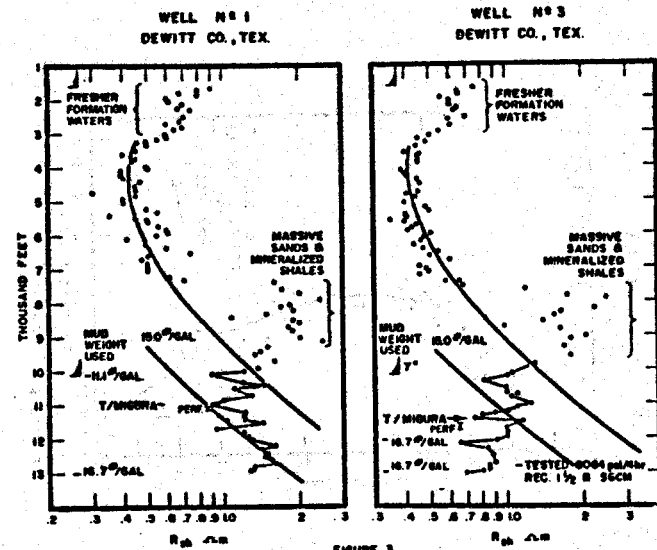
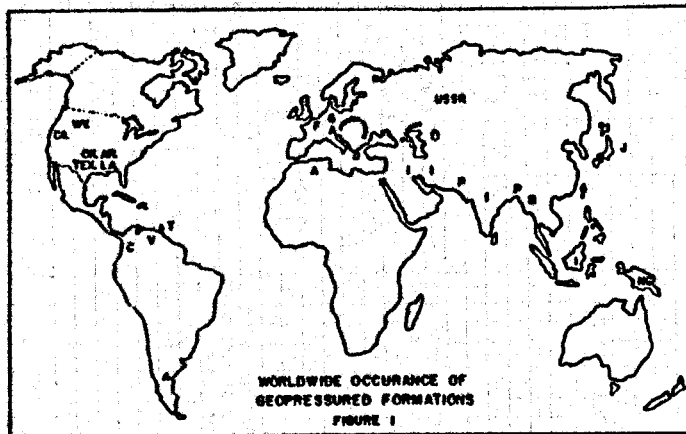
- Boatman, W. A. (1967). "Shale density key to safer, faster drilling": World Oil, August 1, 1967.
- Browning, W. C. and Perricone, A. C. (1963). "Clay chemistry and drilling fluids": SPE 540, AIME, First Conference of Drilling and Rock Mechanics, The University of Texas, January 23-24, 1963.
- Chenevert, M. E. (1969). "Shale hydration mechanics": SPE 2401, AIME, Fourth Conference of Drilling and Rock Mechanics, The University of Texas, January 14-15, 1969.
- Combs, G. D. (1968). "Prediction of pore pressure from penetration rate": SPE 2162, AIME, 43rd Annual Fall Meeting, Houston, Texas, 1968.
- Darley, H. C. H. (1969). "Physical and chemical factors affecting bore hole stability": SPE 2400, AIME, Fourth Conference of Drilling and Rock Mechanics, The University of Texas, January 14-15, 1969.
- DeSitter, L. U. (1947). "Diagenesis of oil-field brines": American Association of Petroleum Geologists Bulletin, V. 31, No. 11, pp. 2030-2040, 1947.
- Dickey, P. A., Shriram, C. R., and Paine, W. R. (1968). "Abnormal pressures in deep wells of Southwestern Louisiana": Science, V. 160, pp. 609-615, May, 1968.
- Dickinson, G. (1953). "Reservoir pressures in Gulf Coast Louisiana": American Association of Petroleum Geologists Bulletin, V. 37, pp. 410-432, 1953.
- Forgotson, J. M. (1969). "Indication of proximity of high pressure fluid reservoir, Louisiana and Texas Gulf Coast": American Association of Petroleum Geologist Bulletin, V. 53, pp. 171-173, Jan., 1969.
- Foster, J. B. and Whalen H. E. (1965). "Estimation of formation pressures from electrical surveys, offshore Louisiana": SPE paper 1200, 1965.

- Fowler, W. A. (1968). "Pressure hydrocarbon accumulation, and salinities, Chocolate Bayou Field, Brazoria County, Texas": SPE 2226, AIME, 43rd Annual Fall Meeting, Houston, Texas, 1968.
- Goins, W. C. (1968). "Guidelines for blowout prevention": World Oil, October, 1968.
- Ham, H. H. (1966). "A method of estimating formation pressures from Gulf Coast well logs": Transactions--Gulf Coast Association of Geological Societies, V. 16, pp. 185-197, 1966.
- Harkins, K. L. and Baugher, J. W. (1969). "Geological significance of abnormal formation pressures": Journal of Petroleum Technology, August, 1969.
- Hottman, C. E. and Johnson, R. K. (1965). "Estimation of formation pressures from log-derived shale properties": Journal of Petroleum Technology, June, 1965.
- Jones, P. H. (1968). "Hydrodynamics of geopressure in the northern Gulf of Mexico Bayou": SPE 2207, AIME, 43rd Annual Fall Meeting, Houston, Texas, 1968.
- Jorden, J. R. and Shirley, O. J. (1966). "Application of drilling performance data to overpressure detection": Journal of Petroleum Technology, November, 1966.
- Kelly, J. A. (1968). "Look at troublesome shale": Oil and Gas Journal, June 3 and 10, 1968.
- Kerr, P. E. and Barrington, J. (1961). "Clays of deep shale zone, Caillou Island, Louisiana": American Association of Petroleum Geologists Bulletin, V. 45, pp. 1697-1712, 1961.
- McGregor, J. R. (1965). "Quantitative determination of reservoir pressures from conductivity log": American Association of Petroleum Geologists Bulletin, V. 49, No. 9, pp. 1502-1511, 1965.
- McKelvey, J. G. and Milne, I. H. (1962). "Flow of salt solutions through compacted clay": Ninth National Clays and Clay Mineral Conference Proc., Pergamon Press, 1962.
- Mondshine, T. C. (1969). "New technique determines oil-mud salinity needs in shale drilling": Oil and Gas Journal, July 14, 1969.
- O'Brien, T. B. and Goins, W. C. (1960). "The mechanics of blowouts and how do you control them": API Drilling and Production Practice, 41, 1960.

- Overton, H. L. and Timko, D. J. (1969). "The salinity principle, a tectonic stress indicator in marine sands": Log Analyst, No. 3, 1969.
- Pennebaker, E. S. (1968). "An engineering interpretation of seismic data": SPE 2165, AIME, 43rd Annual Fall Meeting, Houston, Texas, 1968.
- Pirson, S. J. (1969). "Environmental logging and mapping in the search for minerals": SPWLA Transactions, 1969.
- Timko, D. J. (1968). "Recent trends in formation evaluation": World Oil, June, 1968.
- Timm, B. C. and Maricelli, J. J. (1953). "Formation waters in Southwest Louisiana": American Association of Petroleum Geologists Bulletin, V. 37, No. 2, pp. 394-409, 1953.
- van Olphen H. (1963). "An introduction to clay colloid chemistry": John Wiley and Sons, Inc., New York, 1963.
- Wallace, W. E. (1965). "Abnormal subsurface pressures measured from conductivity or resistivity logs": Log Analyst, No. 4, 1965.
- Young, A. and Low, P. F. (1965). "Osmosis in argillaceous rocks": American Association of Petroleum Geologists Bulletin, V. 49, pp. 1005-1007.

TABLE I

<u>Depth Feet</u>	<u>Montmorillonite (%)</u>	<u>Illite (%)</u>	<u>Kaolinite (%)</u>	<u>Chlorite (%)</u>
6648	18	30	10	3
7116	15	25	14	4
7394	18	31	8	2
7707	15	26	10	4
7803	10	28	11	4
7860	10	34	10	5
8014	11	31	11	4
8094	10	27	10	4
8160	9	30	11	4
8326	21	28	15	6
8438	19	27	11	4
9203	12	17	9	6
9254	12	20	13	5
9593	8	23	9	6
9714	8	22	11	3
9718	7	21	11	5
9821	5	28	15	4
9931	7	22	12	6
9975	6	23	15	6
10057	7	23	13	4
10142	9	21	13	4
10145	3	18	18	7
10303	5	18	14	4
10311	6	19	14	7
10393	12	17	14	5
10415	20	20	12	7



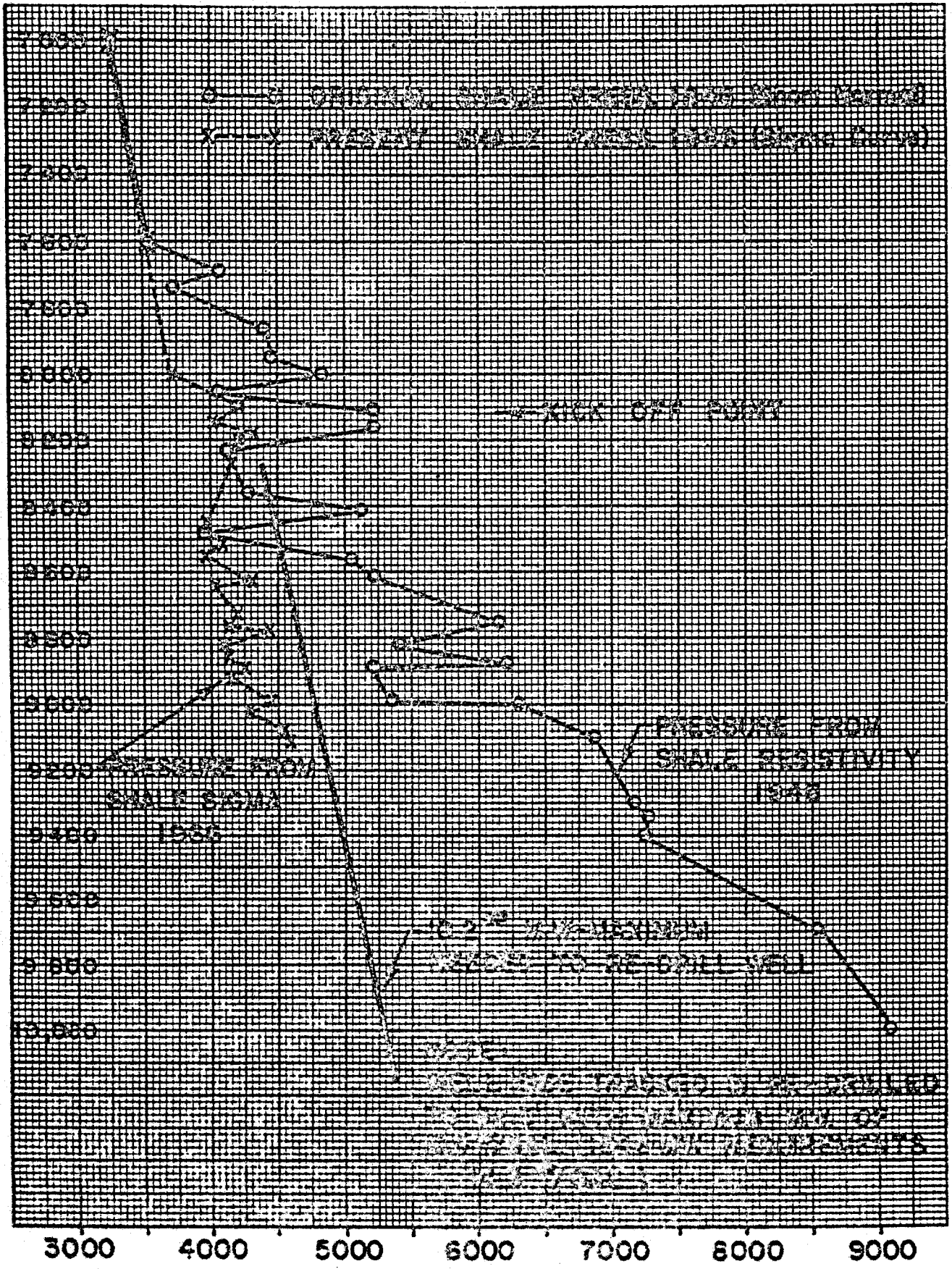


FIGURE 9

PRESSURE PSI

ARDON NO. 2
TEPETATE, LA.

FIGURE 10

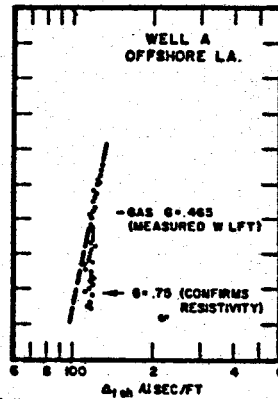
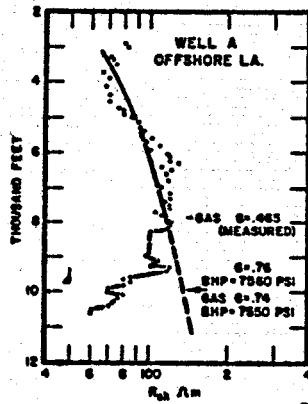
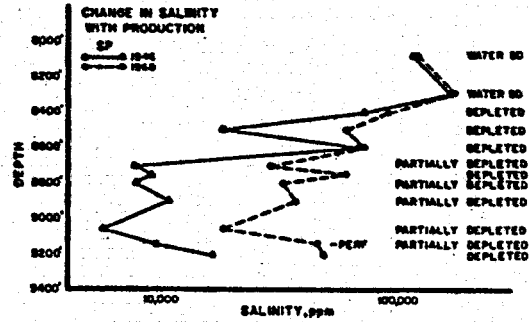


FIGURE 11

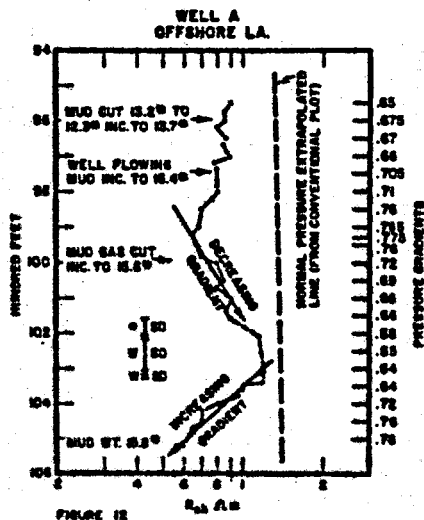


FIGURE 12

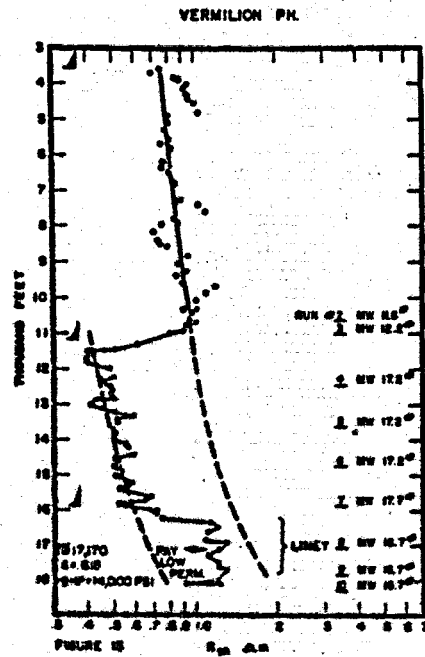


FIGURE 13